Relationship between calcium and metabolism in mouse eggs at fertilisation

Karen Campbell

ProQuest LLC
789 East Eisenhower Parkway
P.O. Box 1346
Ann Arbor, MI 48106-1346

Publications arising from work contained in this thesis

Campbell, K., Dumollard, R., Halet, G., Carroll, J. and Swann, K. (2007) Regulation of cytosolic and mitochondrial ATP levels in mouse oocytes and zygotes. *JBC* (submitted May 2007)

Swann, K., **Campbell, K**., Yu, Y., Saunders, C. and Lai, T. A (2007) Use of luciferase chimaera to monitor PLCζ expression in mouse eggs. *Methods in Molecular Biology*. *In press*

Campbell, K. and Swann, K. (2006a) Ca^{2+} oscillations stimulate an ATP increase during fertilization of mouse eggs. *Dev Biol.* 298, 225-33.

Nomikos, M., Blayney, L. M., Larman, M. G., **Campbell, K.**, Rossbach, A., Saunders, C. M., Swann, K., Lai, F. A. (2005) Role of phospholipase C-zeta domains in Ca^{2+}-dependent phosphatidylinositol 4, 5-bisphosphate hydrolysis and cytoplasmic Ca^{2+} oscillations. *J Biol Chem.* 280, 31011-8

Abstracts

Campbell, K. and Swann, K. (2006b) Ca^{2+} oscillations cause a rise in intracellular ATP in fertilizing mouse eggs. *Proc Physiol Soc* 3 PC177 (Abstract)

Summary

At fertilisation in mammals a series of Ca^{2+} oscillations are initiated that activate development. These Ca^{2+} oscillations cause the reduction of mitochondrial NAD^{+} and flavoproteins, suggesting that they might also stimulate changes in cytosolic ATP levels. Many events at fertilisation are triggered that require ATP; however, the changes in ATP during fertilisation are poorly defined. In this thesis intracellular Ca^{2+} and ATP levels in individual mouse eggs were measured by monitoring the fluorescence of a Ca^{2+} dye (Oregon green bapta dextran) and luminescence of firefly luciferase. During fertilisation of mouse eggs it was found that there are two phases of increase in ATP in both the cytosol and the mitochondria, during the series of sperm-induced Ca^{2+} oscillations. The increase in ATP is Ca^{2+} dependent since it did not occur when Ca^{2+} oscillations were prevented by BAPTA injection and, were abrogated by extracellular Ca^{2+} chelation. Additionally, it was not seen when eggs were activated by cycloheximide, which does not cause a Ca^{2+} increase. The ATP increase is likely to be caused by oxidative phosphorylation by the mitochondria since the ATP levels in substrate free media are recovered by the addition of pyruvate. This recovery is blocked by the pyruvate uptake inhibitor α-Cyano-4-hydroxycinnamic acid. These data suggest that mammalian fertilisation is associated with a sudden but transient increase in cytosolic ATP via oxidative phosphorylation, and that Ca^{2+} oscillations are both necessary and sufficient to cause this increase in ATP.

Work in this thesis has also investigated the functionality of the sperm factor PLCζ. Using luciferase tagged PLC constructs, the Ca^{2+} oscillation inducing ability of a series of PLCζ truncated constructs, PLCδ and PLCγ have been established. Results show that PLCζ activation of mouse eggs cannot be reproduced by other PLCs and that the C2, EF1 and catalytic site on the X domain are all essential for causing Ca^{2+} oscillations.

Contents

List of Figures ..... *IV*
List of Tables ..... *VI*
Abbreviations ..... *VII*

Chapter1- Introduction

1.1 Introduction - Fertilisation *2*

1.2 Oocyte and Sperm Maturation *3*
1.2.1 Oogenesis 3
1.2.2 Ovulation 7
1.2.3 Metabolism in eggs 10
1.2.4 Spermatogenesis and Sperm Characteristics 12
1.2.5 Sperm Metabolism 15
1.2.6 Sperm Capacitation 16

1.3 Fertilisation and Development *17*
1.3.1 Fertilisation 17
1.3.2 Zona Pellucida Structure 19
1.3.3 Embryo Development 23

1.4 Calcium (Ca^{2+}) *23*
1.4.1 A universal intracellular messenger 23
1.4.2 Intracellular Ca^{2+} releasing agents 26
1.4.3 Ca^{2+} change at fertilisation 27
1.4.4 Ca^{2+} Oscillations at Fertilisation 29
1.4.5 Maturation Promoting Factor (MPF) activity 31
1.4.6 Ca^{2+} Oscillations and the $InsP_3$ pathway 36

1.5 Sperm Factor *37*
1.5.1 How does a sperm fertilise an egg? 37
1.5.2 Search for the Sperm Factor 41
1.5.3 PLCζ 45

1.6 Metabolism and Fertilisation *46*
1.6.1 Metabolism 46
1.6.2 Mitochondria 47
1.6.3 Mitochondria and Ca^{2+} 50
1.6.4 Mitochondrial distribution in eggs 50
1.6.5 Mitochondria and Fertilisation 52

1. 7 Bioluminescence *54*
1.7.1 Firefly Luciferase 54
1.7.2 Firefly Luciferase in cells 57

1.8 Aims *59*

Chapter2 - Materials and Methods

2.1 Laboratory reagents and animals *61*
2.1.1 Media and hormone preparation 61

2.2 Chemical Reagents preparation *62*
2.2.1 Reagents injected into eggs 62
2.2.2 Chemicals that manipulate cellular metabolism 63
2.2.3 Cell cycle inhibitors 66
2.2.4 Chemicals that affect Ca^{2+} levels and/or parthenogenetic activation 67

2.3 cRNA constructs *68*
2.3.1 Preparation of cRNA 68
2.3.2 Mitochondrial targeted firefly luciferase cRNA 70

2.4 Immunohistochemistry *70*

2.5 Mouse Egg Experiments *72*
2.5.1 Fire pulled glass pipettes 72
2.5.2 Stimulation of Ovulation and Collection of Oocytes 72
2.5.3 Microinjection of mouse eggs 76

2.6 IVF Procedure *78*

2.7 Imaging and Ca^{2+} and ATP *80*
2.7.1 Imaging of microinjected mouse eggs 80
2.7.2 Measurement of luminescence using a luminometer 87
2.7.3 Measurement of ATP levels in eggs 89
2.7.4 Microinjection of luciferase tagged PLC ζ, δ and β domain constructs 89

2.9 Statistical Analysis *90*

Chapter3 - The relationship between Ca^{2+} and ATP at fertilisation

3.1 Introduction *92*

3.2 Results *93*
3.2.1 Monitoring ATP luminescence in mouse eggs 93
3.2.2 Ca^{2+} and ATP in a mouse egg 97
3.2.3 Ca^{2+} oscillations at fertilisation are correlated with an ATP increase 99
3.2.4 ATP content in a single mouse egg 108

3.3 Discussion *113*

Chapter 4- ATP dependance upon Ca^{2+} changes

4.1 Introduction *117*

4.2 Results *118*
4.2.1 The increase in ATP is Ca^{2+} dependant 118
4.2.2 Parthenogenetic activation without a Ca^{2+} change is insufficient to increase ATP levels 121
4.2.3 Ca^{2+} and ATP changes can be induced by uncaging $InsP_3$ 123
4.2.4 Ca^{2+} releasing agents that act via the $InsP_3$ pathway produce an increase in ATP... 127
4.2.5 Non-physiological Ca^{2+} releasing agents produce an initial decrease in ATP levels 130

4.3 Discussion *132*

Chapter 5 - Regulation of cytosolic and mitochondrial ATP levels in mouse oocytes and zygotes

5.1 Introduction *137*

5.2 Results *139*
5.2.1 Mitochondrial Luciferase 139
5.2.2 Oxidative phosphorylation is required by MII eggs 145
5.2.3 Fertilisation ATP responses to cinnamate addition 151
5.2.4 Pyruvate recovers ATP levels in starved eggs 153
5.2.5 Neither glucose, lactate, or, glutamine can support ATP production in a fertilised egg 156

5.3 Discussion *160*

Chapter 6 - Investigations into the secondary change in ATP levels at fertilisation

6.1 Introduction *163*

6.2 Results *166*
6.2.1 Second PB emission could be responsible for the 2nd change in ATP 166
6.2.2 Cell cycle inhibition inhibits the 2nd increase in ATP levels 170
6.2.3 Mitochondrial activity could increase due to an increase in mitochondrial Ca^{2+} uptake 172
6.2.4 Inhibiting mitochondrial Ca^{2+} uptake into the mitochondria 177

6.3 Discussion *179*

Chapter 7- The mechanism of action of PLCζ

7.1 Introduction *184*

7.2 Results *185*
7.2.1 Quantification of protein expression 185
7.2.2 Preparation of WT mPLCζ-Luciferase and deletion constructs 187
7.2.3 Expression of PLCζ-LUC, ζΔEF1-LUC, ζΔC2-LUC and ζΔD210 constructs in mouse eggs 187
7.2.4 Cloning of PLCδ1-LUC, δ1ΔPH-LUC, ζ-δ1PH and PLCγ1 193
7.2.5 Expression of PLCδ1-LUC δ1-LUC chimeras and PLCγ1 193
7.2.6 hPLCζ and sPLCζ-LUC constructs and chimeras 198

7.3 Discussion *204*

Chapter 8 - Main Discussion

8.1 Firefly luciferase luminescence to measure ATP *210*

8.2 ATP levels during fertilisation *210*

8.3 The Second rise in ATP at fertilisation *212*

8.4 Ca^{2+} release and ATP response *215*

8.5 ATP and aged eggs *219*

8.6 Why does ATP levels matter? *220*

8.7 Metabolism during fertilisation *224*

8.8 PLCζ *232*

References *241*

List of Figures

Fig. 1. 1 Maturation of primary oocyte to a GV oocyte 6
Fig. 1. 2 Maturation and fertilisation of an MII egg 9
Fig. 1. 3 Schematic diagram of a sperm 14
Fig. 1. 4 Diagram of the acrosome reaction 21
Fig. 1. 5 Ca^{2+} oscillations in a mouse egg 30
Fig. 1. 6 MPF regulation in an unfertilised and fertilised egg 35
Fig. 1. 7 Three hypotheses for a Calcium increase at fertilisation 40
Fig. 1. 8 Diagram showing the structure of PLCs 44
Fig. 1. 9 Diagram illustrating the function of mitochondria 49
Fig. 1. 10 The firefly luciferase-luciferin reaction 55

Fig. 2. 1 Cinnamate structure 65
Fig. 2. 2 Retrieval of ampullas from the mouse 74
Fig. 2. 3 MII eggs before and after hyaluronidase treatment 75
Fig. 2. 4 Microinjection of MII mouse egg 77
Fig. 2. 5 Photek imaging system 82
Fig. 2. 6 Schematic and photograph of Photek system 83
Fig. 2. 7 Diagram demonstrating switching mechanism 86
Fig. 2. 8 Luminometer used in lysis assays 88

Fig. 3. 1 Luminescence signal in an unfertilised egg 94
Fig. 3. 2 Luminescence signal in a fertilised egg 96
Fig. 3. 3 Luminescence and fluorescence in the same eggs 98
Fig. 3. 4 ATP and Ca^{2+} in a fertilised egg 100
Fig. 3. 5 Initial increase in ATP at fertilisation 101
Fig. 3. 6 ATP and Calcium during fertilisation 103
Fig. 3. 7 Fertilisation in high Ca^{2+} 107
Fig. 3. 8 Calibration curve for firefly luciferase 109
Fig. 3. 9 Lysis method to determine ATP content 112

Fig. 4. 1 BAPTA injected egg during fertilisation 119
Fig. 4. 2 BAPTA addition during fertilisation 120
Fig. 4. 3 Cycloheximide activation of mouse eggs 122
Fig. 4. 4 Uncaging $InsP_3$ in mouse eggs 125
Fig. 4. 5 Ca^{2+} releasing agents via $InsP_3$ 128
Fig. 4. 6 Ionomycin and thapsigargin induced Ca^{2+} rise 131

Fig. 5. 1 Anti-Luciferase immunohistochemistry 140
Fig. 5. 2 Cytosolic and mitochondrially targeted luciferase probes 141
Fig. 5. 3 Mitotracker orange and mitochondrial luciferase 143
Fig. 5. 4 Mitochondrial localisation in GV oocytes 144
Fig. 5. 5 Oligomycin effect on cytosolic and mitochondrial ATP levels .. 146
Fig. 5. 6 Mitochondrial ATP levels during fertilisation 147
Fig. 5. 7 The effect of cinnamate on unfertilised eggs 149

Fig. 5. 8 The effect of cinnamate on cytosolic and mitochondrial ATP levels 150
Fig. 5. 9 Cytosolic and mitochondrial ATP levels during fertilisation in the presence of cinnamate 152
Fig. 5. 10 Pyruvate can recover ATP and Ca^{2+} levels in starved eggs .. 154
Fig. 5. 11 Cinnamate prevents the recovery action of pyruvate in starved eggs during fertilisation 155
Fig. 5. 12 Glucose, lactate and glutamine addition to unfertilised starved eggs 158
Fig. 5. 13 Glucose, lactate and glutamine addition to starved fertilised eggs 159

Fig. 6. 1 Mitochondrial and cytosolic Ca^{2+} oscillations during fertilisation 165
Fig. 6. 2 A two phase increase in ATP levels during fertilisation 168
Fig. 6. 3 Inhibiting 2nd PB emission during fertilisation 169
Fig. 6. 4 Nocodazole and MG132 fertilised eggs 171
Fig. 6. 5 Mitochondrial ATP during fertilisation 173
Fig. 6. 6 Flavoprotein autofluorescence during fertilisation 174
Fig. 6. 7 Excitation and emission profiles of luciferin and FAD^{++} 176
Fig. 6. 8 Fertilisation in SB202190 178

Fig. 7.1 Calibration for quantification of protein expression 186
Fig. 7. 2 Preparation of PLCζ-LUC and ζ-LUC deletion constructs 190
Fig. 7. 3 Microinjection of PLCζ-LUC and ζ-LUC deletion constructs..... 191
Fig. 7. 4 Preparation of PLCδ1-LUC, δ1 chimeras and PLCγ1-LUC..... 195
Fig. 7. 5 Microinjection of PLCδ1-LUC, δ1-LUC chimeras and γ1-LUC. 196
Fig. 7. 6 Preparation of sPLCζ-LUC and hPLCζ-LUC WTs and chimeras 200
Fig. 7. 7 Microinjection of sPLCζ-LUC and hPLCζ-LUC and chimeras.. 201
Fig. 7. 8 hPLCζ can induce oscillations at low expression levels..... 202

Fig. 8. 1 Pathways taken by exogenously added metabolic substrates. 231

List of Tables

Table 3.1 Ca^{2+} and luciferase luminescence response in eggs at fertilisation....104
Table 4.1 Uncaging data....126
Table 4.2 Ca^{2+} and luciferase luminescence response in eggs exposed to Ca^{2+} releasing agents....129
Table 7.1 WT and mPLCζ-LUC and deletion constructs 192
Table 7.2 PLCδ1-LUC, δ1 chimeras and PLCγ1 197
Table 7.3 hPLCζ-LUC, sPLCζ-LUC and chimeras....203
Table 8.1 Changes in Ca^{2+} concentrations during physiological and non-physiological stimuli....218
Table 8.2 Changes in Ca^{2+} concentrations following injections of either PLCζ or, PLCδ1....238

List of Abbreviations

AC	Adenylyl cyclase
ADP	adenosine diphosphate
AMP	Adenosine monophosphate
ANT	Adenine nucleotide translocase
APC/C	Anaphase promoting complex/cyclosome
ATP	Adenosine trisphophate
AU	Arbitrary units
BAPTA	1,2-Bis(2-aminophenoxy)ethane-N,N,N',N'_tetraacetic acid potassium salt
BMP8b	Bone morphogenetic protein 8b
BSA	Bovine serum albumin
Bub	Budding uninhibited by benzimidazole
[(Ca^{2+})i]	Intracellular Calcium
Ca^{2+}	Calcium
cADPR	cyclic ADP ribose
CaMKII	Calmodulin-dependant kinase II
cAMP	cyclic adenosine monophosphate
Carbachol	Carbamolycholine chloride
CB	Cytochalasin B
CD	Cytochalasin D
CICR	Ca^{2+} induced Ca^{2+} release
Cinnamate	α-cyano-4-hydroxycinnamic acid
CO_2	Carbon dioxide
cps	Counts per second
CSF	Cytostatic factor
DAG	1,2 Diacylglycerol
DMSO	Dimethyl sulfoxide
EGF	Epidermal growth factor
Emi1	Early mitotic inhibitor 1
E-PAP	E-polyadenylate polymerase
ER	Endoplasmic reticulum
Erp1/Emi2	Emi1 related protein 1
FAD^+	Flavin adenine dinucleotide
FCCP	Carbonyl cyanide 4-(trifluoromethoxy) phenylhydrazone
FSH	Follicle stimulating hormone
GDP	Guanosine 5-diphosphate
GTP	Guanosine 5-triphosphate
HKSOM	Hepes buffered potassium simplex optimised media
hCG	Human chorionic gonadotrophin
H_2O	Water
Hoechst 33342	bis Benzimide H 33342
ICCD	Intensified charged coupled device
ICSI	intracytoplasmic sperm injection
IICR	$InsP_3$ induced Ca^{2+} release
GAPD-S	Glyceraldehyde-3 phosphate dehydrogenase
GDNF	Glial cell line derived neutrophic factor
GPR3	G protein receptor 3

GV	Germinal Vesicle
GVB	Germinal vesicle breakdown
$InsP_3$	Inositol 1,4,5-trisphosphate
$InsP_4$	Inositol 1,3,4,5 tetrakisphosphate
InP_3Rs	Inositol 1,4,5-trisphosphate receptors
IP	Intra-peritoneal
IVF	*In vitro* fertilisation
K^+	Potassium
LH	Luteinising hormone
MII	Metaphase II
MAD	Mitotic arrest deficient
MAPK	Mitogen activated protein kinase
MG132	Z-Leu-Leu-Leu-al
MPF	Maturation promoting factor
NAD^+	Nicotinamide adenine dinucleotide
NO	nitric oxide
NAADP	Nicotinic acid adenine dinucleotide phosphate
O_2	Oxygen
OGBD	Oregon green bapta dextran
PAWP	Post acrosomal sheath WW domain binding protein
PI arrest	Prophase I arrest
PB	Polar body
PH	Pleckstrin homology
PIP_2	Phosphatidylinositol 4,5 bisphosphate
PKA	Protein kinase A
Plk	Polo-like kinase 1
PLC	Phospholipase C
PM	Plasma membrane
PMGCs	Primordial germ cells
PMSG	Pregnant mare serum gonadotrophin
PMT	Photomultiplier tube
PN	Pronuclei
PPP	Pentose phosphate pathway
PTK	Protein tyrosine kinase
PVP	Poly(vinyl) alcohol
ROCCs	Receptor operated calcium channels
ROS	Reactive oxygen species
RT	Room temperature
RYR	Ryanodine receptor
SAC	Spindle assembly checkpoint
SOCC	Store operated calcium channels
SR	Sarcoplasmic reticulum
TCA	Tricarboxylic acid
VOCCs	Voltage operated calcium channels
ZP	Zona pellucida

List of Symbols

β	beta
δ	delta
γ	gamma
ζ	zeta

Chapter 1

Introduction

1.1 Introduction - Fertilisation

Fertilisation is the process where two sex cells (gametes) come together to produce a new individual cell that has a genome derived from both parents. When a sperm fertilises an egg, reactions in the egg cytoplasm are initiated that begin development of the embryo. During mammalian fertilisation a series of intracellular calcium [$(Ca^{2+})i$)] oscillations are initiated that last for several hours. Recently, it was discovered that the "sperm factor" Phospholipase C zeta (PLCζ) produces [$(Ca^{2+})i$)] similar to those produced at fertilisation. Part of this thesis investigates the role and function of the PLCζ domains at fertilisation. The downstream effects on metabolism of [$(Ca^{2+})i$] oscillations in the egg, has yet to be fully defined. In this thesis, experiments have been designed to look directly at ATP and [$(Ca^{2+})i$] levels simultaneously in order to characterise the relationship that exists between the two.

This introduction shall act as a general review of areas that are directly relevant to my area of study. I shall begin with an overview of gametogenesis, which is the process that explains the creation of both the male and female gametes. Males and females have different forms of gametogenesis: oogenesis (females) and spermatogenesis (males). This section shall be followed by an overview and discussion of both [$(Ca^{2+})i$] oscillations that occur in an egg at fertilisation and PLCζ. Mitochondria and metabolism, within an egg, shall then be discussed followed by an overview of the firefly luciferase-luciferin system that is used throughout this thesis to study intracellular ATP levels.

1.2 Oocyte and Sperm Maturation

1.2.1 Oogenesis

The female gamete forms, grows and matures during a mechanism known as oogenesis. Before birth, primordial germ cells (PMGCs) develop in the genital ridge of the foetus, and in the mouse ovary (Hogan et al., 1986). These PMGCs are known as oogonia and undergo ~4 mitotic cycles before entering meiosis between days 14 and 16 of a 20 day gestation period (Monk and McLaren, 1981). More than half of these cells, now referred to as primary oocytes (Fig. 1.1), are present in the mouse at birth and will degenerate before the mouse reaches 3-5 weeks of age. The mouse will reach sexual maturity at around 6 weeks (Hogan et al., 1986). Ovarian oocytes are immature and rest in primordial follicles that reside in the ovarian cortex. They measure approximately 12 μm and 30 μm in diameter, in mice and humans, respectively (Grudzinskas and Yovich., 1995).

Each primary oocyte is contained within a primordial follicle surrounded by layers of follicle cells (Fig. 1.1). The follicle cells are essential for growth and differentiation of the oocyte. The primordial follicles undergo a stage of growth and during this time the primary oocytes are able to undergo remarkable enlargement as their growth is not interrupted by mitosis and cleavage of the cytoplasm (Fig. 1.1) (Grudzinskas and Yovivh. 1995). Growing oocytes develop a zona pellucida (ZP), which is 7 μm thick in the mouse oocyte (Fig. 1.1). Oocyte growth is also characterised by the development of a large nucleus called

the germinal vesicle (GV). During this growth stage, oocytes will increase to a diameter of 80 μm and 120 μm, in mice and humans, respectively (Grudzinskas and Yovich., 1995).

Primary oocytes are diploid cells that must undergo meiosis. Meiosis is the process that allows a diploid cell to divide twice to produce haploid cells (gametes) that contain one complete set of chromosomes. GV oocytes are arrested at prophase I (PI arrest) of meiosis I which means that the chromosomes within the oocytes have condensed ready for the 1st meiotic division. PI arrest is regulated by 3, 5 cyclic adenosine monophosphate (cAMP) levels within the oocyte (Conti et al., 2002). cAMP is either produced locally within the oocyte, or transferred into the oocyte from granulosa cells through gap junctions (Dekel, 1988). cAMP holds the oocytes at PI arrest by inactivating maturation promoting factor (MPF – discussed in section 1.4.5) (Duckworth et al., 2002). Measurements of cAMP levels have shown that a drop in oocyte cAMP is associated with germinal vesicle breakdown (GVB), hence progression through meiosis I. Preventing cAMP levels from falling has been shown to block oocyte maturation (Schultz et al., 1983a; Schultz et al., 1983b; Vivarelli et al., 1983). This stage of arrest may also be accomplished by the action of hypoxanthine, which is produced by follicular cells (Eppig et al., 1985).

High cAMP levels that hold the oocyte in meiotic arrest is produced in the oocyte via a pathway that requires the activity of the heterotrimeric G protein G_s (Kalinowski et al., 2004; Mehlmann et al., 2002). It has recently been suggested that the G protein receptor 3 (GPR3) is a

constitutive activator of the G_s G protein (Freudzon et al., 2005). GPR3-Gs seems to be responsible for the activation of adenylyl cyclase (AC) that maintains elevated cAMP in the oocyte.

Fig. 1. 1 Maturation of primary oocyte to a GV oocyte

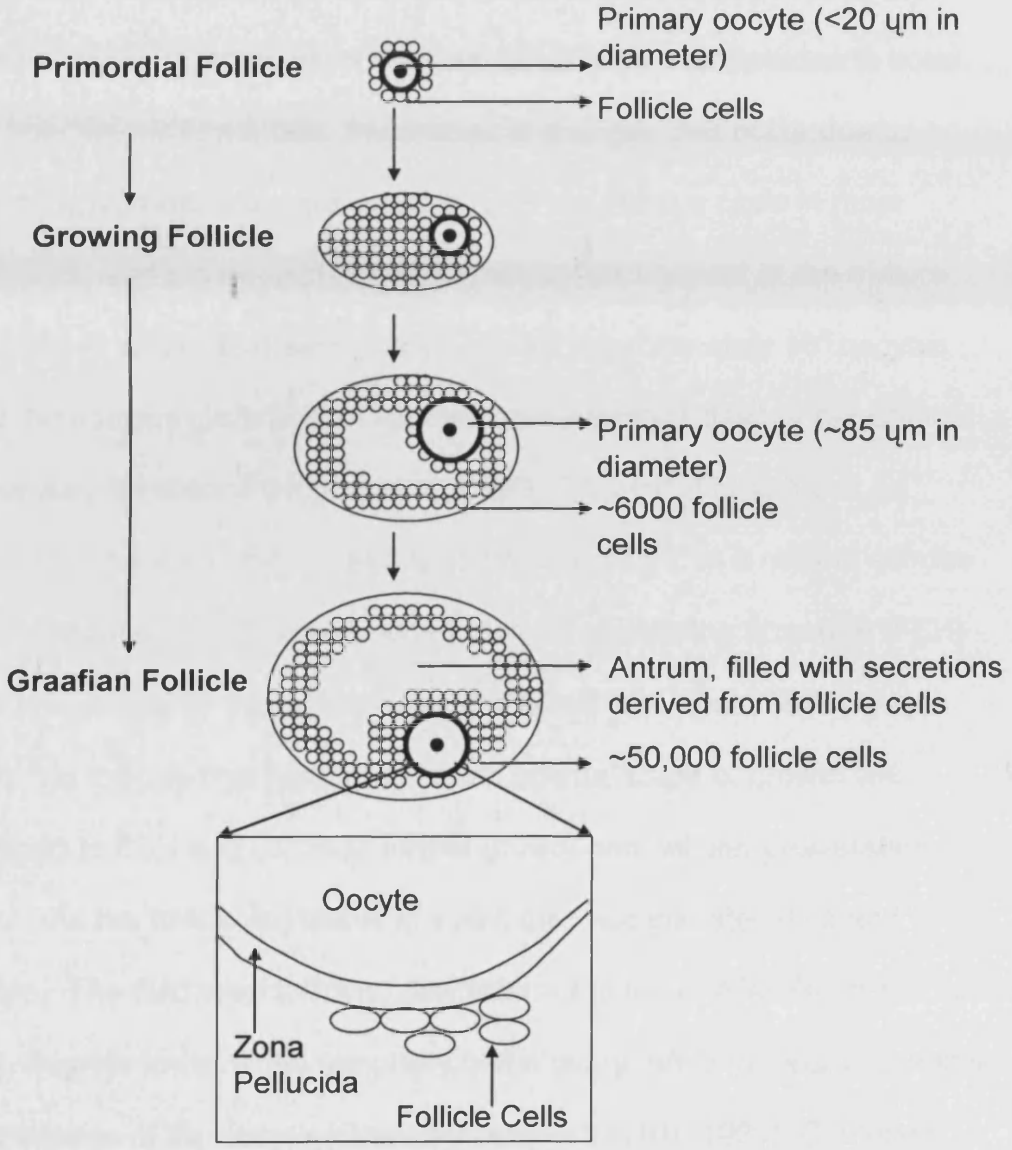

Fig 1.1 Diagram illustrating the growth stages of the ovarian follicle from a primordial follicle to a graafian follicle containing an immature oocyte at the germainal vesicle (GV) stage.

1.2.2 Ovulation

Oocytes arrested at PI will increase in size and when exposed to the correct hormonal stimulation, they will acquire the competence to enter the final stages of meiosis. Physiological changes that occur due to reproductive hormones are referred to as the estrous cycle in most mammals and the menstrual cycle in humans and apes. In the mature mouse (~6 weeks old) each ovary contains approximately 10^4 oocytes and the estrous cycle occurs spontaneously every 4 days under optimal laboratory conditions (Hogan et al., 1986). This cycle length can be influenced by many factors and is strain dependent. In a natural estrous cycle, about 6-15 follicles respond to follicle stimulating hormone (FSH) that is secreted by the pituitary gland (Wassarman et al., 1976). Any maturing follicles that have reached an optimal stage of growth will respond to FSH and continue further growth and cellular proliferation.

As the follicle increases in size it also accumulates fluid and swells. The fluid filled follicles, now referred to as graafian follicles (Fig. 1.1), migrate towards the periphery of the ovary ready for final maturation and release of the oocyte (Grudzinskas and Yovich. 1995). Ovulation occurs in response to a surge in the levels of luteinizing hormone (LH) from the pituitary gland. Following the LH surge, the oocytes undergo nuclear maturation. The nucleus, (GV), will lose its membrane and the chromosomes will assemble on the spindle and move towards the periphery of the cell. It is at this point that the oocyte will undergo the first meiotic division. One set of homologous chromosomes are retained within the oocyte while the other set will become surrounded by a small

amount of the oocytes cytoplasm and be extruded as the first polar body (PB) (Donahue, 1968; Wassarman et al., 1976). Meiosis is complete with the secondary oocyte containing a full set of complement chromosomes: the cell now arrests at metaphase II (MII) of the second meiotic division (Fig. 1.2) (Donahue, 1968). The egg is arrested at metaphase II with the 1st PB present in most species. The exceptions to this are the dog and fox, whose eggs are ovulated as primary oocytes and are, therefore, arrested at the GV, or, 1st meiotic division (Holst and Phemister, 1971). The estrous cycle can be influenced by environmental factors and can be induced artificially by hormone injections (see Chapter 2: section 2.5.2). During natural ovulation, 8-12 eggs are released, depending upon the strain of the mouse. After hormonal injections, to stimulate ovulation, around 20-30 eggs can be collected per mouse.

Fig. 1. 2 Maturation and fertilisation of an MII egg

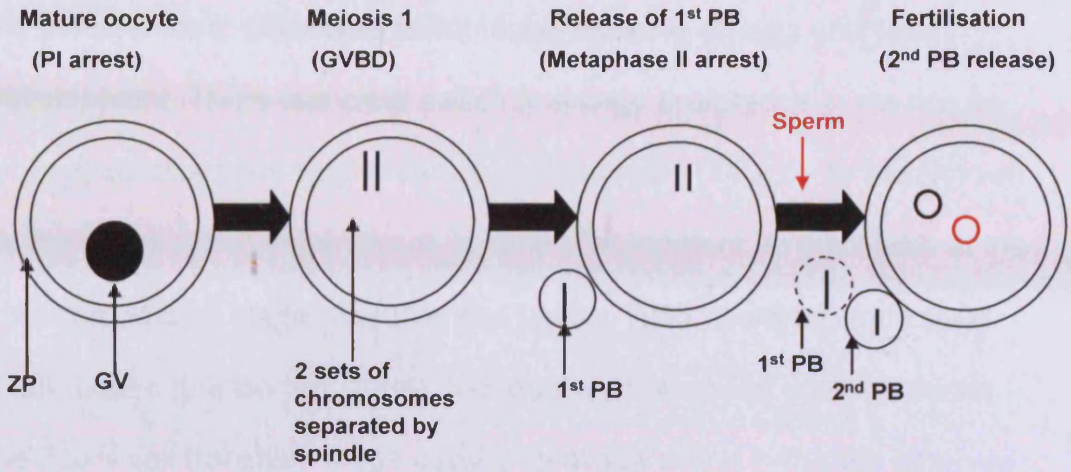

Fig. 1.2 Primary oocytes arrested at PI undergoing meiosis I to contain one complete set of chromsomes and extrude a 1st PB. At sperm entry, an egg is activated and meiosis II is complete with the egg now containing male (red) and female (black) genetic information (diploid cell). The 2nd PB will be released and the 1st PB degenerates. The egg will form pro nuclei (PN) around 5-6 hours post activation.

1.2.3 Metabolism in eggs

An egg is reliant upon energy production via oxidative metabolism from the mitochondria. Glycolysis is not highly active in an egg until later development. There is a clear switch in energy preference in the mouse embryo development from tricarboxylic acid cycle (TCA cycle also known as the krebs cycle) dependence in early development, to glycolysis at the post-compaction stage (Gardner and Leese, 1986; Gardner and Leese, 1988; Leese and Barton, 1984). Indeed the presence of glucose during the 2 to 4 cell transition stage causes cleavage arrest in mouse embryos (Brown and Whittingham, 1991; Brown and Whittingham, 1992; Chatot et al., 1989; Sakkas et al., 1993). This inhibitory effect of glucose has been demonstrated in mouse (Barbehenn et al., 1974), hamster (Schini and Bavister, 1988), cattle (Takahashi and First, 1992) and humans (Conaghan et al., 1993). The eggs preferentially use pyruvate instead of glucose due to a block at the 6-phosphofructokinase level (see Fig. 1.9 page 49) (Barbehenn et al., 1974). Oxidative phosphorylation is, therefore, presumed to be the mechanism responsible for adenosine 5-trisphosphate (ATP) production in unfertilised and fertilised eggs in early development.

Cumulus cells play an important role in oocyte growth and this was first demonstrated when oocyte maturation failed to occur in glucose containing media, unless the cumulus cells or, pyruvate were also present (Biggers et al., 1967). This was further supported when cumulus cells were shown to produce pyruvate from glucose or, lactate (Donahue and Stern, 1968; Leese and Barton, 1985). Cumulus cells play an

acids (Colonna and Mangia, 1983; Haghighat and Van Winkle, 1990). The transport of substrates from cumulus cells to the oocyte occurs via passive transport and gap junctions (Sugiura et al., 2005). The oocyte utilises these substrates via the TCA cycle and hence, produce ATP. Fully grown follicles are mainly active glycolytically as they have been shown to produce steady state levels of mRNAs that encode enzymes involved in glycolysis (Sugiura et al., 2005). It seems that the oocyte regulates the activity of the cumulus cells via secretion of paracrine factors that are secreted by the oocyte (Sugiura et al., 2005). The pentose phosphate pathway (PPP) has also been shown to occur in cumulus cells and has been shown to be required for GV breakdown (Colton et al., 2003; Downs, 1998).

1.2.4 Spermatogenesis and Sperm Characteristics

Spermatogenesis is the production of sperm from PMGCs. Spermatozoa was first described about 300 years ago by Leeuwenhoek in semen and in the testis (Ruestow, 1983). In 1830 spermatozoa were identified as the component of semen required for fertility. The spermatozoa of different species differ in sizė; those of human and other domestic mammals, such as the dog and cat (Austin and Short. 1982) are about 50 μm long while rodent spermatozoa are much longer, measuring 150-250 μm (Austin and Short. 1982). Spermatogenesis is initiated during puberty and in the mouse is thought to be regulated by the synthesis of bone morphogenetic protein 8b (BMP8b; Zhoa et al., 1996). Mice lacking BMP8b are unable to initiate spermatogenesis at puberty and there is a marked increase in male germ cell apoptosis in the adult male mouse (Zhao et al., 1996).

Sperm cells, like oocytes, are derived from PMGCs. When the PMGCs reach the gonad (testicle), they divide 4 times to produce intermediate spermatogonium. Intermediate spermatogonium undergo 2 mitotic divisions to produce primary spermatocytes. Finally, primary spermatocytes undergo meiosis to form spermatids (Dym, 1994). This transition from spermatogonia to spermatocytes appears to be mediated by glial cell line derived neurotrophic factor (GDNF), which is secreted by sertoli cells (Meng et al., 2000).

In humans the progression from spermatogonial stem cells to mature spermatozoa takes 65 days (Dym, 1994). In human testicles 100 million sperm are made per day and each ejaculation releases 200 million sperm (Reijo et al., 1995). Unused sperm are either resorbed or passed

out of the body as urine (Reijo et al., 1995). In the mouse, development from stem cells to spermatozoa takes 34.5 days (Reijo et al., 1995).

The sperm head is characteristic of the species; hook shaped in mice and rodents but flattened and rounded in man and domesticated animals such as the cat and the dog. The head of human sperm are about 5 µm long, 2.5 µm wide and 1.5 µm thick (Austin and Short. 1982). In all mammals the sperm head contains a highly condensed mass of DNA-protein called chromatin combined with protamines (Austin and Short. 1982). The sperm tail, or flagellum, is usually divided into a mid-piece and an end piece (Fig. 1.3). The mid-piece extends from the head to as far as the end of the mitochondrial helix (Fig. 1.3; Austin and Short. 1982). At the centre of the tail is the axoneme complex which is mainly responsible for the sperm motility (Fig. 1.3).

Fig. 1. 3 Schematic diagram of a sperm

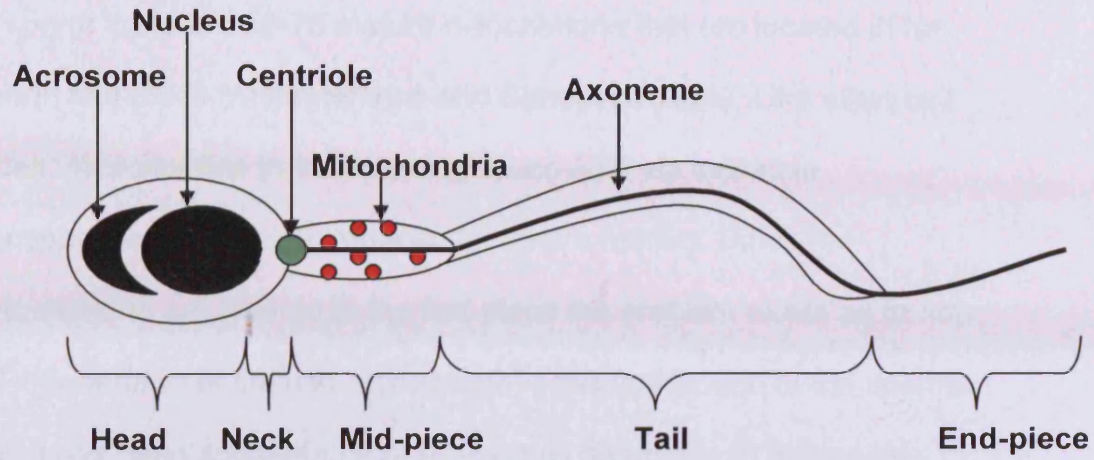

Fig. 1.3 Schematic diagram of a sperm cell (see text for details).

1.2.5 Sperm Metabolism

In sperm there are 50-75 mature mitochondria that are located in the sperm mid-piece (Ankel-Simons and Cummins, 1996). Like other cell types, mitochondria in the sperm produce ATP via oxidative phosphorylation which is required for sperm motility. Since the mitochondria are located in the mid-piece the problem exists as to how ATP generated at the mid-piece reaches the farther end of the sperms tail. It has been suggested that ATP would be unable to diffuse this distance in sufficient time to meet the energy demands of the tail (Turner, 2006). Also, in the mouse it has been demonstrated that if mitochondrial oxidative phosphorylation is defective, fertilisation can still occur (Narisawa et al., 2002). This finding suggests that oxidative phosphorylation is not the only and main source of ATP in the sperm.

Several glycolytic enzymes, including hexokinase, lactate dehydrogenase and glyceraldehyde-3-phosphate dehydrogenase (GAPD-S), have been identified in the tail of mammalian sperm cells e.g. the fox, boar and mouse sperm (Bradley et al., 1996; Bunch et al., 1998; Mori et al., 1998; Travis et al., 1998; Westhoff and Kamp, 1997). ATP production from glycolysis is required for hyperactivated sperm motility and fertilisation whereas inhibition of oxidative phosphorylation does not block fertilisation in the mouse (Fraser and Quinn, 1981). However, this area is very complex since different species have different abilities and requirements for carrying out glycolysis and oxidative phosphorylation. While mouse sperm require glucose for capacitation, bull sperm

capacitation is inhibited by glucose. Therefore, the role of glucose on sperm metabolism in different species is unknown.

1.2.6 Sperm Capacitation

Mammalian spermatozoa are unable to fertilise the oocyte immediately after ejaculation. Ejaculated sperm require a period of incubation in the female reproductive tract where they undergo a series of biochemical modifications in order to acquire the ability to fertilise, a process defined as capacitation. *In vitro* capacitation is achieved by leaving the collected sperm in optimal media for two hours in a humidified incubator set at the appropriate temperature (37°C) and 5% CO_2 levels. During capacitation several intracellular changes occur, such as increases in intracellular Ca^{2+} and cAMP concentrations (Breitbart et al., 1985). Other changes include; cholesterol efflux, protein phosphorylation, increases in membrane fluidity and changes in swimming patterns and chemostatic motility (Breitbart, 2002). Tyrosine phosphorylation of several sperm proteins play an important role in capacitation (Visconti and Kopf, 1998). For example, inhibition of protein kinase A (PKA) can inhibit the capacitation of spermatozoa (Visconti et al., 1995). In humans reactive oxygen species (ROS) have been suggested to play an important role in capacitation-related phosphorylation of several proteins (Aitken, 1989). In addition, epidermal growth factor (EGF) may play a role since its receptor tyrosine kinase, EGFR, has been identified in the head of bovine sperm (Lax et al., 1994). Activation of EGFR leads to two essential processes for the progress of capacitation, tyrosine phosphorylation and activation of PLCγ (Spungin et al., 1995).

1.3 Fertilisation and Development

1.3.1 Fertilisation

In the mouse approximately $5.8x10^7$ sperm are released into the female reproductive tract per ejaculation (Hogan et al., 1986). Some sperm will reach the ampulla in approx 5 minutes (Hogan et al., 1986) but, as discussed above, they are not competent to initiate fertilisation until capacitation has occurred. In order to reach the surface of the egg, the sperm must penetrate both the cumulus masses and the ZP, respectively. During mouse *in vitro* fertilisation (IVF) protocols this process is aided by a hyaluronidase digestion of the cumulus cells surrounding the egg, which allows easier access for the sperm to the egg. A guidance mechanism exists to ensure capacitated sperm successfully reach and fertilise the egg. Chemotaxis and thermotaxis are two mechanisms of sperm guidance that have been demonstrated in mammals (Eisenbach and Giojalas, 2006). Chemotaxis is the movement of cells up a concentration gradient and was originally demonstrated in the mid 1960s in marine species (Eisenbach and Giojalas, 2006). In the last 12 years chemotaxis has now been shown to occur in humans (Ralt et al., 1994), frogs (al-Anzi and Chandler, 1998), mice (Giojalas and Rovasio, 1998; Oliveira et al., 1999) and rabbits (Fabro et al., 2002). Thermotaxis is the movement of cells along a temperature gradient and to date has only been demonstrated in two species; humans and rabbits (Bahat et al., 2003).

Fertilisation triggers the second meiotic division and extrusion of the 2nd PB. The paternal DNA is required for normal embryonic development and must be remodelled at fertilisation since the DNA of the mature sperm is compacted and transcriptionally inactive (McLay and Clarke, 2003). Mammalian sperm DNA differs from somatic cell DNA. It is not associated with histones or, arranged in nucleosomes. Protamines are the major basic protein found in the nuclei of mature sperm cells and are deposited onto the DNA at the end of spermatogenesis (Wouters-Tyrou et al., 1998). At fertilisation, the compacted DNA must be remodelled and the protamines replaced with histones (McLay and Clarke, 2003). Nuclear membranes, including nuclear lamin proteins, form around the maternal and paternal chromosomes, and the haploid female and male pro nuclei (PN) move toward the centre of the egg. During this migration event, DNA replication takes place.

The process by which an egg is activated without any contribution from the male genome is called parthenogenetic activation. Such activation can be caused by treatment with ethanol (Presicce and Yang, 1994), the Ca^{2+} ionophore A23187 (Kline and Kline, 1992b) and cycloheximide (Moses and Kline, 1995). In the mouse parthenogentically activated eggs will die on day 9-10 once the blastocyst stage has been reached. No normal development will occur from parthenogenetically activated embryos. The reason for this seems to be the requirement of the embryo for the paternal chromosomes. Parthenogenetic mouse embryos that do implant are severely growth retarded at day 9.5 due to a defect in extraembryonic tissue formation and most embryos die prior to

birth (McGrath and Solter, 1984; Surani et al., 1984). The embryo seems to require one set of chromosomes that have undergone the imprinting stage in both the male and female germ lines. Despite these results, one live birth from over 400 parthengenetically activated mouse embryos has been reported as a result of manipulating the expression of appropriate imprinted genes (Kono et al., 2004), which emphasises the importance of maternal and paternal imprinted genes.

Imprinted genes are genes where expression is determined by the parent that contributed them. Imprinted genes violate the usual rule of inheritance in that both alleles in a heterozygote are equally expressed. Imprinting begins in the gametes where the allele that is destined to become inactive in the new embryo (either mother or father allele) is marked. The marker has been demonstrated to be methylation of the DNA in the promoter(s) of the gene (Kaneda et al., 2004). The methylation of the promoter site prevents the binding of transcription factors to the promoter and hence shuts down gene expression. Either the maternal allele is exclusively expressed because the fathers is imprinted, or, vice versa. Gene imprinting therefore, means that both parents do not contribute methylated genes and hence explains why parthenogenetic activation of eggs fails to produce a viable embryo.

1.3.2 Zona Pellucida Structure

The ZP is a translucent, extracellular, glycoprotein matrix that surrounds the oocyte (Florman and Wassarman, 1985). This structure is secreted during folliculogenesis and persists throughout the pre-implantation stage of pregnancy. During fertilisation the ZP is the site where sperm egg

recognition occurs and where spermatozoa become activated. During fertilisation the penetrating sperm will undergo the acrosome reaction when it comes in contact with the ZP (Bleil and Wassarman, 1983) (Fig. 1.4). The acrosome is a secretory vacuole like structure that is present in the sperm head, and it is this structure that fuses with the plasma membrane (PM) of the sperm head. The acrosome reaction causes the release of various hydrolytic enzymes that are essential for the sperm to fertilise an egg (Wassarman and Mortillo, 1991). Loss of the acrosome and its visible contents occur prior to the sperm head making its way through the ZP. The ZP plays a vital role in preventing more than one sperm penetrating an egg (polyspermy). The ZP also provides protection for the fertilised egg during its passage through the uterine cavity.

Fig. 1. 4 Diagram of the acrosome reaction

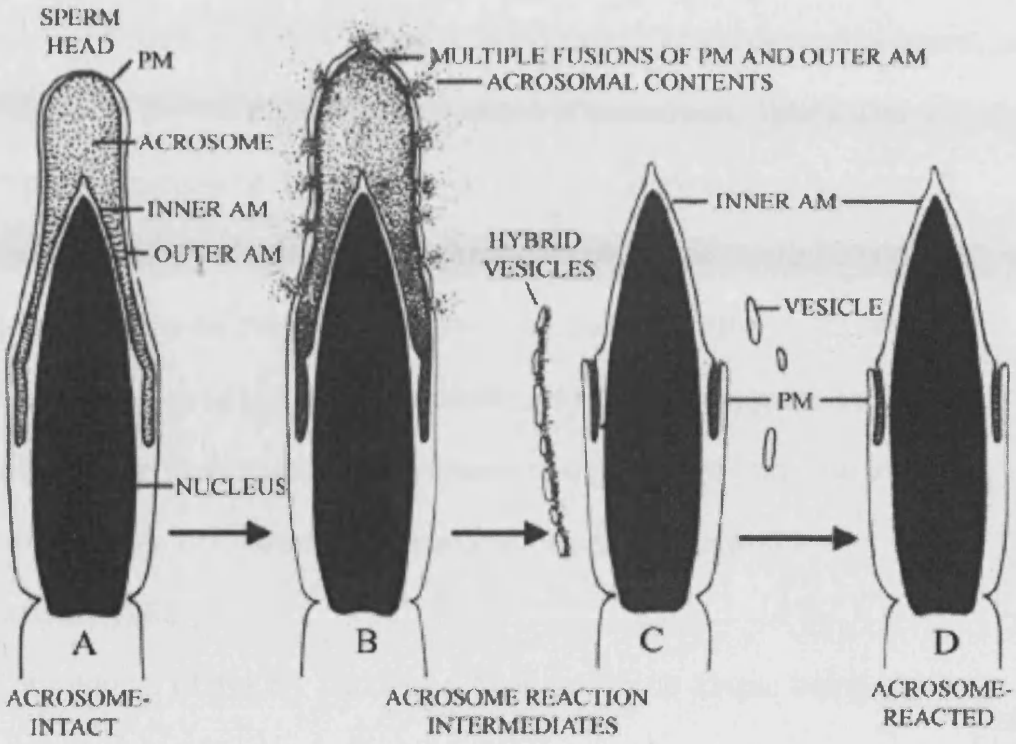

Fig. 1.4 This diagram is showing a mouse sperm undergoing the acrosome reaction. (Drawing by R. Yanagimachi taken from Wassarman et al., 2005)

The mammalian ZP has 3 or 4 major glycoproteins (ZP1-4) and they are named in order of decreasing molecular weight. The major glycoprotein structure of the ZP that is recognised by the sperm has been identified as ZP3 (MW 83kDa in the mouse) (Wassarman, 1988). The glycoprotein structure of ZP3 is highly conserved in evolutionary terms. It exhibits a homology of around 60% between amino acid sequences of species as diverse as the mouse and human. However, the sperm egg recognition process is still species specific and this is thought to be controlled by the carbohydrate side chains of the ZP3 protein, and in particular, a class of O-linked oligosaccharides (Florman and Wassarman, 1985).

Hardening of the ZP, which results in sperm no longer being able to bind or penetrate the egg, normally occurs 2-3 hours following sperm activation. The proteolytic cleavage of ZP2 (MW 120 kDa in the mouse) is thought to account for ZP hardening (Moller and Wassarman, 1989). Modification of the oligosaccarides side chains of ZP3, by glycosides in the cortical granules, results in loss of ZP3 activity and, hence its ability to induce the acrosome reaction (Wassarman, 1991). The sperm that successfully penetrates the egg becomes immotile as it is incorporated into the egg. All of the sperm, including the tail, are drawn into the eggs cytoplasm. The mid-piece of the sperm contributes paternal centrioles and mitochondria to the zygote; however, the sperm's mitochondria will be destroyed by the oocyte, as discussed later (section 1.6.5).

1.3.3 Embryo Development

The development of a fertilised early embryo proceeds via a series of mitotic divisions. The cytoplasm of the fertilised egg will be divided into numerous smaller, nucleated undifferentiated cells, called blastomeres. During the cleavage divisions, the cytoplasmic volume of the embryo does not increase; rather, the cytoplasmic volume is divided increasingly into smaller cells. In the mouse the 1st embryonic cell division begins about 17-20 hours after fertilisation. The zygote is divided in half (2-cell), then quarters (4-cell), then eighths (8-cell) and so on (Hogan et al., 1986).

Up to the mid two cell stage (~27 hours after fertilisation) the embryo appears to rely largely upon protein and RNA synthesised during oogenesis. By the mid-two cell stage many embryonic genes are switched on. *In vivo*, the 2nd cleavage begins 46-54 hours post fertilisation and typically, the embryo will reach the 8-cell stage by 60 hours. Formation of the compacted morula occurs by 60-75 hours and then blastocyst formation will occur 84-96 hours post fertilisation (Hogan et al., 1986). In mice transcription by RNA polymerase II is observed in the late 1 cell embryo, initially from the male PN (Aoki et al., 1997; Bouniol et al., 1995).

1.4 Calcium (Ca^{2+})

1.4.1 A universal intracellular messenger

Ca^{2+} plays an important role in a vast array of cellular processes such as gene transcription, muscle contraction and cellular proliferation. When Ca^{2+} levels are elevated in the cytosolic compartment it can diffuse into

the nucleus (Bootman et al., 2000), or be sequestered into the mitochondria (Montero et al., 2000). The Ca^{2+} concentration within a cell is controlled by channels located on the PM that regulates the supply of extracellular Ca^{2+} as well as channels located on the endoplasmic reticulum (ER) and sacroplasmic reticulum (SR) (Berridge et al., 2000). Ca^{2+} is removed from the cytosol by Ca^{2+}ATPases on the PM, ER/SR and the Na^{+}/Ca^{2+} exchanger. Mitochondria also play an important role in regulating cytosolic Ca^{2+} levels. Resting Ca^{2+} levels in a cellular environment are typically ~100 nM (Bootman et al., 2001). When cells are stimulated by a Ca^{2+} ionophore or, depolarisation cytosolic Ca^{2+} levels can increase to more than 1 μM (Bootman et al., 2001).

Many different types of Ca^{2+} influx channels exist and are grouped according to their activation mechanism. Voltage operated Ca^{2+} channels (VOCCs) are largely present in excitable cells (e.g. muscle and neuronal cells). Such channels are activated via depolarisation of the PM. Receptor operated Ca^{2+} channels (ROCCs) are activated by an agonist binding to the extracellular domain of the channel and are particularly present on secretory cells at nerve terminals. Store operated Ca^{2+} channels (SOCCs) are activated in response to a decrease in intracellular Ca^{2+} stores.

Ca^{2+} release from intracellular stores is mediated by many distinct types of messenger-activated channels. When hormones and/or growth factors bind to specific receptors on the PM, a PLC becomes activated which leads to the hydrolysis of phosphatidylinositol 4,5 bisphosphate (PIP_2) to produce inositol 1,4,5 trisphosphate ($InsP_3$) and diacylglycerol

(DAG). $InsP_3$ diffuses freely in the cytoplasm and acts on $InsP_3$ receptors ($InsP_3Rs$) that are present on the ER and SR to induce a conformational change of these receptors to release Ca^{2+} into the cytosol. $InsP_3Rs$ have a total molecular mass of ~1200 kDa; these large structures are made from 4 subunits (Bootman et al., 2001). $InsP_3R$ activation is also regulated by the Ca^{2+} concentration at their cytosolic surface (Bootman and Lipp, 1999). A Ca^{2+} level of 0.5-1 µM will enhance the receptors function, whereas Ca^{2+} concentrations higher than 1 µM will inhibit their opening. $InsP_3Rs$ are almost ubiquitously expressed in mammalian tissues.

Ryanodine receptors (RyRs) are structurally and functionally similar to $InsP_3Rs$ and are named due to their high affinity for the plant alkaloid ryanodine. However, RyRs have about twice the conductance and molecular mass of the $InsP_3Rs$ (Franzini-Armstrong and Protasi, 1997). Like $InsP_3Rs$, RyRs are highly sensitive to cytosolic Ca^{2+} concentrations, however, they generally require higher Ca^{2+} concentrations to be activated (1-10 µM) and inhibited (>10 µM) (Bootman et al., 2001). RyRs are mostly present in excitable tissues such as muscle and neurons (Bennett et al., 1996).

Mitochondria can also be considered as a Ca^{2+} store. Mitochondria have a large capacity for Ca^{2+} uptake and can also significantly buffer cytosolic Ca^{2+} rises (Montero et al., 2000). Mitochondria sequester Ca^{2+} by a low affinity, high speed uniporter that is driven by the membrane potential of the mitochondria and by high Ca^{2+} levels. Mitochondria are proposed to be located in close proximity to the ER. This has led to the

suggestion that $InsP_3$ induced release of Ca^{2+} exposes the mitochondrial Ca^{2+} uniporter to around 20 fold higher Ca^{2+} concentrations than those Ca^{2+} concentrations in the bulk of the cytosol (Csordas et al., 1999). Increasing Ca^{2+} within the mitochondria activates the enzymes that are involved in the TCA cycle which leads to an enhanced production of ATP synthesis (Hajnoczky et al., 1995). The Ca^{2+} accumulated by the mitochondria is released via the Na^+ dependent exchanger which performs at a significantly slower rate than the uniporter.

1.4.2 Intracellular Ca^{2+} releasing agents

$InsP_3$ is produced via the action of hydrolysis of PIP_2 by a PLC. Although produced at the PM, $InsP_3$ is a highly diffusible molecule that can rapidly pass through the cytoplasm of cells (Allbritton et al., 1992). Once produced, $InsP_3$ has a lifetime of seconds inside the cell before it is metabolised by enzymes that add or remove a phosphate group to terminate the Ca^{2+} releasing ability of $InsP_3$ (Berridge et al., 2000). The addition of a phosphate group to $InsP_3$ produces inositol 1,3,4,5 tetrakisphosphate ($InsP_4$) that has been shown to bind a small GTPase activating protein of the RAS family that modulates Ca^{2+} release (Cullen, 1998).

Cyclic adenosine disphosphate ribose (cADPR) activates RyRs and therefore, releases Ca^{2+}. The Ca^{2+} releasing effect of cADPR was first identified in sea urchin eggs (Bootman et al., 2001). This Ca^{2+} releasing agent has been shown not to be effective in mouse eggs (Kline and Kline, 1994). Nicotinic acid adenine dinucleotide phosphate (NAADP) emerged as another candidate for an intracellular messenger (Genazzani

and Galione, 1997). Its Ca^{2+} releasing properties have been demonstrated in sea urchin, starfish and ascidian oocytes (Albrieux et al., 1998; Chini et al., 1995; Lee et al., 1989; Santella et al., 2000), plants (Navazio et al., 2000), human heart cells (Bak et al., 2001) and kidney cells (Cheng et al., 2001). NAADP response is sensitive to the L-type channel antagonist verapamil and insensitive to the Ca^{2+}ATPase inhibitor thapsigargin (Albrieux et al., 1998). Such demonstrations were performed in ascidian oocytes but the NAADP response appears to be inactive in causing Ca^{2+} release in mammalian oocytes (Swann K; Galione A, unpublished).

1.4.3 Ca^{2+} change at fertilisation

One of the most important cellular processes that Ca^{2+} is responsible for is the stimulation of egg activation at fertilisation. An intracellular rise in Ca^{2+} at fertilisation, is a crucial event in activation in plants, animals and non-mammalian species respectively (Digonnet et al., 1997; Jaffe, 1983; Zucker et al., 1978). In many eggs, this increase in Ca^{2+} is initiated as soon as the sperm penetrates the egg. This Ca^{2+} signal then propagates through the entire egg (Stricker, 1999). In mammals, the Ca^{2+} wave crosses the egg in ~2 sec. In echinoderm eggs (diameter ~0.1 mm) and frog eggs (diameter ~1 mm), the Ca^{2+} wave crosses the egg in ~20 sec and several min, respectively (Whitaker, 2006). In sea urchin eggs the Ca^{2+} wave at fertilisation occurs in Ca^{2+} free media demonstrating that the Ca^{2+} increase comes from the eggs internal stores (Crossley et al., 1988; Schmidt et al., 1982). This has also been demonstrated in mouse eggs,

where the first Ca^{2+} transient still occurs when extracellular Ca^{2+} levels are reduced (Jones et al., 1998b).

The idea of Ca^{2+} being responsible for egg activation arose in the early 1930s from experiments inducing artificial activation. Later experiments showed that the Ca^{2+} ionophore A23187 could activate sea urchin, starfish, toad and hamster eggs (Steinhardt et al., 1974). A large Ca^{2+} increase was recorded at fertilisation in medaka fish and sea urchin eggs using the Ca^{2+} binding luminescence protein aequorin (Whitaker, 2006). Subsequently aequorin was also used to detect a Ca^{2+} wave at fertilisation in the sea urchin, starfish, ascidian and zebrafish egg (Whitaker, 2006). Aequorin was also used to demonstrate changes in Ca^{2+} in mouse eggs (Cuthbertson and Cobbold, 1985; Cuthbertson et al., 1981). Also, a series of hyperpolarisations were demonstrated at fertilisation in hamster eggs suggesting a series of Ca^{2+} oscillations occur in mammals at fertilisation (Miyazaki and Igusa, 1981) because each hyperpolarisation represented an increase in Ca^{2+}-activated potassium (K^+) conductance.

However, some eggs, like those of the marine worm, Urechis caupo (Echiura), do not exhibit Ca^{2+} waves. Instead, they exhibit Ca^{2+} rises simultaneously around the egg cortex and peaks slightly larger in the nucleoplasm (Stephano and Gould, 1997). In most non-mammalians like frogs and sea urchins, the Ca^{2+} signal at fertilisation occurs in the form of a monotonic intracellular Ca^{2+} rise. During fertilisation in some species, it is not the sperm that causes the Ca^{2+} increase. For example, in the zebrafish and brine shrimp the Ca^{2+} rise is induced by ovulation or

contact with pond, or, sea water respectively (Lee et al., 1992; Lindsay and Clark, 1992; Lindsay et al., 1992).

1.4.4 Ca^{2+} Oscillations at Fertilisation

In many eggs such as those from the nemertean worm *Cerabratulus lacteus* (Stricker, 1996), the polychaete worm *Chaetopterus* (Eckberg and Miller, 1995), ascidians (Speksnijder et al., 1989; Yoshida et al., 1998) and mammals (Cuthbertson et al., 1981; Miyazaki et al., 1986). The Ca^{2+} spikes occur separately with an interval in between them. In asicidans, Ca^{2+} oscillations have been shown to follow MPF activity (McDougall and Levasseur, 1998). Ca^{2+} oscillations in ascidian oocytes occur when MPF activity in elevated and pause when MPF is low (McDougall and Levasseur, 1998). In mammalian eggs the long lasting series of Ca^{2+} oscillations persist until PN formation (Fig. 1.5) (Kline and Kline, 1992a; Marangos et al., 2003; Miyazaki et al., 1993). The first spike is distinctively longer in duration and larger in amplitude. The following spikes are lower in amplitude and shorter in duration occurring every 10 minutes (Swann and Ozil, 1994).

Fig. 1. 5 Ca^{2+} oscillations in a mouse egg

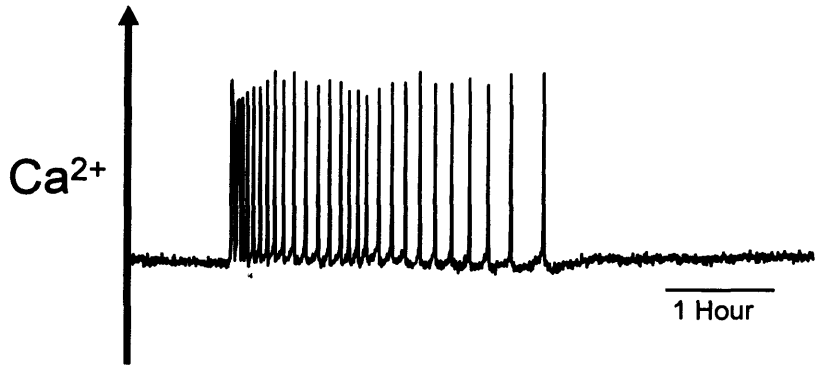

Fig 1.5 This figure shows the long lasting series of Ca^{2+} oscillations that are initiated in a mouse egg by sperm. These oscillations persist until PN formation.

The Ca^{2+} release at fertilisation is from internal stores within the egg and not from the sperm, as shown in the mouse (Jones et al., 1998b). Ca^{2+} oscillations caused by the sperm at fertilisation are both necessary and sufficient to stimulate the many events of egg activation that lead to embryo development (Kline and Kline, 1992a). These activation events include cortical granule exocytosis, changes in the pattern of protein synthesis, and meiotic resumption (Ozil et al., 2005). Inhibition of oscillations by the action of the Ca^{2+} chelator BAPTA-AM blocks egg activation (Kline and Kline, 1992a). Additionally, premature blockage of these oscillations have been shown to inhibit PN formation and, therefore, further development (Lawrence et al., 1998).

Repetitive Ca^{2+} spikes at fertilisation are required to degrade MPF (see next section for full explanation) successfully (Ducibella et al., 2002). If the number of Ca^{2+} spikes are insufficient to cause MPF degradation, eggs remain arrested at metaphase III after formation of the 2^{nd} polar body and fail to form PN (Ducibella et al., 2002). A sufficient number of Ca^{2+} spikes causes the reduction of mitogen activated protein kinase (MAPK) activity and thereby leads to PN formation (Ducibella et al., 2002).

1.4.5 Maturation Promoting Factor (MPF) activity

MPF is responsible for the entry from interphase into meiosis/mitosis (Nurse, 1990) and was first described in amphibians by its ability to trigger oocyte maturation (Masui and Markert, 1971; Smith and Ecker, 1971). MPF is a complex that consists of both a regulatory protein cyclin B1 (in mammals) and a catalytic subunit CDK1 (cdk1/cyclinB). MPF

levels have been shown to remain high until fertilisation, then MPF levels decline and are maintained at a minimal level during cell cleavage (Doree and Hunt, 2002; Jones, 2004).

Cytostatic factor (CSF) is responsible for the stabilisation of MPF (Masui, 2000; Masui and Markert, 1971). CSF was first identified when the cytoplasms of eggs at the later stages of maturation were found to cause metaphase arrest in the blastomeres of zygotes (Masui and Markert, 1971). The identity of CSF remains unresolved and most characterisation has been done in the frog. CSF activity includes a signalling pathway that also involves MAPK and Rsk proteins (Masui, 2000; Murray et al., 1989; Tunquist and Maller, 2003). The *c-mos* gene is part of CSF activity (Masui, 1991; Sagata, 1997) since eggs from *c-mos* null mice are unable to remain arrested at MII and cannot be parthenogenetically activated (Colledge et al., 1994; Hashimoto et al., 1994). The c-*mos* pathway seems to contribute to CFS activity but is not solely responsible for it. CSF activity is likely to be an anaphase promoting complex/cyclosome (APC/C) inhibitor since CSF inhibits the action of the APC/C to hold the eggs at MII phase.

At fertilisation, MPF activity is inactivated by polyubiquitination of its cyclin B component, which targets it for destruction by the proteasome (Murray et al., 1989). Cyclin B is polyubiquitinated by the ubiquitin ligase activity of the APC/C which is a large 1.5 MDa multimeric protein complex (Peters, 2006). Without APC/C, cells are unable to separate their sister chromatids at anaphase which means the cell will not exit from mitosis and produce 2 daughter cells. The initiation of cyclin B proteolysis is

dependent upon APC/C associating with its coactivator Cdc20 (APC/C^{Cdc20}), this association is possible since the phosphoylation of APC/C promotes Cdc20 binding. Proteolysis of cyclin B then occurs via action of the 26S proteasome (Fig. 1.6). The activity of APC/C is kept in check by several mechanisms, the most important of these being the spindle assembly check point (SAC), which inhibits the action of APC/C^{Cdc20} to initiate anaphase until all of the chromosomes are correctly orientated. Several proteins required for functional SAC activity have been identified as members of the mitotic arrest deficient (Mad) and budding uninhibited by benzimidazole (Bud) family as well as Mpsl kinase (Shah and Cleveland, 2000).

A novel APC/C inhibitor Early Mitotic Inhibitor I (Emi1) was identified in frogs and suggested to prevent premature APC/C activity (Reimann et al., 2001a; Reimann et al., 2001b). However, due to its absence during metaphase II arrest, it is unlikely that Emi1 is the correct candidate (Ohsumi et al., 2004; Rauh et al., 2005). A protein related to Emi1, known as Emi1 related protein 1 (Erp1), or Emi2 is stable at meiosis II until fertilisation and is required to maintain CSF arrest (Schmidt et al., 2005; Shoji et al., 2006; Tung et al., 2005). Emi2 is targeted for degradation by a polo-like kinase (Plk) once it has been phosphorylated by calmodulin dependent kinase II (CaMKII) (Hansen et al., 2006; Rauh et al., 2005). Although this has only been demonstrated in frog eggs (Hansen et al., 2006; Liu and Maller, 2005; Rauh et al., 2005; Tung et al., 2005), Emi2 does appear to be significant in mammals since preventing protein synthesis of Emi2 in mouse MII eggs results in

parthenogenetic activation (Shoji et al., 2006). Additionally, it has also been shown in the mouse that Emi2 synthesis inhibition during oocyte maturation results in oocytes failing to arrest (Madgwick et al., 2006). CaMKII becomes activated by a transient increase in [$(Ca^{2+})i$] that occurs at fertilisation. This then allows Emi2 degradation to occur, followed by the subsequent activation of APC/C^{Cdc20} and hence degradation of cyclin B (Madgwick et al., 2006).

Fig. 1. 6 MPF regulation in an unfertilised and fertilised egg

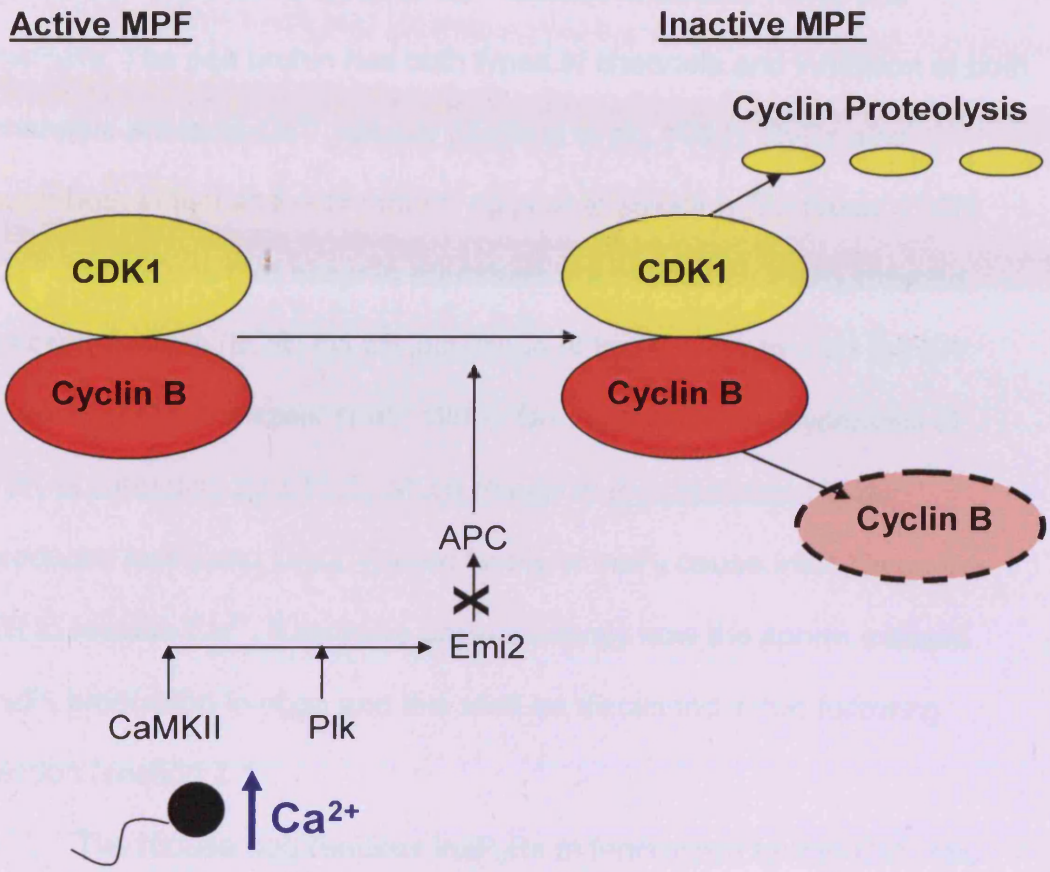

Fig. 1.6 Schematic diagram of active MPF at MII arrest and inactive MPF during fertilisation. Sperm produces an increase in Ca^{2+} that activates both CaMKII and Plk1 that both phosphorylate Emi2. Degradation of Emi2 activates APC activity and hence drives the break down of MPF.

1.4.6 Ca^{2+} Oscillations and the $InsP_3$ pathway

On the ER there are 2 types of Ca^{2+} release channels: RyRs and $InsP_3Rs$. The sea urchin has both types of channels and inhibition of both channels prevents Ca^{2+} release (Galione et al., 1993). RyRs also contribute in fish and echinoderm eggs at fertilisation (Whitaker, 2006). Ca^{2+} oscillations that occur in mammals are caused by $InsP_3$ induced calcium release (IICR) via the activation of $InsP_3$ receptors on the ER (Carroll, 2001; Miyazaki et al., 1993). During fertilisation hydrolysis of PIP_2 is catalysed by a PLC, which results in the production of two products, $InsP_3$ and DAG. Raised levels of $InsP_3$ cause $InsP_3Rs$ on the ER to release Ca^{2+}. It remains unclear exactly how the sperm initiates $InsP_3$ production in eggs and this shall be discussed in the following section (section 1.5).

The mouse egg requires $InsP_3Rs$ at fertilisation for the Ca^{2+} rise suggesting that the phosphoinositide (PI) turnover is essential at fertilisation (Miyazaki et al., 1993; Miyazaki et al., 1992). The increase in Ca^{2+} at fertilisation can be inhibited by microinjection of antibodies that inhibit the $InsP_3Rs$ (Miyazaki et al., 1993; Miyazaki et al., 1992). Downregulation of $InsP_3Rs$ has been demonstrated to inhibit Ca^{2+} release in mouse eggs (Brind et al., 2000; Jellerette et al., 2000), therefore, it has been proposed to partly explain the cessation of Ca^{2+} oscillations 3-4 hours after fertilisation.

1.5 Sperm Factor

1.5.1 How does a sperm fertilise an egg?

$InsP_3$ is produced by the hydrolysis of PIP_2 via the action of a PLC: the phosphatidylinositol pathway. There have been 3 main models to explain Ca^{2+} release via the action of the sperm (Fig. 1.7). The receptor theory (Fig. 1.7a) suggests that Ca^{2+} oscillations are initiated via a signal transduction pathway that involves the interaction of a sperm ligand to a receptor that is situated on the PM of an egg (Foltz and Shilling, 1993; Schultz and Kopf, 1995). Although there are surface proteins that mediate sperm-egg binding there is no direct evidence to suggest they are linked to intracellular signalling (Runft et al., 2002). In sea urchins there is an increase in $InsP_3$ turnover during fertilisation (Ciapa and Whitaker, 1986) and a receptor was thought to cause the activation of an egg PLC that, in turn, caused PIP_2 hydrolysis and $InsP_3$ induced Ca^{2+} oscillations. The egg receptor was thought to be coupled to a tyrosine kinase of a G protein signalling pathway which triggers the Ca^{2+} release inside the egg. Antibodies to the Gq family of G proteins have been unable to prevent the sperm induce Ca^{2+} release at fertilisation (Williams et al., 1998). The most convincing evidence to challenge the receptor theory came from intra-cytoplasmic sperm injection (ICSI). This process bypasses the interaction of the sperm and egg, but still results in successful egg activation and development (Kimura and Yanagimachi, 1995).

The Ca^{2+} conduit hypothesis (Fig. 1.7b) describes a mechanism by which sperm acts as a channel (or pipe) allowing a flow of extracellular

Ca^{2+} into the egg via pores in the sperm membrane (Jaffe, 1991). The Ca^{2+} conduit hypothesis in an example of Ca^{2+} induced Ca^{2+} release (CICR). This is supported by reports where egg fusion occurred before the Ca^{2+} oscillations began (Lawrence et al., 1997; McCulloh and Chambers, 1992). Further, Ca^{2+} injected into fish and frog eggs produced a Ca^{2+} transient (Nuccitelli, 1991). However, in mammals injection of Ca^{2+} did not produce Ca^{2+} oscillations, only a single transient (Swann and Ozil, 1994).

The sperm factor theory describes a mechanism by which a sperm factor is responsible for fertilisation induced Ca^{2+} oscillations (Swann, 1990; Swann and Ozil, 1994). At fertilisation the PM of the sperm head and the egg fuse together, suggesting a soluble factor from the sperm could be released into the egg to induce activation. Injection of hamster sperm extracts into eggs caused Ca^{2+} oscillations similar to those seen at fertilisation (Swann, 1990; Swann and Ozil, 1994). This data led to the proposal of the sperm factor theory in which a soluble cytosolic factor in the sperm is introduced into the egg cytoplasm and initiates Ca^{2+} oscillations (Fig. 1.7c). The sperm factor hypothesis explains many of the observations that could not be explained by the Ca^{2+} receptor and conduit theory. Injection of sea urchin extracts into unfertilised sea urchin eggs produced signs that a Ca^{2+} increase had occurred (Dale et al., 1985). This result never been repeated in the sea urchin, but it does suggest that fertilisation could occur successfully without any sperm-egg surface interaction.

The sperm factor theory appears to be consistent across species. Pig sperm extracts have been shown to cause Ca^{2+} oscillations in cow and mouse eggs (Wu et al., 1997). Also, hamster and cow sperm extracts can both induce oscillations in the hamster egg (Swann, 1990). Further evidence includes the ability of non-mammalian sperm extracts, taken from xenopus or, chicken to induce Ca^{2+} oscillations in the mouse, or, cow (Dong et al., 2000). Furthermore, sperm extracts taken form the fish are also able to induce Ca^{2+} oscillations in mouse eggs (Coward et al., 2003). Mammalian (pig) sperm extracts can also induce Ca^{2+} oscillations in non-mammalian eggs (nemertean worm) (Stricker et al., 2000). Interestingly, however , worm extracts do not induce Ca^{2+} oscillations in mammals (Stricker et al., 2000).

Fig. 1. 7 Three hypotheses for a Calcium increase at fertilisation

A) Receptor Theory

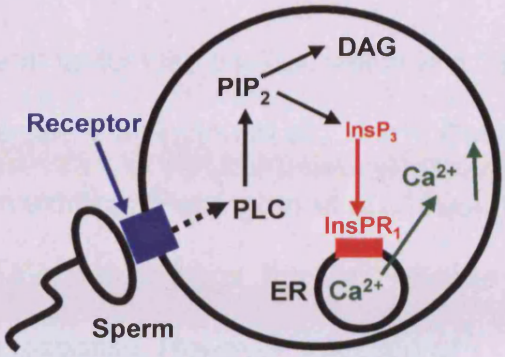

B) Ca^{2+} Conduit Theory

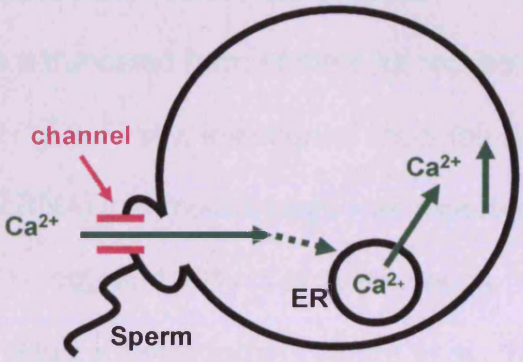

C) Sperm Factor Theory

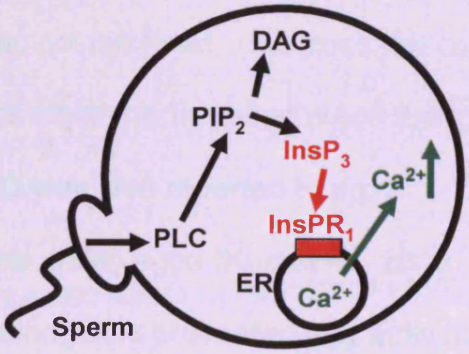

Fig. 1.7 Schematic diagram showing the three main hypotheses for how sperm initiates Ca^{2+} transients in eggs at fertilisation.

1.5.2 Search for the Sperm Factor

A potential candidate for the sperm factor was oscillin, which is a 33 kDa glucosamine-6-phosphate isomerase (Parrington et al., 1996). Oscillin was purified from hamster sperm extracts (Parrington et al., 1996). When this purified extract was injected into mouse eggs, the Ca^{2+} release correlated with a fertilisation like response. However, injection of recombinant oscillin failed to cause Ca^{2+} oscillations (Wolosker et al., 1998), suggesting oscillin may not be the correct sperm factor.

Other candidates include a truncated form of the c-kit receptor called tr-kit and also nitric oxide (NO). Firstly, injection of recombinant tr-kit, or its complementary RNA (cRNA) into mouse eggs was reported to be able to successfully activate an egg and 30% of activated eggs successfully reached the 2-cell stage of development (Sette et al., 1997). There was, however, no evidence to suggest that tr-kit could mimic Ca^{2+} oscillations like those caused by the sperm (Sette et al., 1997). Also, tr-kit was present in the sperm mid-piece, not the head. This does not correlate with the sperm factor characteristics since it is the head piece that causes activation of an egg during ICSI. NO was also reported to produce Ca^{2+} oscillations and egg activation in sea urchin eggs (Kuo et al., 2000). Although the NO scavenger oxyhaemoglobin prevented egg activation in the sea urchin, it fails to meet other criteria as a potential candidate for the sperm factor since mouse and ascidian eggs did not show that Ca^{2+} oscillations were associated with NO (Hyslop et al., 2001).

The identification of the sperm factor has been investigated by isolation and purification of sperm extracts. Since the PI pathway appears

to be responsible for Ca^{2+} release at fertilisation, PLCs are obvious candidates for the sperm factor and several are known to be expressed in mammalian sperm, including PLC beta (β)1, gamma (γ)1, γ2, delta (δ)1 and δ4 (Dupont et al., 1996; Lee and Rhee, 1996; Mehlmann et al., 1998). Evidence for a sperm derived PLC has been shown in experiments where depletion of PIP_2 with a bacterial PLC in sea urchin egg homogenates prevents sperm, but not $InsP_3$, from producing Ca^{2+} release. The sperm response is recovered with the homogenate receiving exogenous PIP_2 (Jones et al., 1998a). Additionally, pre-incubation of mouse eggs in U73122, a PIP_2-PLC inhibitor, blocks sperm induced Ca^{2+} oscillations (Dupont et al., 1996). However, recombinant forms of PLCβ1, γ1, γ2, and δ1 all failed to mimic the pattern of Ca^{2+} oscillations seen at fertilisation that are caused by sperm and sperm extracts (Jones et al., 2000).

Recently, a novel PLC, PLCζ, was identified that is specifically expressed in sperm (Saunders et al., 2002). Microinjection of cRNA, encoding this novel PLC, into mouse eggs produced fertilisation like Ca^{2+} transients. Additionally, the Ca^{2+} oscillation inducing activity of sperm extracts is lost when PLCζ activity is immonudepleted (Saunders et al., 2002; Swann et al., 2004). The amount of PLCζ required to initiate Ca^{2+} oscillations correlated with the approximate content of PLCζ in one sperm (20 -50 fg) (Saunders et al., 2002). Microinjection of PLCζ caused activation and development to blastocysts with success rates similar to IVF rates. Human and monkey (*simian*) PLCζ can also stimulate activation and development of mouse eggs to the blastocyst stage (Cox

et al., 2002). PLCζ is also present in non-mammalian vertebrates, e.g. the domestic chicken (*gallus gallus*) suggesting that PLCζ could be conserved in other non mammalian vertebrates (Coward et al., 2005). The recombinant form of chicken PLCζ cRNA is able to cause Ca^{2+} oscillations when it is microinjected into mouse eggs (Coward et al., 2005). Fig 1.8 compares the structure of all known PLCs to highlight the difference between PLCζ and other PLCs.

Fig. 1. 8 Diagram showing the structure of PLCs

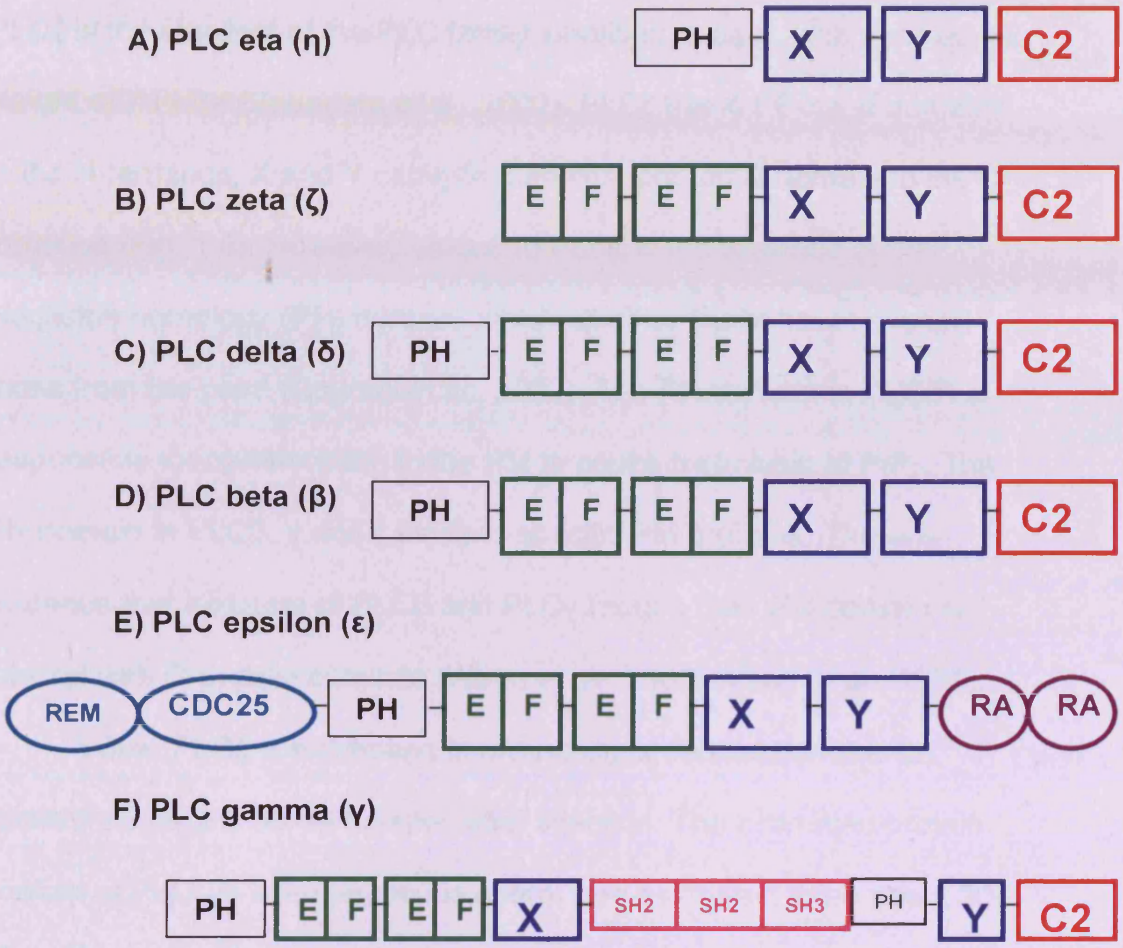

Fig. 1.8 Schematic diagram and comparison of the different domains in all known PLCs. The plecktrin homology (PH) domain targets the PLC to membrane bound proteins. The X and Y are the catalytic domains. The C terminal domain (C2) is a lipid binding domain, while the EF hands bind Ca^{2+}. Scr homology (SH) domains bind to phoshorylated tyrosine residues in target proteins. Cell division cycle 25 (CDC25) and ras exchanger motif (REM) domains catalyse guanosine diphosphate (GDP) to guanosine diphosphate (GTP) and their activity is regulated by Ras associating (RA) domains. See text for details.

1.5.3 PLCζ

PLCζ is the smallest of the PLC family identified to date, with a molecular weight of 70 kDa (Saunders et al., 2002). PLCζ has 4 EF-hand domains in the N-terminus, X and Y catalytic domains, and a C2 domain in the C-terminus (Fig. 1.8). However, unique to PLCζ is the absence of the pleckstrin homology (PH) domain, which all other PLCs have; except those from the plant (Coursol et al., 2002). The PH domain in PLCδ1 is responsible for translocation to the PM to cause hydrolysis of PIP_2. The PH domain in PLCβ, γ and ε binds to specific PM proteins. There is evidence that isoforms of PLCβ and PLCγ require their PH domain to interact with G-protein subunits (Wang et al., 2000; Wang et al., 1999).

When PLCζ is expressed in mouse eggs, fertilisation like Ca^{2+} oscillations begins 30-40 minutes after injection. The estimated protein content of PLCζ in a single mouse sperm was estimated to be about 20-50 fg (Saunders et al., 2002). PLCζ is similar to PLCδ1, it shares 38% identity and 49% homology in 647 residues of PLCζ, despite the absence of the PH domain (Miyazaki and Ito, 2006). Other types of PLCζ that do not to contain the PH domain include; human, monkey, chicken and rat (Coward et al., 2005; Cox et al., 2002).

The mechanism of action of PLCζ remains unknown since, unlike other PLCs, it lacks a regulatory domain such as the G protein binding site of PLCβ, or, the SH domain of PLCγ for phosphorylation by protein tyrosine kinase (PTK). PLCζ has Ca^{2+} activity at levels as low as 10 nM and 70% maximal activity at 100 nM Ca^{2+} (Kouchi et al., 2004). The EC_{50} for PLCζ and PLCδ 1 are 52 nM and 5.7 μM, respectively.

1.6 Metabolism and Fertilisation

1.6.1 Metabolism

ATP contains high energy phosphate bonds and is used to transport energy to cells for processes that include muscle contraction and enzymatic metabolism. ATP produces energy when it is hydrolysed into adenosine disphosphate (ADP). Aerobic oxidation occurs in nearly all cells and is the process that drives the production of ATP. In aerobic oxidation, fatty acids and sugars, principally glucose, are metabolised to carbon dioxide (CO_2) and water (H_2O). The energy released from this reaction is converted to the chemical energy of phosphoanhydride bonds in ATP. The oxidation of glucose is called glycolysis and the initial steps of this process, which do not require oxygen, occur in the cytosol. The latter stages of aerobic oxidation, which do require oxygen, occur in the mitochondria and these stages are referred to as the oxidative phosphorylation process. Glycolysis produces a small amount of ATP (4 molecules) and the 3-carbon compound pyruvate (2 molecules). Pyruvate is then transported into the mitochondria where it is generated into CO_2, in the process producing a large amount of ATP (~30molecules).

Pyruvate is transported into the mitochondria of a cell and it is converted into acetyl CoA, this conversion results in the oxidation of nicotinamide adenine dinucleotide (NAD^+) to NADH. Fatty acids are also transported into the mitochondria where they are also converted to acetyl CoA, producing NADH and oxidising flavin adenine dinucleotide (FAD^{++}) to $FADH_2$ (discussed in next section).

1.6.2 Mitochondria

Mitochondrial organelles were first described in 1881 (Ernster and Schatz, 1981) and have a very distinctive structure (Figure 1.9). Mitochondria contain their own DNA and are able to replicate independently from the nuclear cell cycle. The cytoplasm is bound by two membranes termed the inner and outer mitochondrial membranes. The inner membrane is the more impermeant of the two membranes and therefore, is the main barrier.

The TCA cycle and the respiratory transport chain are the most important enzymatic components of the mitochondria and are responsible for breaking down the carbon substrates acetyl CoA to produce CO_2 (Duchen, 2004; Dumollard et al., 2007). This process also results in the reduction of NAD^+ and FAD^{++} to NADH and $FADH_2$, respectively. NADH and $FADH_2$ are intermediates that provide reducing equivalents to the respiratory chain. The respiratory chain consists of a series of enzyme systems that are referred to as complexes I through to IV. These intermediates produce a transfer of energy from a reduced to an oxidised state. From NADH, an electron is donated to complex I and from $FADH_2$, 2 electrons are donated to complex II. Both complexes then each transfer electrons to the ubiquinol cytochrome c reductase complex (complex III) (Duchen, 2004; Dumollard et al., 2007). The cytochrome c reductase complex is then responsible for shuttling electrons to complex IV, the cytochrome c oxidase complex (Arnold and Kadenbach, 1997; Follmann et al., 1998).

The chemiosmotic theory was first hypothesised in 1961 (Mitchell, 1961) and proposed that ATP synthesis came from the electrochemical gradient that was established across the inner membranes of mitochondria by using the energy of NADH and $FADH_2$. Transfer of protons from the matrix into the inner membrane space are associated with reactions of complexes I, III and IV. This transfer of protons establishes an electrochemical proton gradient which results in the membrane potential of mitochondria to be 150-180 mV, negative to that of the cytosol (Duchen, 2000). The mitochondrial membrane potential is very important for the normal function of cells as it allows the production of ATP and movement of Ca^{2+} into the mitochondria down its electrochemical gradient (Duchen, 2000; Rizzuto et al., 2000). The proton channel F_1F_0-ATP synthase (complex V) allows the influx of protons into the mitochondria. This proton influx results in depolarisation of the mitochondrial membrane and drives the enzyme to phosphorylate ADP to produce ATP (Stock et al., 1999). The newly generated ATP molecule is then transported out of the mitochondria via the adenine nucleotide translocase (ANT) (Stock et al., 1999).

Fig. 1. 9 Diagram illustrating the function of mitochondria

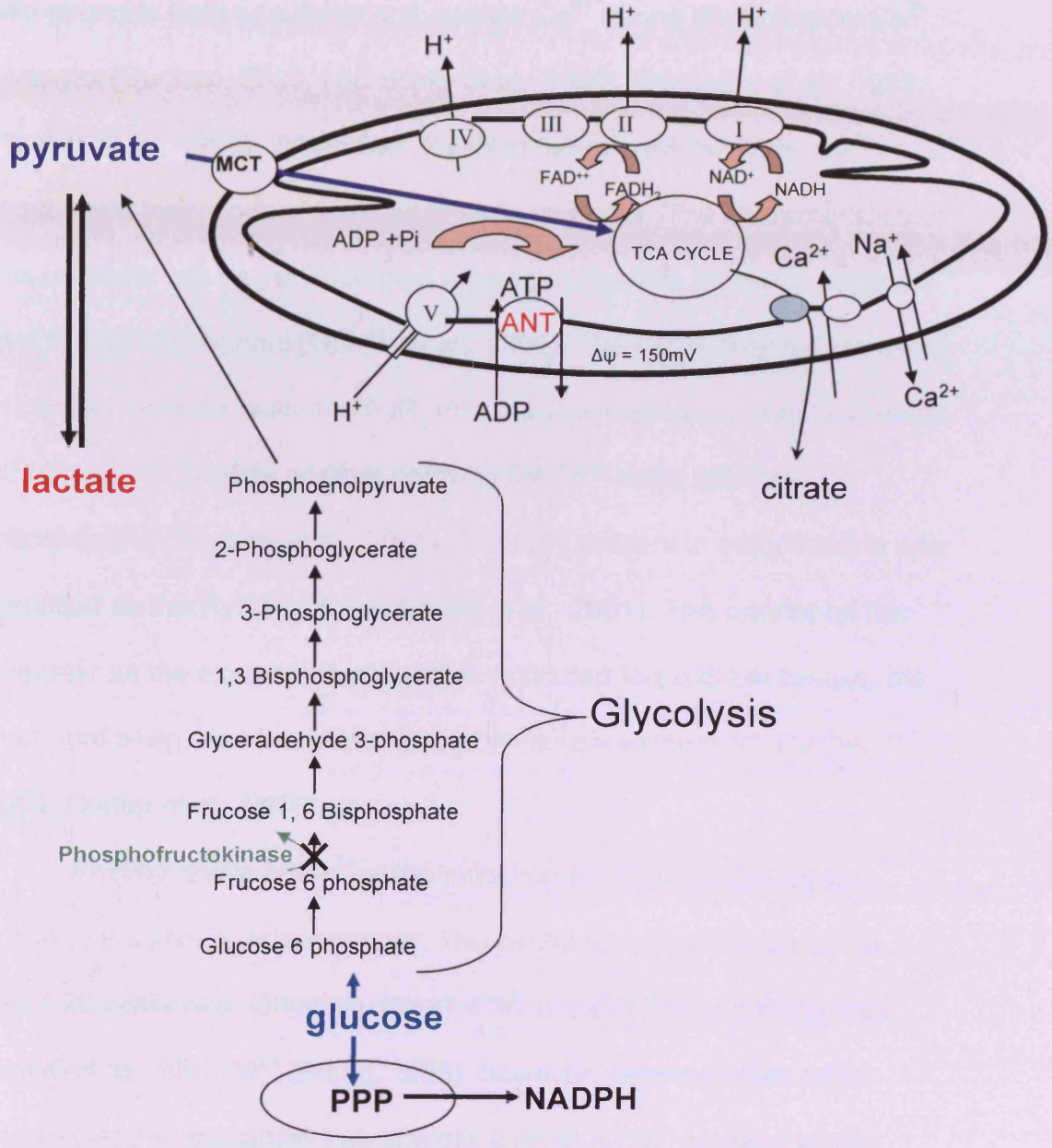

Fig. 1.9 Diagram showing the structure and processes that occur in mitochondria. Complex I is NADH dehydrogenase; complex II is succinate dehydrogenase; complex III is cytochrome c reductase and complex IV is cytochrome c oxidase. Complex V is the F_1F_0 ATPase that allows an influx of protons to produce ATP from ADP (see text). Glycolysis produces pyruvate which feed into the TCA cycle, however in eggs glycolysis is switched off due to a block at the phosphofructokinase level.

1.6.3 Mitochondria and Ca^{2+}

Mitochondria both sequester and release Ca^{2+} during physiological Ca^{2+} changes (Duchen, 2000; Hajnoczky et al., 1999; Hajnoczky et al., 1995; Rizzuto et al., 1992). When Ca^{2+} levels in the cytosol increase, Ca^{2+} moves into the mitochondrial matrix via a uniporter. The characteristics of this uniporter are as yet undefined although collective evidence suggests that it is an ion channel (Gunter et al., 2000). The CICR channel identified in cardiac muscles cells, the RyR, may also be expressed in mitochondria and therefore, provide another pathway for Ca^{2+} entry into the mitochondria (Beutner et al., 2001). The RyR present in mitochondria was identified as the RyR1 isoform (Beuter et al., 2001). This cannot be the uniporter as the expression of RyR1 is restricted to excitable tissues, the heart and brain, and the uniporter is ubiquitously expressed (Duchen, 2004; Gunter et al., 2000).

Resting levels of Ca^{2+} in the mitochondria are kept low by the action of the xNa^{+}/Ca^{2+}exchanger. This exchanger was first identified about 20 years ago. Originally the stoichiometry of the exchanger was identified as $2Na^{+}/Ca^{2+}$ (Brand, 1985), however, recent studies have shown that the exchanger can operate against a Ca^{2+} gradient whose energy is twice that of the Na^{+} gradient (Jung et al., 1995). Thus, recently a stoichiometry of $3Na^{+}/ Ca^{2+}$ has been defined (Jung et al., 1995).

1.6.4 Mitochondrial distribution in eggs

In somatic cells mitochondria commonly take the form of elongated double-walled sacs with cristae, which are formed by the infolding of the

inner membrane. However, in mouse (Dumollard et al., 2004) and human (Motta et al., 2000) eggs mitochondria are more spherical in shape and contain few cristae, which are more flattened against the wall of the mitochondria (Shepard et al., 2000; Trimarchi et al., 2000).

Estimates of mtDNA copy number in eggs is between 150000-300000 and 150000-800000, for sea urchin (Soukhomlinova et al., 2001) and mammals (Cummins, 2004; Poulton and Marchington, 2002), respectively. Mitochondrial replication begins at oogenesis and halts at the end of maturation. The oocyte has an increase in mitochondria from about 10 mitochondria per human PMGC, to several hundred thousand in a mature oocyte (Poulton and Marchington, 2002). Before it is fertilised, the mitochondria in the egg are capable of supporting the egg through fertilisation until blastocyst stage. The egg can still be successfully fertilised and develop to blastocyst stage during inhibition of mtDNA replication or translation (Huo and Scarpulla, 2001; Piko and Chase, 1973).

Before maturation, mitochondria in the mouse and human oocyte are located in the large nucleus known as the GV where they concentrate in one or several clusters (Jansen, 2000). In the mouse oocyte, mitochondria accumulated around the GV move away from the nuclear region towards the animal pole, this occurs during formation and migration of the first meiotic spindle (Nishi et al., 2003). In the mature mouse egg arrested at metaphase II, mitochondria are situated in the centre of the egg and around the meiotic spindle (Calarco, 1995). Early during maturation, mitochondria are found in clusters in close proximity to

the ER (Roegiers et al., 1999). This close positioning of these two structures supports the hypothesis that functional interactions exists between these two organelles (Roegiers et al., 1999).

1.6.5 Mitochondria and Fertilisation

Ca^{2+} oscillations at fertilisation stimulate the mitochondria (Dumollard et al., 2003; Schomer and Epel, 1998). Recordings demonstrated an increase in oxygen (O_2) consumption that reached a peak during sperm induced Ca^{2+} release in the sea urchin, starfish and ascidian eggs (Dumollard et al., 2003; Schomer and Epel, 1998). It has been demonstrated that the sperms mitochondria are destroyed by the egg at fertilisation (Sutovsky et al., 2000) and the reason for this is still unclear. However, in some rare cases, patients inherit mitochondrial defects from the paternal mitochondria (Schwartz and Vissing, 2002). Despite the immature appearance of mitochondria in the egg, the mammalian oocyte is still strongly dependent on these structures to maintain ATP turnover and minimise oxidative stress (Dumollard et al., 2003; Igarashi et al., 2005).

As the fertilised embryo proceeds through development, the mitochondria develop more cristae and become more like those seen in the somatic cell. Mitochondria at fertilisation influence the buffering of cytosolic Ca^{2+} levels and also the production of ATP (Dumollard et al., 2003; Dumollard et al., 2004; Liu et al., 2001). In mouse, human and pig eggs the presence of poorly polarized, displaced or damaged, mitochondria is associated with poor embryo development and apoptosis (Van Blerkom et al., 1995). Mitochondria are also thought to play an

important role in regulating the production of reactive oxygen species (ROS) during fertilisation. Aged mouse eggs and mouse eggs exposed to hydrogen peroxide have lower developmental potential and a higher rate of embryo fragmentation (Liu and Keefe, 2000; Liu et al., 2000; Takahashi et al., 2003).

Ca^{2+} increases at fertilisation in ascidian and mouse eggs leads to an increase in Ca^{2+} in the mitochondrial matrix (Liu et al., 2001). In ascidian and mouse eggs the Ca^{2+} oscillations are associated with oscillations in autofluorescence of NADH and flavoproteins (Dumollard et al., 2003; Dumollard et al., 2004). These data suggest that Ca^{2+} oscillations might stimulate an increase in ATP production in the mitochondria. An increase in ATP could be expected since a Ca^{2+} increase in some somatic cells leads to increases in cytosolic ATP levels (Jouaville et al., 1999; Kennedy et al., 1999). However, some somatic cells show a decrease in ATP during a Ca^{2+} transient (Allen et al., 2002; Jouaville et al., 1999). Moreover, measurements of total ATP levels in sea urchin and fish eggs suggest a substantial decrease in ATP during egg activation (Epel, 1969; Monroy, 1965; Wendling et al., 2004). Monitoring of cytosolic and mitochondrial ATP directly in living eggs can be achieved by recording luminescence emission from the natural ATP indicator firefly luciferase (Dumollard et al., 2004; Kennedy et al., 1999; Manfredi et al., 2002).

1. 7 Bioluminescence

1.7.1 Firefly Luciferase

Bioluminescence is a naturally occurring process in which living organisms convert chemical energy into visible light. The luciferase-luciferin system has long been used as an indicator for monitoring ATP. Most bioluminescent insects are beetles and belong to the families of Elateridae (e.g. click beetles), Phengodidae (the railroad worm) and Lampyridae (the fireflies) (Wilson and Hastings, 1998). The firefly (also called lightning bug) is a beetle and belongs to the family, Lampyridae. During nocturnal courting rituals the tails of these fireflies emit flashes of light which allow the flying males to locate the non-flying females. The flashes are the result of an oxygen-dependent bioluminescent reaction that occurs between the luciferase enzyme and its substrate, luciferin (Fig. 1.10). Each species of firefly has a distinctive pattern of flashes in order to provide distinction from other species in the area. Fireflies emit light in a range of colours from green to yellow in the wavelength range from 550-580 nm. Studies using immunochemical labelling have shown that peroxisomes are the organelles in the photocytes of the North American firefly *Photinus pyralis* that contain luciferase (Wilson and Hastings, 1998).

Fig. 1. 10 The firefly luciferase-luciferin reaction

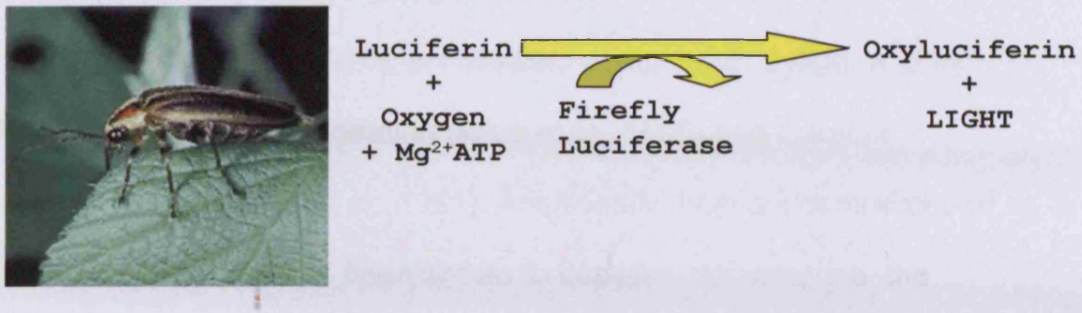

Fig. 1.10 Picture of the firefly beetle and schematic diagram of the firefly luciferase-luciferin reaction.

Many factors have been shown to influence the luciferase-luciferin signal such as temperature (Seliger and Mc, 1960), ionic strength (Denburg and McElroy, 1970), pH (Bowers et al., 1993; Seliger and Mc, 1960), high protein concentration (Allue et al., 1996) and chloride concentration (Ugarova et al., 1981). Additionally, high concentrations of the substrate luciferin has been shown to depress, not enhance, the luminescence signal and this is proposed to be an inhibitory effect of oxyluciferin (Gandelman et al., 1994). It has been proposed that 100 µM is the optimal concentration of luciferin in media for luminescent recordings (Gandelman et al., 1994).

In the luciferase-luciferin system ATP is important, but is not required as an energy source (Campbell, 1988). ATP converts the luciferin into a form capable of being catalytically oxidised by the luciferase protein (Campbell, 1988). Numerous previous studies have used firefly luciferase to report relative changes in ATP levels in mammalian somatic cells (Allen et al., 2002; Allue et al., 1996; Bowers et al., 1993; Dumollard et al., 2004; Jouaville et al., 1999; Kennedy et al., 1999). The Km value for the luciferase-luciferin reaction *in vitro* is in the µM range in solution. However, the Km for this reactions shifts to the mM (2mM) range when in the cytoplasm of cells due to the presence of intracellular proteins (Allue et al., 1996).

During this study the luciferase chemistry used was developed from a North American firefly called the *Photinus Pyralis*. In the *Photinus Pyralis* the light organs are situated on the ventral (under-belly) surface of the sixth and seventh abdominal segments. Firefly luciferase is a 100 kDa

euglobulin, protein dimer with a binding site for 1 $Mg^{2+}ATP^{4-}$ molecule. The reaction of the luciferin occurs in 2 stages; first adenosine monophosphate (AMP)-luciferin is formed, followed by its oxidation by O_2 to the excited state oxyluciferin. Cellular ATP content can be measured by direct lysis of the cell with a detergent, in the presence of the luciferase-luciferin cocktail, in front of a luminometer.

1.7.2 Firefly Luciferase in cells

The firefly luciferase-luciferin reaction is the most sensitive method available detecting [ATP] as low as 0.01 fmol. When injected or expressed in the cytoplasm of mammalian cells or bacteria, the luminescence from firefly luciferase can be used to measure the dynamics of ATP changes during physiological stimulation, growth, or stress (Allen et al., 2002; Dumollard et al., 2004; Schneider and Gourse, 2004).

Firefly luciferase has been used to monitor both cytosolic and mitochondrial ATP levels in both HeLa cells and primary cultures of skeletal myotubes (Jouaville et al., 1999). When HeLa cells were perfused with glycolytic substrates and then exposed to a Ca^{2+} increase, the luciferase luminescence signal decreased indicating a decrease in both cytosolic and mitochondrial ATP levels. On perfusion with oxidative substrates and exposure to a Ca^{2+} rise, the ATP in both the mitochondria and cytosol increased. The increase in ATP was dependent upon a Ca^{2+} increase within the cells, because the ATP rise was abolished when cells were loaded with the Ca^{2+} buffer BAPTA-AM. Mitochondrial Ca^{2+}

accumulation triggers an activation of the cells mitochondria which results in ATP production.

Firefly luciferase has also been used in MIN-6 and primary β cells (Kennedy et al., 1999). Cytosolic, PM and mitochondrial targeted luciferase constructs were used to measure ATP at these three sites (Kennedy et al., 1999). The cells responded to extracellular glucose with a sustained increase in mitochondrial and PM ATP levels. Also, cytosolic ATP levels responded with a large increase that peaked before returning to basal levels (Kennedy et al., 1999). This glucose induced increase in ATP was more significant when Ca^{2+} was present, and therefore, shows that Ca^{2+} plays an important role in stimulating an ATP response in cells.

Previously, ATP was monitored during fertilisation in mouse eggs by measuring the luminescence of intracellularly injected firefly luciferase (Dumollard et al., 2004). A small increase in ATP during fertilisation was recorded, but this was only seen in 9/25 eggs (Dumollard et al., 2004). Since ($[Ca^{2+}]i$) was not monitored simultaneously, it was not possible to establish any relationship between ATP and Ca^{2+} oscillations. Other studies have used Mg^{2+} sensitive fluorescent dyes to monitor ATP in an indirect manner (Igarashi et al., 2005). This suggested a transient decrease followed by a sustained increase in ATP during Ca^{2+} oscillations at fertilisation, but only in freshly ovulated eggs. Aged eggs showed a decrease in ATP during fertilisation (Igarashi et al., 2005). Therefore, the relationship between Ca^{2+} and ATP in eggs at fertilisation, and indeed how ATP levels change at fertilisation, are still largely undefined.

1.8 Aims

From this study, my overall objective is to monitor the dynamics of cytosolic Ca^{2+} and ATP levels in the same set of mouse eggs during fertilisation. In Chapter 3, I shall investigate the relationship between Ca^{2+} and ATP during sperm induced activation until PN formation. Chapter 4 shall involve exploring the dependence of the ATP change upon intracellular Ca^{2+} levels. In Chapter 5 the metabolic status and substrate utilisation in eggs during fertilisation shall be surveyed, whilst Chapter 6 will investigate the changes in ATP that occur during fertilisation more thoroughly. The final results chapter, Chapter 7, will look at the domains of PLCζ that are required for successful PLCζ activation of mouse eggs. Chapter 8 will summarise the overall results from Chapters 3 to 7 and provide a detailed discussion of all the findings in this thesis.

Chapter 2
Materials and Methods

2.1 Laboratory reagents and animals

All chemicals and reagents were obtained from Sigma or Calbiochem, unless otherwise stated. Female MF1 mice were obtained from Harlan and male mice (CBAxC57) were obtained from colony (Dr S. Paynter). cRNA constructs were supplied by Chris Saunders, Michail Nomikos and Jose Gonzalez Garcia.

2.1.1 Media and hormone preparation

Hepes buffered potassium simplex optimized media (HKSOM) (no BSA) was prepared as described previously (Summers and Biggers, 2003) and was required for imaging purposes to ensure the eggs remained in place during an experiment. The osmolarity of the media was confirmed prior to experiments (280 mOsm/kg) and the pH was adjusted to pH to 7.3. For experimental purposes, glass cover slips were coated with Poly-D- lysine hydrobromide MW 70,000-150000 (cell culture tested) to ensure eggs stayed in place during imaging. Poly-D-lysine promotes cell adhesion and was prepared in clinical grade water to a working concentration of 1 mg/ml.

Cumulus cells that surround eggs following retrieval from the ampullas must be removed prior to experiments and hyaluronidase is an enzyme used to remove these cells. A working concentration of 300 µg/µl of hyaluronidase was used throughout experiments. Female MF1 mice (~6 weeks old) underwent hormonal treatment to induce ovulation (see section 2.5.2). The hormones that were used to stimulate ovulation were pregnant mare serum gonadotrophin (PMSG) and human chorionic gonadotrophin (hCG). PMSG mimics the action of FSH and stimulates

Hepes buffered potassium simplex optimised media (HKSOM) and Tyrodes 6 (T6)

Chemical	HKSOM (10x stock in 500 ml of sterile water)	T6 media (1x stock in 1000 ml of sterile water)
Sodium Chloride	27.75 g	- -
Potassium Chloride	0.925 g	- -
Monopotassium Phosphate	0.238 g	- -
Sodium Pyruvate	0.11 g	0.055 g
L-Glutamine	0.73 g	- -
Streptomycin sulphate	0.25 g	0.05 g
Benzylpenicillin	0.315 g	0.06 g
EDTA	0.019 g	- -
Magnesium sulphate	0.2465 g	- -
Sodium Lactate (syrup)	7.37 ml	3.5 ml
Sodium Bicarbonate	1.68 g	2.106 g
Phenol red	0.05 g	0.005 g
Hepes	23.8 g	- -
Tyrodes Salt	- -	1 Vial

HKSOM stocks can be stored at -20°C while T6 should be stored at 4°C for a maximum of 6 weeks.

Prepare a working stock of HKSOM on day of experiment by diluting 1ml of the prepared 10x stock in 9 ml of clinical grade water. To this add 10 µl of 0.2 M glucose, 10 µl of 1.71 M calcium chloride and 20 µl of sodium hydroxide. Filter before use.

T6 should be prepared the day before required by dissolving 16 mg/ml of BSA into 10 ml of T6 media and equilibrated in the incubator overnight.

the growth and development of ovarian follicles. The resulting concentration of PMSG injected into mice was 5 IU. hCG mimics the action of LH and promotes ovulation in the mature follicles. The final concentration of this hormone that was used for experimental procedures was 10 IU.

Tyrodes 6 (T6) is a solution that is mainly used for the capacitation of sperm in the incubator (38°C, 5% CO_2 in air). For capacitation of sperm T6 was prepared with bovine serum albumin (BSA) (16 mg/ml). Potassium chloride (KCL) Hepes buffer was used for preparing reagents that were being injected into eggs. This buffer was prepared to pH 7.5 and chelex 100 beads were used to remove any ions that were present.

2.2 Chemical Reagents preparation

2.2.1 Reagents injected into eggs

Oregon green bapta dextran (potassium salt) (OGBD) is a visible wavelength Ca^{2+} indicator that is excited at 488 nm. When OGBD binds to Ca^{2+}, an increase in fluorescence emission occurs, therefore, allowing changes in intracellular Ca^{2+} to be measured. OGBD was prepared in clinical grade water to a stock concentration of 2 mM (Molecular Probes O6798, MW 10,000) and for most experiments was injected at a pipette concentration of 0.5 mM.

The aim of this thesis is to determine the behaviour of ATP levels in mouse eggs during various conditions, therefore, it was essential that a reliable indicator of ATP was used. Firefly luciferase is derived from the firefly beetle and is the enzyme responsible for the reaction that converts luciferin to oxyluciferin which results in the production of emitted light

(550-580 nm). This reaction can be used as a measure of ATP and stock concentrations of 10 mg/ml were prepared in clinical grade water. The pipette concentration that was typically injected was 7.5 mg/ml. D-Luciferin (sodium salt) is the substrate for firefly luciferase, and must be present in the extracellular media surrounding the eggs. The firefly luciferase-luciferin reaction can then be measured via luminescence levels. Luciferin was prepared in clinical grade water as a 100 mM stock and used as a working concentration of 100 µM.

If Ca^{2+} oscillations within an egg could be artificially initiated and controlled, then the response of ATP levels during various oscillation patterns can be explored in a controlled manner. Caged $InsP_3$ allows this possibility to be explored and has previously been used for this purpose (Jones and Nixon, 2000). Caged $InsP_3$ is a photolabile derivative of Ins(1, 4, 5)P_3 which is neither active nor metabolized by endogenous phosphatases. Caged $InsP_3$ has extra chemical groups present on either the 4 or 5 position and can be selectively released by irradiation with a pulses of UV light of about 360 nm to produce a concentration jump in intracellular levels of $InsP_3$. Caged $InsP_3$ was obtained from Calbiochem (cat no. 407135) and a stock of 2 mM was prepared in KCL Hepes, the injecting concentration in the pipette was 0.4 mM.

2.2.2 Chemicals that manipulate cellular metabolism

Carbonyl cyanide 4-(trifluoromethoxy) phenylhydrazone (FCCP) is an uncoupler of oxidative phosphorylation in the mitochondria. A stock concentration of 1 mM was prepared in dimethyl sulfoxide (DMSO) and for experiments; a final concentration of 1 µM was used. Eggs are

thought to rely on oxidative phosphorylation for ATP production (Dumollard et al., 2003; Dumollard et al., 2004) and, therefore, require pyruvate in their media. To explore this more pyruvate uptake into the mitochondria was inhibited. The chemical, α-Cyano-4-hydroxycinnamic acid (Cinnamate – see figure 2.1), blocks pyruvate transport into the mitochondria (Barnard et al., 1993; Williams et al., 1996). A fresh stock (0.25 M) of cinnamate was produced every week in ethanol. To dissolve the powder the mixture was heated to 60°C and vortexed every 20 minutes. The powder dissolved typically after 1 hour. The final concentration of cinnamate used on eggs was 0.5 mM.

Mitochondria sequester Ca^{2+} during fertilisation induced Ca^{2+} oscillations (Dumollard et al., 2004). To investigate how reliant the eggs are upon their mitochondria buffering cytosolic Ca^{2+}, the uptake of Ca^{2+} by the mitochondria must be inhibited. Ca^{2+} is taken up via a mitochondrial uniporter whose exact identity is still undefined. SB202190 is a MAP Kinase inhibitor that has been suggested to inhibit the Ca^{2+} uniporter on the mitochondria (Montero et al., 2000). A stock concentration of 100 mM was prepared in DMSO and during experiments; a working concentration of 10 μM was used.

Although glycolysis activity has been demonstrated to be low in eggs (Barbehenn et al., 1974) it is possible that glycolysis may be switched on when the eggs ATP levels are compromised. Iodoacetate has an inhibitory effect on glycolysis (Downs, 1995) and a stock of 10 mM stock was prepared in DMSO with the final concentration of 10 μM being used during experiments.

Fig. 2. 1 Cinnamate structure

A) Cinnamate

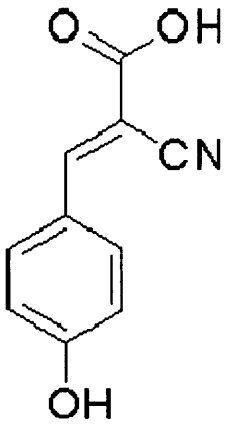

B) Pyruvic acid

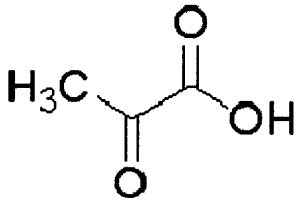

C) Sodium lactate

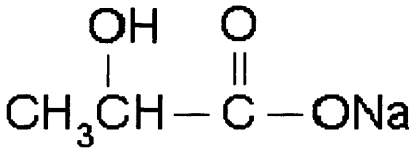

Fig. 2.1 Chemical structure of A) the pyruvate uptake inhibitor cinnamate (α-cyano-4hydroxycinnamic acid), B) pyruvic acid and C) sodium lactate.

2.2.3 Cell cycle inhibitors

The progression of a cell through the cell cycle can be manipulated by the presence of different chemicals depending upon the stage that is being explored. The following agents were used to establish if a relationship existed between ATP levels and cell cycle progression. Nocodazole is an antimitotic agent that disrupts microtubules by binding to β-tubulin and preventing formation of one of the two interchain disulfide linkages, thus inhibiting microtubule dynamics, disruption of mitotic spindle function, and fragmentation of the Golgi complex. Nocodazole arrests the cell cycle at metaphase, therefore, preventing formation of PN and 2nd PB emission. A 10 mM stock in DMSO was prepared for experiments; a final concentration of 10 μM was used. Z-Leu-Leu-Leu-al (MG132) is a potent, membrane-permeable proteasome inhibitor. 50 mM of MG132 was prepared in DMSO and during experiments, a final concentration of 50 μM MG132 was used.

Second PB emission is an event that occurs during the first hour of fertilisation. This event can be prevented by the presence of cytochalasin B or, D (CB or, CD). CB is a permeable toxin which induces the disruption of contractile microfilaments by inhibiting actin polymerization. Therefore, DNA fragmentation is induced which will inhibit cell division, and also cause the disruption of many cell processes. A stock of 5 mg/ml was prepared in DMSO and the working concentration required was 5 μg/ml. CD, like CB, is also a cell permeable toxin that inhibits actin polymerization. Actin microfilaments are disrupted and the p53-dependent pathways are activated causing arrest of the cell cycle at the

G1-S transition. A 2 mM stock was prepared in DMSO and the working concentration required was 2 µM.

2.2.4 Chemicals that affect Ca^{2+} levels and/or parthenogenetic activation

Sperm is the physiological stimulus that induces Ca^{2+} transients in an egg; however, non-physiological stimuli can be used to attain further knowledge of the cellular mechanisms that occur within the egg. Ionomycin is a Ca^{2+} ionophore of which a 10 mM stock was prepared in DMSO and a final concentration of 10 µM was used for experimental purposes. Thapsigargin is a potent, cell-permeable, $InsP_3$-independent intracellular Ca^{2+} releaser. Thapsigargin inhibits sacro/endoplasmic reticulum Ca^{2+} ATPase (SERCA) and allows an influx of Ca^{2+} into the cytosol. A stock concentration of 10 mM was prepared in DMSO and a final working concentration of 5 µM was used throughout experiments. The $InsP_3$ pathway is the natural mechanism by which an egg produces Ca^{2+} transients, carbamoylcholine chloride (carbachol) is a muscarinic agonist that releases Ca^{2+} via the $InsP_3$ pathway. Eggs were treated with 10 µM carbachol during experiments from a 10 mM stock that was prepared in DMSO.

To investigate the Ca^{2+} and ATP relationship during fertilisation, Ca^{2+} was chelated by the presence of 1,2-Bis(2-aminophenoxy)ethane-N,N,N',N'-tetraacetic acid tetrapotassium salt (BAPTA). BAPTA is a Ca^{2+} buffer and chelator. A 100 mM stock of BAPTA was prepared in clinical grade water and a final concentration of 2 mM was used in the media surrounding eggs during experiments. Alternatively, for experiments

when BAPTA was injected into the eggs, the stock of 100 mM was dissolved 1:5 so that the pipette concentration before injections was 20 mM.

Parthenogenesis is the activation of an unfertilised egg without mating or, fertilisation. Parthenogenetic activation can occur via exposure of unfertilised eggs to cycloheximide. Cycloheximide can parthenogenetically activate eggs without an increase in Ca^{2+} levels. Cycloheximide blocks 90% of protein synthesis and has been shown to cause parthenogenetic egg activation in a Ca^{2+} independent manner (Moses and Kline, 1995). A stock of 20 mg/ml was prepared in DMSO and the final concentration used was 20 µg/ml.

2.3 cRNA constructs

2.3.1 Preparation of cRNA

PLCζ and PLCδ constructs were prepared by Michail Nomikos, Chris Saunders, or, Jose Gonzalez Garcia. Diagrammatic structural details of the cRNA constructs are provided in Chapter 7. Briefly, a two-step cloning strategy was used to create the PLCζ-luciferase (LUC), PLC δ1-LUC and PLCγ1-LUC constructs. The appropriate DNA was amplified using appropriate primers to incorporate a 5'-EcoRI site and a 3'-NotI site, for cloning into pCR3 vector. The luciferase was amplified by PCR reaction and then cloned at the 3'-end of each PLC construct using the NotI restriction enzyme. The PLC construct and LUC were tagged together via either a 3, or, 4 amino acid linker sequence (AAA, YAAA or, CAAA).

The DNA (PLC-LUC) was amplified using Qiagen's Plasmid Maxi Kit according to the manufacturing instructions. The circular plasmid DNA then had to be linearised to prevent the production of extremely long cRNA molecules. The restriction enzyme NdeI was used to linearise the plasmid as it does not cut the plasmid between the promoter site and the gene of interest. The linearised DNA is cleaned by phenol/chloroform extraction before it is precipitated. Precipitation is carried out by incubation in isopropanol and sodium acetate (pH 5.2) for an hour. This mixture is then pelleted by microcentrifugation at 1400 g for 20 minutes. The supernatant is removed and the pellet is washed and then dried.

The DNA pellet is then resuspended in nuclease free water and a transcription reaction is assembled at room temperature with 2xNTP/CAP mix, reaction buffer and the appropriate enzyme (2 hours). After the 2 hour incubation a poly-A tail is added to the construct to enhance cRNA longevity; this is achieved by incubating for a further 2 hours at 37°C in the presence of high (10 mM) ATP and the enzyme *E*-polyadenylate polymerase (E-PAP). The polyadenylated cRNA is then precipitated by the addition of lithium chloride precipitate solution and incubated at -80°C for more than 1 hour. The pellet is washed (supernatant discarded) with 80% ethanol and then centrifuged for 15 minutes before being allowed to dry. The cRNA is then resuspended in nuclease free water and SUPERase-In-RNAase inhibitor.

The absorbance of the cRNA at 260 nm is measured in order to quantify the concentration of the cRNA. The amount of RNA can then be calculated using the appropriate equation (cRNA conc (μg/μl) = 40 x A_{260}

x 500) and the cRNA can then stored at -80°C. When the cRNA is injected, it will be diluted with OGBD.

2.3.2 Mitochondrial targeted firefly luciferase cRNA

Mitochondrial luciferase was prepared by Remi Dumollard and the mitochondrial targeting sequence from coxVIII was obtained from Rosario Rizzuto. Briefly, the coxVIII targeting sequence was cloned at the N-terminus site of luciferase into the EcoRI/NotI sites of pRN3. From this construct, polyadenylated capped cRNA was produced using mMessage mMachine kits and poly(A) tailing kits from Ambion. Eggs were injected with 0.675 µg/µl mitochondrial luciferase with 0.5 mM OGBD.

2.4 Immunohistochemistry

bisBenzimide H 33342 trihydrochloride (Hoechst 33342) stains DNA, chromosomes and nuclei. A stock of 10 mg/ml was prepared in DMSO and 1 µg/ml is the concentration that eggs were exposed to for an incubation time of 30 minutes.

The immunohistoochemistry method used to verify mitochondrial targeted luciferase was as follows. Eggs injected with 0.675 µg/µl mitochondrial luciferase were washed with PBS (+1 mg/ml poly(vinyl alcohol) (PVA)) and fixed with 4% formaldehyde for 30 minutes, at room temperature (RT). After washing 3 times with PBS, eggs were then incubated for 15 minutes in 50 mM NH_4Cl (in PBS + PVA). The eggs were washed again 3 times with PBS and then permeabilised with 0.25% Triton X-100 (in PBS + PVA) for 5 minutes, at RT. After washing once with PBS, the eggs were then blocked for 30 minutes with image-iT™ FX signal enhancer (Invitrogen, I36933) before a further blocking step for 30

minutes with 10% normal goats serum in PBS. Following another wash with PBS, cells were incubated with 10 µg/µl rabbit anti luciferase antibody (Sigma L0159) for 30 minutes at RT. Eggs were then washed with PBS six times for 30 minutes at RT and then incubated with 20 µg/µl of the secondary antibody goat anti-rabbit (Alexa fluor 488 nm obtained from Invitrogen A11008) for 30 minutes at RT. Following incubation with the secondary antibody, the eggs were then washed 3 times for 60 minutes (total time) and finally mounted on glass slides using FluoroGuard antifade reagent. All washing steps were carried out at RT in PBS (+ 1 mg/ml PVA). Stained eggs were imaged using SP5 confocal microscope. GV eggs were also imaged and underwent the same protocol as described for MII eggs.

MII and GV eggs were also stained with the mitochondrial probe Mitotracker orange (M7510 Invitrogen). A stock concentration of 5 mM Mitotracker orange was prepared in DMSO and eggs were incubated in 0.5 µM for 30 minutes. It is important to note that along side the above experiment, controls were performed by omitting the incubation with the primary antibody. This ensured that the fluorescence seen did not result from non-specific binding of the secondary antibody.

2.5 Mouse Egg Experiments

Eggs were collected from female MF1 mice that were approximately 6 weeks old. For IVF experiments, sperm were collected from male F1 hybrid mice (CBA x C57) that were approximately 12-24 weeks old.

2.5.1 Fire pulled glass pipettes

Fine bore glass pipettes were prepared prior to every experiment and were used to transfer eggs from one solution to another by attaching a mouth pipette to the large end of the glass pipette. The pipettes were prepared by holding the narrowing end of a disposable glass pipette over a small flame, on a Bunsen burner. The pipette was rotated whilst it was in the flame to ensure the pipette was evenly heated and when the glass began to melt the pipette was pulled apart in one fast motion. The pipette was then broken approximately 5cm away from the original point that was melted in the flame. The resulting diameter of the opening of the pipette was slightly larger than that of the diameter of the eggs, to allow the eggs to be easily picked up (>80μm).

2.5.2 Stimulation of Ovulation and Collection of Oocytes

Metaphase II (MII) eggs were collected from female MF1 mice (~6 weeks old) that had been administered 5 IU of PMSG (Folligon) via intra-peritoneal (I.P.) injection using a syringe, at 4-6pm on day 1. The same mice were then given a second injection of 10 IU of human hCG (Folligon) at 6pm of day 3 (i.e. 50 hours after initial PMSG injection).

At 8am on day 4, (therefore, 14 hours post hCG), the superovulated female mice were sacrificed via cervical dislocation. The ampullas were collected as shown in Fig. 2.2 and then placed into M2

media. The cumulus masses were retrieved from within the ampullas and released into a dish containing 300 µg/ml of the enzyme hyaluronidase, which was prewarmed to 38°C. The eggs remained in the hyaluronidase for no longer than 5 minutes. Fig. 2.3 shows eggs before and after hyaluronidase treatment. Following hyaluronidase treatment, eggs were washed at least 3 times in M2 media and left to recover for at least 10 minutes before any experimental procedure was carried out on them.

GV eggs were imaged for mitochondrial localisation. Briefly, immature oocytes were collected from unprimed MF1 female mice. Cumulus cells surrounding the oocytes were mechanically removed using a fine pipette. GV oocytes were then maintained at the GV stage by incubation in M2 media containing 250 µM cAMP. GV eggs were either incubated in 0.5 µM Mitotracker orange or, injected with mitochondrial firefly luciferase before being fixed and stained as described in section 2.4.

Fig. 2. 2 Retrieval of ampullas from the mouse

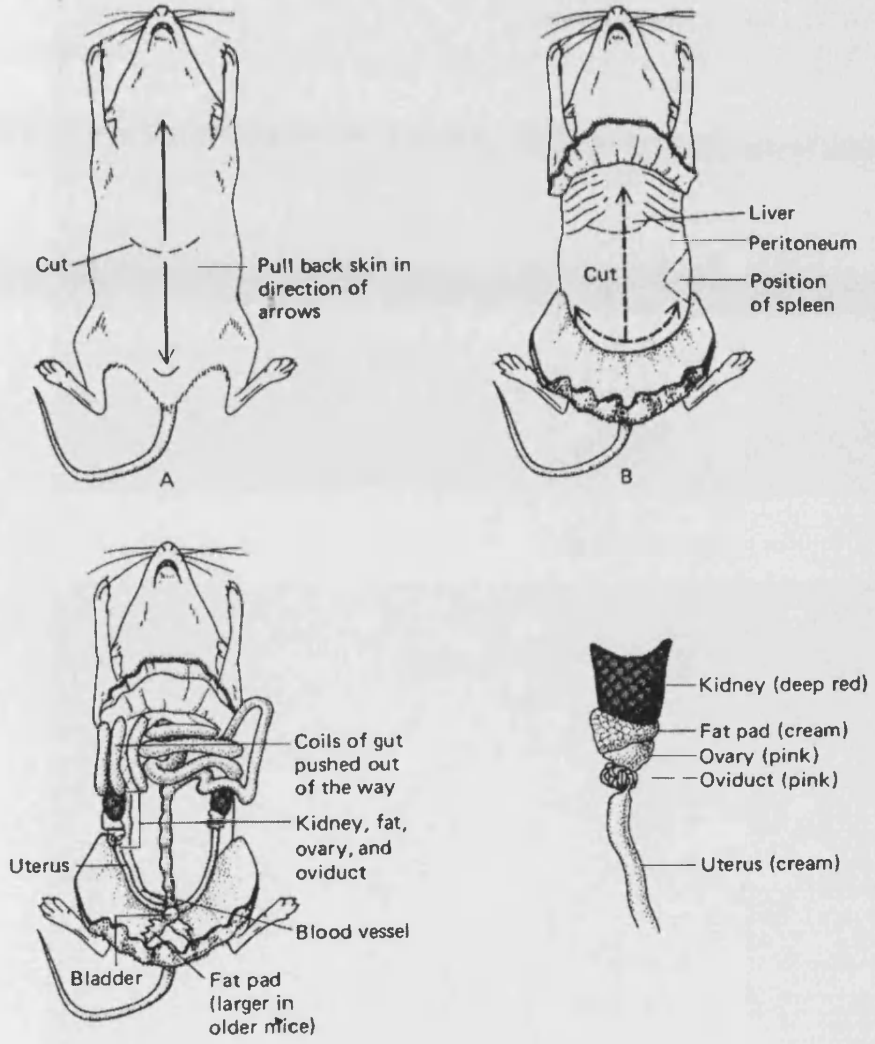

Figure 2.2 Diagram showing the dissection and removal of female mouse ovary. (Hogan et al., 1986)

Fig. 2. 3 MII eggs before and after hyaluronidase treatment

A

B

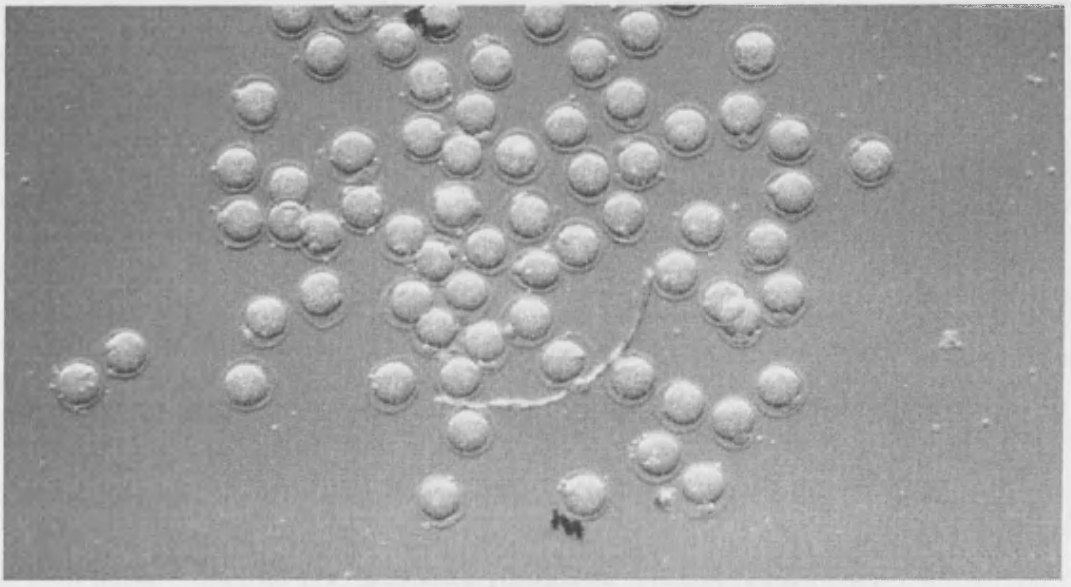

Fig 2.3 Mouse eggs before (A) and after (B) treatment with hyaluronidase enzyme.

2.5.3 Microinjection of mouse eggs

Mouse eggs were washed in M2 and microinjected (Fig. 2.4) with 0.5 mM OGBD and 7.5 mg/ml firefly luciferase for most experiments. Injections of other agents are described in more detail in the appropriate results section. Borosilicate glass capillaries (Harvard Apparatus Ltd. 1.5 mm outer diameter and 0.86 mm inner diameter) with an internal filament were pulled on a vertical pipette puller (Model P-30; Sutter Instruments). The volume of solution injected was estimated by the diameter of cytoplasmic displacement caused by the injection; which was approximately 3-5%.

Injection needles are backfilled with <1 µl of the injection solution using sterile micropipettes (Ependorff). The filled injection needles are then clamped in a holder with a silver wire and side port (World precision instruments www.wpi-europe.com). The holder is connected to a preamplifier that is electrically connected to an intracellular amplifier (Cyto 721; WPI). The egg is held in place by a holding pipette (Cook) using suction. The eggs are then individually microinjected using pressure pulses applied to the back of micropipettes inserted into eggs, using overcompensation of the negative capacitance of a serially connected electrical amplifier. Both the preamplifier, needle holder and the holding pipette are mounted on hydraulic manipulators (Narashige) that are fixed to an inverted microscope (TE2000, Nikon).

Fig. 2. 4 Microinjection of MII mouse egg

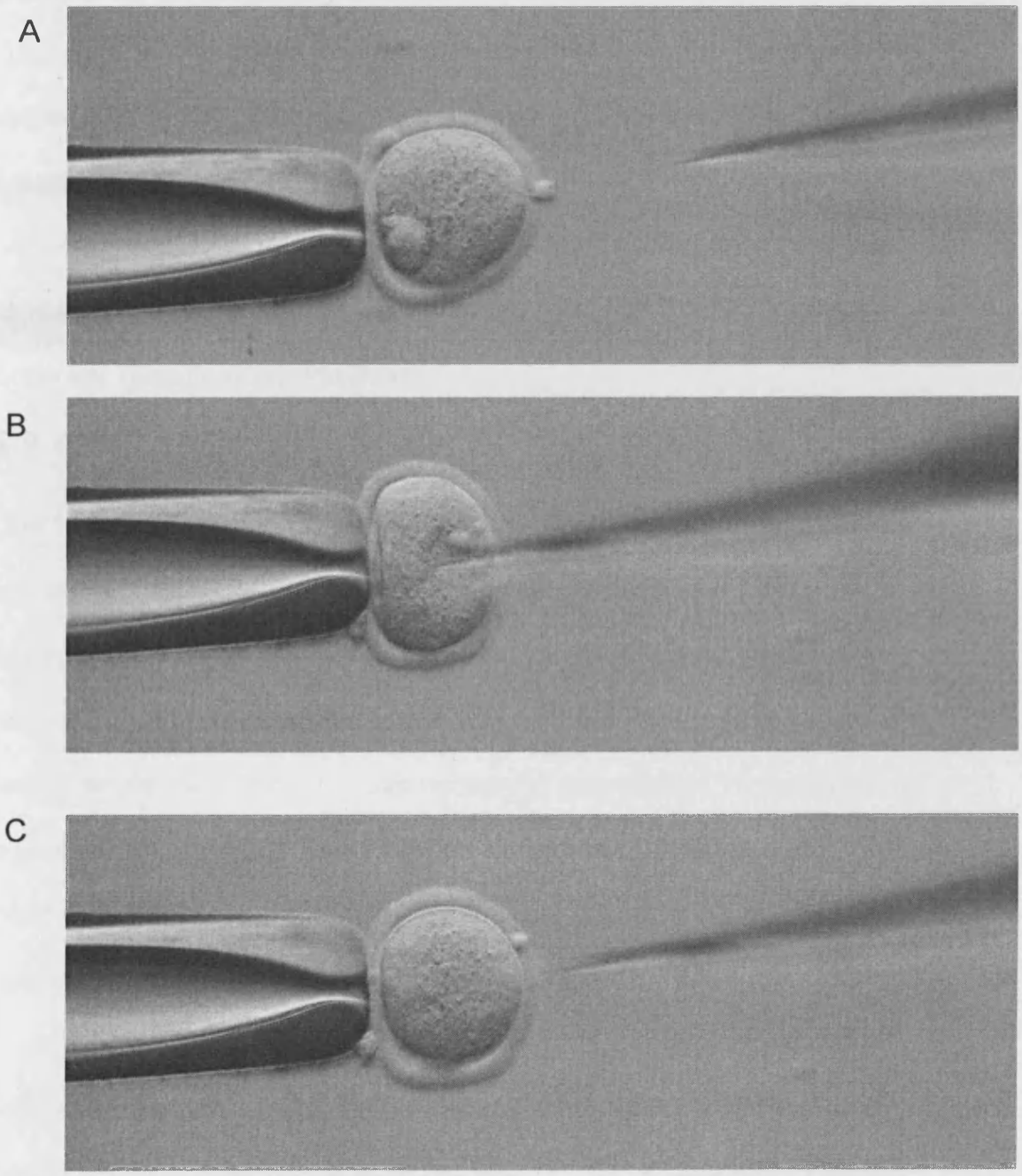

Fig. 2.4 Sequence (A to C) of images showing a single mouse egg being microinjected.

For PLCζ experiments, eggs were injected with (pipette concentration) 1 mM OGBD and the desired concentration of cRNA PLC-LUC which will be stated in Chapter 7 when the PLCs are discussed further. For BAPTA experiments, eggs were injected with 20 mM BAPTA, 0.4 mM OGBD and 6 mg/ml firefly luciferase (pipette concentrations). For Caged compound experiments, eggs were injected with an appropriate concentration of the caged compound, 0.4 mM OGBD and 6 mg/ml firefly luciferase (pipette concentrations).

2.6 IVF Procedure

One 12-week old male mouse (CBA x C57) was sacrificed and the cauda epididymis, vas deferens and testis were excised from each side. Spermatozoa were extracted from the tissue using fine needles and released into the surrounding media and left for a few minutes before being transferred into a 5 ml tube containing capacitated T6 media (16 mg/ml of BSA, pH 7.6). This tube containing the sperm was then incubated at 38°C in a humidified atmosphere (38°C, 5% CO_2 in air) for 2 hours to allow capacitation to occur.

ZPs were removed from microinjected eggs via brief treatment with acidic tyrodes solution before being placed onto a poly lysine coated 1 ml chamber containing HKSOM (no BSA) + 100 µM luciferin, covered with mineral oil. The luminescence signal was left to equilibrate for approximately 1 hour before 10 µl of capacitated sperm were added to the chamber.

In some IVF experiments, 10 µM of nocodazole, 50 µM MG132, 10 µM SB202190, or, 0.5 mM cinnamate were present in the HKSOM (no

BSA) media. For other IVF experiments, 2 mM (final concentration) of BAPTA-AM was added to the chamber 1-2 hours after sperm addition to stop Ca^{2+} oscillations. At the end of all IVF experiments, eggs were checked for PN formation and 2nd PB emission. For IVF experiments where BAPTA had been injected, eggs were stained with 1 µg/ml of Hoechst 33342 for 30 minutes before being viewed in the blue spectra to verify sperm penetration.

2.7 Imaging and Ca^{2+} and ATP

2.7.1 Imaging of microinjected mouse eggs

Fluorescence (OGBD) and luminescence (firefly luciferase) were both imaged in the same sets of eggs using a Nikon TE2000 microscope equipped with a 20x 0.65NA Fluor objective lens that was encased within a purpose built dark box (see Fig. 2.5A, 2.6A and 2.6B for system diagram and photographs). The light (100%) was directed via a sideport to a cooled intensified charged coupled device (ICCD) camera (Fig. 2.5B) equipped with an intensifier with a S20 type photocathode that was cooled to 0°C. The ICCD camera, a peltier cooler and software for control and analysis were supplied by Photek Ltd (www.photek.co.uk).

The system could be used in two different ways by manipulating the opening and closing of the shutters present on the system (Fig. 2.6A). Firstly, either fluorescence or luminescence could be measured individually for an indefinite period of time. Continuous measurement of fluorescence could be achieved for a specified time by programming S1 to stay open and S2 to stay closed (for fluorescence measurements). When S1 was open, the fluorescent excitation light (465-495 nm) from a halogen lamp passed through a fluorescence filter block and was used with a 505 nm dichroic mirror and 500 nm longpass (LP) filter. Similarly, continuous measurement of luminescence could be achieved by programming S1 and S2 to stay closed. Secondly, alternative measurements of both fluorescence and luminescence, in the same experiment, could be achieved by programming S1 to open and close

systematically. The timing of S1 opening/closing could be changed to tailor the needs of various experiments.

Fig. 2. 5 Photek imaging system

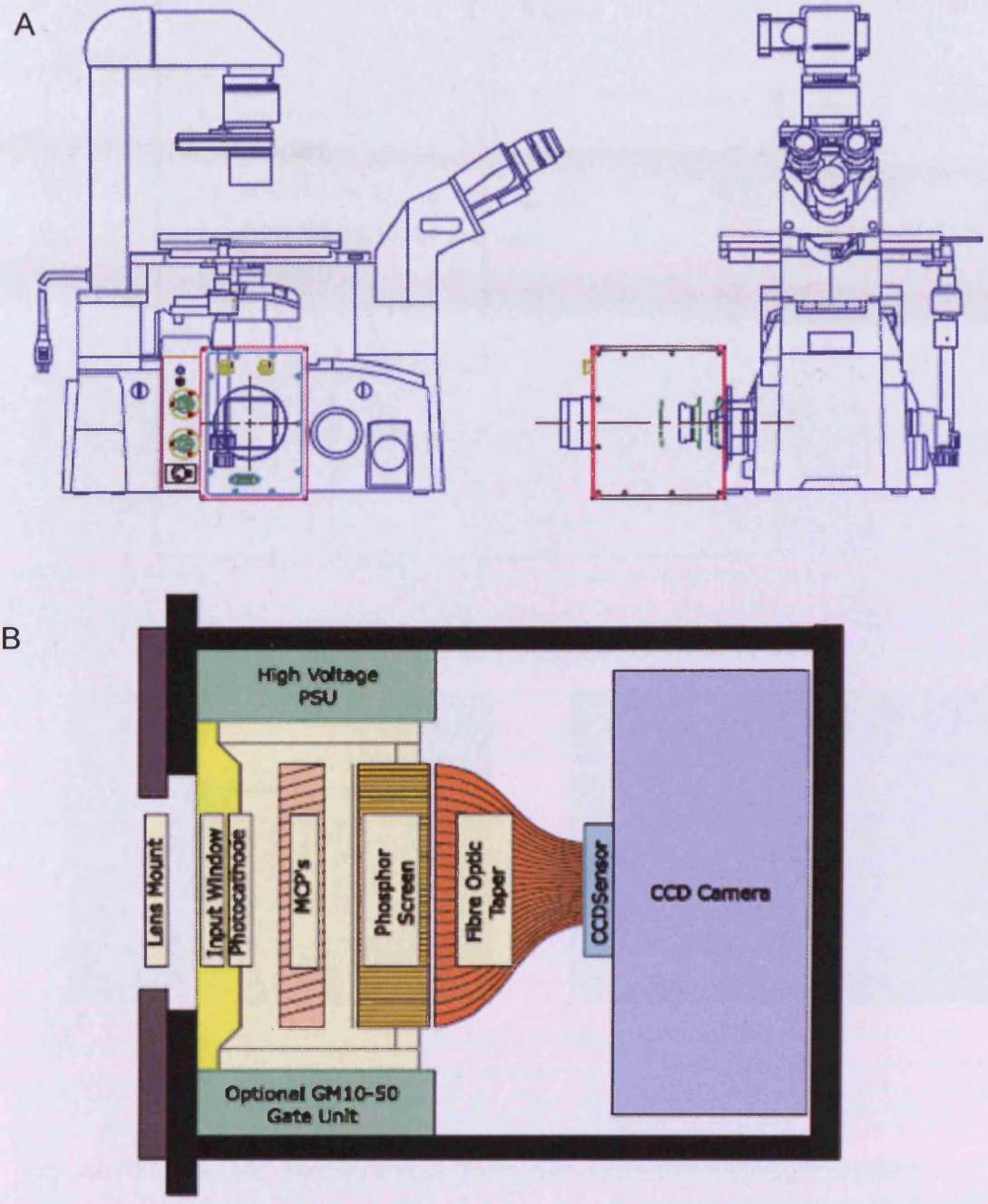

Fig. 2.5 A) Technical drawing showing the microscope and camera assembled together (Photek.com) and B) diagram of ICCD camera (from Photek.com). Light is collected onto the front of the camera before it is intensified and imaged.

Fig. 2. 6 Schematic and photograph of Photek system

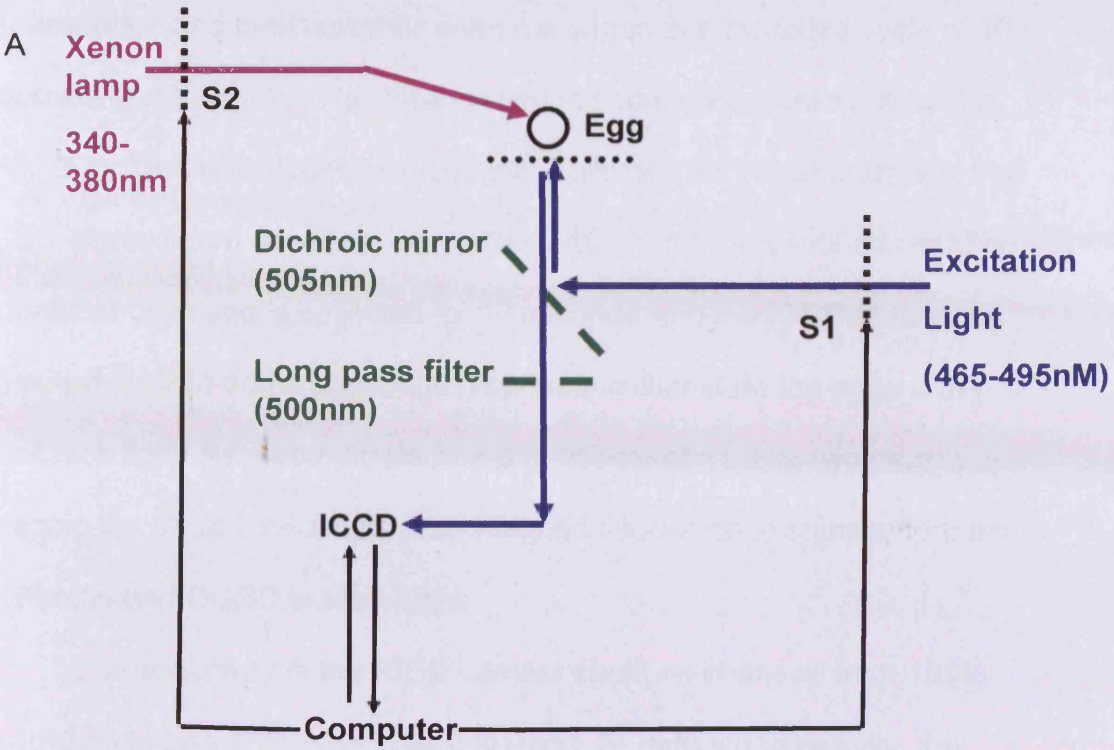

Fig. 2.6 A) Schematic diagram and B) photograph of the Photek imaging system

During switching experiments throughout work in this thesis the fluorescence and luminescence were measured in a repeated cycle of 10 seconds and the image files were stored in separate but linked data files (Fig. 2.7). The luminescence image was collected for 10 seconds with the ICCD at maximum sensitivity and with all illumination sources closed. The fluorescence image is collected for 10 seconds with the ICCD at reduced sensitivity (10%) and a shutter (S1) opened to illuminate the eggs with excitation light. By switching back and forth between these two modes of imaging we could collect luminescence and fluorescence signals from the luciferase and OGBD loaded eggs.

The sensitivity of the ICCD camera could be changed from 100% to 10% during each cycle of data collection. At reduced sensitivity, the camera is still collecting 100% of the photons but the computer only images 10% of these emitted photons. In most cases the fluorescence was recorded with the camera sensitivity on 10% and the fluorescence was 10-100 times greater than luminescence. When fluorescence and luminescence were recorded on both 100% sensitivity, the mean of the luminescence signal just before and after each fluorescence measurement was subtracted from the value obtained from the intensity obtained during fluorescence excitation to obtain the real fluorescence value from each egg. The luminescence values in experiments represent the absolute number of measured photon counts per second (cps). In contrast the intensity of fluorescence is displayed in arbitrary units (AU) and the offset of traces in the y-axis was adjusted for the sake of presentation. For UV excitation of caged $InsP_3$ another shutter (S2), was

opened that allowed light from a mercury lamp to be directed onto the eggs via a fibre optic cable. UV light was directed onto the eggs using a UG11 filter (270-380 nm BP) obtained from Cairn (www.Cairnweb.com). The voltage on the intensifier of the ICCD camera was switched off for the duration of the UV excitation light pulse.

Autofluorescence was measured using the Photek system described above, with all illuminations sources closed and using a 450 nm BP filter. Autofluorescence was also measured using a Nikon Diaphot upright microscope that was equipped with Photometrics (*in vivo*) software (www.photomet.co.uk). The 450 BP filter was arranged with a 510 dichroic mirror and 520 LP filter and excitation was supplied from a metal halide lamp. The eggs were kept at 37°C with a Biotech delta T4 culturedish temperature controller and were imaged using a Coolsnap HQ camera. Autofluorescence was measured every 10s with an exposure time of 400 ms.

Fig. 2. 7 Diagram demonstrating switching mechanism

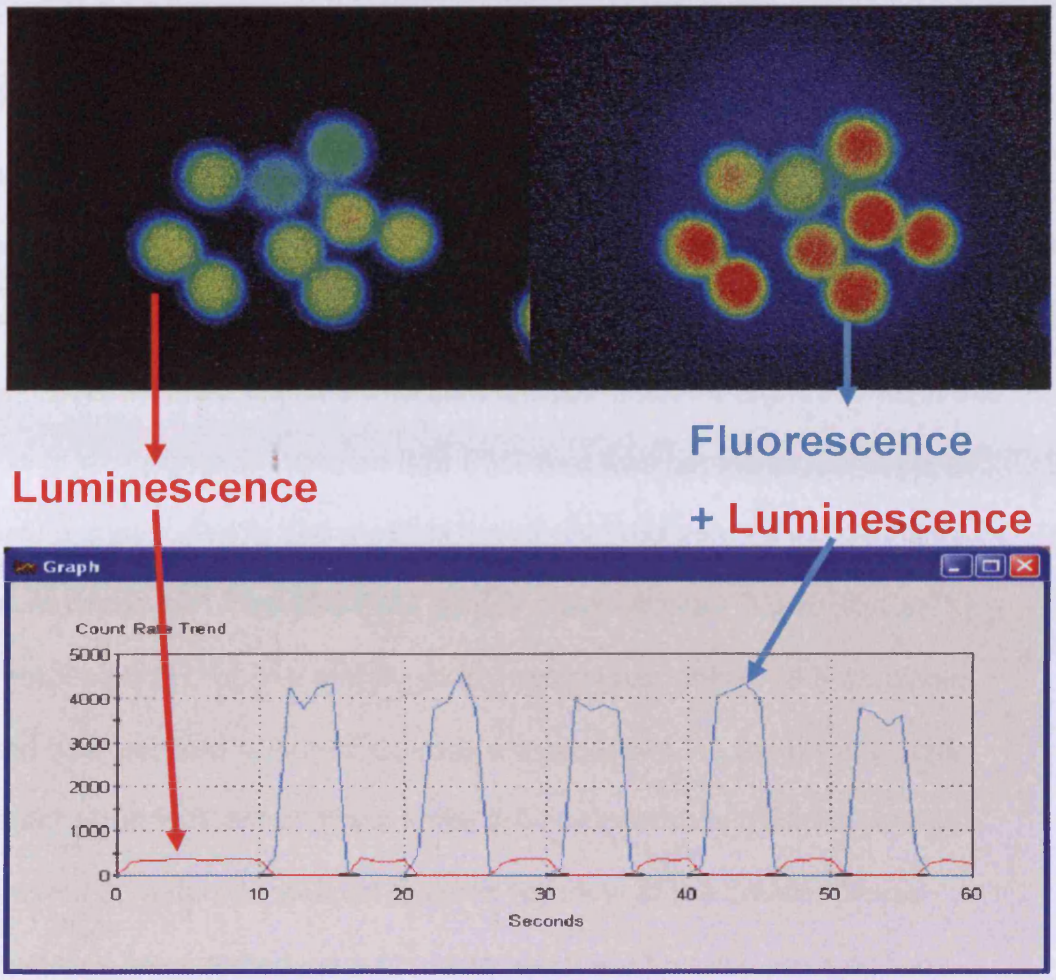

Fig. 2.7 Data collection via switching mechanism. In this diagram, switching is occurring every 5 seconds, however, for most experiments in this thesis, switching occurred every 10 seconds.

2.7.2 Measurement of luminescence using a luminometer

To measure absolute ATP content in single eggs and also to establish the amount of cRNA expression in PLC-LUC injected eggs, a custom made luminometer was used (Fig. 2.8). Luminometers are used to detect and measure light. Light is detected by a photomultiplier tube (PMT) which is an extremely sensitive detector of light in the ultraviolet, visible and near infrared spectra. The luminometer used for experiments in this thesis was equipped with an S20 PMT that was cooled to -20°C via a peltier cooler. PMTs can multiply the signal produced by incident light by as much as 10^8. The S20 PMT contains a multialkali (Na-K-Sb-Cs) photocathode that has a high, wide spectral response in the ultraviolet and near infrared region. Electrons are produced via the photoelectric effect when incident photons strike the photocathode material, which is present as a thin deposit on the entry window of the device. These electrons are directed via a focusing electrode towards the electron multiplier. The electron multiplier is responsible for multiplying electrons by the process of secondary emission.

Fig. 2. 8 Luminometer used in lysis assays

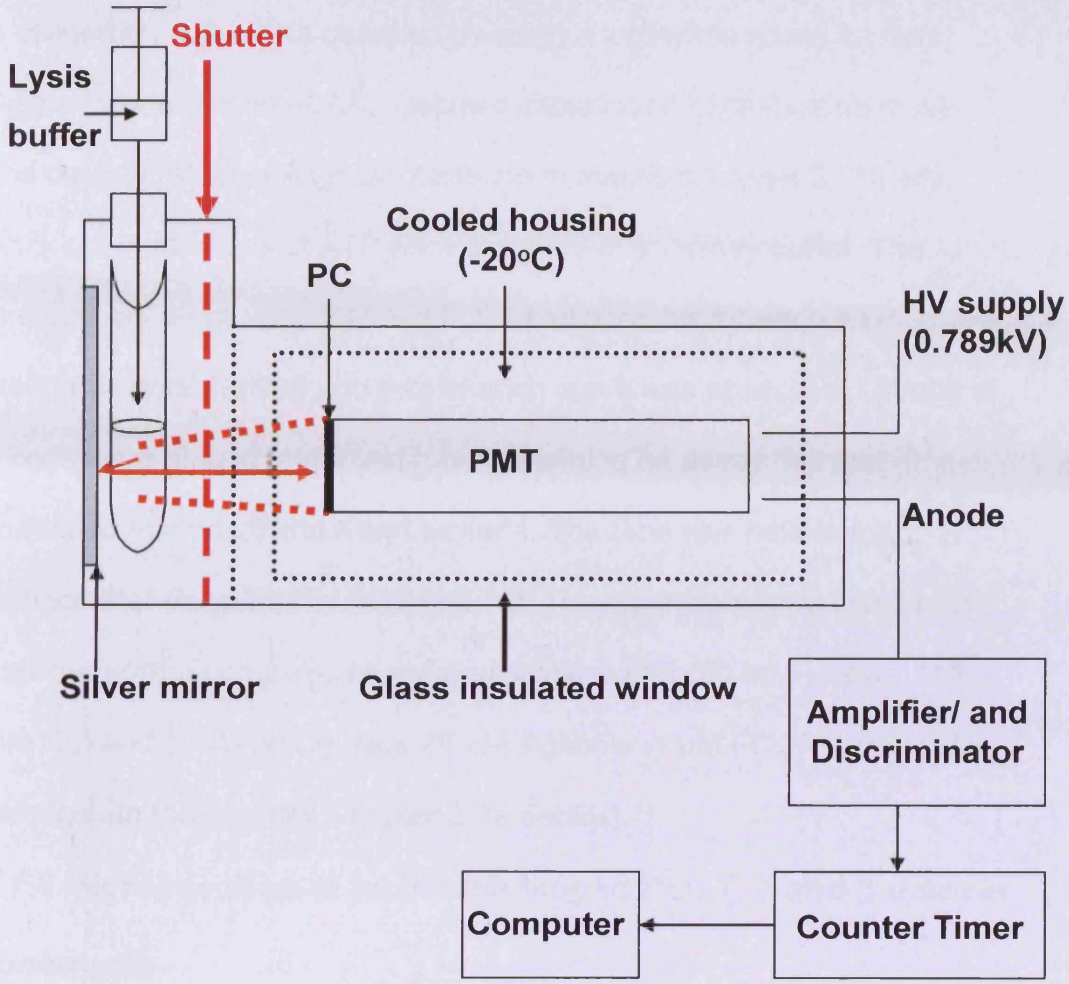

Fig. 2.8 Schematic diagram of a custom made luminometer. The sample is placed into a 5 ml tube and all shutters are closed. The lysis buffer is then injected into the tube and the light emitted from the sample is collected and amplified via the photocathode (PC) and dynodes within the PMT. The amplified signal is collected by the anode and finally arrives at the computer in the form of photons per second.

2.7.3 Measurement of ATP levels in eggs

A calibration curve was obtained by using a luciferase assay kit from Sigma (product code FLAA). Detailed explanation of calibration curve and concentration of ATP can be found in results (Chapter 3). Briefly, stock concentrations of ATP were prepared in an assay buffer. The luminescence cps was obtained in the luminometer for each ATP standard concentration and a calibration curve was produced. Groups of 5 eggs were placed into a test tube containing an assay mix that contained firefly luciferase and luciferin. The tube was held in the luminometer described in section 2.7.2. The eggs were then lysed with a lysis buffer that consisted of an intracellular buffer (20 mM Hepes, 140 mM KCl and 5 mM NaCl), plus 20 μM digitonin, 1 μM FCCP and 10 μM iodoacetate (see results Chapter 3 for details).

2.7.4 Microinjection of luciferase tagged PLC ζ, δ and β domain constructs

For experiments with luciferase-tagged PLC cRNA, eggs were microinjected with the appropriate cRNA mixed with an equal volume of 1 mM OGBD. Eggs were then maintained in H-KSOM with 100 μM luciferin and imaged. Fluorescence was monitored in these eggs for 4 hours after injection by measuring the OGBD fluorescence with low-level excitation light from a halogen lamp. Fluorescence and luminescence measurements were carried out separately. At the end of the fluorescence measurements, the same set of eggs were then monitored for luminescence by integrating light emission (in the absence of fluorescence excitation) for 30 minutes using the same cooled ICCD

camera, with all illumination sources closed. The fluorescence signals were typically 10-100 times greater than the luminescence signals. Ca^{2+} measurements for an egg were considered valid only if the same egg was also luminescent. Groups of eggs verified as being luminous, were then collected and placed in a test tube containing PBS with 1 mM $MgCl_2$, 1 mM ATP and 100 µM luciferin that was held in a custom-made luminometer equipped with a cooled S20 photomultiplier tube (see section 2.7.2 for details). The eggs were then lysed with 0.5% Triton X-100 and the steady state light was compared to that emitted from calibrated amounts of recombinant firefly luciferase (Sigma). The amount of luciferase activity measured for each group of eggs was then divided by the number of luminous eggs to obtain the mean value for protein expression of each type of PLC-LUC (see Chapter 7 for more details).

2.9 Statistical Analysis

All values stated throughout this thesis are the mean $\pm$ s.e.m, also all comparisons were done using the student's unpaired t-test (unless otherwise stated) and were stated as significant when a P value of less that 5% was obtained.

Chapter 3
The relationship between Ca^{2+} and ATP at fertilisation

3.1 Introduction

At fertilisation in mammals the sperm initiates a long lasting series of Ca^{2+} oscillations that persist until PN formation (Kline and Kline, 1992a; Marangos et al., 2003; Miyazaki et al., 1993). The Ca^{2+} signal in eggs of some species is associated with the activation of metabolism. In ascidian and mouse eggs Ca^{2+} oscillations have been shown to be associated with oscillations in autofluorescence of NADH and flavoproteins (Dumollard et al., 2003; Dumollard et al., 2004) suggesting that Ca^{2+} oscillations might stimulate an increase in ATP production in the mitochondria. In a previous study ATP was monitored during fertilisation in mouse eggs by measuring the luminescence of intracellularly injected firefly luciferase (Dumollard et al., 2004). This study reported a small increase in ATP during fertilisation in 36% of all mouse eggs imaged (Dumollard et al., 2004). Since it was not possible to measure Ca^{2+} at the same time when monitoring ATP, the relationship between ATP and Ca^{2+} could not be defined.

The main aim of this Chapter is to establish the relationship that exists between Ca^{2+} oscillations and ATP levels at fertilisation. Luminescence (ATP) and fluorescence (Ca^{2+}) shall be measured simultaneously from the same group of mouse eggs during fertilisation. This will enable a relationship between Ca^{2+} and ATP at fertilisation to be defined.

3.2 Results

3.2.1 Monitoring ATP luminescence in mouse eggs

Fig. 3.1a shows the luminescence from a single mouse egg injected with a pipette concentration of 7.5 mg/ml firefly luciferase and incubated in 100 μM luciferin for 24 hours. As reported previously in eggs and other cells, there was an initial decline in the luminescence signal that occurred whilst the luciferase and luciferin reached equilibrium (Dumollard et al., 2004; Gandelman et al., 1994). This initial run-in phase typically lasted around 30-40 minutes and was always complete within the first hour of recording (Dumollard et al., 2004). For this reason, the eggs were always allowed a run in period of 1 hour before any experimental procedure was carried out. This phase was then followed by a relatively stable period of light emission that lasted for many hours (8 hours; Fig. 3.1b). In many eggs there was then a slight increase in luminescence signal of 129% ± 1.7 (n=15), however, this typically occurred over 6 hours of recording. In prolonged recordings the luminescence was found to eventually decline to half the starting value in about 16 hours. This shows that the luciferase from single eggs is relatively stable for several hours. In subsequent traces the initial decline in luminescence is not shown since the luminescence was allowed to stabilise before the start of experiments.

Fig. 3. 1 Luminescence signal in an unfertilised egg

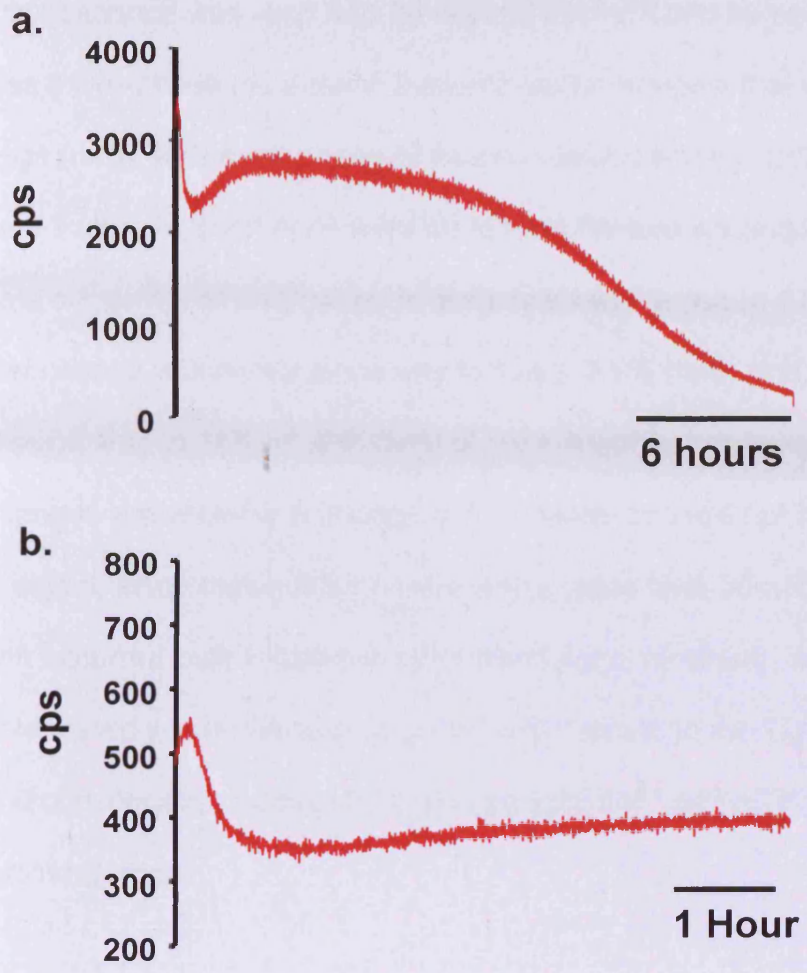

Fig. 3.1 a) Shows the typical luminescence signal (y-axis represents cps = counts per second) from a mouse egg injected with luciferase over the initial 24 hours of recording (n=15). b) The luminescence recorded from a single egg injected with firefly luciferase over the first 6 hours.

Fig. 3.2 shows the trace obtained when eggs were fertilised and luminescence was recorded for several hours. It can be seen that there was a two-phase increase in the luminescence signal that occurred in all eggs (n=6), with each phase of increase taking place over a 30 minute time frame. All such eggs went on to form PN and second PBs. These data suggest that fertilisation is associated with a rise in ATP levels. The first change in luminescence was to 124 $\pm$ 3.9% (n=6) and the second change was to 148 $\pm$ 6.3% (n=6) of the prefertilisation level. These changes are showing a change in ATP levels and are not due to the drift in signal, since these changes are taking place over 30 minutes and the drift occurred over 6 hours in unfertilised eggs. However, it could not be determined when changes occurred with respect to the Ca^{2+} oscillations and consequently I sought to measure both Ca^{2+} and ATP in the same fertilising eggs.

Fig. 3. 2 Luminescence signal in a fertilised egg

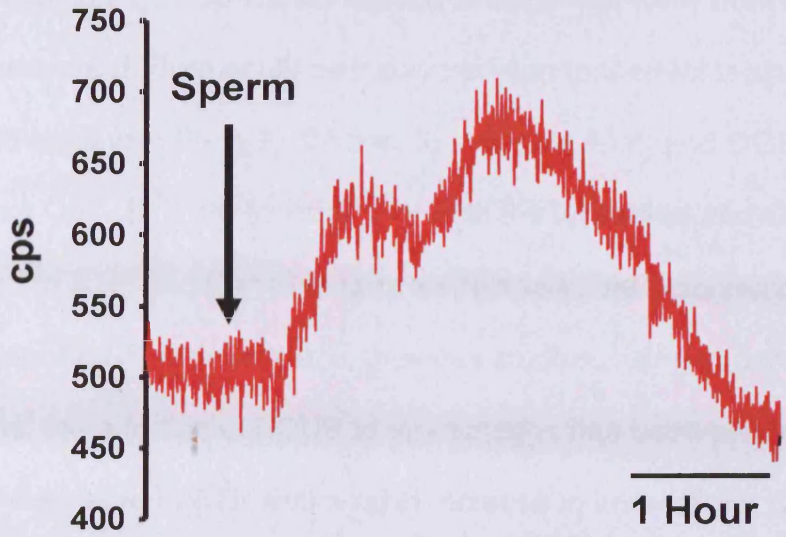

Fig. 3.2 Luminescent signal from a single egg injected with 7.5 mg/ml (pipette concentration) of firefly luciferase. The eggs were fertilised with sperm (as indicated with arrow) and after 6 hours, eggs were checked for signs of activation (i.e. 2nd PB and 2 PN) n=6.

3.2.2 Ca^{2+} and ATP in a mouse egg

The image in Fig. 3.3a shows a group of eggs that were both luminescent and fluorescent. Both could be measured due to the fact that we had co-injected eggs with firefly luciferase, to measure ATP, and OGBD, to measure Ca^{2+}. In order to verify that both the luciferase and OGBD could respond to ATP and Ca^{2+} changes respectively, the mitochondrial uncoupler FCCP was added. In previous studies, using separate imaging systems, the addition of FCCP to mouse eggs has been shown to cause a large decrease in ATP and a rapid increase in intracellular Ca^{2+} (Dumollard et al., 2004; Liu et al., 2001)

Fig. 3.3b shows the changes recorded when 1 μM FCCP was added to mouse eggs injected with luciferase and OGBD. There was a rapid decrease in luciferase luminescence. The Ca^{2+} levels indicated by OGBD fluorescence showed an initial rapid increase followed by a slower and sustained rise. The patterns of change for both probes are similar to those seen in previous studies carried out on different sets of eggs (Dumollard et al., 2004). This data supports the idea that mouse eggs are dependent on mitochondria for ATP production and that continuous ATP production is required to maintain resting Ca^{2+} levels. In addition, these results suggest that we can monitor the dynamic changes in intracellular ATP and Ca^{2+} over the same time period in the same sets of eggs.

Fig. 3. 3 Luminescence and fluorescence in the same eggs

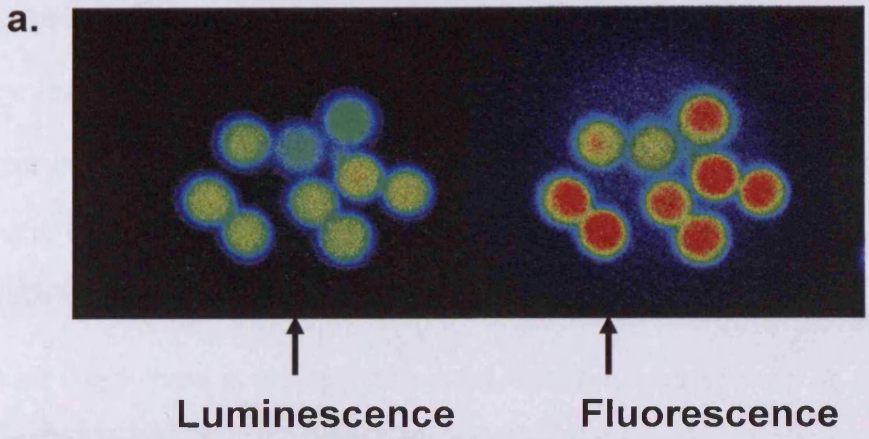

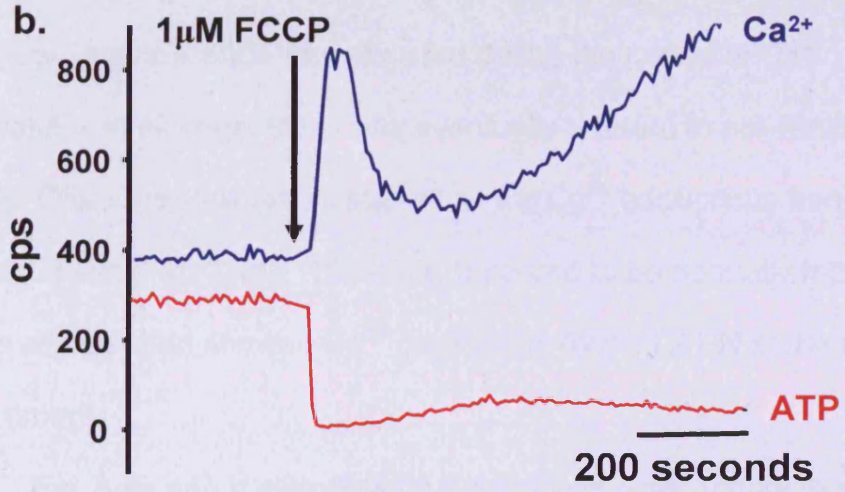

Fig. 3.3. a) The fluorescence and luminescence images are shown of a group of eggs that had been injected with both firefly luciferase and OGBD. The left side of the image is the luminescent signal; the right side of the image is the same group of eggs showing their fluorescent signal. b) Shows a trace of the changes in luciferase luminescence (red) and OGBD fluorescence (blue) when an egg was exposed to 1μM FCCP (typical of 15 eggs).

3.2.3 Ca^{2+} oscillations at fertilisation are correlated with an ATP increase

Eggs that had been injected with OGBD and luciferase were imaged as above and inseminated with capacitated sperm. Fig.3.4a and b show the familiar characteristic pattern of Ca^{2+} oscillations in fertilising mouse eggs, as well as the changes in ATP as indicated by luciferase luminescence. It can be seen there is an increase in luciferase luminescence as soon as the Ca^{2+} oscillations start at fertilisation. Fig. 3.5 shows that the start of the luminescence increase could be seen to occur during the first Ca^{2+} transient at fertilisation and this was typical of all 38 eggs imaged. Although luminescence was elevated during the period of Ca^{2+} oscillations in all eggs, there was eventually a return to pre-fertilisation levels. Often the slow return started as the Ca^{2+} oscillations frequency slowed down (Fig. 3.4b). The eggs appeared to be normally fertilised since all eggs that showed Ca^{2+} oscillations formed 2 PN at the end of the experiment.

Fig. 3.4a and b also show that there was a secondary increase in luciferase luminescence. This secondary rise in luciferase signal occurred in 34/38 eggs and occurred 60 $\pm$ 23.1 minutes after the onset of Ca^{2+} oscillations that corresponds to the 9^{th} Ca^{2+} oscillation ($\pm$ 0.9, n=34).

Fig. 3. 4 ATP and Ca^{2+} in a fertilised egg

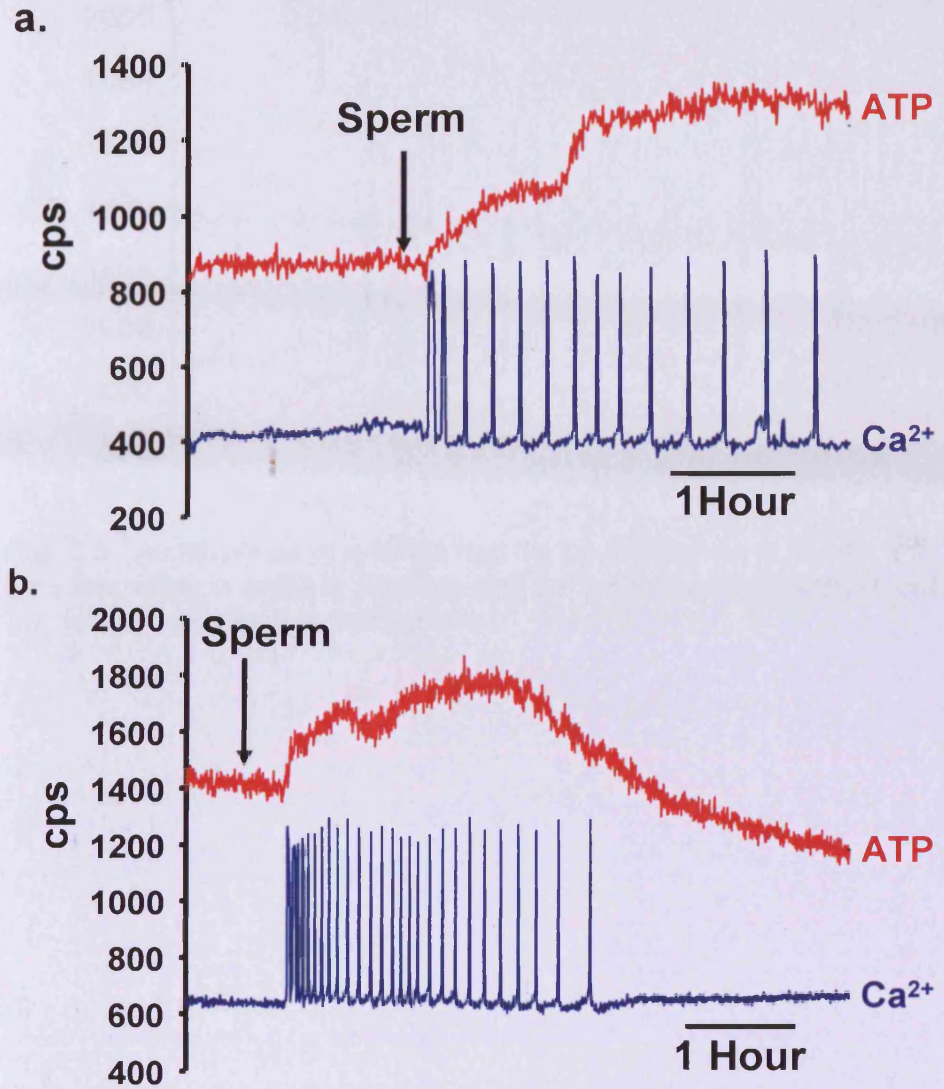

Fig. 3.4. a) Shows a trace of both the luminescence and fluorescence signal from a single egg. The graph shows an initial and secondary change in luminescence occurring during sperm induced Ca^{2+} oscillations. In b) a similar experiment is shown to a) but the recording display is extended to show the full extent of the luminescence change during and after Ca^{2+} oscillations at fertilisation.

Fig. 3. 5 Initial increase in ATP at fertilisation

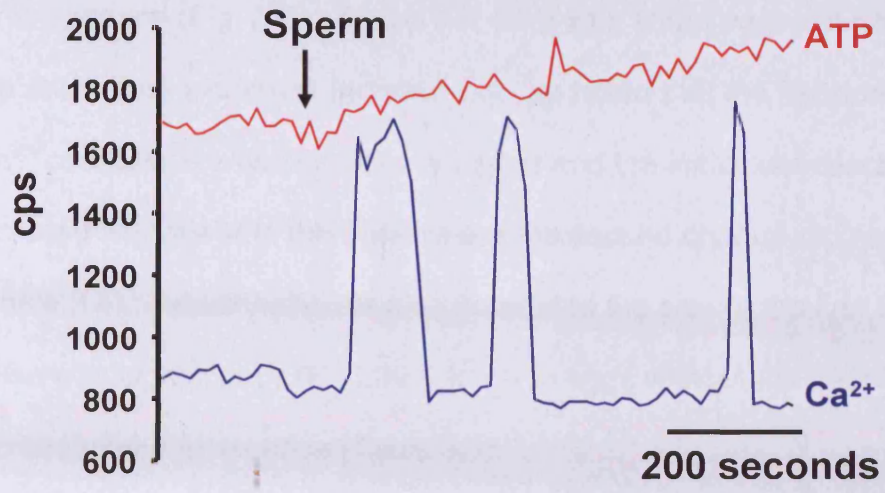

Fig. 3.5 The response of a single egg during fertilisation is shown with a shorter time resolution in order to illustrate that the luminescence increase occurs during the 1st Ca^{2+} increase at fertilisation.

Only 4 of the observed eggs showed no substantial 2nd increase in luminescence (Fig. 3.6a). It was not clear why some eggs did not show the secondary luciferase increase but, we noted that the frequency of Ca^{2+} oscillations was significantly higher and the initial luminescence increase was lower in the eggs where the second change did not occur (Table 3.1). Additionally, we also noted that the size of the first Ca^{2+} spike was significantly ($P<0.005$) lower in eggs without the secondary increase in luminescence (Table 3.1).

The increase in luciferase luminescence was a highly consistent result throughout all experiments. It occurred in all the above eggs that were collected and fertilised within 18 hours after hCG injection. When eggs were inseminated that had been aged *in vitro* and fertilised 20-22 hours after hCG injection, few eggs underwent Ca^{2+} oscillations. In cases where Ca^{2+} oscillations were seen, the oscillations were of a significantly higher frequency compared to fertilised fresh eggs. However, an increase in luciferase luminescence was still observed (Fig. 3.6b and Table 3.1) despite the age of the eggs and high frequency Ca^{2+} oscillations.

Fig. 3. 6 ATP and Calcium during fertilisation

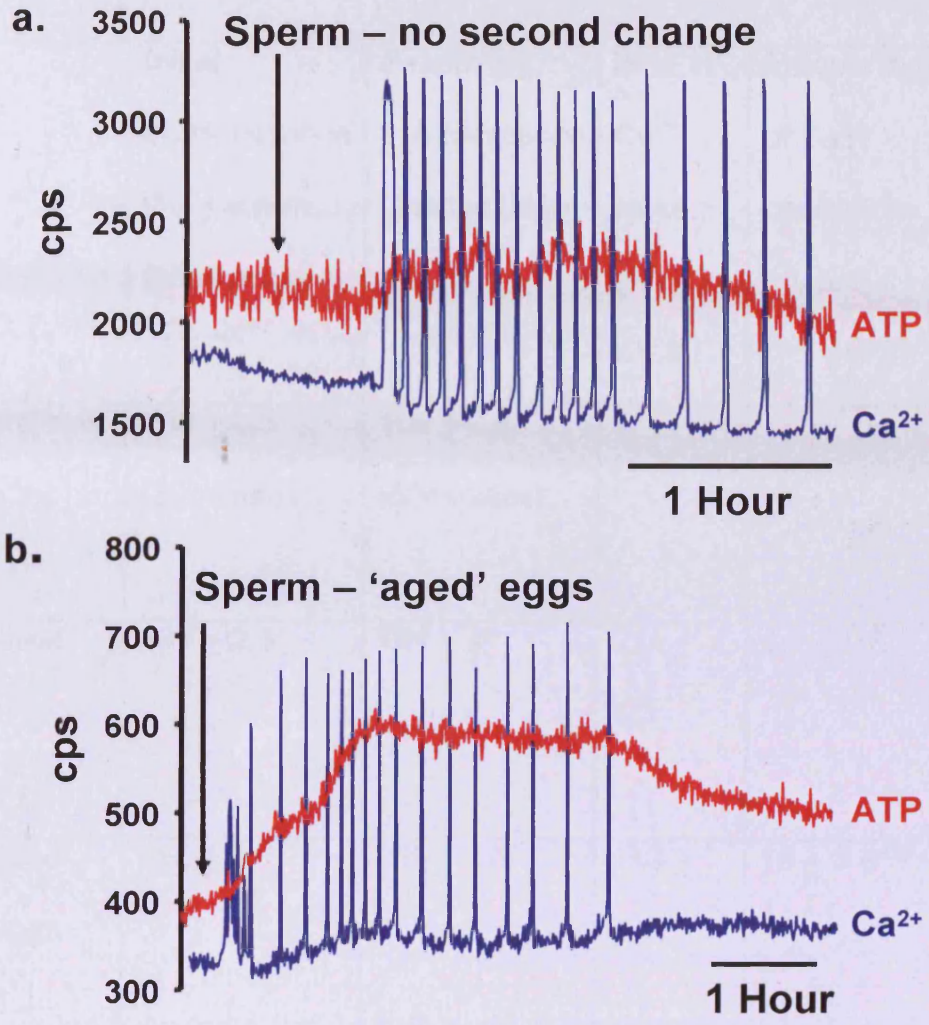

Fig. 3.6. In a) a recording is shown from an egg that underwent the initial change in luminescence at fertilisation but failed to show the secondary increase (n=4). In b) the luminescence change is shown for an egg that was fertilised 22 hours after hCG injection (n=4).

Table 3.1 – Ca^{2+} and luciferase luminescence response in eggs at fertilisation

	Initial Luminescence (%) ± s.e.m (1^{st} change)	Secondary Luminescence Change (%) ± s.e.m	Size 1^{st} Ca^{2+} spike (%) ± s.e.m	Frequency/hour of Ca^{2+} oscillations ± s.e.m
Unfertilised eggs (n=15)	102 ± 0.3 (30minutes)	104 ± 0.2 (60minutes)	-	-
Fertilised eggs (n=34)	131 ± 2.3*	161 ± 4*	211 ± 8.3	8.7 ± 0.6
Fertilised Old eggs (n=4)	125 ± 11*	150 ± 6.6*	183 ± 1.7**	15 ± 3.8***
Fertilised eggs (no 2^{nd} change) (n=4)	109 ± 2.7*		188 ± 7.8**	13 ± 1.3***

Table 3.1 Eggs were exposed to different conditions and both the luminescence and Ca^{2+} response were measured for approximately 6 hours. The percentage change is expressed in relation to the initial luminescence value before the Ca^{2+} stimulus was applied. All values are the mean from the stated total number of eggs ± the s.e.m. The luminescence response from fertilised were each compared to luminescence values from unfertilised eggs using student's unpaired t-test (*$P<0.005$). The size of the 1^{st} Ca^{2+} transient at fertilisation was compared to the size of the 1^{st} Ca^{2+} transient at fertilisation in aged eggs

and fertilised eggs that showed no 2nd change in luminescence (**P<0.005). The frequency of Ca^{2+} oscillations at fertilisation was compared to the eggs fertilised with sperm that had both the first and second change in luminescence (***P<0.005).

In aged eggs the second change in luminescence was detected at the 15th spike ($\pm$ 4.0, n=4), but still typically around 60 $\pm$ 6 minutes (n=4) after the 1st spike occurred. The overall increase of luminescence in aged eggs was significantly lower than that of fresh eggs ($P<0.005$). These data suggest that Ca^{2+} oscillations at fertilisation are associated with a sudden elevation of ATP levels in eggs, regardless of post-ovulatory age.

Furthermore, the increase in ATP lasts throughout most of the period that Ca^{2+} oscillations occur. Since high frequency oscillations in aged eggs still led to an increase in luciferase luminescence, we fertilised fresh eggs in high Ca^{2+} (10 mM) to test if ATP levels still increased when abnormally high Ca^{2+} oscillations were induced (Fig. 3.7). Indeed, a very high frequency of Ca^{2+} oscillations were obtained, however, the luminescence signal still consistently increased with the first Ca^{2+} transient, suggesting that at fertilisation ATP will always increase despite the frequency of oscillations the egg undergoes.

Fig. 3. 7 Fertilisation in high Ca^{2+}

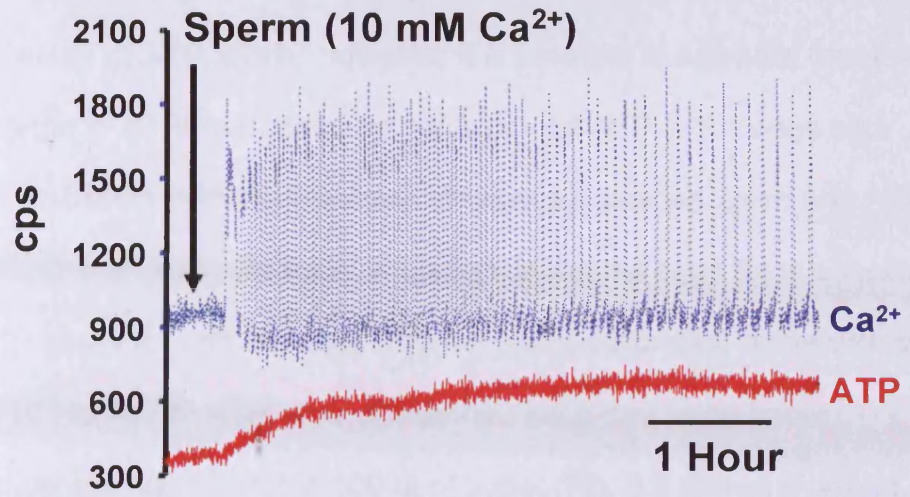

Fig. 3.7 Eggs were fertilised in the presence of high Ca^{2+} (10 mM) and displayed an increase in luminescence with a very high frequency of Ca^{2+} oscillations (n=8).

3.2.4 ATP content in a single mouse egg

The luminescence of luciferase being measured is only a relative measure of ATP levels. However, it is possible to estimate the absolute change in ATP from measurements of total ATP in the eggs and extrapolation from the relationship between luminescence and ATP. To establish an estimate for ATP content in mouse eggs for this thesis, an ATP assay kit was obtained (Sigma) and a calibration curve with a range of 10^{-5} to 10^{-9} M ATP, was established each day using known concentrations of ATP in 100 µl of buffer (Fig. 3.8 shows a typical calibration curve). A linear regression analysis was performed (Sigma Plot) on the curve to obtain the linear regression equation (Fig. 3.8). For this equation the unknown ATP concentration from the sample is x and the luminescence cps obtained from the sample is y. Once the ATP concentration from the sample has been calculated (M), the number of moles of ATP present in the sample can be obtained by multiplying by $1x10^{-4}$ since the sample was 100 µl. Finally, the ATP concentration in a single egg can be established by dividing the number of moles of ATP by the volume of an egg.

Fig. 3. 8 Calibration curve for firefly luciferase

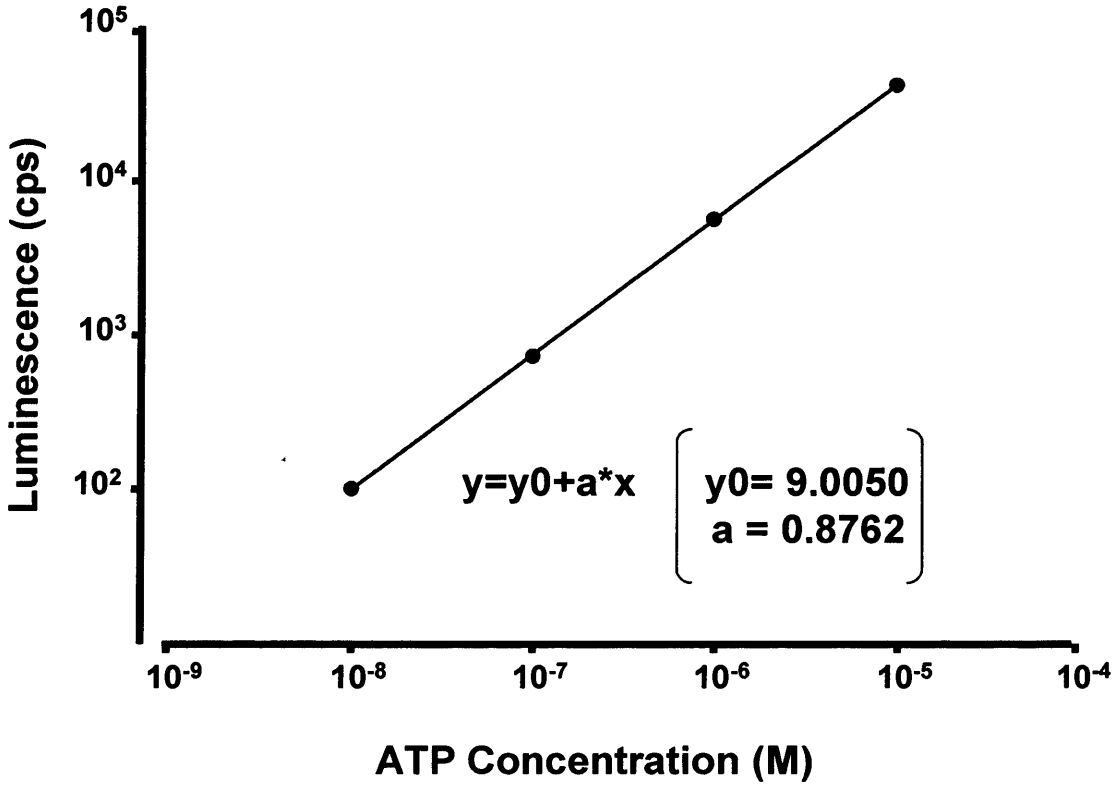

Fig. 3.8 Calibration curve obtained by using known concentrations of ATP in 100 µl. The equation was obtained by linear regression analysis of the data and was used to establish the ATP content when eggs were lysed.

The first approach was to lyse 5 eggs with 40 µM digitonin (Fig. 3.9a, n=10, 2 runs) where a value of over 1000 cps was obtained. Using the equation (example shown in Fig. 3.8), it was estimated that each egg had an ATP protein content of 4 pmoles. Assuming a volume of 200 pl for a single egg and using the estimate of 4 pmoles, a value of 20 mM ATP was obtained for a single egg. This value is far from expected and there was concern the ATP stocks may be contaminated. However, when fresh ATP was used high ATP values were still obtained (16.5 mM, data not shown).

Digitonin lysis produced a continual increase in the luminescence signal suggesting ATP turnover was still occurring due to the non-specific action of digitonin. Oxidative phosphorylation and glycolysis could still be producing ATP after the digitonin addition, giving the impression of abnormally high ATP values for our absolute measure. Therefore, oxidative phosphorylation and glycolytic pathways were targeted directly using specific poisons to ensure ATP turnover was stopped completely during the lysis. When 40 µM digitonin was added with 1 µM FCCP (to uncouple the mitochondria – Fig. 3.9b, n=15, 3 runs) the overall cps were lower than digitonin alone and after the appropriate calculations an ATP content of 8 mM was established per egg. However, a secondary late, and unexpected, increase in luminescence was detected during the lysis that occurred in all 3 runs. This result suggested that there was still ATP turnover via another pathway, which was thought to be glycolysis. Although glycolysis has low activity in eggs (Barbehenn et al., 1974), it is possible that a small turnover of ATP via this pathway is encouraged

during abnormal and stressful conditions. Bearing this in mind, the next approach was to lyse 5 eggs using 40 μM digitonin and 10 μM iodoacetate (to block glycolysis – Fig. 3.9c, n=15, 3 runs). The ATP content per egg was estimated to be around 10 mM but, it was difficult to determine an absolute value since the luminescence level was continually increasing. The continual increase in luminescence suggests that ATP production is still continuing (via oxidative phosphorylation, since FCCP was not present).

The final approach was to use all three agents (40μM digitonin, 10 μM iodoacetate and 1 μM FCCP – Fig. 3.9d) in the lysis mixture. This resulted in a relatively steady level of luminescence and when calculated, over 5 runs lysing 5 eggs at a time, an average ATP content in a single mouse egg was found to be 1.88 mM. From the relationship between ATP and luciferase luminescence that was established using the same conditions as described previously (Allue et al., 1996), I can estimate that the peak luminescence increase to 160% we found in our typical fertilisation experiments, corresponds to an ATP increase to 3.02mM.

Fig. 3. 9 Lysis method to determine ATP content

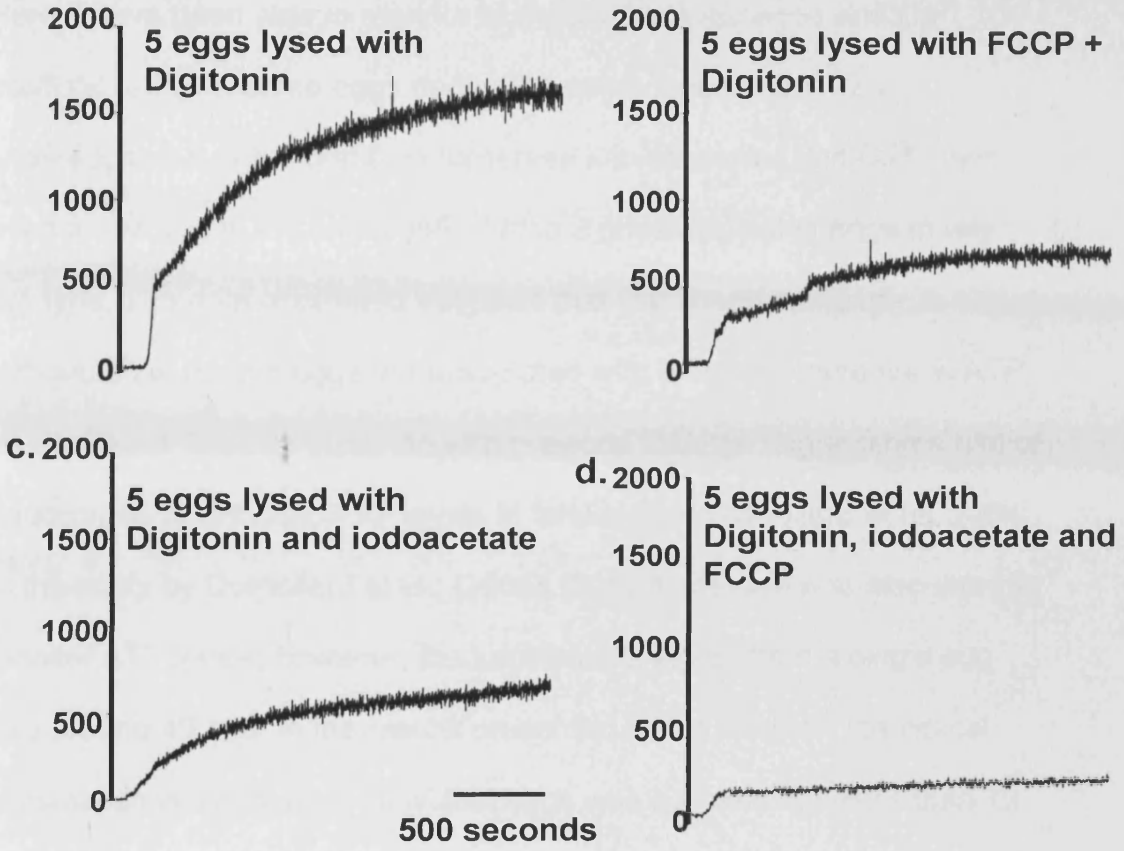

Fig. 3.9 Groups of 5 eggs were lysed in a luminometer using a) 40 μM digitonin (n=10, 2 runs) b) 40 μM digitonin and 1 μM FCCP (n=15, 3 runs) c) 40 μM digitonin and 10 μM iodoacetate (n=15, 3 runs) d) 40 μM digitonin, 1 μM FCCP and 10 μM iodoacetate (n=25, 5 runs) Time bar applies to all graphs.

3.3 Discussion

Here, I have been able to monitor luciferase luminescence and Ca^{2+} oscillations in the same eggs during the same time period. To my knowledge, this is the first time luciferase luminescence and Ca^{2+} have been monitored in the same cells during a physiological change in any cell type. The data presented suggests that Ca^{2+} oscillations at fertilisation in mouse eggs are associated with a definite increase in ATP levels. These findings correlate with previous findings suggesting a hint of an increase in cytosolic ATP levels at fertilisation (Dumollard et al., 2004). In the study by Dumollard et al., (2004), firefly luciferase was also used to monitor ATP levels; however, the luminescent signal from a single egg was around 40 cps. In the results presented in this chapter, the typical luminescence signal from individual eggs was consistently more than 10 times greater than previously published (Dumollard et al., 2004), which is probably why the results presented show a more definitive change in luminescence levels during fertilisation.

Fluorescence measurements in mouse eggs with an Mg^{2+} sensitive dye has shown that Ca^{2+} oscillations at fertilisation are associated with a transient increase and then a prolonged decrease in intracellular free Mg^{2+} concentrations. These changes were interpreted as being due to an initial decrease followed by an increase in ATP at fertilisation in fresh mouse eggs (Igarashi et al., 2005). The secondary increase in ATP is consistent with my current data using firefly luciferase as indicator of ATP levels, and supports the idea that ATP increases at fertilisation in the mouse. However, unlike Igarashi *et al.* (2005), I did not

find any evidence for a transient decrease in ATP during each Ca^{2+} transient. In addition the ATP increase also occurred in aged eggs 20-22 hours after hCG injection, despite recent indirect evidence for a decrease in ATP levels in aged eggs 18.5 hours post hCG injection (Igarashi et al., 2005). The Mg^{2+}-Green dye method is an indirect method for monitoring ATP, compared with firefly luciferase, since Mg^{2+}-Green can also be used as a Ca^{2+} indicator (Chen and Regehr, 1999; Regehr and Atluri, 1995; Regehr and Tank, 1991), so it is possible that some of the apparent changes in ATP are due to the confounding effects of changes in other factors at fertilisation such as Ca^{2+} and Mg^{2+}. Since firefly luciferase is a specific indicator of ATP, the luciferase luminescence increase that we see at fertilisation is highly likely to reflect an increase in ATP concentration.

A main factor that should be considered for firefly luciferase is that its luminescence depends upon intracellular pH (Koop and Cobbold, 1993). However, there are no changes in intracellular pH in mouse eggs during either fertilisation, or, parthenogenetic activation (Kline and Zagray, 1995; Phillips and Baltz, 1996). This appears to be due to the lack of an active Na^+/H^+ antiporter in the PM of mouse eggs (Kline and Zagray, 1995; Phillips and Baltz, 1996).

Resting ATP levels in individual mouse eggs was found to correspond to a cytoplasmic concentration of about 1.88mM. This is in the middle of the range (0.8-5mM) of the resting ATP concentrations in mouse eggs, which have been reported by various groups (Albertini et al., 2003; Igarashi et al., 2005; Van Blerkom et al., 1995). Previous studies

used rapid freeze/thaw lysis methods to establish ATP content in single mouse eggs and use undefined lysis media. It is likely that these techniques produce inconsistent values since the eggs are being stressed prior to the lysis and the oxidative phorphorylation and glycolytic pathways are not being targeted. Taking our value of 1.88mM we can estimate that at the peak ATP concentration at fertilisation, ATP levels have increased to around 3.02mM. This is consistent with the evidence that mouse eggs predominantly rely on mitochondrial oxidative phosphorylation (Dumollard et al., 2004). Unfortunately, it was not possible to examine the effects of Ca^{2+} on mitochondria more directly with ruthenium red derivatives, because they appear to be ineffective in blocking Ca^{2+} uptake into mitochondria in mouse eggs (unpublished observations Campbell and Swann. 2005; Dumollard et al., 2006).

This chapter has identified that cytosolic ATP levels undergo a significant increase at fertilisation. The increase in ATP appears to occur at fertilisation despite post ovulatory age of the eggs and frequency of Ca^{2+} oscillations, suggesting that a rise in ATP is essential for successful activation. Whether Ca^{2+} oscillations control the rise in ATP is undefined and shall be further investigated in the next chapter. In addition, this chapter has also discovered a 2^{nd} increase in ATP levels that was an unexpected result. This nature of this secondary ATP rise will be looked at in greater detail at a later point in this thesis (Chapter 6).

Chapter 4
ATP dependence upon Ca^{2+} changes

4.1 Introduction

In chapter 3 it was established that during IVF a rise in ATP levels occurs during Ca^{2+} oscillations. The tight correlation between Ca^{2+} oscillations and the luciferase luminescence increase suggests that Ca^{2+} oscillations cause the rise in ATP levels.

Mitochondria are the main regulators of intracellular Ca^{2+} homeostasis (Duchen, 2004; Rizzuto et al., 2000). The mitochondria of sea urchin (Eisen and Reynolds, 1985) and ascidian eggs (Dumollard et al., 2003) have been demonstrated to sequester Ca^{2+} during sperm induced Ca^{2+} oscillations. Mitochondrial accumulation of Ca^{2+} triggers the activation of mitochondrial metabolic processes, which increases the synthesis of ATP in the mitochondria and hence, ATP levels in the cytosol increase. It has been demonstrated in other cell types (HeLa, pancreatic β and MIN6 cells) that cytosolic ATP levels increase when Ca^{2+} levels in the cytosol increase (Jouaville et al., 1999; Kennedy et al., 1999). When the mitochondrial Ca^{2+} uptake is reduced in the mitochondria of skeletal myotube cells, the ATP response is significantly reduced. Also, in HeLa cells the presence of the Ca^{2+} buffer BAPTA prevents both a Ca^{2+} and ATP response when the cells were challenged with histamine.

This would suggest that the ATP response in mouse eggs is finely regulated by the different patterns of cytosolic Ca^{2+} levels in response to different Ca^{2+} stimuli. This shall be further investigated in the following chapter by looking at the Ca^{2+} and ATP relationship that exists in response to different Ca^{2+} releasing agents.

4.2 Results

4.2.1 The increase in ATP is Ca^{2+} dependent

To test if Ca^{2+} oscillations are necessary for the ATP change, eggs were injected with firefly luciferase, OGBD, and the Ca^{2+} chelator BAPTA (~1 mM final concentration). When sperm were added to these eggs there was no change in Ca^{2+} levels or, luciferase luminescence (Fig. 4.1a). In 9 such eggs we verified that sperm entry had occurred at the end of the 6-hour recording period by staining the eggs with Hoechst dye (Fig. 4.1b) (Raz et al., 1998). In some cases polyspermy occurred due to the absence of the ZP. Since the eggs were activated without a change in Ca^{2+} or, ATP this suggests that a Ca^{2+} increase is necessary for an ATP increase at fertilisation.

The next approach was to investigate if the continuous presence of Ca^{2+} is required to maintain the apparent increase in ATP. To explore this, eggs were fertilised and BAPTA was added to the medium around the eggs (final concentration 2 mM) after Ca^{2+} oscillations were observed to have began. The presence of BAPTA in the extracellular media chelates the extracellular Ca^{2+}. As reported previously, this procedure to chelate extracellular Ca^{2+} stops, or reduces the frequency of, Ca^{2+}oscillations. Figure 4.2 shows that when Ca^{2+} oscillations stopped after the addition of BAPTA, the luminescence signal started to decline. This suggests that Ca^{2+} transients are not only required to initiate a rise in ATP levels, but that Ca^{2+} oscillations are necessary to maintain continuous increases in ATP levels.

Fig. 4. 1 BAPTA injected eggs during fertilisation

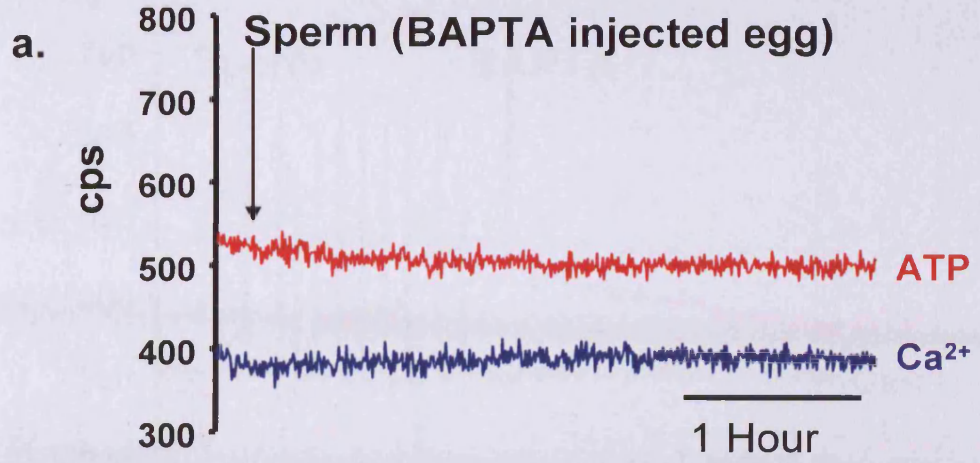

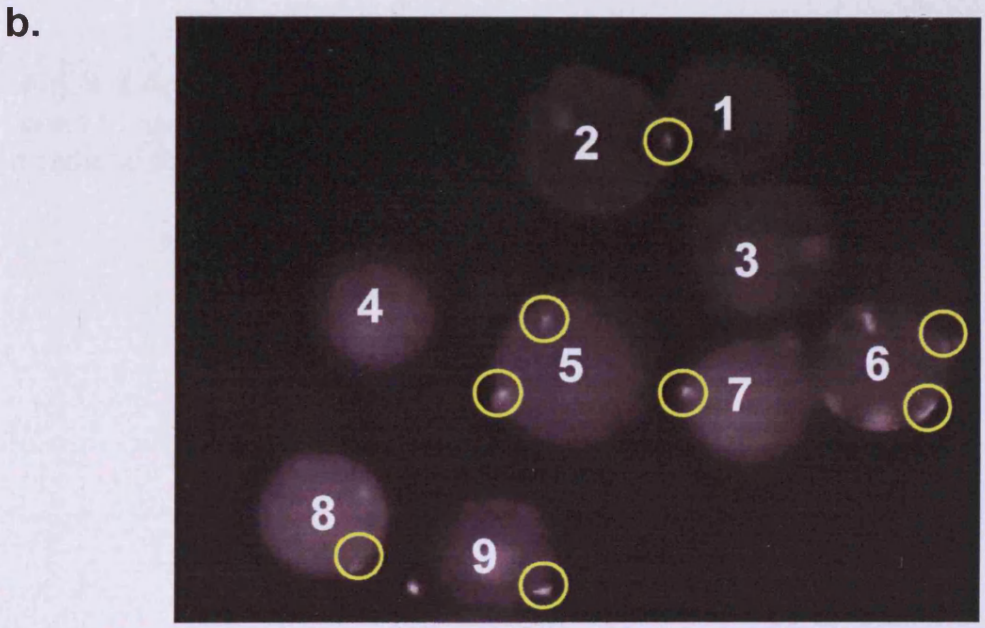

Fig. 4.1 a) eggs were injected with 20 mM BAPTA (pipette concentration) before being fertilised (n=9) b) fertilised eggs injected with BAPTA were stained with Hoechst 33342 to confirm sperm entry as shown by yellow circles in eggs 2, 5, 6, 7, 8 and 9 (eggs were numbered in ascending order starting from the top of the image)

Fig. 4. 2 BAPTA addition during fertilisation

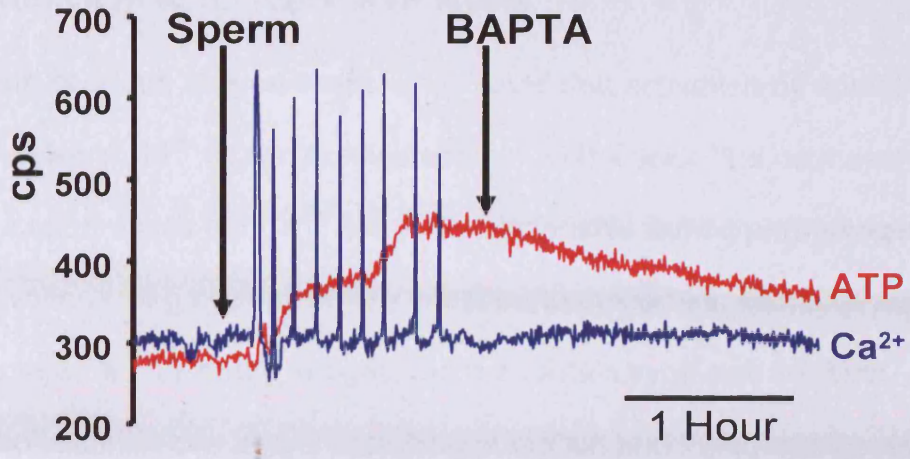

Fig. 4.2 An egg was fertilised with sperm and after Ca^{2+} oscillations were seen to have started, BAPTA (2 mM final concentration) was added to the media to stop the Ca^{2+} oscillations (n=10).

4.2.2 Parthenogenetic activation without a Ca^{2+} change is insufficient to increase ATP levels

In the previous section it was established that activation by sperm produces a Ca^{2+} dependent increase in ATP levels. The next avenue to be explored was the Ca^{2+} and ATP relationship during parthenogenetic activation using cycloheximide. Most parthenogenetic stimuli in mammals cause a Ca^{2+} increase in eggs, but the protein synthesis inhibitor cycloheximide can trigger meiotic resumption and PN formation without causing any Ca^{2+} increase (Bos-Mikich et al., 1995). When eggs were treated with 20 μg/ml cycloheximide no change in Ca^{2+} was seen and only a slight increase in luminescence was recorded (Fig. 4.3). All eggs activated with cycloheximide were checked for PN and 2nd PB formation to confirm successful activation. The slight drift up in luciferase luminescence to 115% (± 5.0, s.e.m, n=16) was recorded over 4 hours, but this is not significantly different from the drift up in signal over 4 hours that is shown in Fig. 3.1b (116 ± 1.2, n=15). This suggests the meiotic resumption or cell cycle resumption as such, is the not the cause of the increase in ATP during fertilisation of mouse eggs. From the data presented in this section it seems most likely that changes in cytosolic Ca^{2+} levels is the cause of changes in ATP levels in the cytosol.

Fig. 4. 3 Cycloheximide activation of mouse eggs

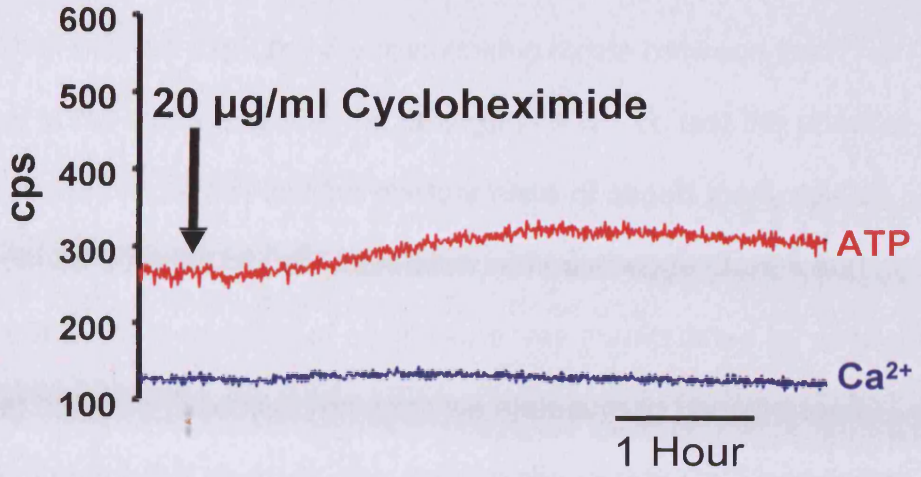

Fig. 4.3 Eggs were pathenogenetically activated with cycloheximide (n=16)

4.2.3 Ca^{2+} and ATP changes can be induced by uncaging $InsP_3$

Now it has been established that the ATP change is dependent upon Ca^{2+}, it shall now be explored if a relationship exists between the frequency of the transients and the change in ATP. To test the effect of $InsP_3$ increases more directly the photorelease of caged $InsP_3$ can be used to cause a series of Ca^{2+} increases in mouse eggs (Jones and Nixon, 2000). The frequency of oscillations was manipulated by uncaging $InsP_3$ that had been injected into eggs via exposure to UV light for 10 seconds at controlled intervals. Fig. 4.4 a-c shows that Ca^{2+} transients could be generated. The transients were not always constant and the amplitude of the Ca^{2+} increase was not as large as those seen at fertilisation (see Table 4.1).

Although an increase in luminescence occurred when $InsP_3$ was uncaged every 10 and 5 minutes, the increase did not occur with the 1st Ca^{2+} oscillation, as shown in fertilising eggs in Chapter 3. This suggests that $InsP_3$ alone is unable to recreate the physiological response produced by sperm activation. When $InsP_3$ was uncaged every 10minutes (Fig. 4.4a), the luminescence increased to 114 $\pm$ 3.2% (n=6), typically after spike 2, 10 minutes after the 1st spike occurred. When the frequency was increased to every 5 minutes (Fig. 4.4b), the luminescence signal increased after 15 minutes at spike 3 and to 119 $\pm$ 2.9% (n=10). However, at a frequency of 1 pulse every 2.5minutes (Fig. 4.4c), the luminescence decreased by 14.5 $\pm$ 2.4% (n=8) with the 1st Ca^{2+} spike and only recovered when no more $InsP_3$ could be uncaged. This result suggests that when too much $InsP_3$ is released into the egg, the ATP

supply and demand becomes unbalanced leading to a decrease in cytosolic ATP levels. Referring back to Chapter 3, when eggs were fertilised in high (10 mM) Ca^{2+}, despite a very high frequency of Ca^{2+} oscillations the ATP still increased. Together, these results would further imply that the physiological relationship of Ca^{2+} and ATP at fertilisation is difficult to reproduce artificially, but reinforces the suggestion that Ca^{2+} and ATP exist within cells in close harmony.

All changes in luminescence recorded with uncaging of $InsP_3$ in all explored conditions (i.e. 10, 5 or, 2.5 minutes) were significantly different to the control drift in luminescence observed in non-fertilised eggs over 30 minutes ($P<0.005$) (see Chapter 3 Table 3.1). These data suggest that repetitive Ca^{2+} increases generated by the uncaging of $InsP_3$ can cause changes in cytosolic ATP levels.

Briefly, caged Ca^{2+} and ATP were also explored, but it was difficult to uncage a sufficient amount of each of these compounds to mimic the changes at fertilisation (unpublished observations).

Fig. 4. 4 Uncaging $InsP_3$ in mouse eggs

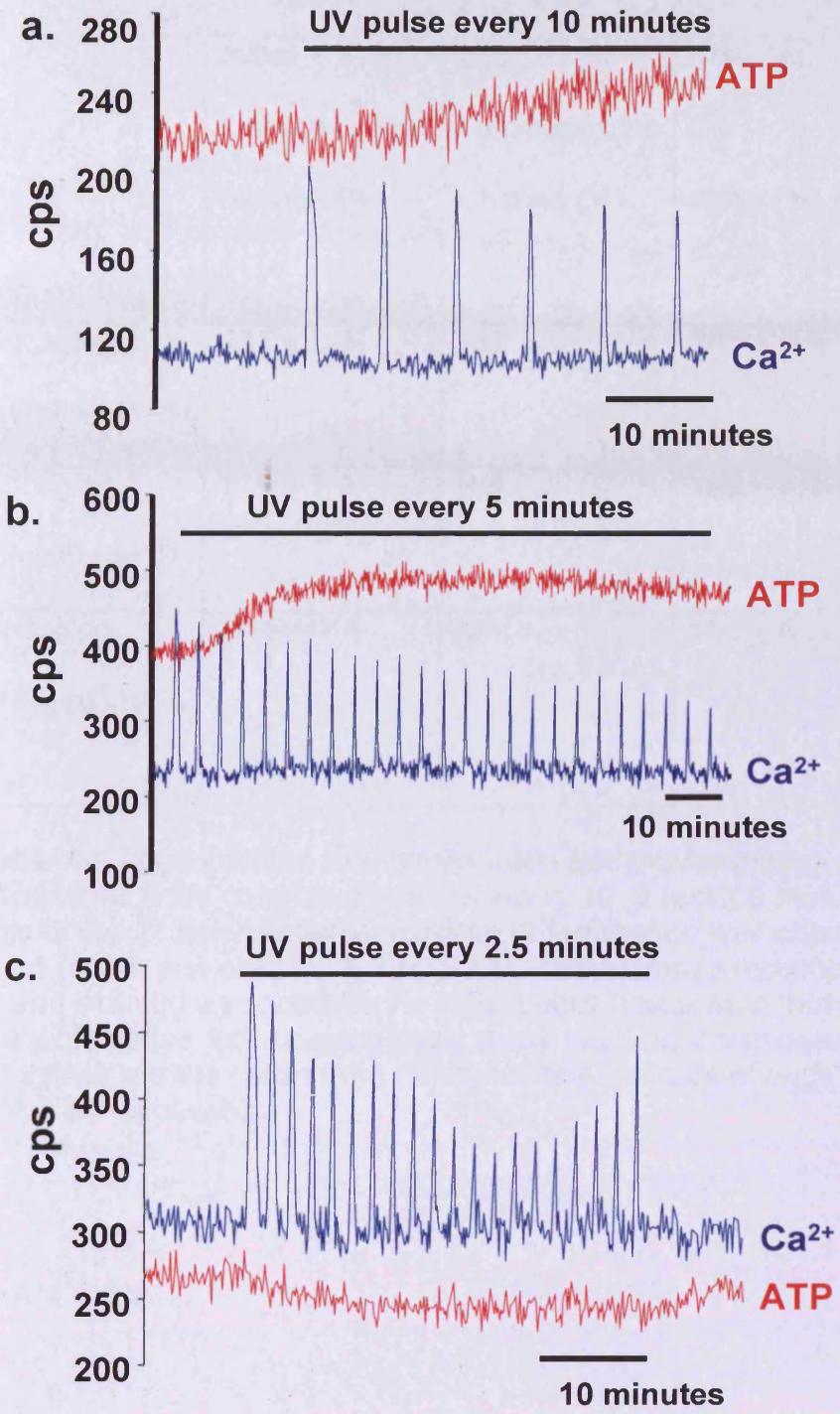

Fig. 4.4 Ca^{2+} oscillations were triggered in eggs when caged $InsP_3$ was injected and eggs were exposed to UV light for 10 seconds at controlled intervals. Ca^{2+} transients were triggered every a) 10mins (n=6), b) 5mins (n=10) and c) 2.5mins (n=8)

Table 4.1 Uncaging data

	Initial Luminescence change (%)	2nd Luminescence Change (%)	Size 1st Ca^{2+} spike (%)	Frequency of Ca^{2+} oscillations (spikes/hr)
Uncaging (10mins) (n=6)	114 ± 3.3	N/A	203 ± 6.9	6
Uncaging (5mins) (n=10)	119 ± 2.9	N/A	183 ± 7.1	12
Uncaging (2.5mins)(n=8)	85.5 ± 2.4	N/A	150 ± 5	24

Table 4.1 Eggs injected with caged $InsP_3$ and the frequency of oscillations were controlled to occur every 10, 5 and 2.5 minutes. The size of the 1st luminescence increase at fertilisation was shown to be 131 ± 3.1 (n=38, see chapter 3, Table 3.1). This increase recorded during sperm induced egg activation is significantly higher than those detailed in the table above for uncaging $InsP_3$ every 10, 5 or, 2.5 minues ($P<0.005$). All values are the mean from the stated total number of eggs ± the s.e.m. N/A = not applicable

4.2.4 Ca^{2+} releasing agents that act via the $InsP_3$ pathway produce an increase in ATP

Since it has been established that ATP changes are dependent upon Ca^{2+} levels, the next approach was to investigate if the source of the Ca^{2+} release produced different ATP responses. At fertilisation, Ca^{2+} increases occur via the $InsP_3$ pathway and so to mimic this source of Ca^{2+} production, carbachol and PLCζ were used since they both act via this pathway.

The addition of extracellular carbachol, or, injection of (0.02 mg/ml) PLCζ cRNA both caused oscillations in unfertilised mouse eggs. Fig. 4.5 a and b show that both of the stimuli caused Ca^{2+} oscillations in mouse eggs, which was associated with a gradual increase in luciferase luminescence (see also Table 4.2). The increase in luminescence was markedly slower with carbachol and since the oscillations do not persist the increase in luminescence tended to occur after Ca^{2+} oscillations had ceased. With injection of PLCζ cRNA, the rise in luminescence occurred in most eggs about 10 minutes after the first transient (Fig. 4.5b), which is significantly later than the increase in luminescence that occurs during fertilisation. The frequency of Ca^{2+} oscillations were significantly lower in eggs injected with PLCζ compared to normally fertilised eggs (8.7 $\pm$ 0.6 spikes/hour: see Chapter 3, Table 3.1). The size of the luminescence response is also significantly different to control changes in luminescence observed in unfertilised eggs over 30 minutes (102 $\pm$ 0.3: see Chapter 3, Table 3.1).

Fig. 4. 5 Ca^{2+} releasing agents via $InsP_3$

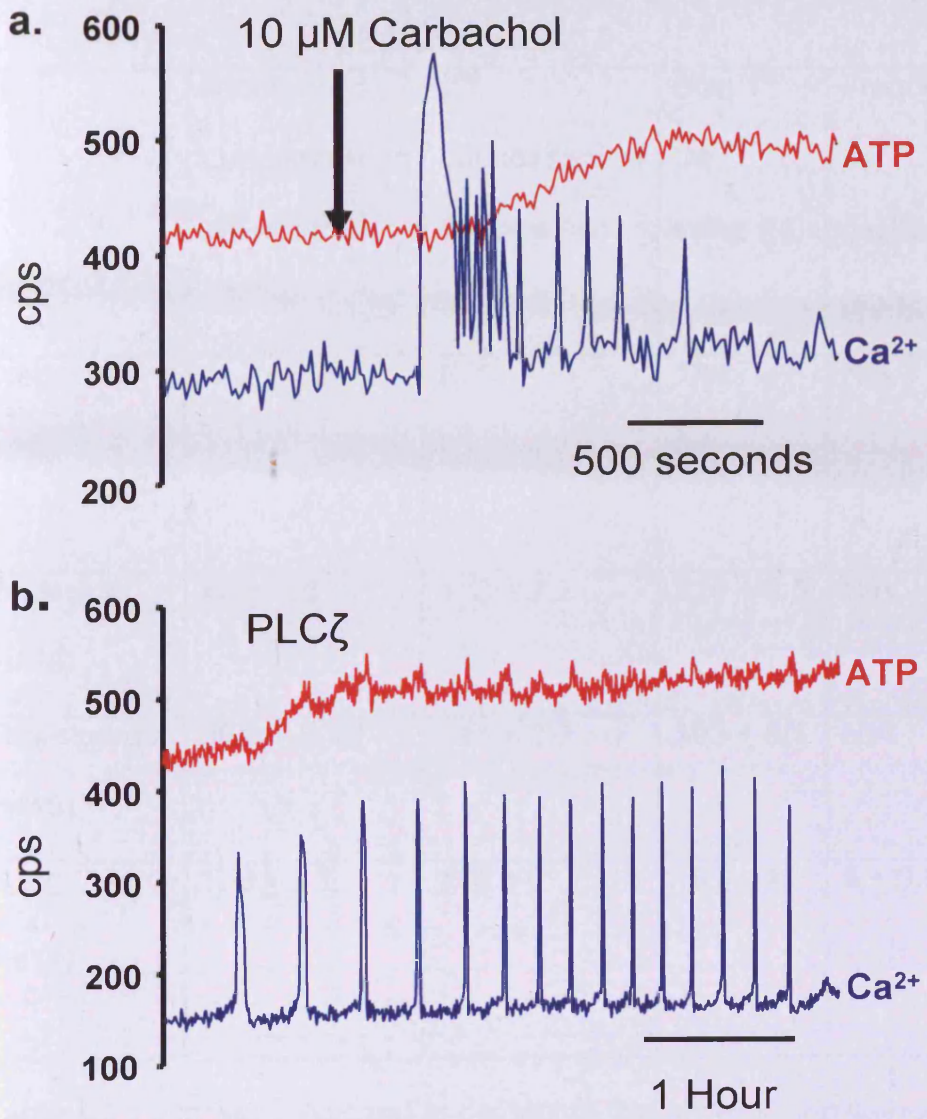

Fig. 4.1.5 a) Eggs were exposed to carbachol to produce a Ca^{2+} rise (n=10) and b) Eggs were activated by injecting cRNA PLCζ (0.02 mg/ml-pipette concentration) (n=12)

Table 4.2 Ca^{2+} and luciferase luminescence response in eggs exposed to Ca^{2+} releasing agents

	Initial Luminescence change (%)	2nd Luminescence Change (%)	Size 1st Ca^{2+} spike (%)	Frequency of Ca^{2+} oscillations (spikes/hr)
Carbachol (n=9)	117 ± 3.3	N/A	189.7 ± 9.6	N/A
Ionomycin (n=16)	80 ± 1.6	112 ± 2.2	226 ± 9.5	N/A
Thapsigargin (n=16)	86.9 ± 0.93	114 ± 2.3	193 ± 5.1	N/A
PLCζ (n=12)	125 ± 2.7	133 ± 2	195 ± 12	4 ± 0.5

Table 4.2 Eggs were exposed to carbachol, ionomycin, thapsigargin, or, PLCζ to initiate an increase in Ca^{2+}. Both the Ca^{2+} and luminescence response were measured for several hours after the stimulus was applied or injected. The percentage change is expressed in relation to the initial luminescence value before the Ca^{2+} stimulus was applied. All values are the mean from the stated total number of eggs ± the s.e.m.

4.2.5 Non-physiological Ca^{2+} releasing agents produce an initial decrease in ATP levels

Section 4.2.4 confirmed that Ca^{2+} releasing agents that act via the $InsP_3$ pathway are able to produce a rise in ATP levels. Ca^{2+} releasing agents that are non-physiological shall now be examined.

A number of agents can cause a rise in Ca^{2+} in mouse eggs. Figure 4.6a and b shows that the addition of the Ca^{2+} ionophore ionomycin, or, the Ca^{2+} ATPase inhibitor thapsigargin both cause an increase in Ca^{2+} in mouse eggs (Kline and Kline, 1992b). They both also lead to a transient decrease in luciferase luminescence. Thapsigargin stimulated eggs showed an increase in luminescence after the initial decrease that was significantly different ($P<0.005$) to the drift in luminescence signal recorded over 30 minutes (Table 4.2 and see Chapter 3,Table 3.1). For ionomycin stimulated eggs, 10/16 eggs also showed an increase (after the initial decrease) that was significantly different ($P<0.005$) to the control drift over 30 minutes. The remaining 6 eggs showed a recovery of luminescence to values similar to those seen before stimulation. Both these stimuli cause a single increase in Ca^{2+} and an initial transient ATP decrease.

These data confirm that the pathway used during fertilisation induced Ca^{2+} oscillations produce a distinct rise in ATP that is unique to the $InsP_3$ pathway. Although other Ca^{2+} stimuli produce an increase, this increase fails to be as substantial and only occurs after an initial decrease in ATP. However, this data still confirms that Ca^{2+} and ATP exist within eggs in a closely related manner.

Fig. 4. 6 Ionomycin and thapsigargin induced Ca^{2+} rise

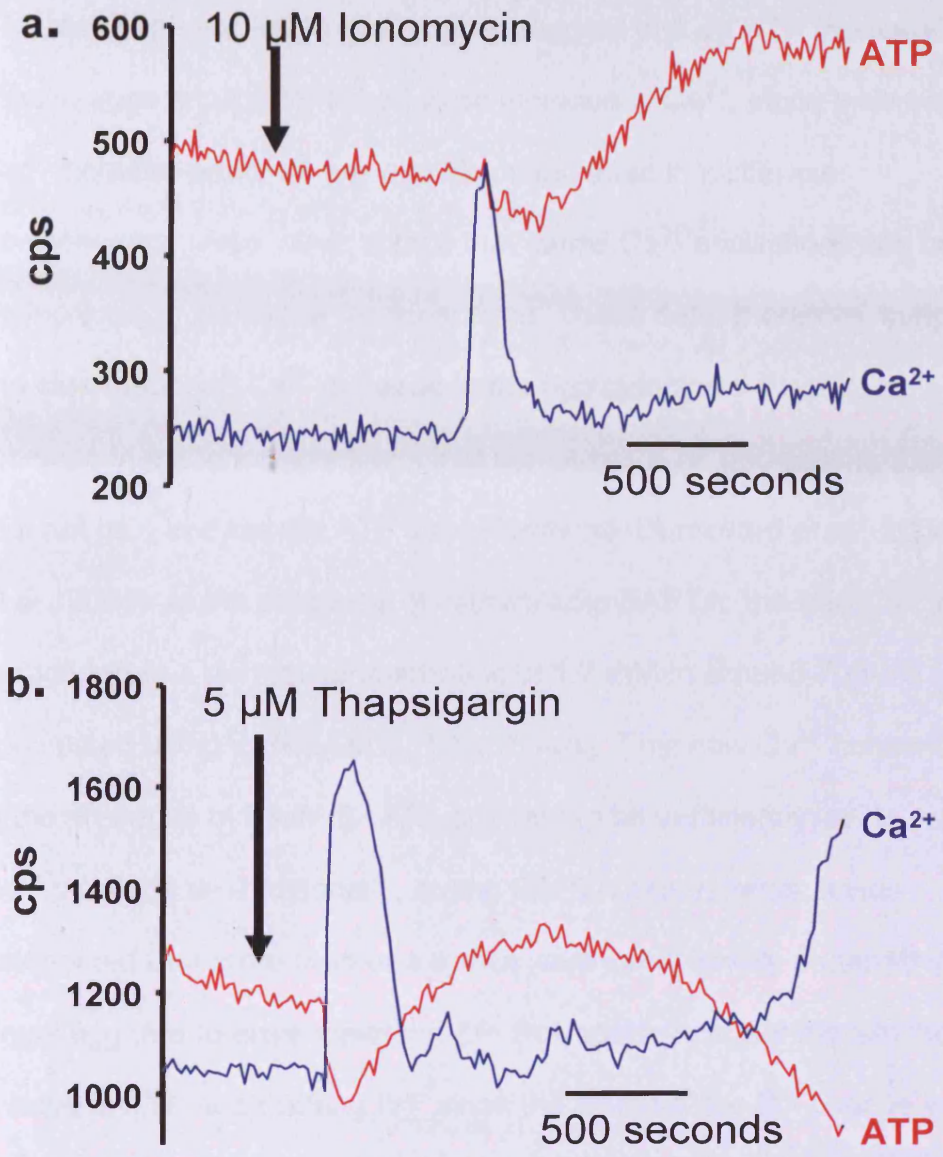

Fig. 4.6 Eggs were exposed to agents that produce a rise in Ca^{2+} a) 10 µM ionomycin (n=16) and b) 5 µM thapsigargin (n=22)

4.3 Discussion

The results presented in this chapter suggest that an ATP increase in mouse eggs is causally linked to an increase in Ca^{2+}, since preventing the Ca^{2+} increase prevents any significant increase in luciferase luminescence. Also, other stimuli that cause Ca^{2+} oscillations can cause an increase in luciferase luminescence. These data, therefore, support the idea that each Ca^{2+} increase in the egg cytoplasm leads to an increase in mitochondrial Ca^{2+}, that stimulates ATP generation, that leads to a net gain in cytosolic ATP concentrations (Dumollard et al., 2004; Liu et al., 2001). In the presence of extracellular BAPTA, the free Ca^{2+} is reduced from a normal concentration of 1.7 mM to around 700 nM (calculated using WINMAXC 2.10 software). This new Ca^{2+} concentration in the presence of 2 mM BAPTA appears to be sufficiently low to prevent Ca^{2+} oscillations. Additionally, during BAPTA experiments, it was determined that more than one sperm were occasionally penetrating a single egg due to absence of the ZP. Polyspermy cannot explain the 2nd change in ATP seen during IVF since the timing of the 2nd change would be variable. From the results in Chapter 3 it was established that the 2nd change was occurring in eggs at a specific time point (60 minutes after fertilisation).

In contrast the Ca^{2+} changes at fertilisation via the $InsP_3$ pathway were mimicked by the addition of carbachol, injection of PLCζ, or repetitive pulses of $InsP_3$ delivered by photolysis of its caged derivative. All three of these stimuli could lead to an increase in ATP levels. This suggests that the induction of $InsP_3$ mediated Ca^{2+} release in eggs

provides a more effective way of stimulating mitochondria to generate ATP without causing excessive ATP consumption. This may be facilitated by close contact between mitochondria and $InsP_3$ receptors in the endoplasmic reticulum (Duchen, 2000; Dumollard et al., 2004; Hajnoczky et al., 1995).

Both PLCζ and caged $InsP_3$ were used to investigate the effects of a prolonged series of repetitive Ca^{2+} rises in eggs. Both of these stimuli caused an ATP increase that progressed as Ca^{2+} increases continued. It was, however, noteworthy that the rate of rise in ATP was slower with these stimuli than with fertilisation. This may have been partly due to the fact that either the amplitude or duration of the Ca^{2+} rise generated by these agents was not identical to that seen at fertilisation. Only one concentration of PLCζ was reported in this section and the Ca^{2+} oscillations induced by PLCζ were of a lower frequency than those seen at fertilisation. This was due to a technical feature of the way the experiments were carried out. Injecting higher concentrations of PLCζ cRNA can cause higher frequency Ca^{2+} oscillations (Saunders et al., 2002), but when greater amounts of PLCζ were injected into eggs, the Ca^{2+} oscillations invariably started within 30 minutes, that was before the 'run in' period for the luciferase signal.

Repetitive photolysis of caged $InsP_3$ was another means of artificially inducing Ca^{2+} oscillations in eggs. Again, it was not possible to entirely mimic fertilisation and maintain a precise pattern of $InsP_3$-induced Ca^{2+} transients with this technique and we found that obtaining responses with caged $InsP_3$ was critically dependent upon the time between injection

and the start of photolysis (Campbell and Swann, unpublished observations). However, a series of Ca^{2+} rises could be induced in eggs and this lead to an increase in ATP when the frequency of transients was 6 or 12 transients per hour, but a decrease in ATP was seen when 24 transients per hour occurred. This again suggests that there is a balance between the ATP production and consumption and that over stimulation of Ca^{2+} release can lead to more ATP consumption than can be supplied by the mitochondria. It was notable that this decrease in ATP was not evident in any fertilising eggs, even when the extracellular Ca^{2+} was increased to drive high frequency Ca^{2+} oscillations (see Chapter 3 results).

Other agents that can cause a Ca^{2+} increase of some type also lead to changes in ATP levels as measured by luciferase luminescence. Both ionomycin and thapsigargin cause a single Ca^{2+} increase in mouse eggs (Kline and Kline, 1992a; Kline and Kline, 1992b), and they initially produced a decrease in ATP levels followed by a recovery to, or slightly above pre-treatment levels. The initial decrease in ATP is similar to that reported in some somatic cells that are exposed to stimuli that cause a large rise in cytosolic free Ca^{2+} which can cause excessive ATP consumption by Ca^{2+} recovery mechanisms outweighing any stimulation of ATP production (Jouaville et al., 1999). Both ionomycin and thapsigargin probably cause a non-physiological amount of Ca^{2+} to be released.

This chapter has confirmed that the ATP change recorded at fertilisation in mouse eggs is dependent upon changes in cytosolic Ca^{2+}

levels that arise via the $InsP_3$ pathway. The ATP response seems to be unique to sperm induced oscillations that cannot be reproduced by other Ca^{2+} producing agents. The source of ATP synthesis that is activated via this Ca^{2+} signal shall be explored in the next chapter.

Chapter 5
Regulation of cytosolic and mitochondrial ATP levels in mouse oocytes and zygotes

5.1 Introduction

In Chapter 3, Ca^{2+} oscillations at fertilisation produced a two-fold rise in cytosolic ATP levels. In Chapter 4, it was then demonstrated that the ATP response seen at fertilisation was dependent upon cytosolic Ca^{2+} changes. The predominant source of ATP production is an area within the field that is still ill-defined and shall be looked at in detail in this chapter.

In mammalian MII eggs and fertilised eggs, several lines of evidence exist that suggest ATP is mainly supplied by mitochondrial oxidative phosphorylation while glycolysis contributes poorly (Barbehenn et al., 1974; Dumollard et al., 2007b; Urner and Sakkas, 2005). Mitochondrial poisons (FCCP and oligomycin) have been shown to inhibit the completion of meiosis triggered by fertilisation (Dumollard et al., 2004; Liu et al., 2001). Furthermore, in mouse eggs, inactivating the mitochondrial enzyme that feeds the TCA (pyruvate dehydrogenase) at the beginning of follicular growth impairs development beyond the one cell stage (Johnson et al., 2007). In addition, cytosolic Ca^{2+} oscillations have been shown to stimulate repetitive oxidation and reduction in the mitochondria (Dumollard et al., 2004).

From the above evidence it was thus hypothesised that up-regulation of energetic metabolism during fertilisation is due to stimulation of mitochondrial oxidative phosphorylation by sperm induced Ca^{2+} oscillations. (Dumollard et al., 2007a; Dumollard et al., 2006). However, no direct measure of mitochondrial ATP production has ever been measured to support such a hypothesis. In this chapter, cytosolic and

mitochondrial ATP levels shall be measured during sperm induced Ca^{2+} oscillations.

When eggs are starved of substrates at fertilisation, Ca^{2+} oscillations are impaired and this can be recovered by the addition of extracellular pyruvate (Dumollard et al., 2004). Pyruvate is not the only substrate available to eggs and developing embryos. Glucose, glutamine and lactate are also available in follicular fluid and all egg/embryo culture media. Even though it is known that glycolysis is repressed in mouse eggs, it has been shown that glucose uptake increases at fertilisation and is subsequently metabolised by glycolysis and the pentose phosphate pathway (PPP). However, the actual contribution of these metabolites during egg activation remains undefined. This chapter shall assess the contribution of exogenous pyruvate, glucose, glutamine and lactate during preimplantation development.

5.2 Results

5.2.1 Mitochondrial Luciferase

A luciferase probe that has a mitochondrial targeting sequence was prepared by collaborator Dr Remi Dumollard (see methods for construct details). To ensure this construct was being targeted to the mitochondria, anti-luciferase immunohistochemistry was performed on eggs that had been injected with this construct. First, to confirm that the antibodies and staining protocol were working efficiently, uninjected eggs were stained to confirm the absence of background staining (Fig. 5.1a and b). To confirm that the protocol was sufficient to measure luciferase expression, eggs were injected with cytosolic luciferase protein and stained (Fig. 5.1c and d). All images in Fig 5.1 were taken on a conventional epifluorescence microscope equipped with a CCD camera.

To view the mitochondria in eggs, a confocal (SP5) microscope was used. Firstly, cytosolic luciferase was imaged (Fig 5.2a and b). Next, eggs injected with mitochondrially targeted luciferase were imaged (Fig. 5.2c, d, e, and f) to confirm mitochondrial localisation.

Fig. 5. 1 Anti-Luciferase immunohistochemistry

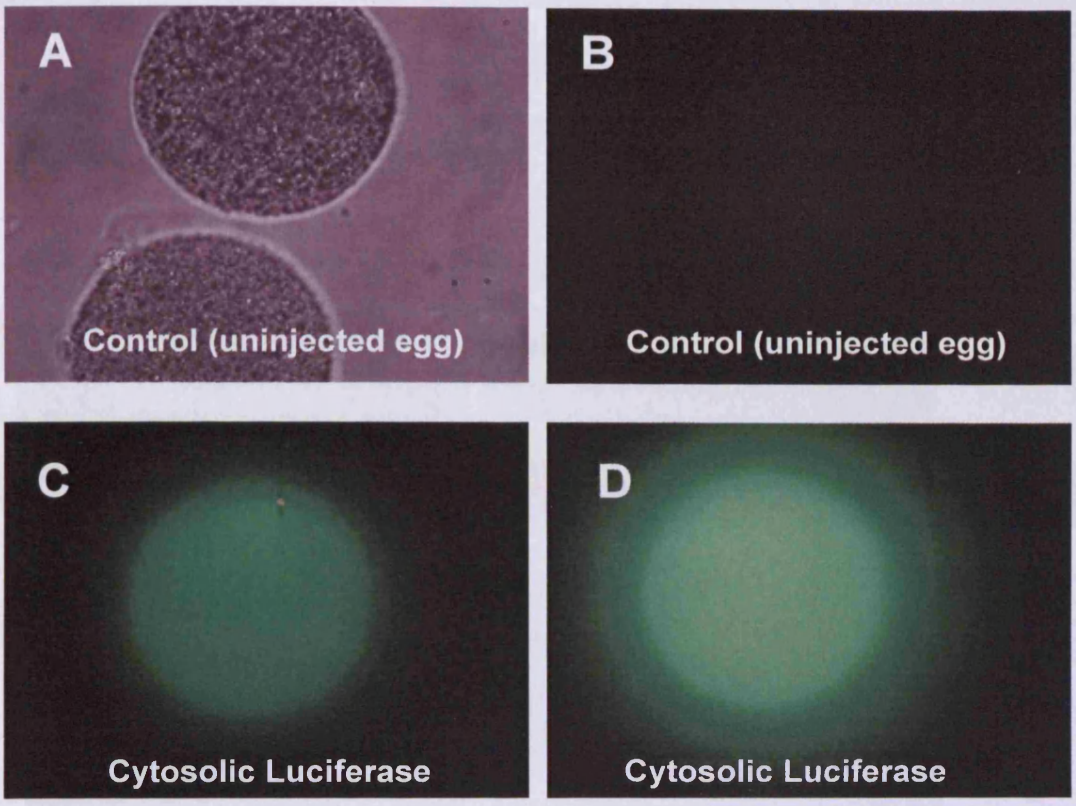

Fig. 5.1 Bright field image of uninjected eggs (A) that were stained to detect the presence of background staining (B). C) and D) show two examples of eggs that were injected with cytosolic luciferase and were stained to detect the presence of luciferase in the cytosol. Images (A-D) were taken on a conventional epifluorescence microscope equipped with a CCD camera.

Fig. 5. 2 Cytosolic and mitochondrial targeted luciferase probes

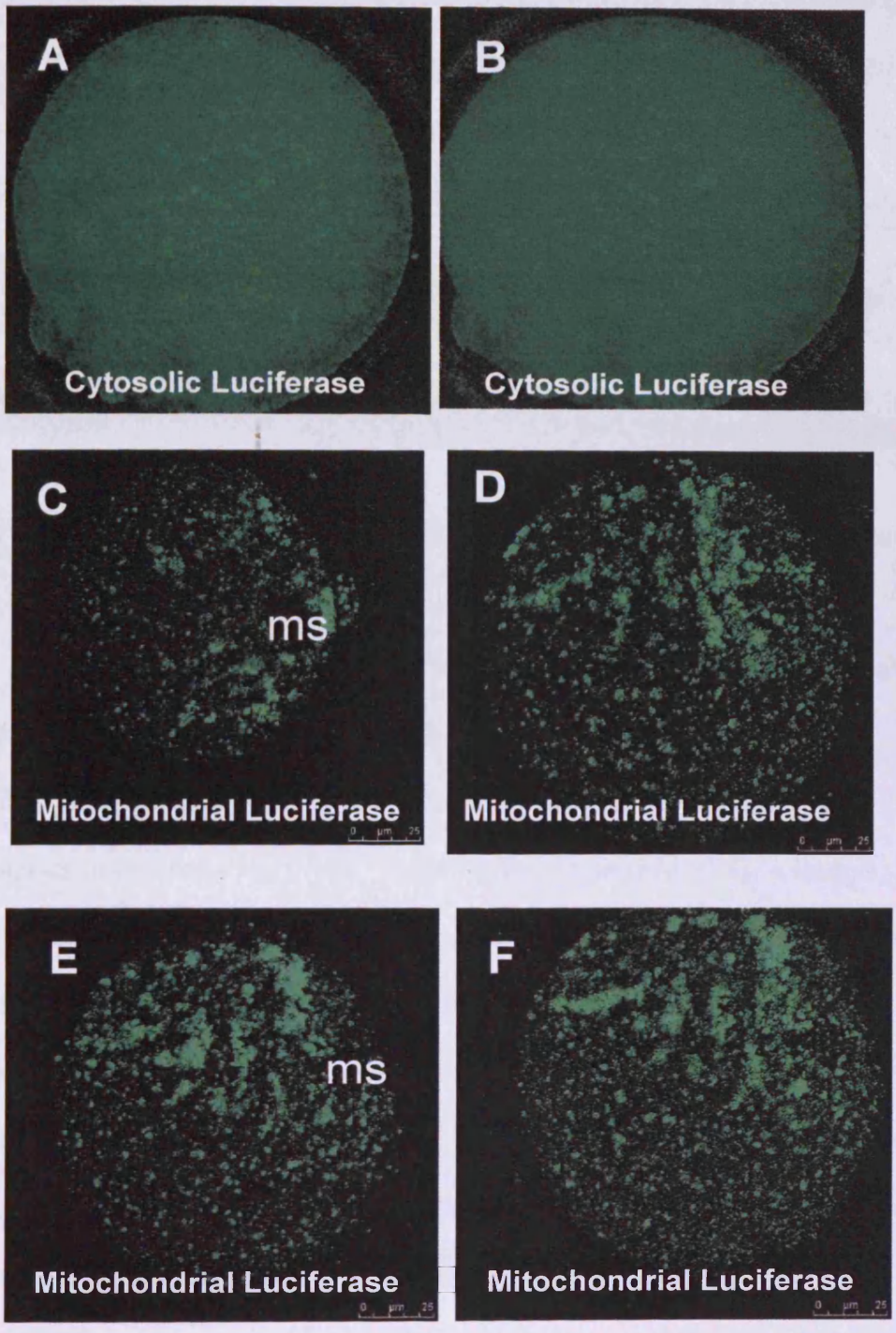

Fig. 5.2 A) and B) Two examples of eggs injected with cytosolic luciferase and stained to confirm the presence of luciferase in the cytosol. C), D), E) and F) Show four examples of eggs injected with mitochondrial luciferase that were stained and imaged. ms = meiotic spindle. Images A-F were taken on a SP5 confocal microscope.

The next step was to use a mitochondrial probe (mitotracker orange) and compare these results to the mitochondrial luciferase (Fig. 5.3a and b). Mitotracker orange was used since its fluorescence emission spectrum (576 nm) does not overlap with signal from the 2nd antibody (488 nm). The mitochondria imaged from the antibody protocol versus the mitotracker highlighted (Fig. 5.3b) concerns regarding the efficiency of the mitotracker probe. Areas within the egg were being stained that appeared too large to be mitochondria suggesting unspecific staining (Fig. 5.3b and c). When images from mitotracker and mitoluciferase were overlapped (Fig. 5.3c) it was clear that the mitotracker was labelling other organelles in addition to the mitochondria.

To further confirm that the mitochondrial luciferase probe was being targeted to the mitochondria, GV eggs were investigated. Mitochondria have been shown to accumulate around the oocytes nucleus via measuring FAD^{++} autofluorescence (Fig. 5.4a – image supplied by Remi Dumollard), hence providing a clear indication of where the mitochondria are distributed. When GV eggs injected with mitochondrial luciferase were fixed and stained, similar images were obtained to those seen using FAD^{++} autofluorescence (Fig. 5.4b, c and d). GV eggs were also stained using mitotracker orange (Fig. 5.4e and f) and again the images were inconsistent with those using both FAD^{++} autofluorescence and mitochondrial luciferase protocol (Fig. 5.4a, b, c and d). The staining pattern did not show the obvious accumulation of mitochondria around the nucleus further suggesting that the mitotracker probe may be staining more organelles than just the mitochondria

Fig. 5. 3 Mitotracker orange and mitochondrial luciferase

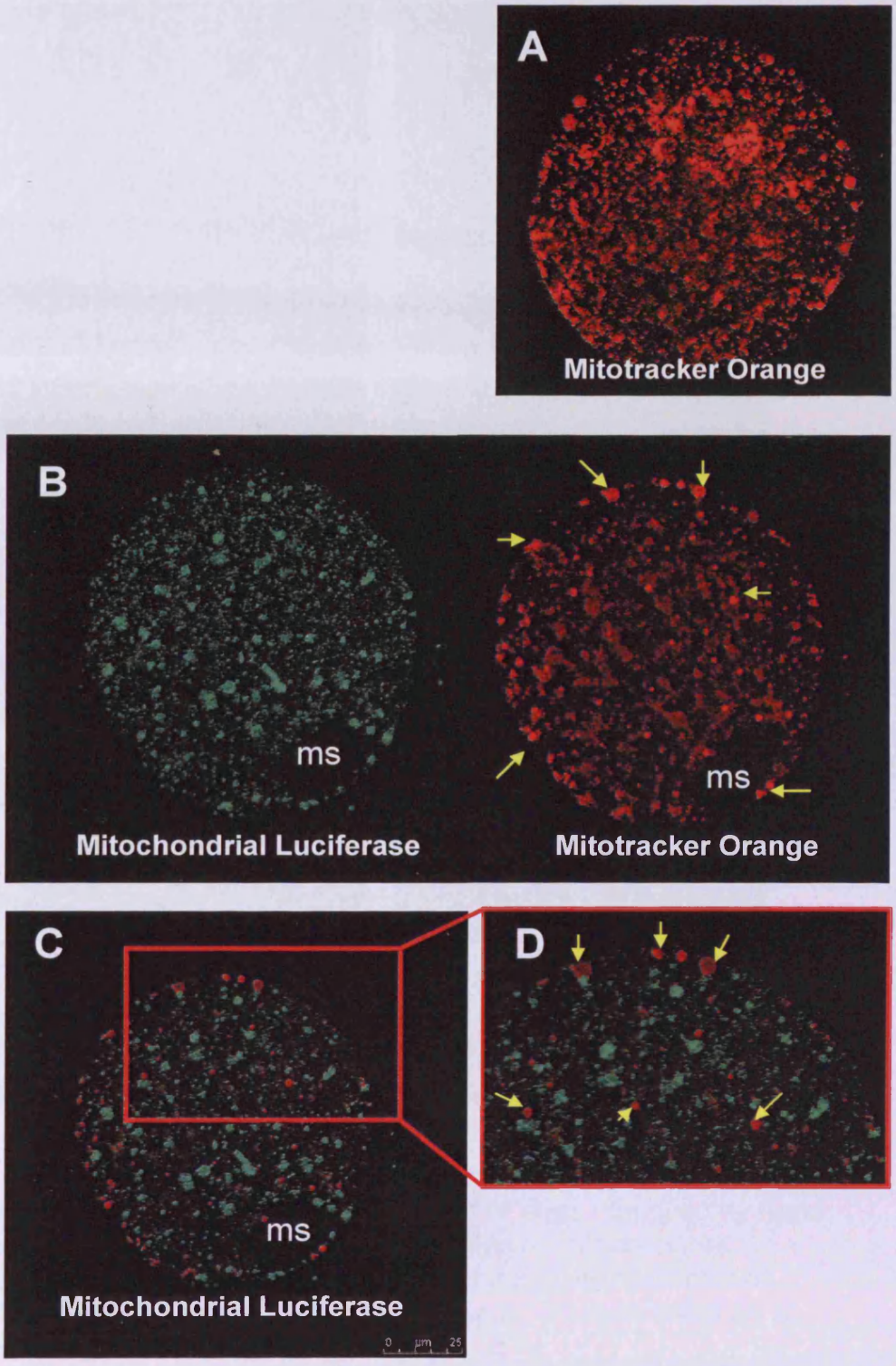

Fig. 5.3 A) mitotracker localisation, B) Mitochondrial luciferase and mitotracker staining, C) an overlap of both mitochondrial luciferase and mitotracker and D) an enlargement of C (yellow arrows indicates unspecific targeting of mitotracker probe)

Fig. 5. 4 Mitochondrial localisation in GV oocytes

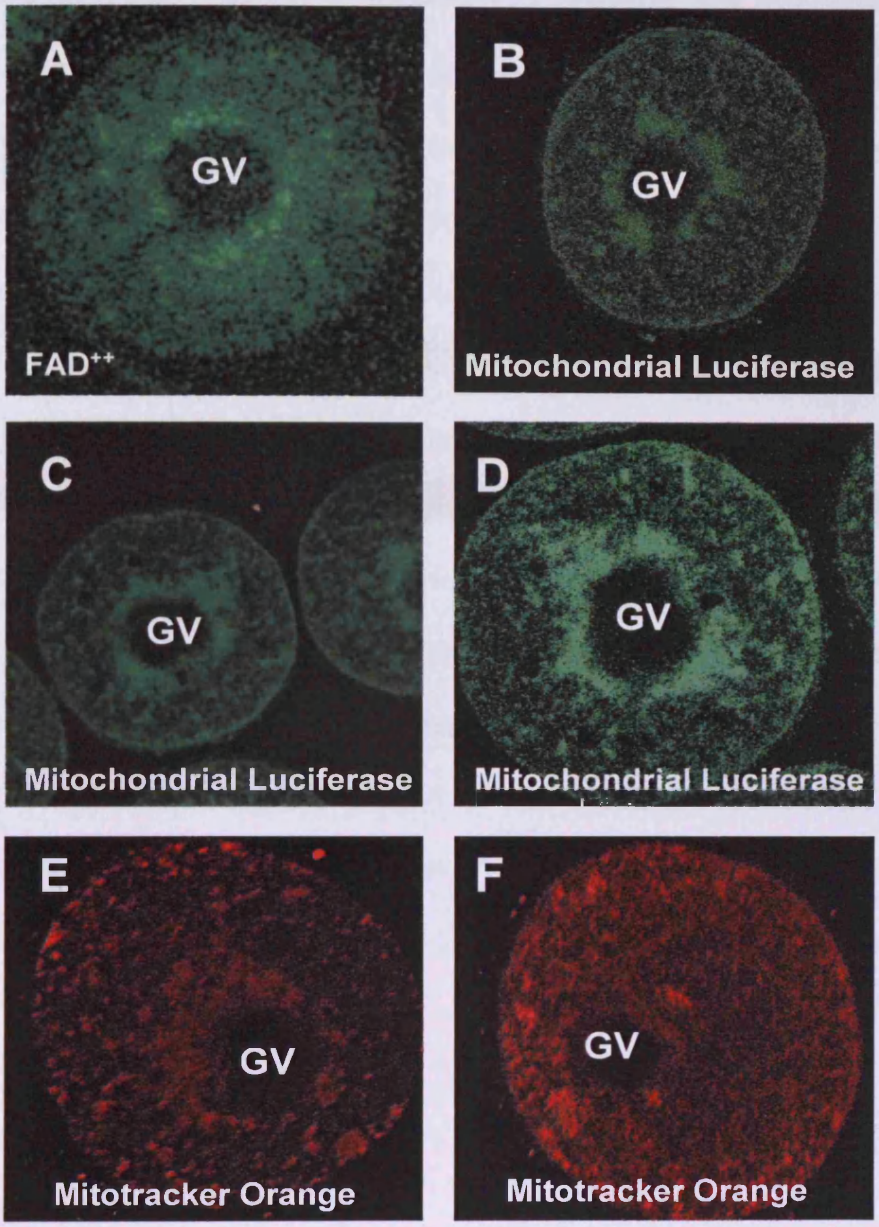

Fig. 5.4 A) FAD^{++} autofluorescence in GV eggs (supplied by Remi Dumollard) B), C) and D) Three examples of mitochondrial luciferase localisation in GV eggs. E) and F) Two examples of mitotracker orange localisation in GV eggs. (Images taken on an SP5 confocal).

5.2.2 Oxidative phosphorylation is required by MII eggs

To test the response of the mitochondrial luciferase probe in unfertilised mouse MII eggs, the mitochondrial F_1F_0 ATPase inhibitor oligomycin was added to eggs that had been injected with either cytosolic or mitochondrial luciferase (Fig. 5.5a, n=6 and b, n=9). Since the result indicated that cytosolic and mitochondrial responses were different this further indicates that the luciferase probe was in fact being targeted to the mitochondria. ATP demands in the cytosol are higher, and therefore, the decrease in the cytosol is more noticeable than that of the mitochondria. Mitochondrial luciferase injected eggs were fertilised with sperm (Fig. 5.6a and b n=22) and the changes in ATP recorded were similar (identical) to those seen in the cytosol (see Chapter 3). The initial increase in ATP occurred with the 1^{st} Ca^{2+} spike and the 2^{nd} change was recorded typically after 1 hour of Ca^{2+} oscillations with the 10^{th} spike.

Fig. 5. 5 Oligomycin effect on cytosolic and mitochondrial ATP levels

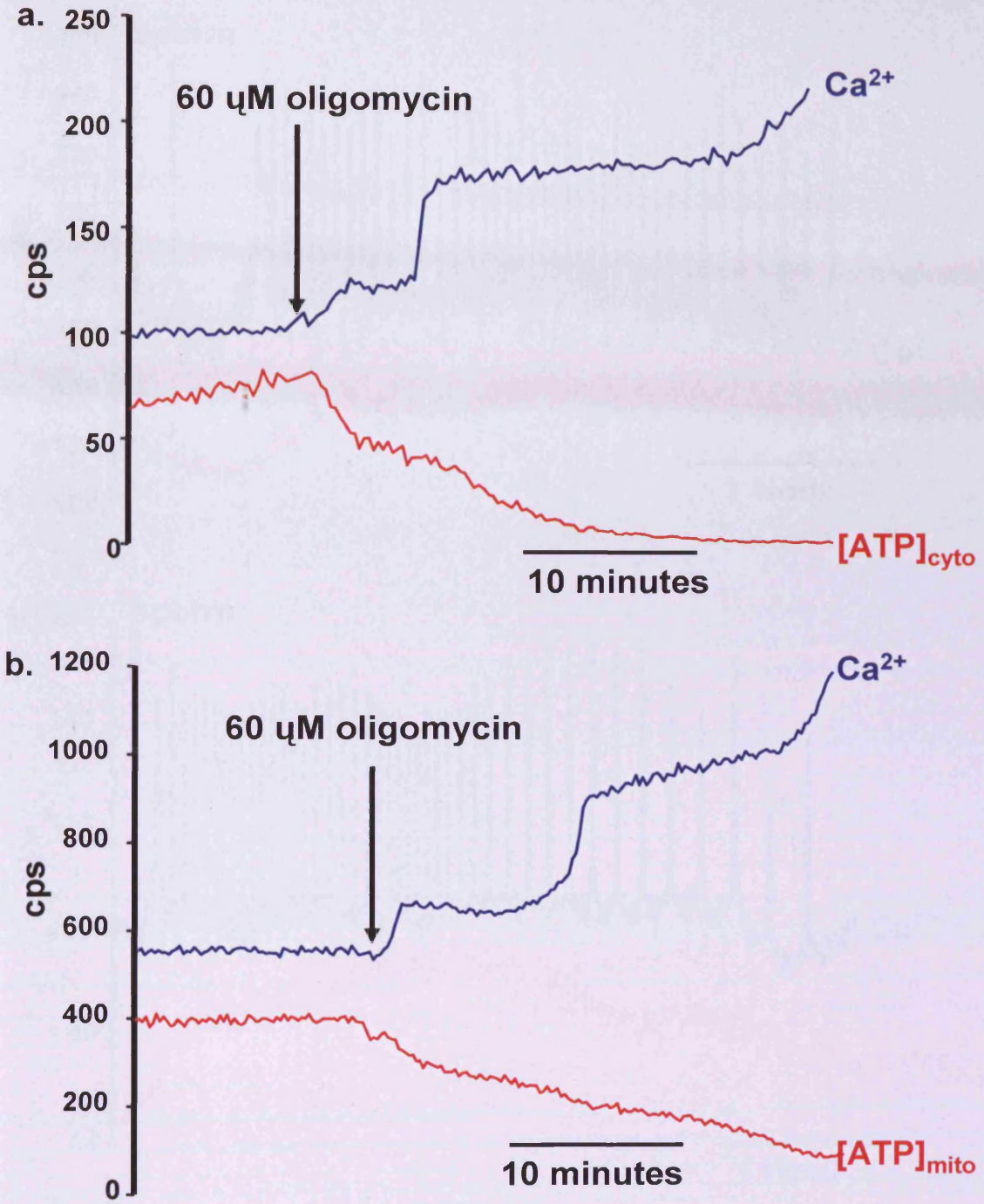

Fig. 5.5 a) Cytosolic (n=6) and b) mitochondrial luciferase (n=9) injected eggs were exposed to oligomycin. $[ATP]_{cyto}$ represents cytosolic luciferase and $[ATP]_{mito}$ represents mitochondrial luciferase

Fig. 5. 6 Mitochondrial ATP levels during fertilisation

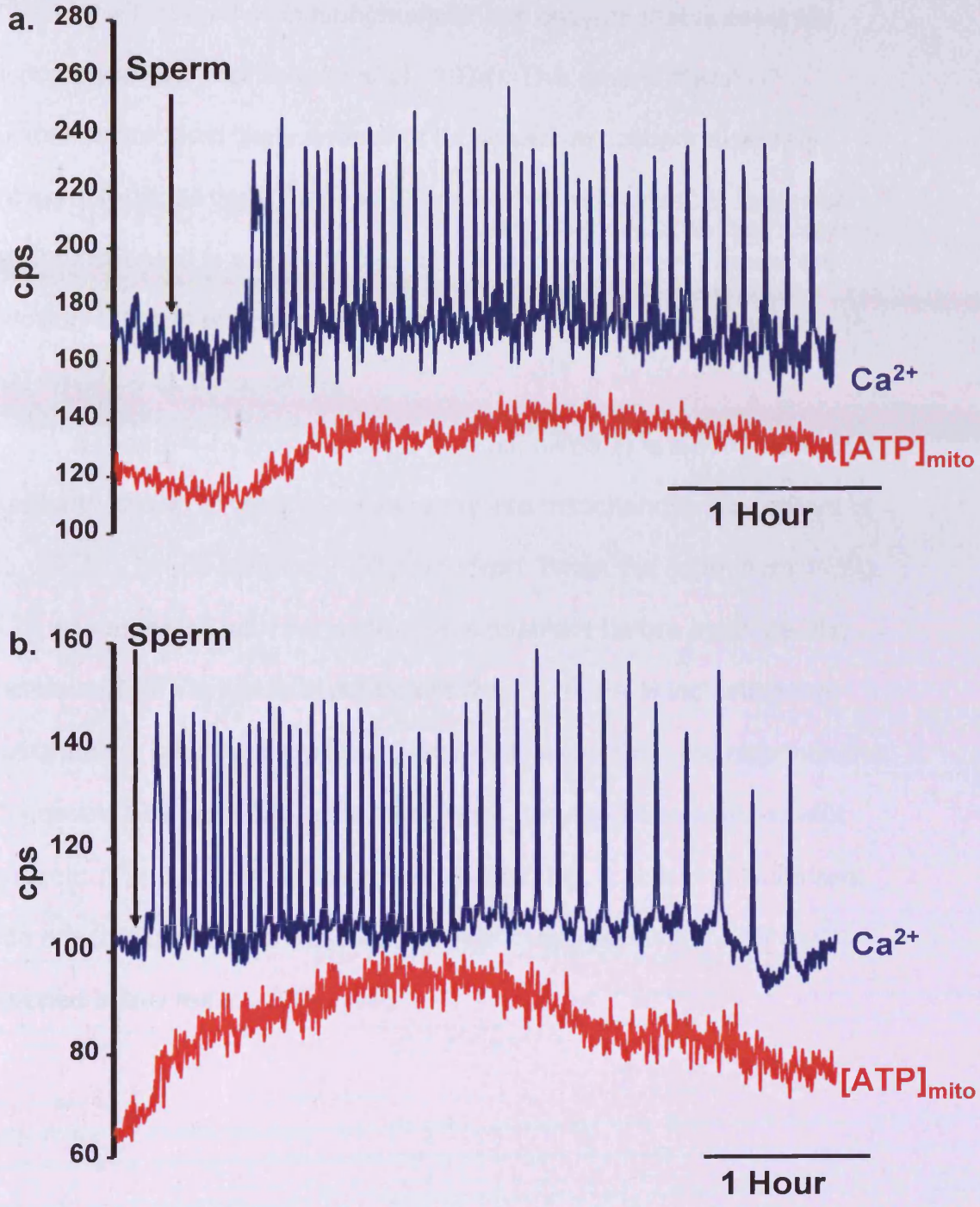

Fig. 5.6 a) and b) Show two examples of eggs injected with mitochondrial luciferase and fertilised with sperm (n=22, 4 runs).

Glycolysis activity is low in eggs, due to high citrate levels having an inhibitory effect on the phosphofructokinase enzyme that is essential during glycolysis (Barbehenn et al., 1974). This means that ATP increases are most likely a result of increased mitochondrial activity. When unfertilised eggs that had been injected with cytosolic luciferase where incubated in substrate free media for greater than 2 hours, the addition of 2 mM pyruvate (final concentration) produced an increase in ATP levels (Fig. 5.7a, n=18).

α-Cyano-4-hydroxycinnamic acid (cinnamate) is a compound that has been shown to block pyruvate entry into mitochondria (Dumollard et al., 2007b), hence blocking ATP production. When the experiment in Fig. 5.7a was repeated with the addition of cinnamate before pyruvate, the increased ATP response was blocked (Fig. 5.7b, n= 4) indicating that cinnamate is effectively blocking pyruvate transport into the mitochondria. Cinnamate was added to unfertilised eggs that had been injected with cytosolic (Fig. 5.8a n=18) and mitochondrial (Fig. 5.8b n=11) luciferase. The effect of cinnamate was clear as in both conditions the ATP levels dropped below resting ATP levels.

Fig. 5. 7 The effect of cinnamate on unfertilised eggs

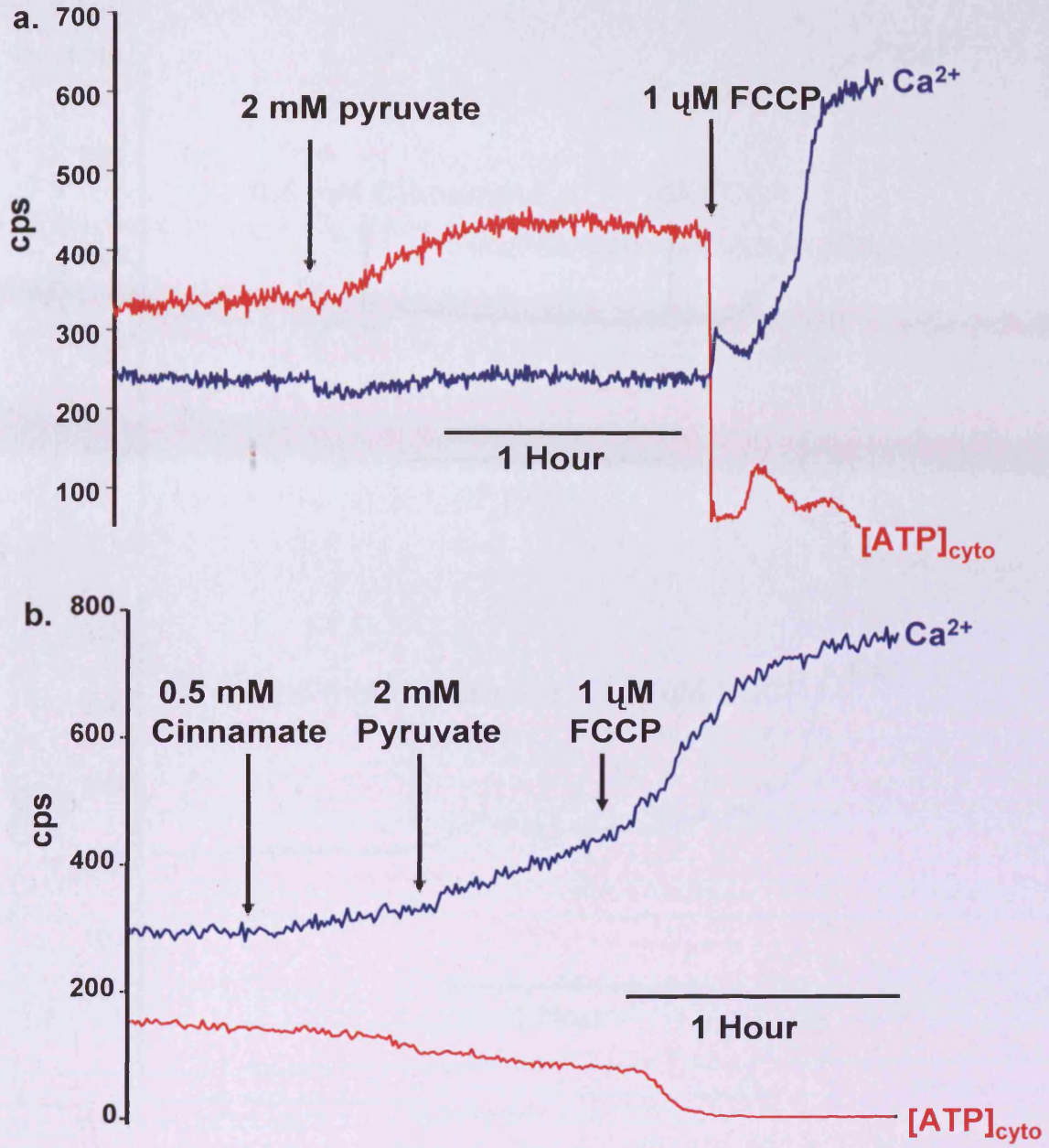

Fig. 5.7 a) eggs were injected with cytosolic luciferase and incubated in substrate free media before pyruvate was added (n=18) and b) cytosolic luciferase injected eggs were starved before the addition of cinnamate followed by pyruvate (n=4).

Fig. 5. 8 The effect of cinnamate on cytosolic and mitochondrial ATP levels

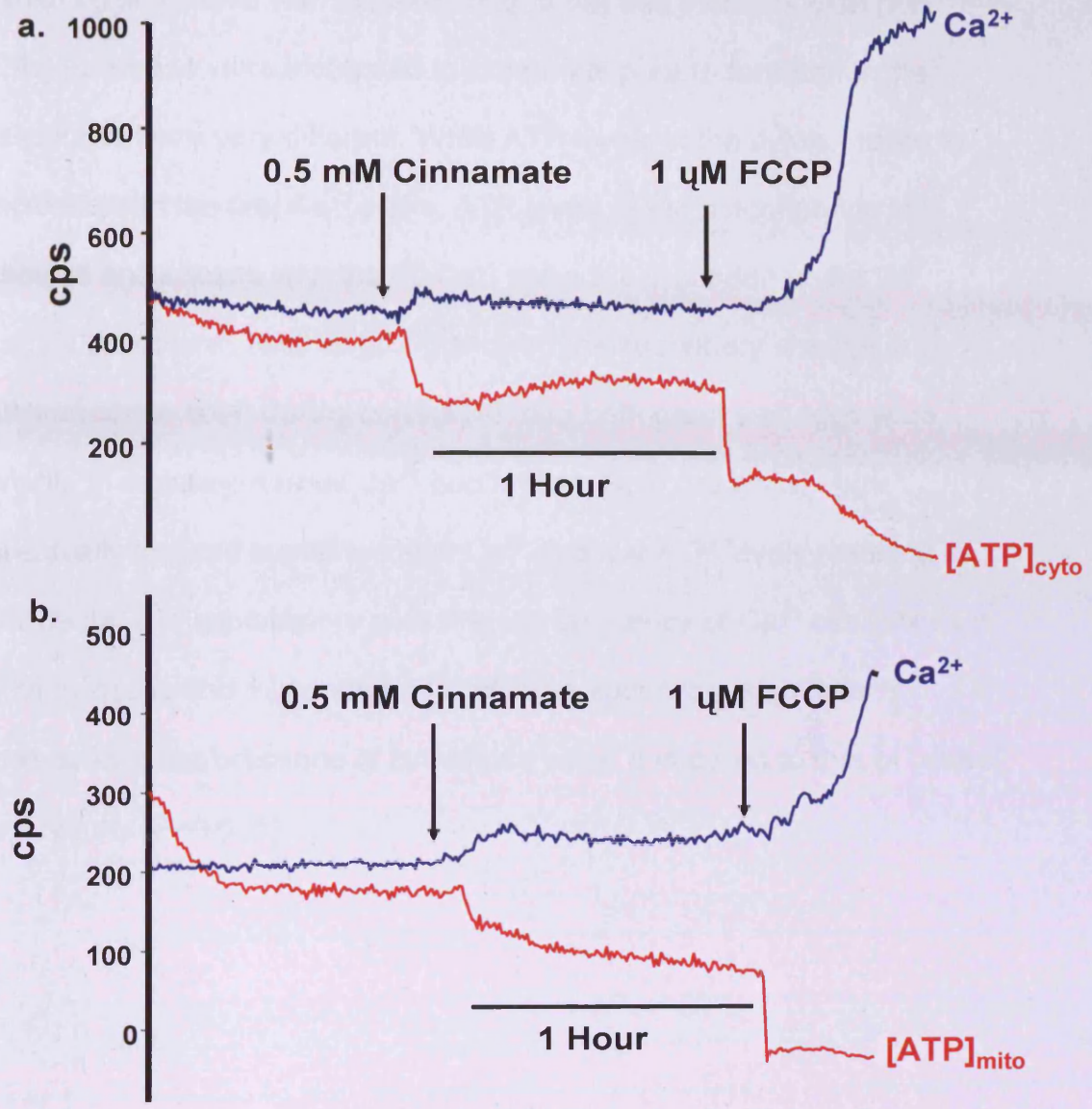

Fig. 5.8 a) cytosolic (n=18) and b) mitochondrial (n=11) luciferase injected eggs exposed to cinnamate followed by FCCP.

5.2.3 Fertilisation ATP responses to cinnamate addition

When eggs injected with cytosolic (Fig. 5.9a) and mitochondrial (Fig. 5.9b) luciferase were incubated in cinnamate prior to fertilisation the responses were very different. While ATP levels in the cytosol failed to increase with the first Ca^{2+} spike, ATP levels in the mitochondria still showed an increase with the 1^{st} Ca^{2+} spike like that seen under IVF control conditions. Neither group showed the secondary change in luminescence seen during control IVF and both groups of eggs were unable to maintain normal Ca^{2+} oscillations. Both groups of eggs eventually showed sustained high Ca^{2+} and low ATP levels resulting in cell death. It is important to note that the frequency of Ca^{2+} oscillations in both cytosolic and mitochondrial luciferase eggs were significantly increased in the presence of cinnamate when compared to that of control IVF results ($P>0.005$).

Fig. 5. 9 Cytosolic and mitochondrial ATP levels during fertilisation in the presence of cinnamate

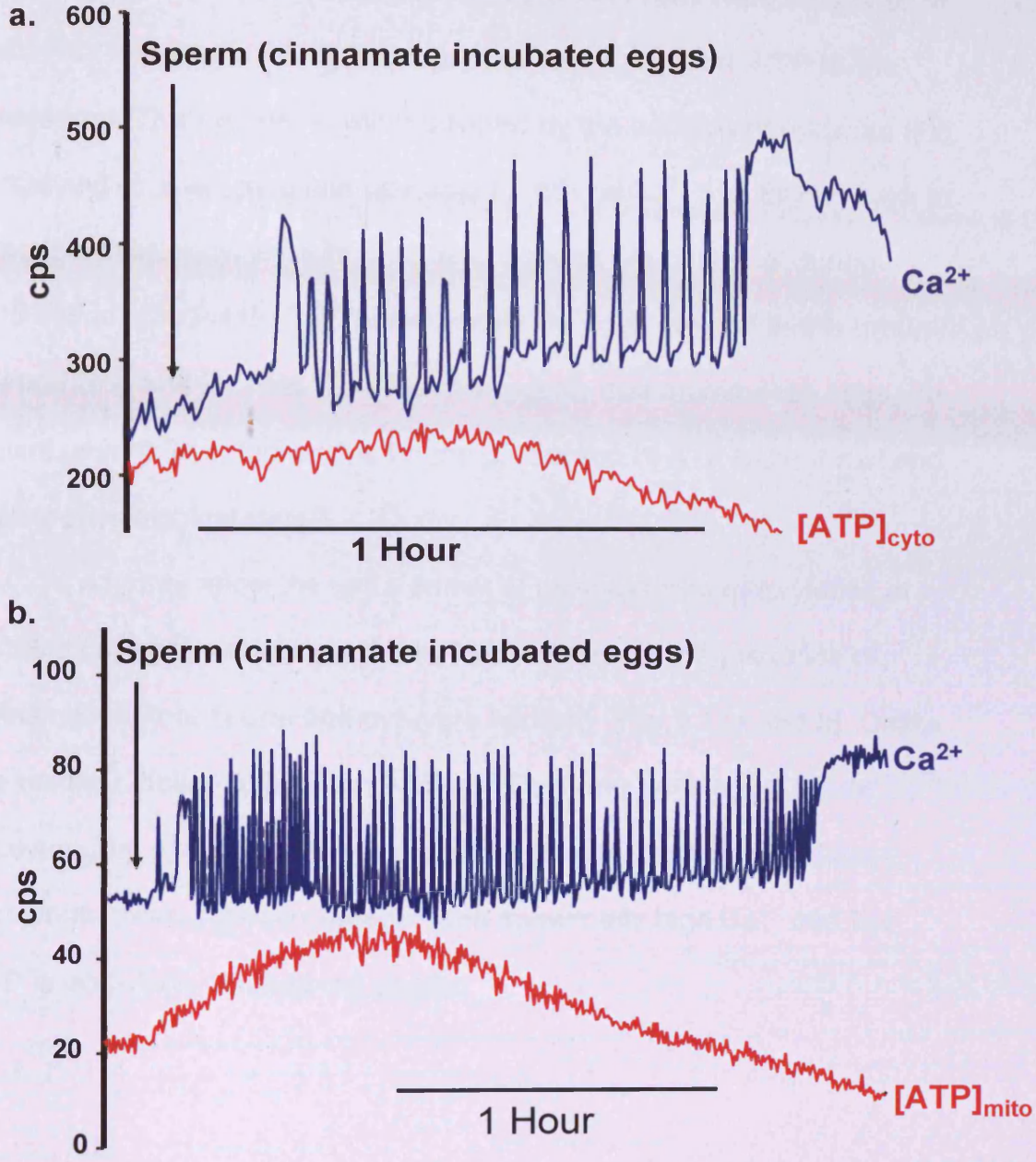

Fig. 5.9 a) cytosolic (n=18) and b) mitochondrial (n=10) luciferase injected eggs were incubated in 0.5 mM cinnamate before sperm addition.

5.2.4 Pyruvate recovers ATP levels in starved eggs

When eggs that were injected with cytosolic luciferase were incubated in substrate free media for >2 hours prior to sperm addition, ATP levels decreased. This decrease was recovered by the addition of pyruvate (Fig. 5.10a and b). Also, pyruvate was able to restore Ca^{2+} oscillations back to a normal frequency, implying that mitochondria are essential during fertilisation to maintain Ca^{2+} homeostasis. All eggs imaged in this group formed 2PN and 2nd PBs. This result suggests that mammalian eggs are reliant upon their mitochondria for the production of ATP both at rest and during physiological stimuli.

To further show the requirement of oxidative phosphorylation at fertilisation, eggs were starved and then fertilised in the presence of cinnamate before sperm and pyruvate addition (Fig. 5.11a and b). Unlike the results detailed above, the ATP and Ca^{2+} response could not be recovered by pyruvate in the presence of cinnamate. All eggs in the cinnamate treated group demonstrated abnormally high Ca^{2+} and low ATP levels which resulted cell death.

Fig. 5. 10 Pyruvate can recover ATP and Ca^{2+} levels in starved eggs

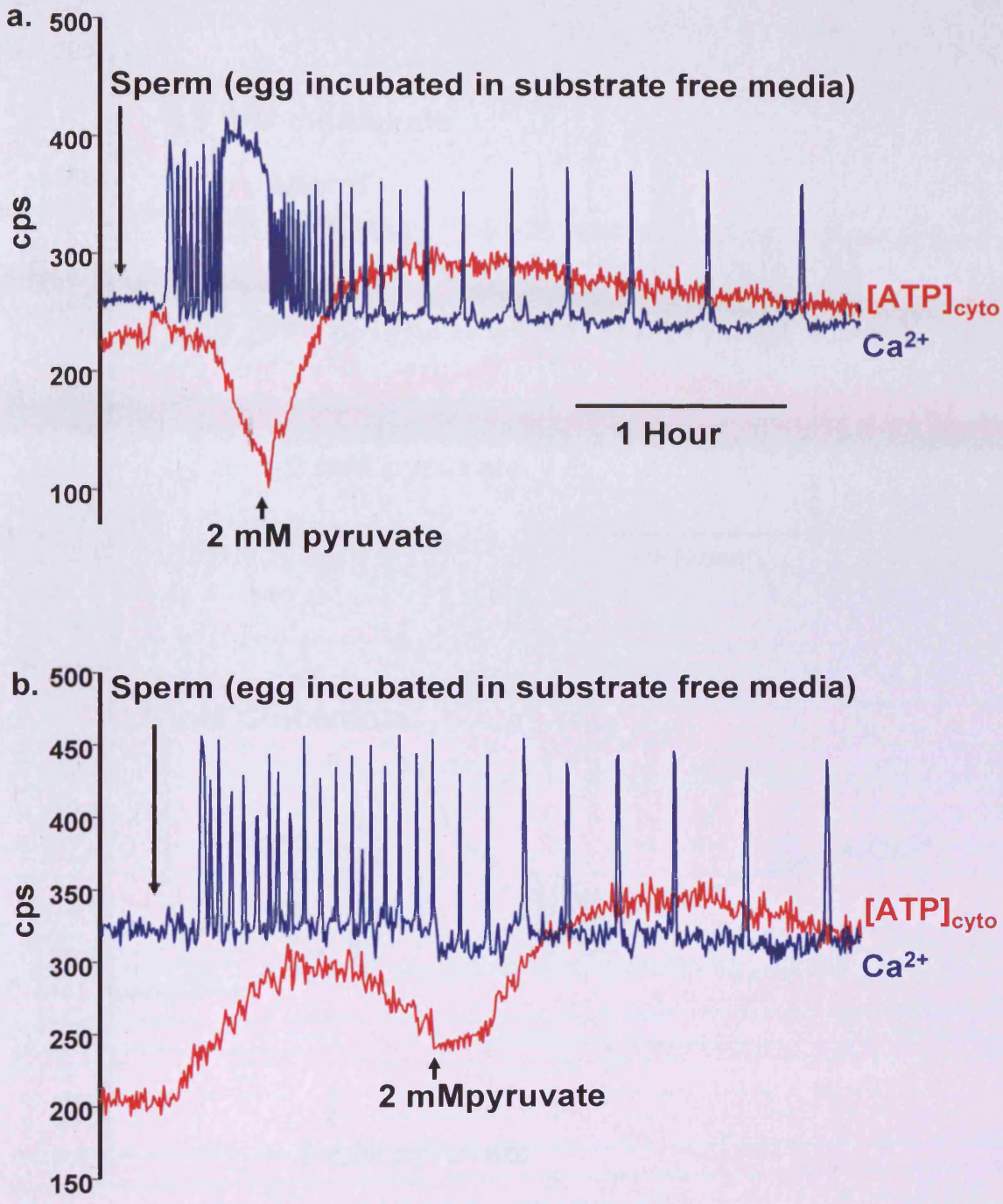

Fig. 5.10 a) and b) Show two examples of eggs that were injected with cytosolic luciferase and fertilised in substrate free media before the addition of pyruvate (n=21). Time bar applies to both graphs.

Fig. 5. 11 Cinnamate prevents the recovery action of pyruvate in starved eggs during fertilisation

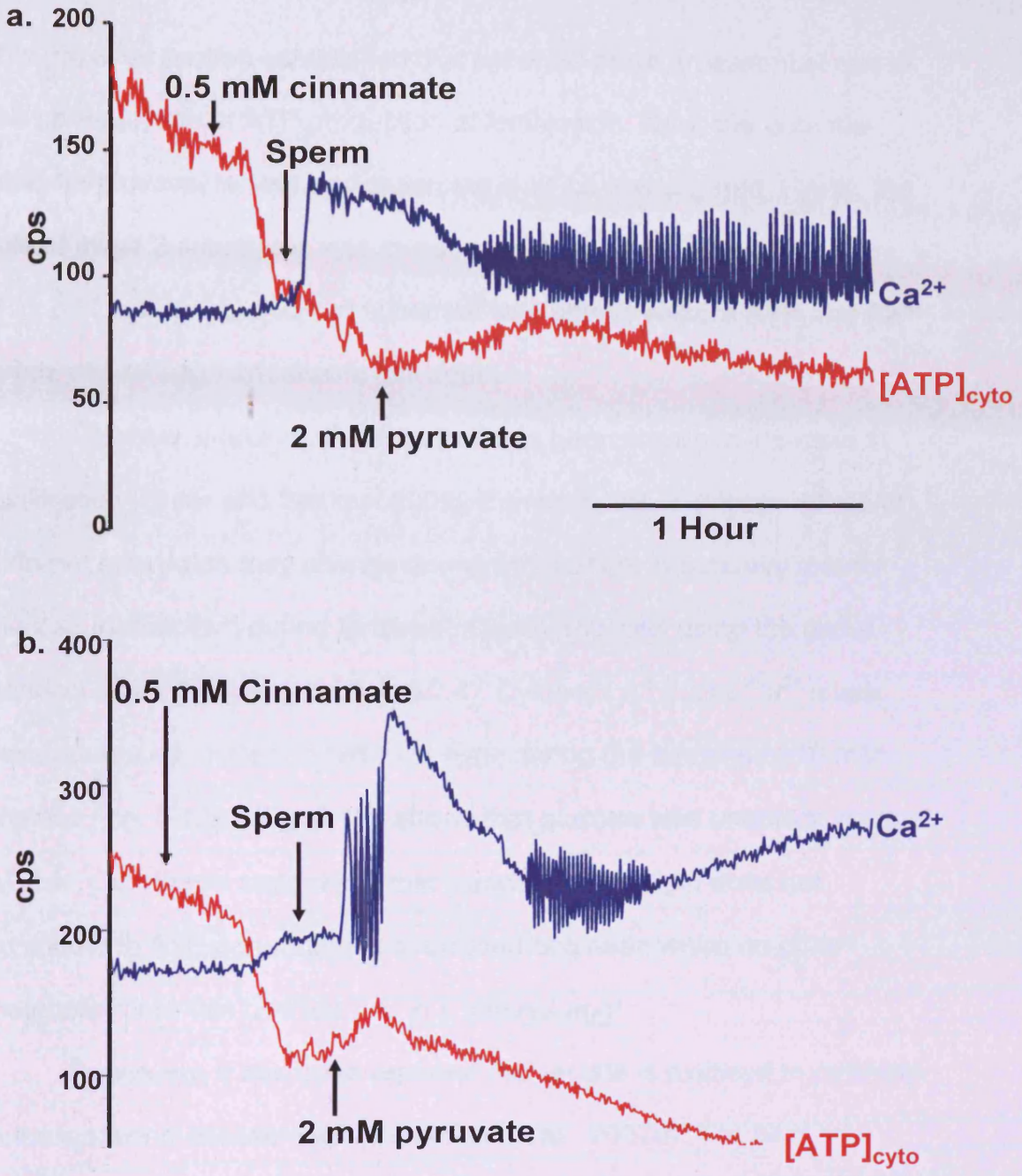

Fig. 5.11 a) and b) shows the response of two eggs injected with cytosolic luciferase and fertilised in substrate free media. Cinnamate was present before the addition of sperm that was followed by pyruvate addition (n=8). Time bar applies to both graphs.

5.2.5 Neither glucose, lactate, or, glutamine can support ATP production in a fertilised egg

The previous section established that pyruvate plays an essential role in the up-regulation of ATP production at fertilisation. Now, the potential roles for glucose, lactate and glutamine shall be investigated. Firstly, the role of these 3 substrates was investigated in starved, unfertilised eggs (Fig. 5.12a, b and c). Neither substrate was able to restore ATP and Ca^{2+} levels and all eggs underwent cell death.

Glucose uptake and metabolism has been shown to increase at fertilisation (Urner and Sakkas, 2005), therefore, the metabolic usage of different substrates may change during fertilisation. A potential role for glucose metabolism during fertilisation was assessed using the same protocol as for pyruvate (section 5.2.4). Cytosolic ATP and Ca^{2+} levels were measured in starved fertilised eggs during the addition of 10 mM glucose (Fig. 5.13a). Fig. 5.13a shows that glucose was unable to restore ATP or, Ca^{2+} levels suggesting that glucose metabolism does not contribute to ATP generation in a fertilised egg even when no other metabolic route can operate (i.e. in a starved egg).

Previously, it has been reported that lactate is oxidised to pyruvate in the cytosol of mouse eggs (Dumollard et al., 2007b). The next experiment sought to establish if pyruvate derived from lactate can support ATP production in a fertilised egg. Therefore, as above, eggs were starved and fertilised before 20 mM lactate was added (Fig. 5.13b). Lactate could not rescue ATP or, Ca^{2+} levels suggesting lactate derived pyruvate cannot supply mitochondrial ATP production in starved eggs.

Finally, 10 mM glutamine was added to starved fertilised eggs. Glutamine can be oxidised to α-ketoglutarate and feed into the TCA cycle. Also, glutamine has been shown to promote development of preimplantation embryos (Biggers et al., 2000; Summers and Biggers, 2003). Fig. 5.13c shows that glutamine addition, like glucose and lactate, is unable to restore ATP and Ca^{2+} back to normal levels.

Fig. 5. 12 Glucose, lactate and glutamine addition to unfertilised starved eggs

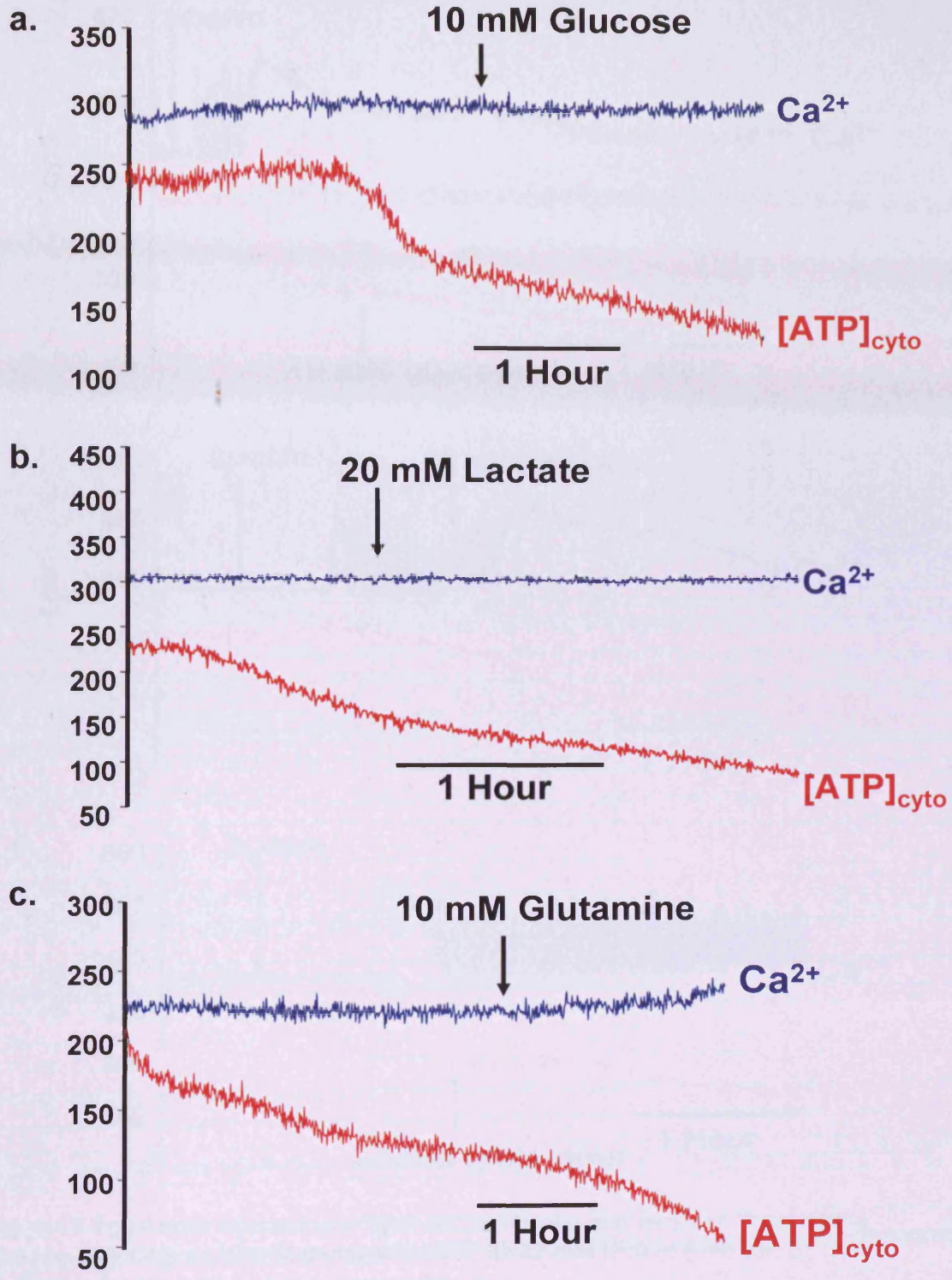

Fig. 5.12 Eggs were injected with cytosolic luciferase and incubated in substrate free media before a) 10 mM glucose (n=10), b) 20 mM lactate (n=8) or, c) 10 mM glutamine (n=15) was added to the media.

Fig. 5. 13 Glucose, lactate and glutamine addition to starved fertilised eggs

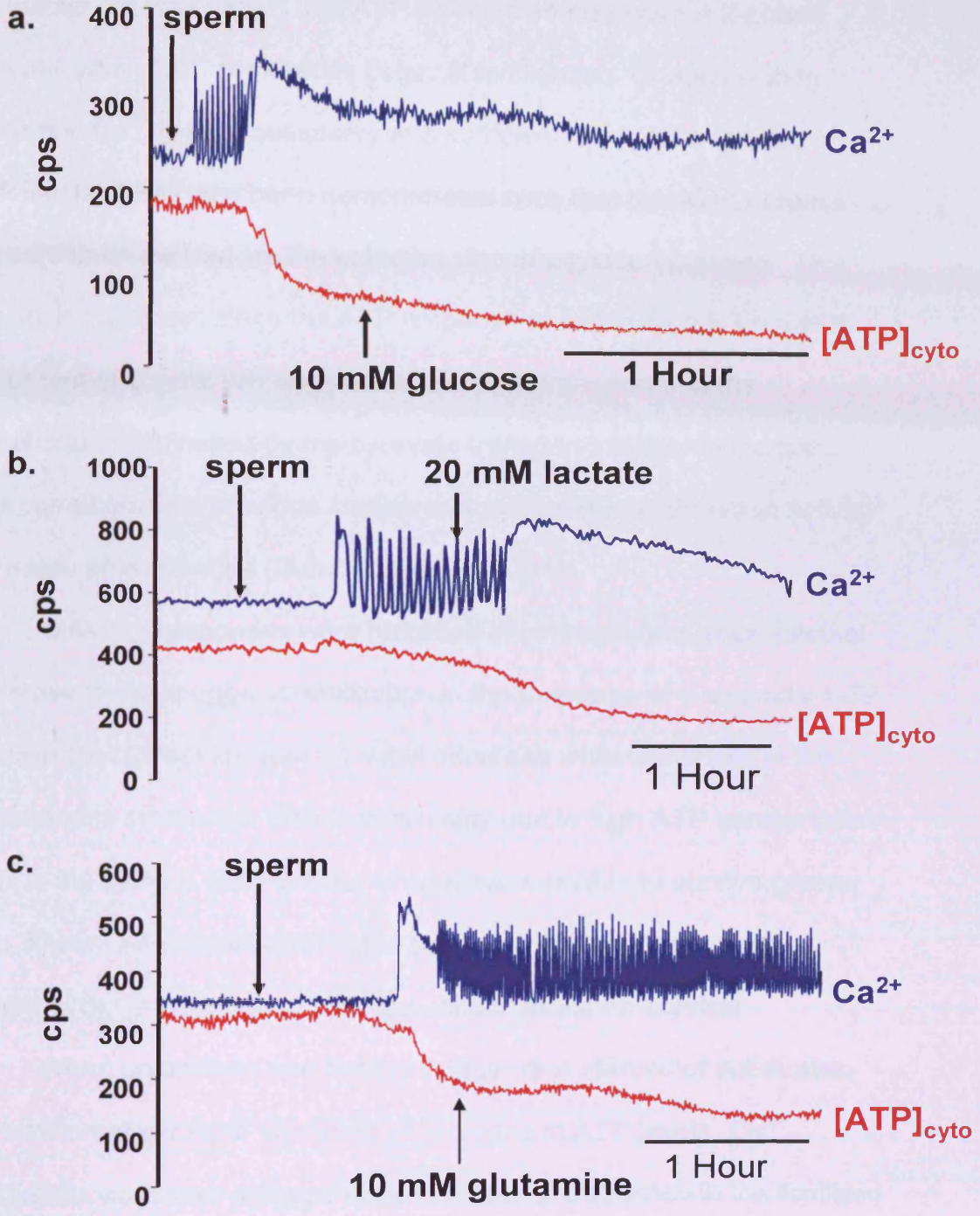

Fig. 5.12 Eggs were injected with cytosolic luciferase and fertilised in substrate free media before a) 10 mM glucose (n=10), b) 20 mM lactate (n=8) or, c) 10 mM glutamine (n=15) was added to the media.

5.3 Discussion

In Chapter 3 it was shown that ATP levels in an egg have a 2-phase increase when Ca^{2+} oscillations begin at fertilisation. Chapter 4 then confirmed Ca^{2+} is both necessary and sufficient to produce the rise in ATP levels. It has now been demonstrated here that the ATP increase appears to be derived via the oxidative phosphorylation pathway. This conclusion is drawn since the ATP response at fertilisation is unable to mirror that of control IVF eggs when pyruvate transport into the mitochondria is blocked by the pyruvate transport inhibitor cinnamate. This correlates with previous studies that suggests mitochondrial activity increases at fertilisation (Dumollard et al., 2004).

Different responses were recorded in cytosolic and mitochondrial luciferase injected eggs at fertilisation in the presence of cinnamate. ATP levels in the cytosol showed an initial decrease while the levels in the mitochondria increased. This is most likely due to high ATP consumption rates in the cytosol. Both groups of eggs were unable to survive greater than 3 hours after fertilisation in the presence of cinnamate which highlights the importance of the eggs mitochondria on survival.

When unfertilised and fertilised eggs were starved of substrates, the addition of pyruvate produced an increase in ATP levels. Ca^{2+} oscillations were also restored back to a normal frequency in the fertilised egg. The recovery by pyruvate addition was consistent and resulted in normal egg activation with all eggs forming PN and 2^{nd} PB.

Glucose and glutamine were unable to stimulate ATP production in starved unfertilised or, fertilised eggs. This suggests that although these

substrates may make minor contributions to MII eggs, they are unable to make a major contribution in the absence of pyruvate. Lactate is converted to pyruvate, but the addition of lactate to starved eggs failed to restore the eggs metabolic status. This result further implies that pyruvate derived from lactate is not taken up by mitochondria as previously suggested (Dumollard et al., 2007b). It has been proposed that pyruvate derived from lactate stays in the cytosol where it is converted to alanine (see main discussion; (Dumollard et al., 2007b).

Chapter 6
Investigations into the Secondary Change in ATP levels at fertilisation

6.1 Introduction

In Chapter 3 it was discovered that an initial rise in ATP levels occurred when Ca^{2+} transients began at fertilisation. This first change was followed by a secondary change in ATP levels that was recorded around 60 minutes post fertilisation with typically the 9^{th} Ca^{2+} spike. The reason for this secondary increase in ATP levels is unexplained and shall be the focus of this chapter.

Studies that have looked at autofluorescence changes in the mitochondria during fertilisation have not reported a secondary change (Dumollard et al., 2004). This is surprising considering the change in ATP recorded after 1 hour in Chapter 3 was so pronounced. Perhaps the change in mitochondrial reduction of NADH and flavoproteins are minor, or, are accumulative over the 1^{st} hour that leads to a dramatic increase in ATP. Additionally, Ca^{2+} oscillations within the eggs mitochondria have been measured simultaneously with cytosolic Ca^{2+} (Rhod2-AM) oscillations using a mito-pericam probe (Fig. 6.1). Mito-pericam (Nagai et al., 2001) was produced by Remi Dumollard and has one mitochondrial targeting sequence that was cloned into pRN3 vector from which cRNA was produced using a T3 promoter kit. *In vitro* matured eggs expressing mito-pericam were imaged and ratiometric measurements of Ca^{2+} within the mitochondria are shown in Fig. 6.1. This data (from Remi Dumollard) does not suggest an increase in mitochondrial Ca^{2+} uptake around the 1-hour mark but this data is not clear enough to draw any conclusions from.

When an egg becomes fertilised, the metaphase II arrest is lifted and the egg is free to continue the cell cycle. This means that many events and changes occur in the fertilised egg, all of which require ATP to drive them. Cortical granule exocytosis, 2nd PB emission and PN formation are some of the many events that could require increased ATP levels (Dumollard et al., 2007; Kline and Kline, 1992). It was established in Chapter 4 that Ca^{2+} and ATP exist in a close relationship which could suggest that Ca^{2+} entry into the mitochondria is driving a change within the mitochondrial matrix as many kinase signalling pathways can be stimulated (PKA, PKB, PKC and p38 are just a few) (Horbinski and Chu, 2005). The ATP levels during fertilisation represent a balance so whether the fertilised eggs requirement for ATP decreases or, an event occurs that triggers excess ATP production shall be explored.

Fig. 6. 1 Mitochondrial and cytosolic Ca^{2+} oscillations during fertilisation

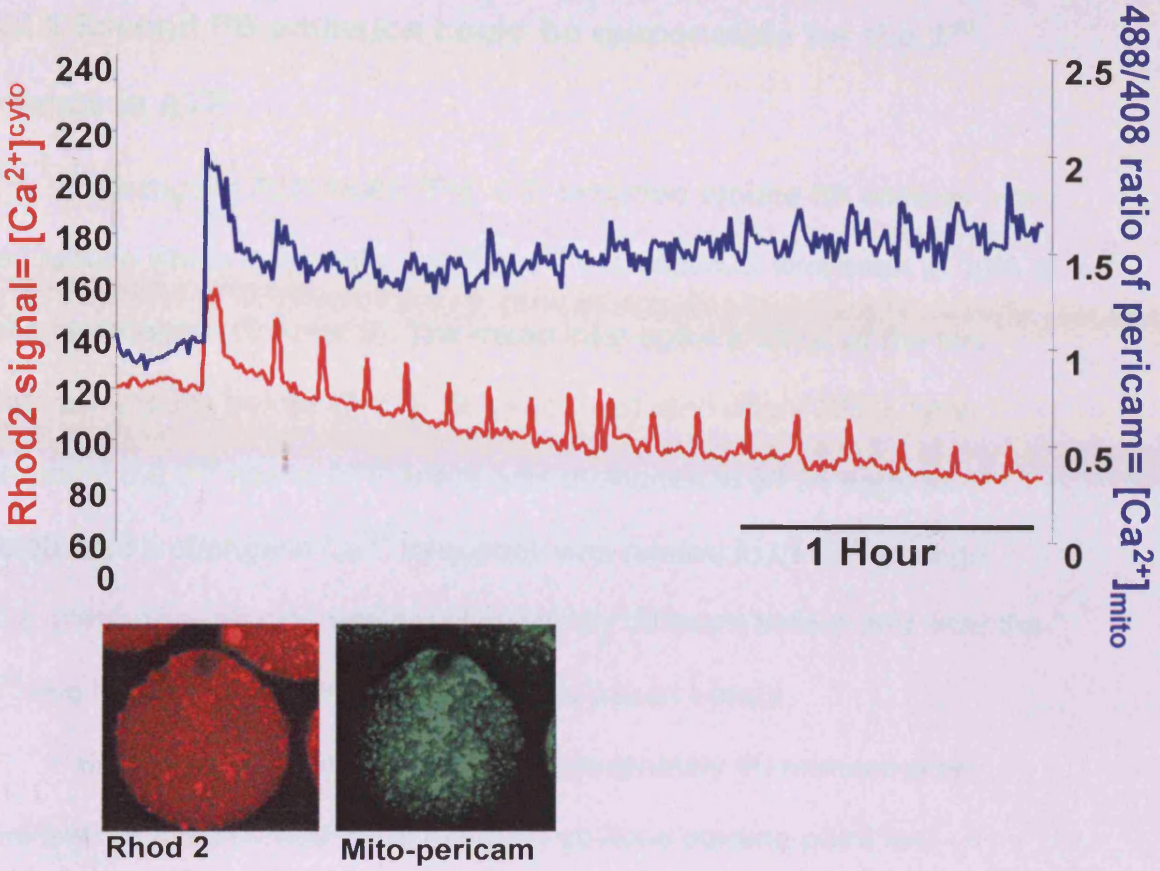

Fig. 6.1 Simultaneous measurements of cytosolic Ca^{2+} (using Rhod2) and mitochondrial Ca^{2+} oscillations (using mito-pericam) (n=15 oocytes - data from Remi Dumollard). Rhod 2 AM was excited at 543 nm and emission was collected at 580 nm through a 580 nm LP filter. Mito-pericam had a duel excitation at 408 and 488 nm (emission 505-550 nm). Confocal imaging was carried out on Ziess LSM 510 meta confocal microscope.

6.2 Results

6.2.1 Second PB emission could be responsible for the 2nd change in ATP

The 2nd change in ATP levels (Fig. 6.2) occurred around 60 minutes after fertilisation which is typically the 9th Ca^{2+} oscillation. It was seen in 90% of all eggs imaged (Chapter 3). The mean inter-spike interval of the two Ca^{2+} oscillations before (730 ± 19.8 seconds), and after (721 ± 18.9 seconds) the 2nd rise in ATP levels was evaluated in all 34 eggs to establish if a change in Ca^{2+} frequency was related to the 2nd change. The inter-spike interval was not significantly different before and after the 2nd rise in ATP levels ($P<0.005$, student's paired t-test).

Since 2nd PB emission occurs approximately 60 minutes after fertilisation, this seemed to be the most obvious starting point for investigating the nature of the 2nd ATP change. Cytochalasin D (CD) prevents the release of the 2nd PB and so fertilisation was carried out in the presence of this substance (Fig 6.3a). The frequency of Ca^{2+} oscillations in the presence of CD (52 ± 0.8 spike/hour) were severely and significantly increased when compared to the frequency (8.7 ± 0.6 spikes/hour) of control IVF experiments from Chapter 3 ($P<0.005$). This prevented the 2nd change in ATP from being investigated thoroughly since the environment within the egg was different to that of the control. It is important to note that low fertilisation rates were obtained during CD experiments. Only 5/12 eggs (over 2 runs) were successfully activated by

sperm. The fertilised 5 eggs had 4 or, 5 PN indicating a high incidence of polyspermy.

In an attempt to overcome the problem of abnormally high frequency Ca^{2+} oscillations using CD, the next approach was to use an alternative inhibitor to prevent 2nd PB emission. Cytochalasin B (CB) also prevents release from MII arrest like CD and so this was tried in order to try and keep the frequency of Ca^{2+} oscillations the same as in control IVF experiments. Fig. 6.3b shows that the frequency of Ca^{2+} oscillations (3 $\pm$ 0.3 spikes/hour) in CB eggs were significantly reduced when compared to control IVF experiments (8.7 $\pm$ 0.6 spikes/ hour) ($P<0.005$). The 2nd change in luminescence still seemed to occur but it was not as pronounced as that seen in control experiments so it is difficult to draw a conclusion from these results. Fertilisation rates for CB eggs were also reduced like eggs treated with CD. Only 5/15 eggs (over 2 runs) were successfully activated and all 5 eggs had 3 PN, indicating no polyspermy.

Fig. 6. 2 A two phase increase in ATP levels during fertilisation

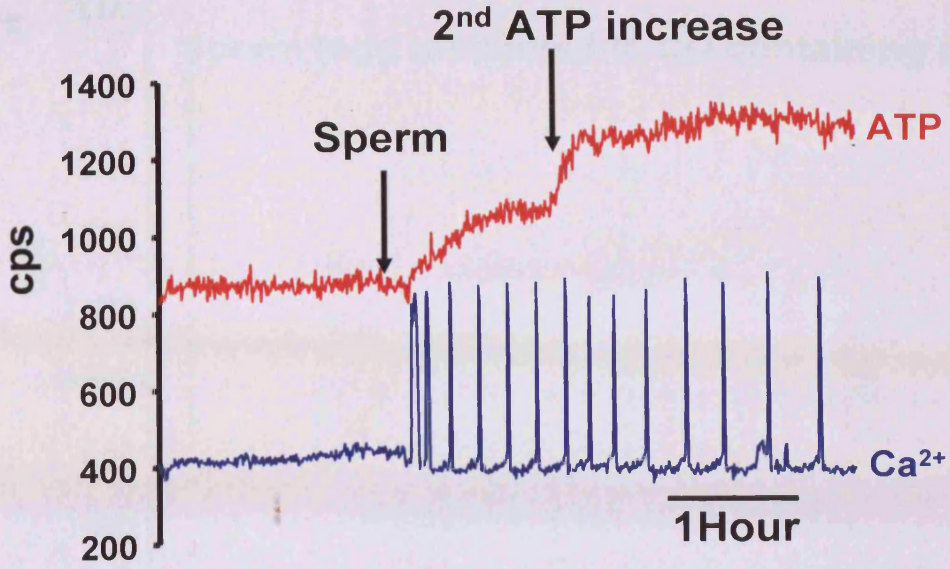

Fig.6.2 An egg fertilised with sperm (see Chapter 3, n=34).The secondary increase in ATP was evident in 34/38 eggs imaged.

Fig. 6. 3 Inhibiting 2nd PB emission during fertilisation

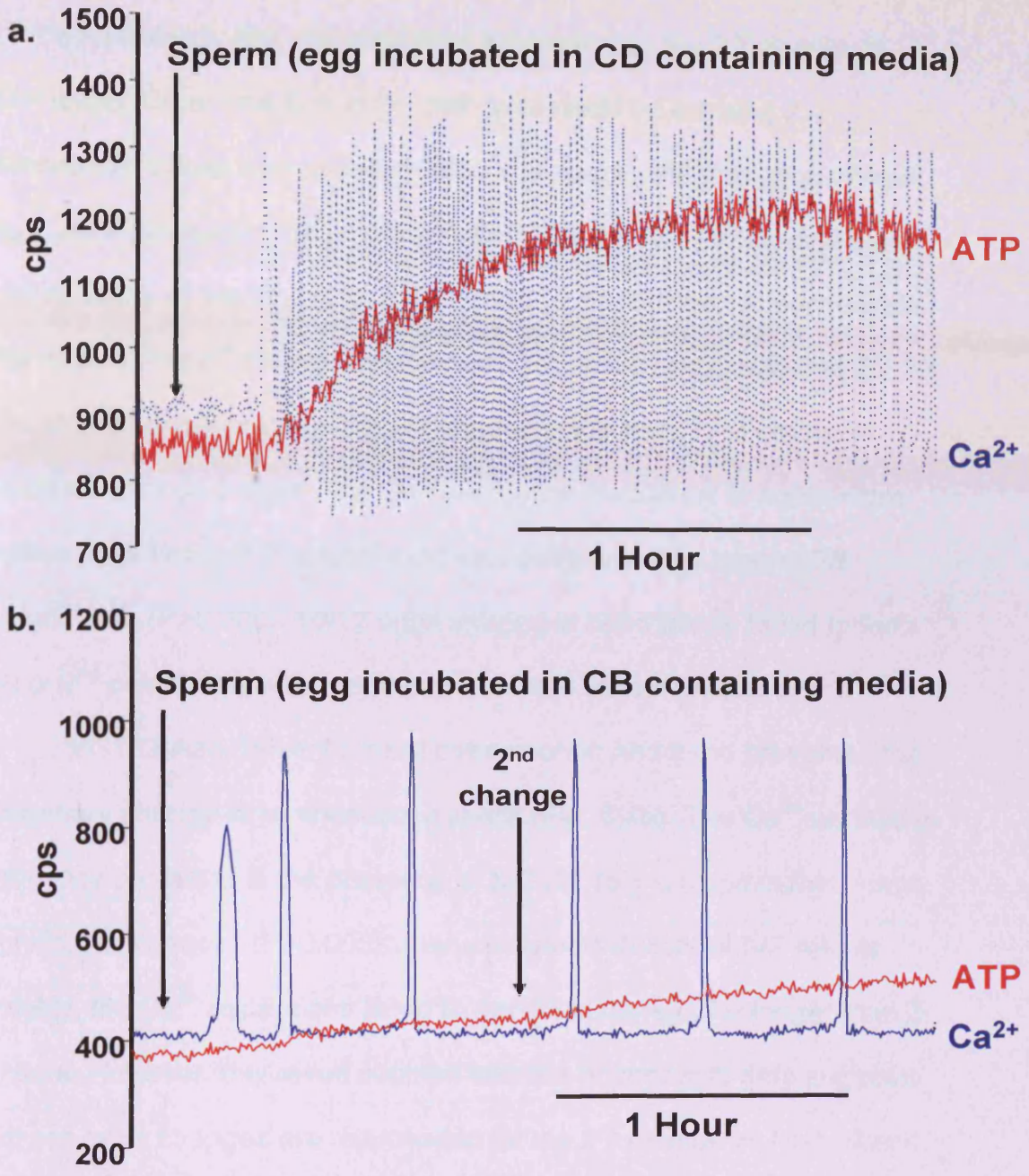

Fig. 6.3 a) A single egg fertilised with sperm in the presence of 2 ug/ml CD (n=5/12 fertilised). All eggs fertilised in CD formed 4 or, 5 PN. b) A single egg fertilised with sperm in the presence of 5 ug/ml CB (n=5/15 fertilised). All eggs fertilised in CB formed 3 PN.

6.2.2 Cell cycle inhibition inhibits the 2nd increase in ATP levels

2nd PB emission is just one candidate for producing the 2nd change in ATP levels. Other changes in the cell cycle could be causing it. Nocodazole blocks meiotic resumption and hence, PN formation. When eggs were fertilised in the presence of nocodazole the 2nd change was inhibited 83% of the time (Fig. 6.4a). The 2 eggs fertilised in nocodazole that showed the 2nd change still formed 3 PN, which suggests that 2nd PB emission does not produce the 2nd change since no 2nd PB emission occurred in these 2 eggs. The Ca^{2+} oscillation frequency in nocodazole treated eggs (9.5 $\pm$ 0.2 spikes/hour) was comparable to control IVF experiments ($P>0.005$). 10/12 eggs imaged in nocodazole failed to form PN or 2nd polar bodies and remained arrested at metaphase II.

MG132 also prevents meiotic resumption and it too prevented the secondary change in luminescence levels (Fig. 6.4b). The Ca^{2+} oscillation frequency produced in the presence of MG132 (5 $\pm$ 0.5 spikes/hour) was significantly reduced ($P<0.005$) when compared to control IVF results. Notably, the Ca^{2+} oscillations failed to persist in the egg for longer than 2-3 hours. However, this result coupled with the nocodazole data suggests that cell cycle changes are responsible for the 2nd change in ATP. These results suggest that some part of the cell cycle could explain the increase in ATP. All eggs fertilised in MG132 remained arrested at metaphase II.

Fig. 6. 4 Nocodazole and MG132 fertilised eggs

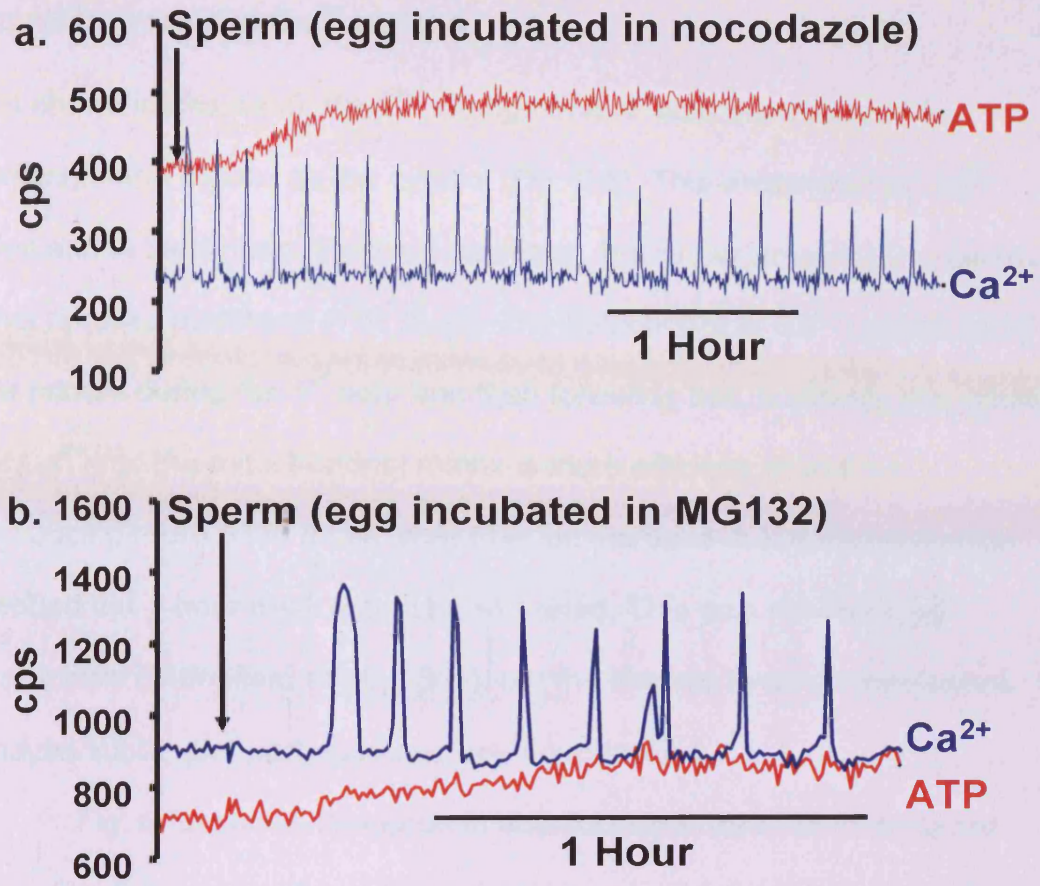

Fig. 6.4 Eggs were fertilised in the presence of a) 10 μM nocodazole (n=10/12 showed no 2nd change in ATP) or, b) 50 μM MG132 (n=8). Ca^{2+} oscillations and the initial increase in ATP were still recorded however, the secondary rise in ATP levels was not evident.

6.2.3 Mitochondrial activity could increase due to an increase in mitochondrial Ca^{2+} uptake

As shown in chapter 5, the 2nd change in ATP also occurred in the mitochondria as well as the cytosol (Fig. 6.5). This suggests that ATP demand in the cytosol does not decrease, but rather an event is triggered that requires additional ATP levels. The mitochondrial Ca^{2+} uptake could be primed during the 1st hour and then following this, suddenly the uptake of Ca^{2+} into the mitochondrial matrix is more efficient, therefore, producing more ATP. If this were true, an increase in autofluorescence around the 1-hour mark would be expected. This was not reported previously (Dumollard et al., 2004), but the change in autofluorescence maybe subtle and perhaps have been overlooked.

Fig. 6.6a shows flavoprotein autofluorescence in an unfertilised egg. Fig. 6.6b and c shows the reduction and oxidation of flavoproteins during the first few hours of fertilisation using different imaging techniques (see Chapter 2: Methods). Different measuring techniques were explored to ensure a second change in autofluorescence was not being overlooked due to sampling technique or, background noise. In both traces there appears to be no distinct secondary change in the rate of reduction/oxidation of flavoproteins occurring.

Fig. 6. 5 Mitochondrial ATP during fertilisation

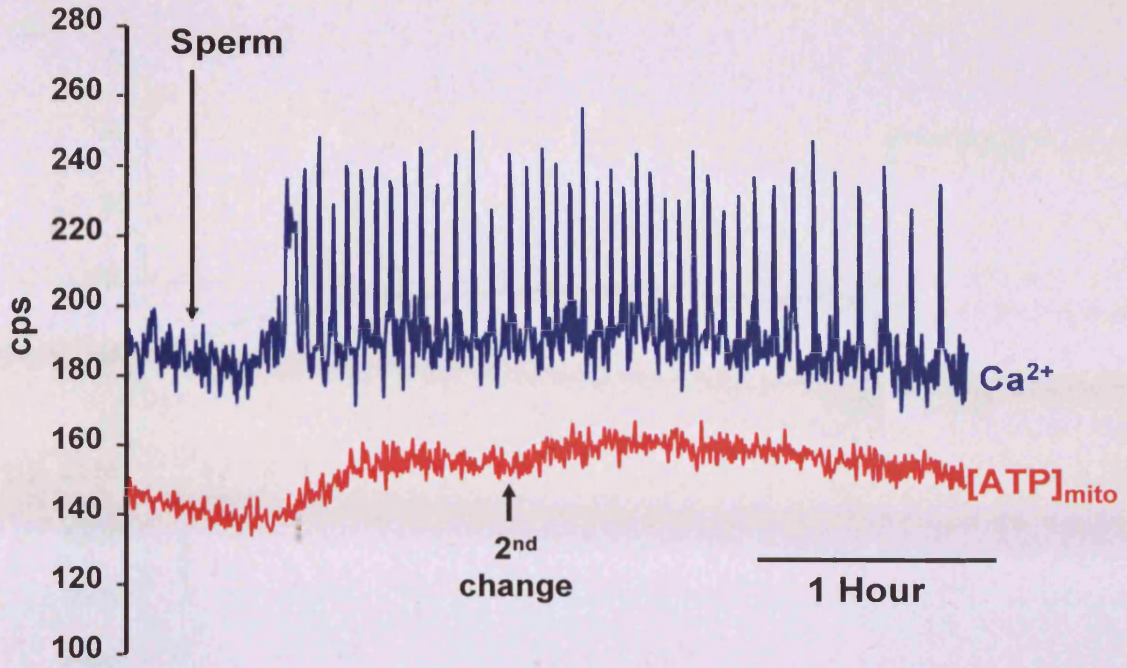

Fig. 6.5 Eggs were injected with 0.675ug/ul cRNA (pipette concentration) of firefly luciferase with a mitochondrial targeting sequence (see Chapter 2: Methods). After expression of lucfierase (4 hours) eggs were then fertilised. The increase in mitochondrial ATP also occurs in two phases during the Ca^{2+} oscillations like that seen with cytosolic luciferase.

Fig. 6. 6 Flavoprotein autofluorescence during fertilisation

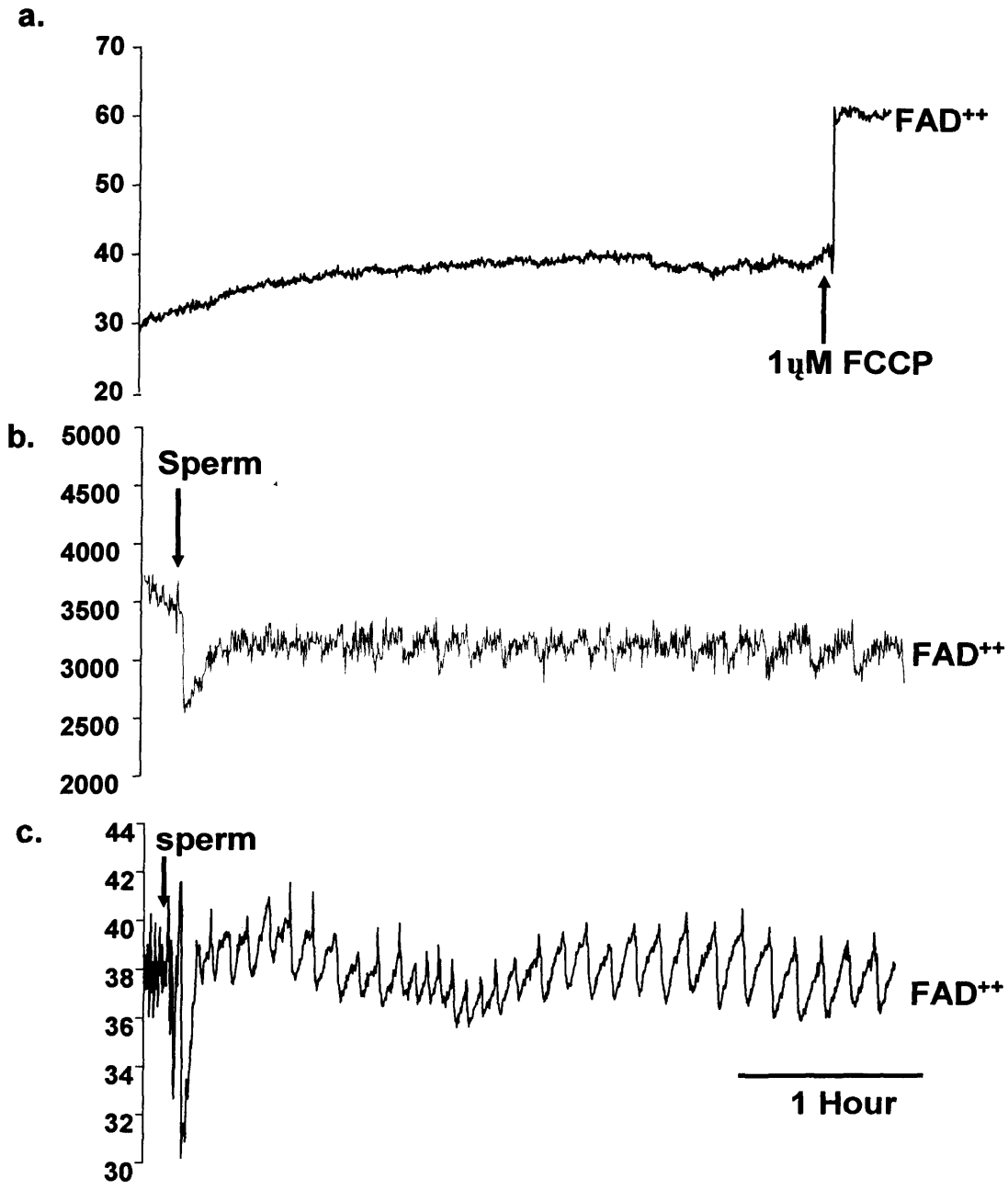

Fig. 6.6 a) FAD^{++} autofluorescence was measured in unfertilised eggs for 4 hours and FCCP was added to confirm FAD^{++} was being measured (n=10) using photometric software. b) and c) Eggs were fertilised with sperm and Flavoprotein reduction and oxidation was measured for 4 hours. All eggs were confirmed to have formed PN and 2nd PB. FAD^{++} autofluorescence was measured b) continuously on a Photek imaging system (n=7) or, c) every 10s using photometric software (n=5) (see Chapter 2: Methods for details).

Ideally, autofluorescence would have been measured with luminescence during fertilisation, as this would give a clear indication of when the 2nd change in ATP increase was occurring. However, FAD^{++} fluorescence emission is collected through a 520 nm LP filter and is excited through a 450 nm BP filter (10 nm width). Luciferin is fluorescent and the excitation and emission values for FAD^{++} autofluorescent are within the range of luciferin excitation and emission values (Fig. 6.7) and hence FAD^{++} autofluorescence was undetectable with luciferin present. Although FAD^{++} excitation is towards the end of the spectrum for excitation of luciferin, enough luciferin is becoming fluorescent to prevent detection of FAD^{++} autofluorescence.

Fig. 6. 7 Excitation and emission profiles of luciferin and FAD^{++}

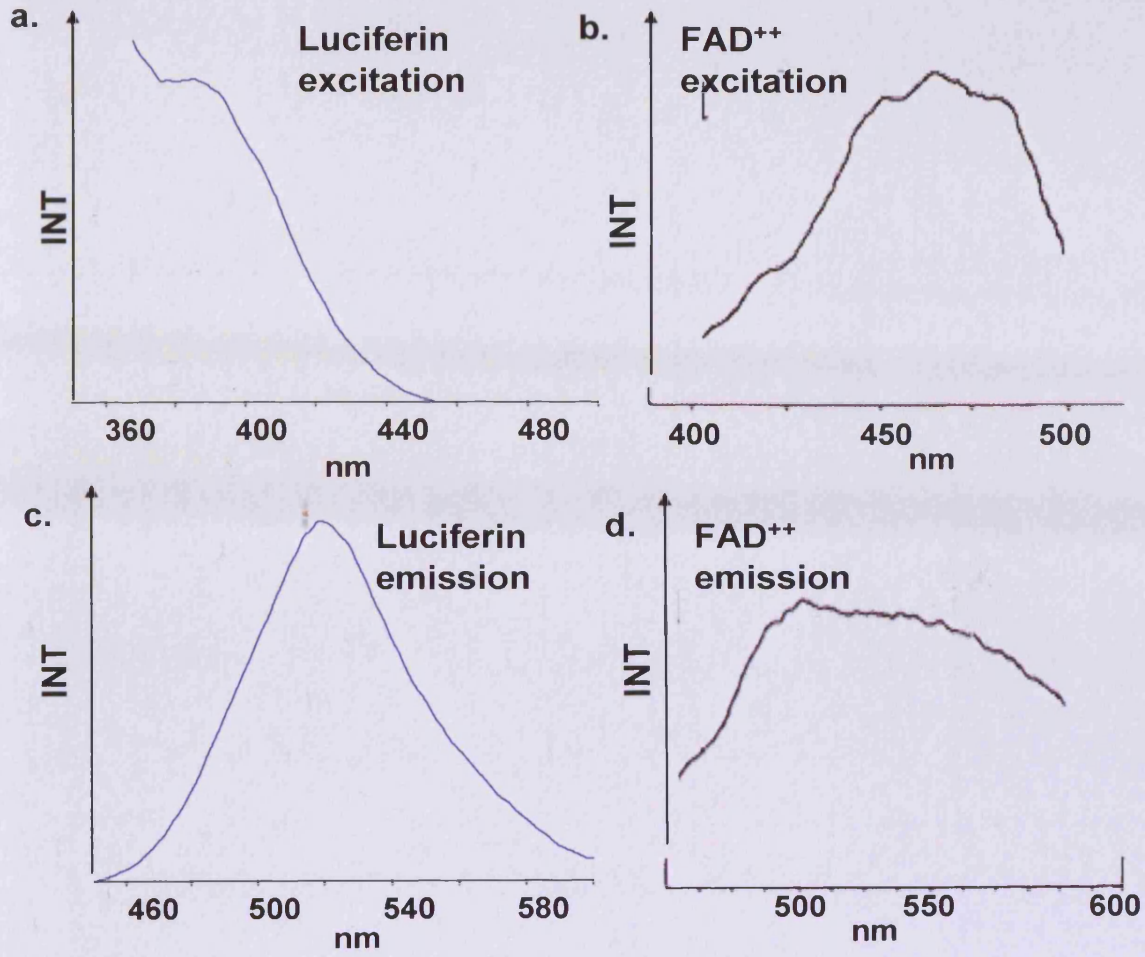

Fig. 6.7 Luciferin fluorescence a) excitation and c) emission profiles obtained using a fluorimeter. FAD^{++} fluorescence b) excitation and d) emission profiles. (b and d spectral images taken from Kunz. 1986). INT = fluorescence intensity

6.2.4 Inhibiting mitochondrial Ca^{2+} uptake into the mitochondria

If Ca^{2+} uptake into the mitochondria increases, it is likely to occur through the uniporter. The Ca^{2+} uniporter in the mitochondria has proposed to be regulated via p38 MAP kinase activity (Montero et al., 2002). SB202190 is a highly specific inhibitor of the p38 MAP kinase (Montero et al., 2002). SB202190 inhibits p38 MAP kinase phosphorylation and, therefore, causes opening of the uniporter. Therefore, fertilisation in the presence of SB202190 would not be expected to produce a 2^{nd} rise in ATP since the uniporter is already allowing the maximum flow of Ca^{2+} into the mitochondria. When eggs were fertilised in the presence of this agent, the 2^{nd} change was not inhibited (Fig. 6.8). This could suggest that Ca^{2+} influx into the mitochondria does not change during fertilisation. Or, it could suggest that the uniporter in mouse eggs is not sensitive to this protein kinase inhibitor, implying that it is regulated via another mechanism.

Fig. 6. 8 Fertilisation in SB202190

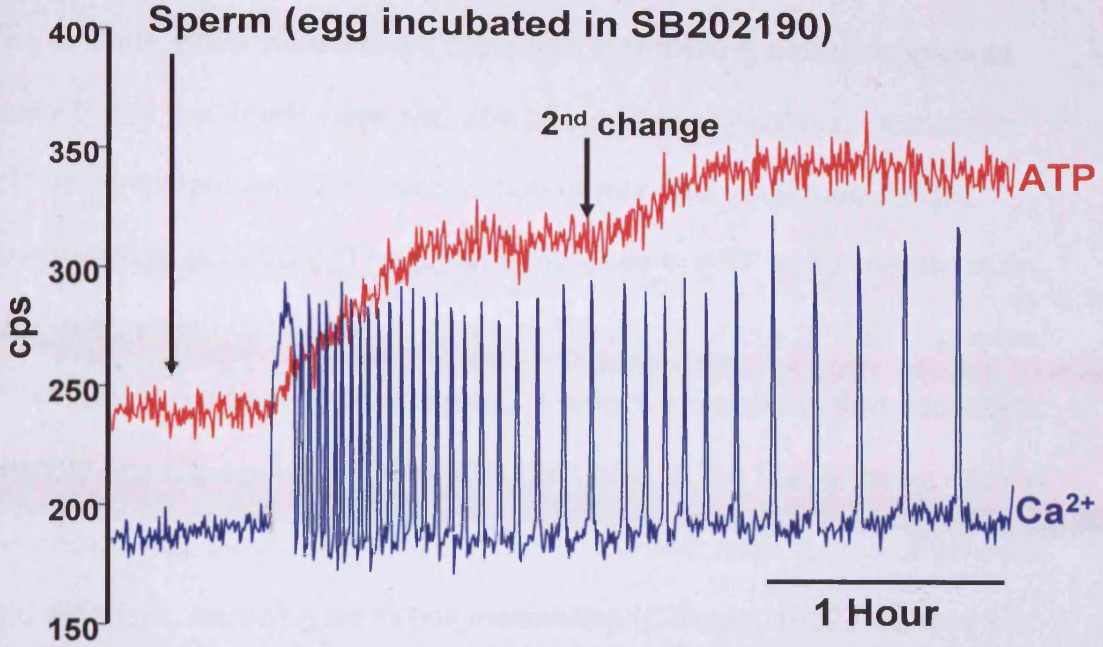

Fig. 6.8 Eggs were fertilised in the presence of the p38 MAP kinase inhibitor SB202190 (20 μM) (n = 4).

6.3 Discussion

The luminescence increase we observed in fertilising mouse eggs was distinctive in that there were two abrupt increases. An initial increase in ATP is consistent with Ca^{2+} stimulation of mitochondrial metabolism (Dumollard *et al.*, 2004). The second increase in ATP occurred about an hour later, which corresponds to around the time of the 9th Ca^{2+} increase. 2nd PB could not be fully investigated due to the problems that occurred with CD and CB agents. CD and CB both bind to the fast growing ends of microfilaments, blocking the addition of monmeric actin to microfilaments, and therefore, reducing actin polymerisation (Cooper, 1987; McAvey et al., 2002) and hence 2nd PB release. CD has been shown to be more effective than CB, as CB has an additional effect in that it inhibits glucose transport (Cooper, 1987). It has been demonstrated that CD treatment increases polyspermy (McAvey et al., 2002) which correlates with the data presented in this chapter. CD treatment increased polyspermy (>3PN) and hence high Ca^{2+} oscillation frequencies were observed. CB treated eggs showed a low Ca^{2+} oscillation frequency which could be related to glucose transport in the sperm being affected by CB. Both agents produced low fertilisation rates.

The microtubule inhibitor nocodazole has been shown to prevent meiotic resumption and to block all changes in cell cycle proteins in xenopus and mouse eggs respectively, (Gerhart et al., 1984; Kubiak et al., 1993). Figure 6.4a shows that when sperm were added to eggs that were incubated in nocodazole there was a familiar series of Ca^{2+} oscillations and an increase in luciferase luminescence similar to that

seen in control fertilised eggs. Most eggs (10/12) fertilised in nocodazole failed to show the secondary increase in luminescence that was seen in the majority of eggs fertilised in normal media. The frequency and size of the first Ca^{2+} spike during fertilisation with nocodazole was comparable to normally fertilised eggs. Despite the absence of the secondary change the data does suggest that the first and major rise in ATP levels at fertilisation only requires the generation of Ca^{2+} oscillations. Cell cycle inhibition would prevent many events from taking place, so although this data suggests cell cycle involvement in the 2^{nd} change it does not allow any major conclusions to be drawn. Other agents investigated were the MAPK inhibitor UO126, the cyclin B inhibitor roscovitine and the protein kinase inhibitor 6 DMAP. All these agents were unsuccessful as they altered the sperm induced Ca^{2+} oscillations (data not shown). This correlates with other groups that proposed UO126 alters sperm induced Ca^{2+} oscillations (Matson and Ducibella, 2007) and roscovitine suppresses sperm induced Ca^{2+} oscillations (Deng and Shen, 2000).

Measurements of mitochondrial flavoproteins and NADH, or, mitochondrial Ca^{2+} changes at fertilisation show oscillatory changes in synchrony with Ca^{2+} oscillations (Dumollard et al., 2004). These measurements have not shown any sign of a two-phase change so it is not clear why there should be such a marked secondary increase in ATP (Dumollard et al., 2004). One possibility may be that the secondary change in ATP reflects a balance between the stimulation of mitochondrial ATP production and ATP consumption. This idea would imply a decrease in ATP consumption about one hour into fertilisation

which may be related to a cell cycle event. However, since the 2nd change in ATP is seen in the mitochondria this implies that ATP consumption in the cytosol does not decrease, rather ATP production is increasing. Ca^{2+} activates the dehydrogenases of the Krebs cycle (McCormack et al, 1990) and the electron transport chain (Gunter et al., 1994). Ca^{2+} also has a direct effect on the F_0-F_1 ATP synthase (Territo et al., 2000). Therefore, this would suggest that Ca^{2+} influx into the mitochondria undergoes an increase which translates into an increase in ATP production. Ideally Ca^{2+} oscillations in the mitochondria should be measured simultaneously with cytosolic Ca^{2+} oscillations. This experiment would confirm if Ca^{2+} oscillations in the mitochondria are responsible for the 2nd change in ATP levels. Mitochondrial aequorin would be suitable for this experiment however; this probe was unavailable for further investigations to take place.

Changes in ATP in the mitochondria are very similar (identical) to the changes observed with cytosolic luciferase. This result is surprising as it means that the transfer of ATP from the mitochondria to the cytosol is very fast. Also, it means that ATP can diffuse into the cytoplasm which is not so unexpected because of results previously published (Campbell and Swann, 2006; Dumollard et al., 2004). As mentioned above, increased Ca^{2+} entry into the mitochondria could explain the 2nd change. The p38 MAP kinase inhibitor SB202190, that has been shown to block the Ca^{2+} uniporter in HeLa cells (Montero et al., 2002), failed to inhibit the 2nd change in fertilising mouse eggs. This result would suggest that Ca^{2+} entry into the mitochondria is not changing around 1 hour post

fertilisation. Another possibility is that p38 MAP kinase is not responsible for regulating the Ca^{2+} uniporter channel in eggs. Since the activity of this kinase has not yet been investigated in mouse eggs, it is difficult to interpret this result. If increased Ca^{2+} entry into the mitochondria is responsible for the 2nd change this could also involve a change in ER positioning. It has been shown that ER reorganisation occurs during fertilisation (FitzHarris et al., 2003). This would mean the mitochondria are in closer proximity and hence, exposed to higher Ca^{2+} levels leading to an increased efficiency of Ca^{2+} transport into the mitochondria resulting in increased ATP production (refer to Chapter 8: Main discussion).

However, Ca^{2+} influx into the mitochondria is just one of many possibilities that could explain the phenomenon of the 2nd change in ATP levels at fertilisation since Ca^{2+} entry into the mitochondria produces many effects. Ca^{2+} causes the phosphorylation of 45 proteins and also the dephosphorylation of PDH and manganese superoxide dismutase (MnSOD) (Hopper et al., 2006). Therefore, many avenues have to be explored in this complex process to define the second change in ATP levels during fertilisation. Also, a chain of events, rather that one specific event, could be responsible for the second increase in ATP.

Chapter 7
The mechanism of action of PLCζ

7.1 Introduction

PLCζ was recently identified as the protein present in sperm that can produce fertilisation-like Ca^{2+} oscillations (Saunders et al., 2002). PLCζ is unlike other mammalian PLCs in that it has no PH domain. The PH domain of PLCδ is well characterised as being responsible for targeting to PIP_2 that resides in the PM (Yamamoto et al., 1999). Therefore, how PLCζ initiates a Ca^{2+} response via the $InsP_3$ pathway is still undefined.

Before PLCζ was proposed to be the sperm factor other PLCs were thought to be responsible for egg activation. PLCδ and PLCγ are two such families that been looked at in detail. Two mammalian PLCγ isoforms have been identified; PLCγ1, and PLCγ2. PLCγ is distinguished from other PLCs by the presence of three Src homology domains (two SH2 domains followed by a SH3 domain) that are present in the XY linker region. Egg derived PLCγ1 has been suggested to play a role in sea urchin, starfish and ascidian eggs at fertilisation (Jaffe et al., 2001) but its role in mammalian fertilisation continues to be discussed. Four distinct PLCδ isoforms have been identified in mammals and PLCδ1 is the most abundant and widely expressed.

This chapter shall focus on the domains of PLCζ that are essential for successful egg activation. Also, the Ca^{2+} oscillation inducing activity of both human (h) and monkey (*simian* (s)) PLCζ shall be discussed. Additionally, the ability of both PLCδ1 and PLCγ1 to induce Ca^{2+} in oscillations in mouse eggs shall be investigated in this chapter.

7.2 Results

7.2.1 Quantification of protein expression

Studies have looked at the ability of PLC constructs to induce Ca^{2+} oscillations in mouse eggs, however, the protein expressed in these eggs has never been confirmed (Cox et al., 2002; Kouchi et al., 2004; Kuroda et al., 2006; Mehlmann et al., 2001; Saunders et al., 2002). In this chapter PLC constructs tagged with luciferase (LUC) were used and protein expression was verified and quantified as previously described (Campbell. 1988). To establish the amount of PLC-LUC protein that was being expressed in eggs following cRNA injections, a calibration was performed. Briefly, eggs were injected with known amounts of firefly luciferase protein (1 ng, 100 pg, 10 pg and 1 pg). Single eggs, from each group of known luciferase concentrations, were then lysed with 1% Triton X100 in a PBS buffer containing 1 mM $MgCl_2$, 1 mM ATP and 100 µM luciferin. The lysis took place in a custom made luminometer (see Chapter 2: Materials and Methods) and the average signal (cps) was taken over 60 seconds. A log-log plot was established (Fig. 7.1) using the 4 known protein concentrations and the counts recorded over the 60 second period. Following linear regression, an equation was obtained (Fig. 7.1) that was used throughout the rest of this chapter to calculate the unknown protein content in eggs that had been injected with a luciferase tagged PLC construct.

Fig. 7.1 Calibration for quantification of protein expression

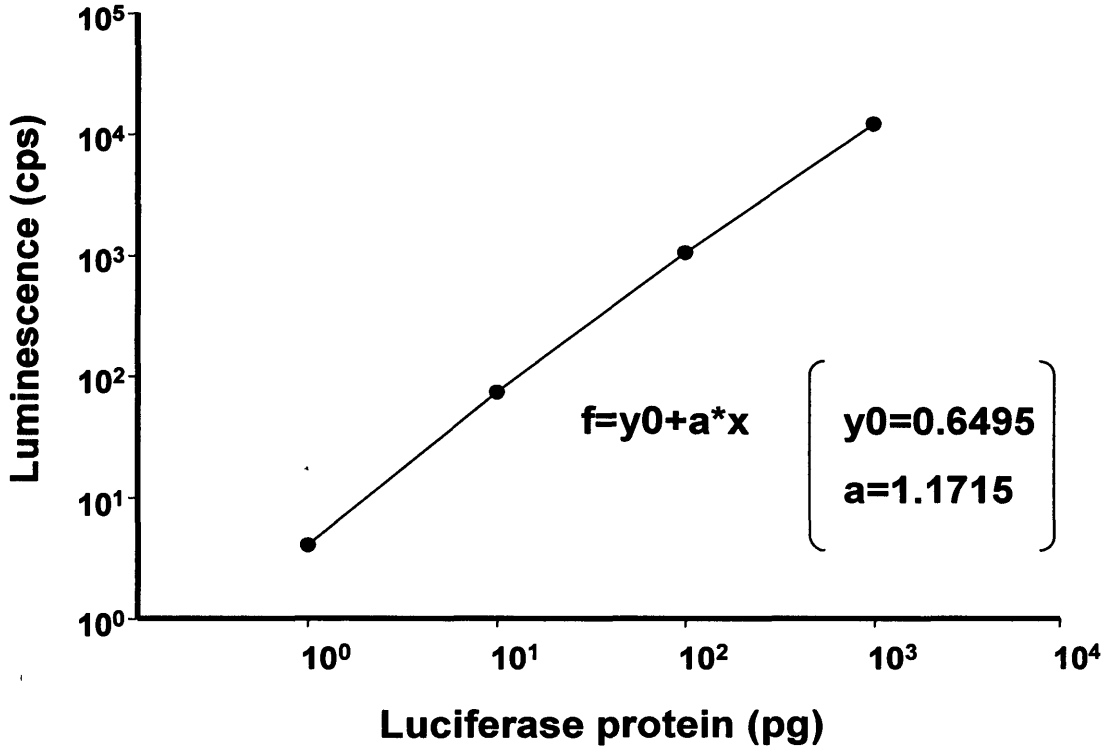

Fig. 7.1 Calibration curve to calculate the amount of PLC-LUC protein being expressed. Following linear regression analysis the equation and unknowns were determined where f, is the cps obtained from lysing eggs in the luminometer and x is the unknown protein content value.

7.2.2 Preparation of WT mPLCζ-Luciferase and deletion constructs

The constructs used throughout this chapter were prepared and expression was confirmed by either Michail Nomikos, Chris Saunders, or, Jose Gonzalez Garcia. For all constructs, expression was confirmed with either western blots using an anti-luciferase antibody, or, using a TNT reaction. Fig. 7.2A-D shows an illustration of the cloning strategy used to prepare the series of 4 constructs. Mouse (m) PLCζ-luciferase (LUC), ζΔEF1-LUC, ζΔC2-LUC and ζΔD210-LUC were amplified by PCR and cloned into the pCR3 vector. Luciferase was then amplified via PCR before being inserted into the pCR3 vector that already contained the appropriate PLCζ construct. Expression of PLCζ-LUC, ζΔEF1-LUC, ζΔC2-LUC and LUC control, was confirmed by western blot analysis (Figure 7.2E).

7.2.3 Expression of PLCζ-LUC, ζΔEF1-LUC, ζΔC2-LUC and ζD210R constructs in mouse eggs

cRNAs corresponding to LUC constructs were prepared (as described in Chapter 2: Section 2.3.1) and microinjected (as described in Chapter 2: Section 2.5.3) into mouse eggs. A concentration of 0.02 μg/μl WT mPLCζ was injected as this has previously been shown to be effective at producing a series of Ca^{2+} oscillations similar to fertilisation (Saunders et al., 2002). In Fig. 7.3A the graph demonstrates that eggs injected with cRNA encoding PLCζ-LUC produced a series of Ca^{2+} oscillations in the eggs that lasted several hours. This shows that the luciferase tagged at

the C-terminus of PLCζ did not prevent PLCζ from generating Ca^{2+} oscillations, as has previously been shown for N-terminal tags (Saunders et al., 2002). The Ca^{2+} signal within the injected eggs were measured for 4 hours. At the end of this 4 hour interval, luminescence was then measured from the same set of eggs (in the absence of fluorescence excitation) to confirm luciferase expression (Figure 7.3A right image). All eggs injected with PLCζ-LUC cRNA that showed clear luciferase expression after 4 hours (n=23), had also exhibited Ca^{2+} oscillations at a frequency of 6 spikes/hour (see Table 7.1). A further 2 concentrations of PLCζ were investigated (1 μg/μl and 0.1 μg/μl) to establish a relationship between expression of PLCζ and the frequency of Ca^{2+} oscillations that were induced (Table 7.1). These results show that increasing the concentrations does not necessarily increase the frequency of oscillations. Additionally, the highest (1 μg/μl) concentration induced premature stoppage of the oscillations after around 2 hours.

When eggs were injected with ζΔEF1-LUC cRNA, all 26 eggs showed no change in intracellular Ca^{2+} levels (Fig. 7.3B). However, these eggs did possess luciferase activity that was confirmed by the intense luminescence signal detected at the end of the experiment (Figure 7.3B). Similarly, after injection of ζΔC2-LUC cRNA, all 26 eggs failed to show any Ca^{2+} increase (Fig. 7.3C) despite strong luciferase luminescence (Fig. 7.3C). In addition, when ζD210R-LUC was injected into eggs no Ca^{2+} oscillations were recorded even though the presence of luciferase expression was detected (Fig. 7.3D)

The exact level of luminescence in cells can depend upon the amount of luciferase protein, the intracellular pH and the ATP concentration (Allue et al., 1996). Consequently, the relative level of luciferase expression was quantified by lysing the group of luminescent eggs in a buffer with a fixed concentration of ATP (1 mM). Upon lysing the eggs in a luminometer, the level of protein expressed could be determined at the end of the experiment (4.5 hours post injection). Table 7.1 lists the level of protein expression that was determined for each construct. A mean value of 0.19pg of WT mPLCζ-LUC (0.02 μg/μl) protein was expressed per egg (n=23). For ζΔEF1-LUC, ζΔC2-LUC and ζD210R-LUC a mean value of 0.98 pg (n=26), 2.7pg (n=26) and 2.1 pg (n=30) of protein was expressed per egg respectively. All three deletion constructs were expressed in eggs at levels that were 5 to 15 fold higher than that of PLCζ-LUC suggesting that the absence of Ca^{2+} oscillations is due to the constructs and not poor expression levels. It has been published that the threshold for PLCζ to cause Ca^{2+} oscillations in an egg is around 50 fg (Saunders et al., 2002). This means that the three domain-deletion constructs were expressed at levels that are 20-50 times the amount required to cause Ca^{2+} oscillations with the full-length PLCζ.

Fig. 7. 2 Preparation of PLCζ-LUC and ζ-LUC deletion constructs

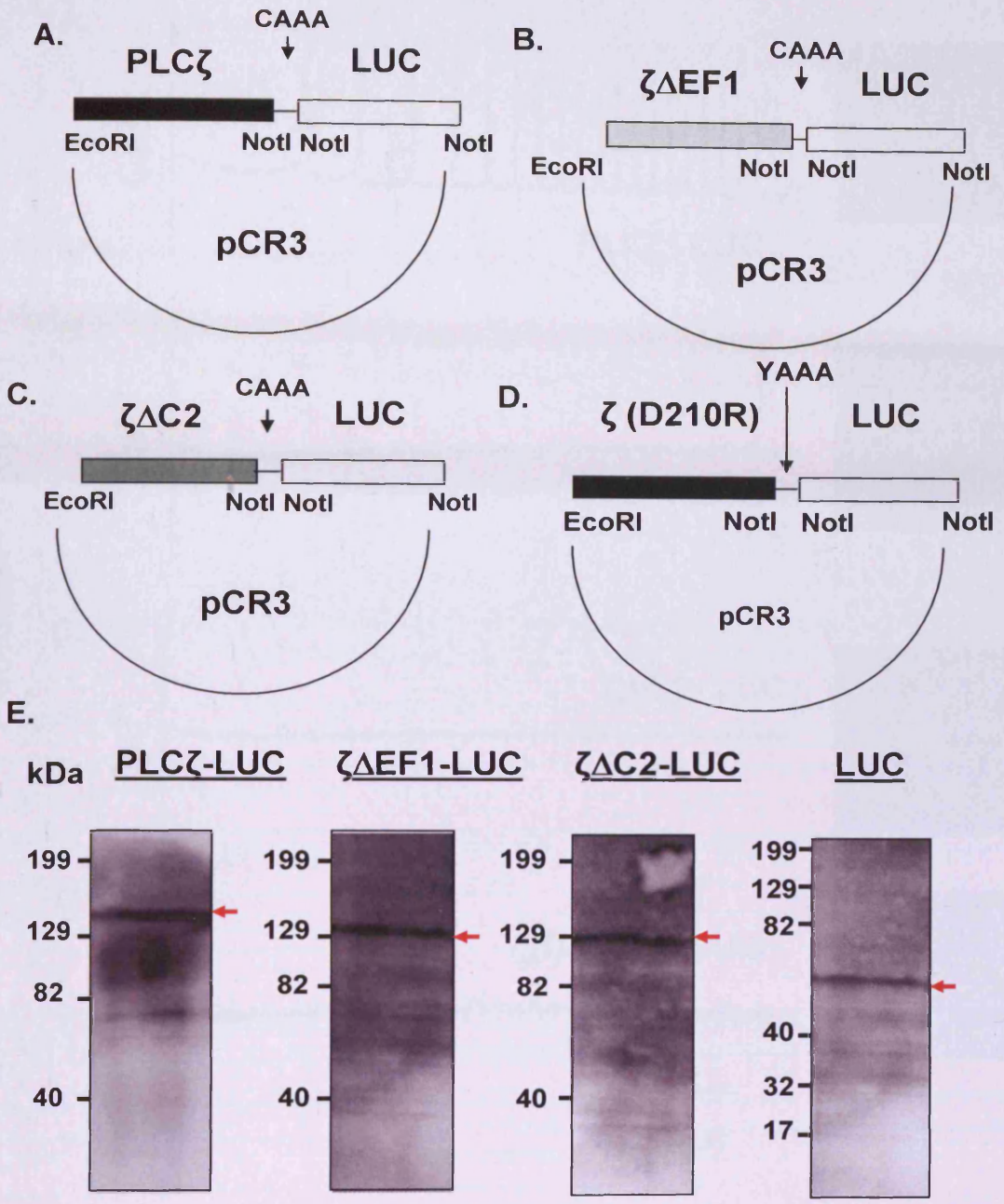

Fig. 7.2 Diagrams showing the cloning strategy used for mPLCζ-LUC (A), ζΔEF1-LUC (B), ζΔC2-LUC (C) and PLCζ with the aspartate residue at position 210 mutated to an arginine residue (ζD210R-LUC) (D). E) Western blots were performed to confirm luciferase was correctly tagged onto the PLCζ domain constructs, using an anti-luciferase antibody – red arrow indicates protein band of the appropriate molecular weight (MW of PLCζ is 74 kD and MW of luciferase is 60 kDa). Control luciferase cRNA was prepared to confirm the correct size of the luciferase protein.

Fig. 7. 3 Microinjection of PLCζ-LUC and ζ-LUC deletion constructs

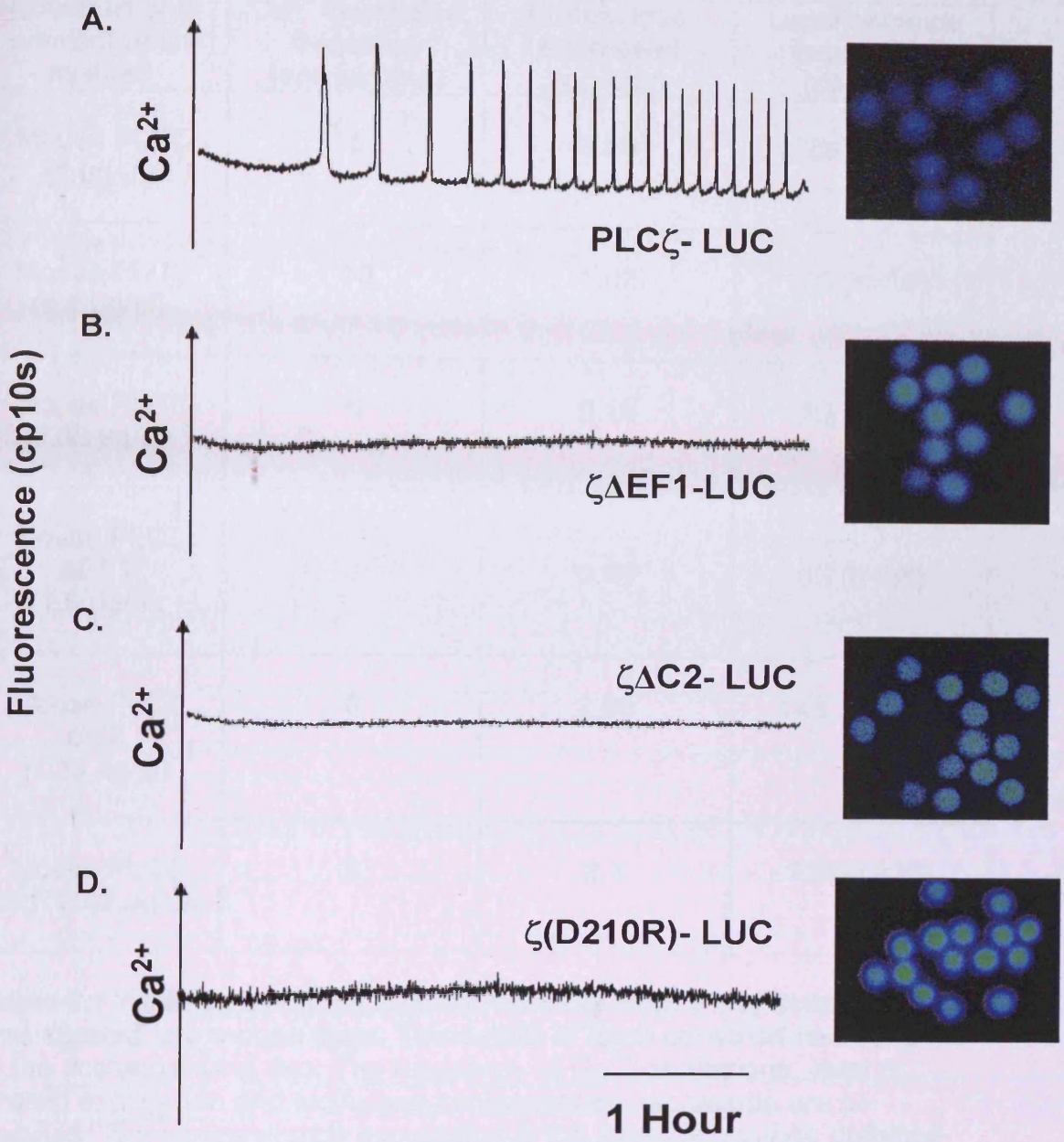

Fig. 7.3 Eggs were injected with OGBD and a PLCζ-LUC constructs. The left graph shows the changes in intracellular Ca^{2+} levels that were measured continuously for 4 hours. The right panel shows an integrated image over 30 minutes of the luciferase-luminescence signal from the same eggs from which Ca^{2+} measurements were taken.

Table 7.1 – WT mPLCζ-LUC and deletion constructs

Construct and concentration injected	Ca^{2+} Oscillation frequency (spikes/hour)	Protein level expressed (pg/egg)	Luminescence expression (cps/egg)
Mouse PLCζ (1 µg/µl)	5	3.59	700 (n=15)
Mouse PLCζ (0.1 µg/µl)	10	1.02	70 (n=16)
Mouse PLCζ (0.02 µg/µl)	6	0.18	10 (n=23)
Mouse PLCζ ΔEF1 (1.5 µg/µl)	0	0.98	55 (n=26)
Mouse PLCζ ΔC2 (1.35 µg/µl)	0	2.68	148.5 (n=26)
Mouse PLCζ D210R (3 µg/µl)	0	2.1	120 (n=30)

Table 7.1 Table showing the concentrations of each PLCζ construct that was injected into mouse eggs. The details of each construct can be found in the accompanying text. The frequency of Ca^{2+} oscillations, level of protein expression and luciferase-luminescence expression are all detailed. The luminescence expression is the average cps/egg obtained by luminescence imaging on the Photek system.

7.2.4 Cloning of PLCδ1-LUC, δ1ΔPH-LUC, ζ-δ1PH and PLCγ1

For the preparation of PLCδ1-LUC and δ1ΔPH-LUC constructs the same cloning strategy was used for those constructs in section 7.2.2 (Fig. 7.4A-B). For PLCδ1-LUC and δ1ΔPH-LUC expression was confirmed as described in section 7.2.2 (Fig. 7.4E). The same cloning protocol was also used for both PLCγ1 and PLCζ-δ1PH-LUC (Fig. 7.4C and D) and expression for these two constructs were confirmed using TNT reactions (Fig. 7.4F).

7.2.5 Expression of PLCδ1-LUC δ1-LUC chimeras and PLCγ1

cRNAs corresponding to PLCδ1-LUC and PLCγ1-LUC constructs were prepared and microinjected into mouse eggs. The graph in Fig. 7.5A shows that eggs injected with the cRNA encoding PLCδ1-LUC caused a series of Ca^{2+} oscillations in all 24 eggs that were injected. The frequency of Ca^{2+} oscillations produced by PLCδ1-LUC was 2 spikes/hr (see table 7.2), which was significantly lower than the 6 spikes/hour triggered by PLCζ-LUC ($P<0.005$). Following 4 hours of monitoring the changes in Ca^{2+}, the luminescence level from the same set of eggs (in the absence of fluorescence excitation) was measured (Fig. 7.5A). The mean level of protein expressed was 3.3pg of PLCδ1-LUC protein per egg (n=24). PLCγ1-LUC failed to induce Ca^{2+} oscillations (Fig. 7.5B) despite high expression levels (1.76 pg/egg (n=16) see Table 7.2. Both PLCγ1-LUC and PLCδ1-LUC were expressed at levels that were 10-17-fold higher than that of mPLCζ-LUC yet they still could not mimic the action of mPLCζ.

When eggs were microinjected with PLCδ1ΔPH-LUC cRNA, all eggs failed to undergo any changes in intracellular Ca^{2+} levels (n=20), (Figure 7.5C). However, these eggs were clearly expressing luciferase since an intense luminescence signal was detected at the end of the experiment (Figure 7.5C). The protein level expressed per egg in this experiment was 7.6pg of δ1ΔPH-LUC protein (n=20) (Table 7.2).

PLCζ is unique in that it has no PH domain. Since it produces increased Ca^{2+} via the $InsP_3$ pathway it is surprising that it has no targeting sequence to the PM where PIP_2 stores are known to reside. The PH domain from δ1 when tagged onto PLCζ produced Ca^{2+} oscillations of a similar frequency and duration to that of WT mPLCζ (Fig. 7.4D). However, the size of the 1st Ca^{2+} spike (134 $\pm$ 2.7 % Ca^{2+} increase) produced by PLCζ-δ1PH was significantly smaller than the 1st Ca^{2+} spike (208 $\pm$ 8.3 % Ca^{2+} increase) produced by WT PLCζ ($P<0.005$). The amount of PLCζ-δ1PH-LUC tagged protein expressed, per egg, was around 0.65 pg (n=11) (Table 7.2).

Fig. 7. 4 Preparation of PLCδ1-LUC, δ1 chimeras and PLCγ1-LUC

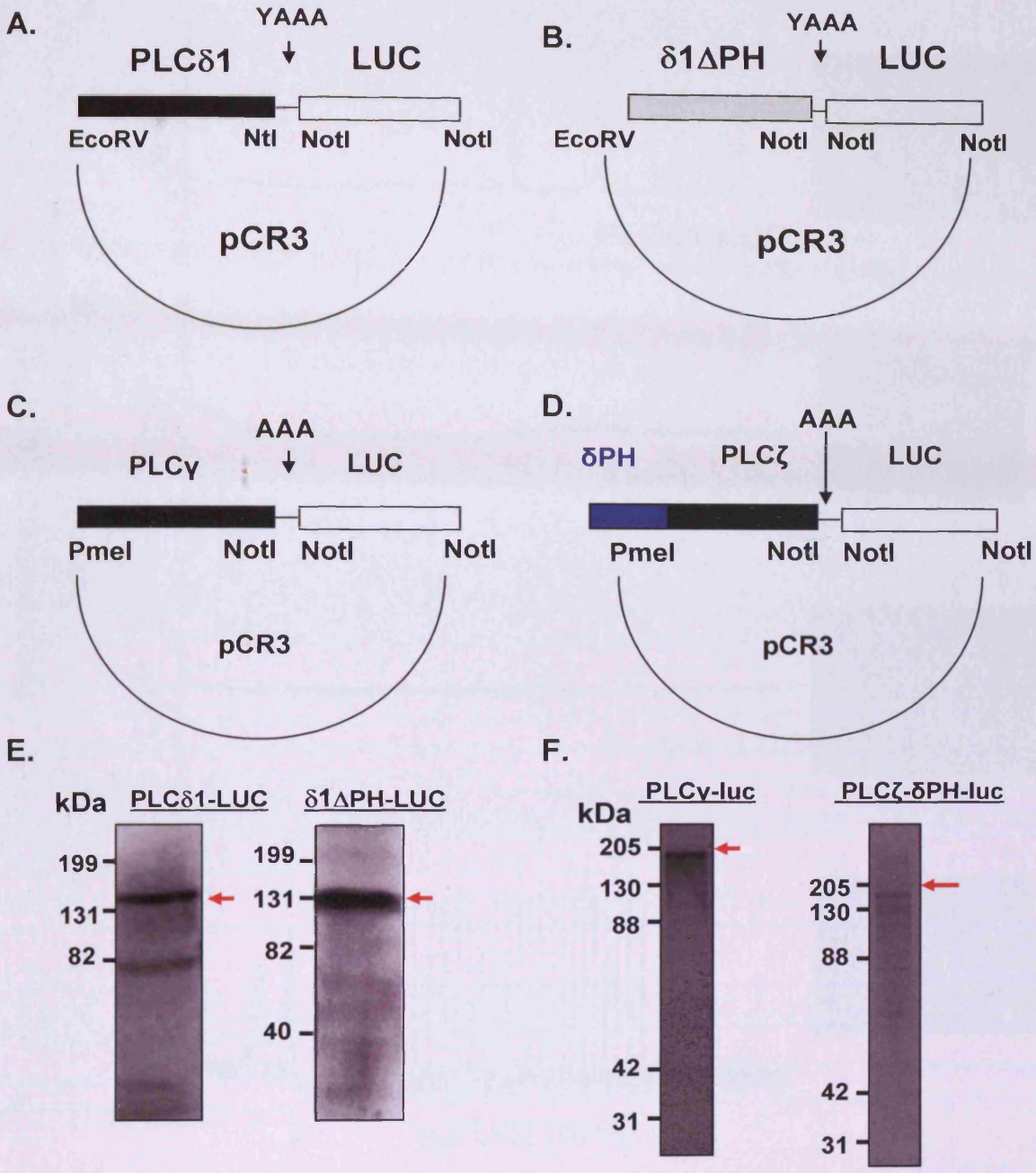

Fig. 7.4 Diagrams showing the cloning strategy for rat PLCδ1-LUC (A) and δ1ΔPH-LUC (B). Western blots of A and B using the anti-luciferase antibody are shown in E. Preparation of bovine PLCγ-LUC (C) and mPLCζ-δ1PH-LUC (D) ^{35}S methionine labelled TNT reactions for C and D are shown in F. Red arrows indicate protein band of appropriate MW. MW of PLCδ is 85 kDa and PLCγ is 148 kDa.

Fig. 7. 5 Microinjection of PLCδ1-LUC, δ1-LUC chimeras and γ1-LUC

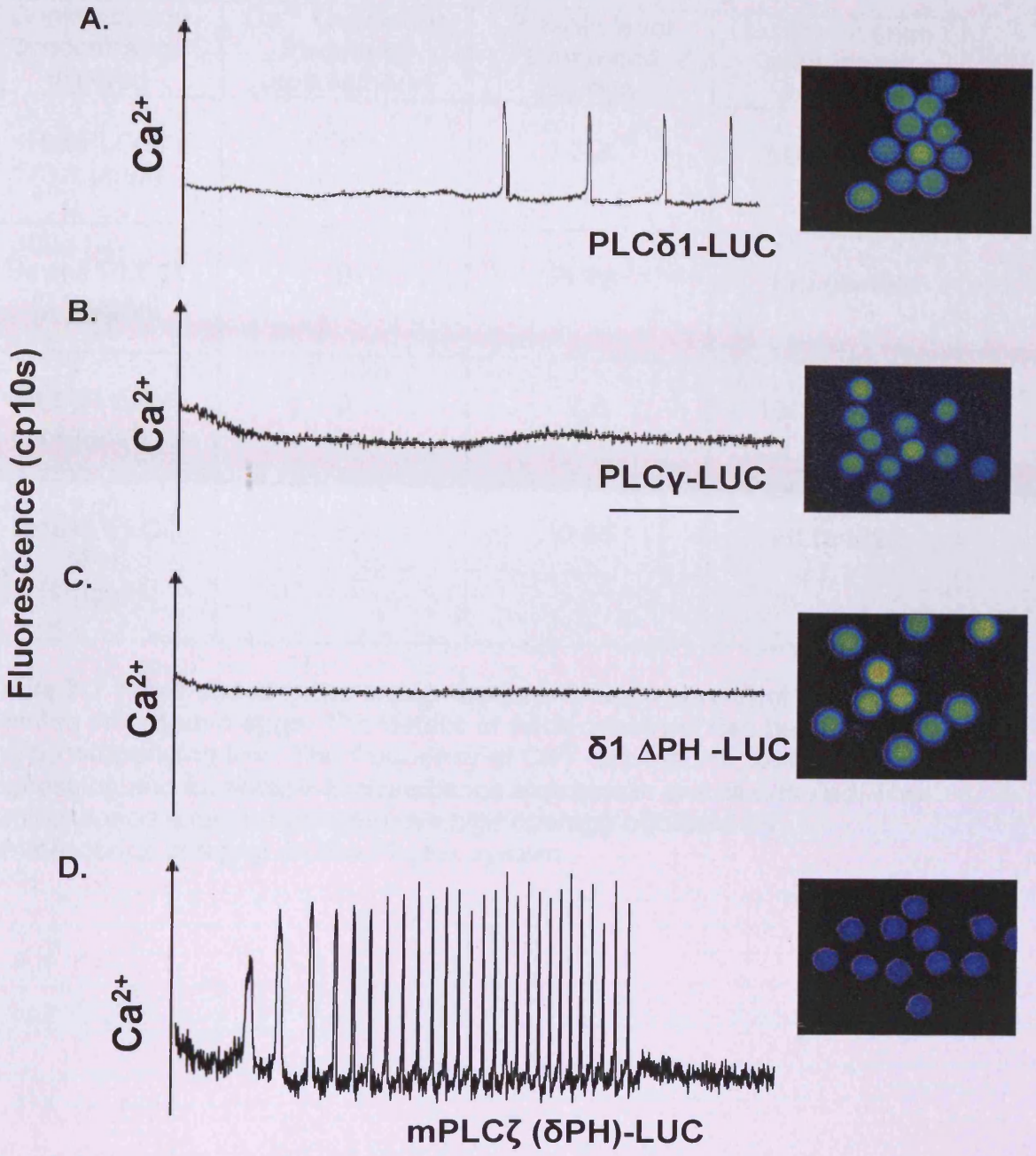

Fig. 7.5 Left graphs show Ca^{2+} oscillations measured in a single egg over a 4 hour period. The right image shows an 30 minute integrated luciferase-luminescence image of the same eggs from which Ca^{2+} measurements were taken from.

Table 7.2 PLCδ1-LUC, δ1 chimeras and PLCγ1

Construct and concentration injected	Ca^{2+} Oscillation frequency (spikes/hour)	Protein level expressed (pg/egg)	Luminescence expression (cps/egg)
Rat PLCδ1 (3.1 µg/µl)	2	3.3	500 (n=24)
Bovine PLCγ1 (2.3 µg/µl)	0	1.76	110 (n=16)
PLCδ1 ΔPH (4 µg/µl)	0	7.6	1000 (n=20)
Mouse PLCζ δPH (1 µg/µl)	8	0.55	20 (n=22)

Table 7.2 Table showing the concentrations of each construct that was injected into mouse eggs. The details of each construct can be found in the accompanying text. The frequency of Ca^{2+} oscillations, level of protein expression and luciferase-luminescence expression are all detailed. The luminescence expression is the average cps/egg obtained by luminescence imaging on the Photek system.

7.2.6 hPLCζ and sPLCζ-LUC constructs and chimeras

Monkey (s) and human (h) PLCζ-LUC constructs were prepared and the cloning strategy used is illustrated in Fig. 7.6. High concentrations (1 µg/µl and 0.5 µg/µl) of sPLCζ-LUC and hPLCζ-LUC was injected to ensure luciferase expression was detectable, since previous observations (Dr Yuansong Yu, unpublished) have shown low sPLCζ and hPLCζ concentrations are able to produce high frequency Ca^{2+} oscillations at undetectable expression levels. Both sPLCζ and hPLCζ constructs produced Ca^{2+} oscillations (Fig. 7.7A and B) and sPLCζ-LUC produced two phases of Ca^{2+} oscillations in all 27 injected eggs (Fig. 7.7A). The first burst of oscillations were of a significantly lower frequency than those of the secondary group of oscillations (see Table 7.3, $P<0.005$, students T-test). The amount of sPLCζ-LUC protein expressed per egg was 0.15 pg (Table 7.3).

hPLCζ-LUC produced one long series of Ca^{2+} oscillations that typically persisted for 2 hours of the 4-hour recording (Fig. 7.7B). The premature stoppage of these oscillations could be due to the high concentration that was injected since Table 7.1 shows that increasing the concentration of mPLCζ increased luciferase expression but decreased oscillation duration. A protein concentration of 1.08 pg was expressed, per egg, for the WT hPLCζ-LUC (Table 7.3). A concentration of 0.02 µg/µl mPLCζ was demonstrated in Fig. 7.3 to cause oscillations similar to fertilisation. When the same concentration of hPLCζ (0.02 µg/µl) was injected into mouse eggs, a series of oscillations were obtained that

lasted for the duration of the recording (Fig. 7.8). However, expression was not detected indicating high potency of the hPLCζ-LUC construct.

The XY linker from hPLCζ was cloned into sPLCζ: sPLCζ-hXY-LUC. This construct produced high frequency Ca^{2+} oscillations that were significantly higher ($P<0.005$) than those recorded using the WT hPLCζ despite similar expression levels (Fig. 7.7C and Table 7.3). Also, the secondary oscillations recorded using WT sPLCζ were absent when this chimera was used. A protein content of 1.4 pg of sPLCζ-hζXY-LUC was expressed per egg which is comparable to WT hPLCζ-LUC.

To further investigate the role of the XY domain, the sXY domain was cloned into hPLCζ, hPLCζ-sXY-LUC. This construct produced 3 bursts of Ca^{2+} oscillations in all 10 eggs investigated (Fig. 7.7D). All eggs experienced sustained high Ca^{2+} levels in the 3rd series of oscillations. Both the 1st and 2nd series of Ca^{2+} oscillations were of a frequency that was comparable to WT sPLCζ-LUC (Table 7.3). The amount of protein expression per egg was 0.7 pg for this construct. It should be noted that both chimeras failed to produce uniform expression levels that can be seen in both images (Fig. 7.7C and D). The lack of uniform expression did not affect the pattern of Ca^{2+} oscillations recorded with each chimera.

Fig. 7. 6 Preparation of sPLCζ-LUC and hPLCζ-LUC WTs and chimeras

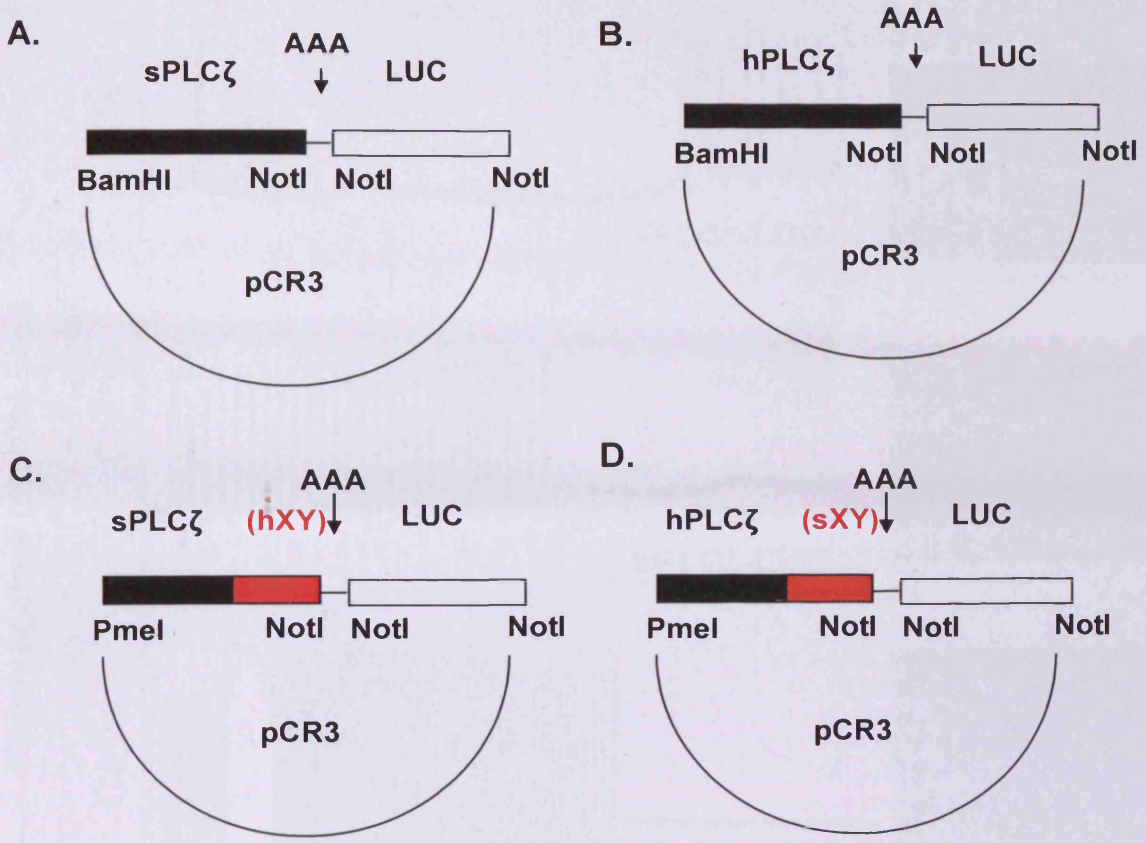

Fig. 7.6 Diagrams showing the cloning strategy used to prepare sPLCζ-LUC and hPLCζ-LUC (A, B). Chimeras were also prepared to investigate the role of the XY linker: sPLCζ-hXY-LUC (C) and hPLCζ-sXY-LUC (D).

Fig. 7. 7 Microinjection of sPLCζ-LUC and hPLCζ-LUC and chimeras

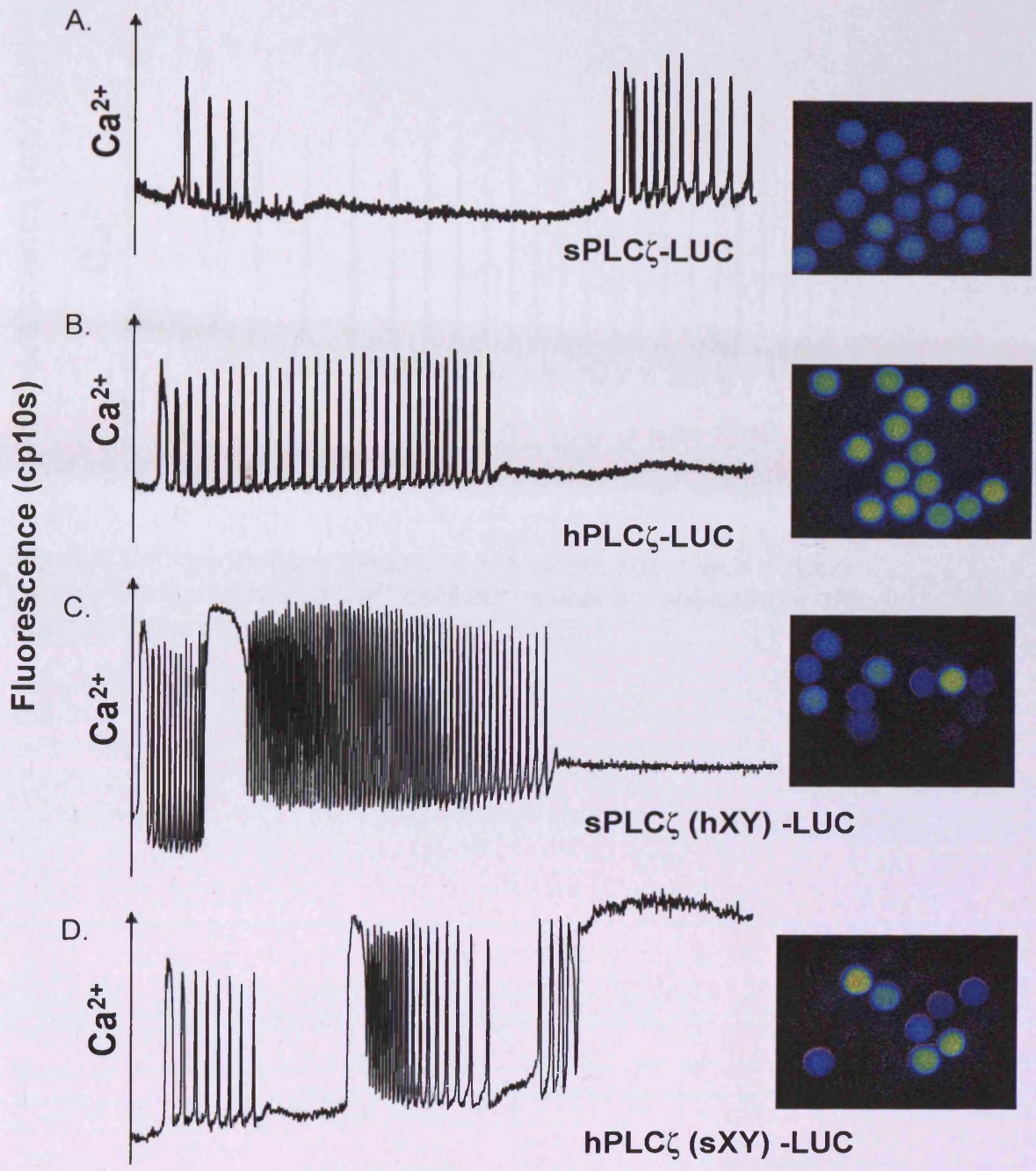

Fig. 7.7 Left graphs show Ca^{2+} oscillations measured in a single egg over a 4 hour period. The right image shows an 30 minute integrated luciferase-luminescence image of the same eggs from which Ca^{2+} measurements were taken from.

Fig. 7. 8 hPLCζ can induce oscillations at low expression levels

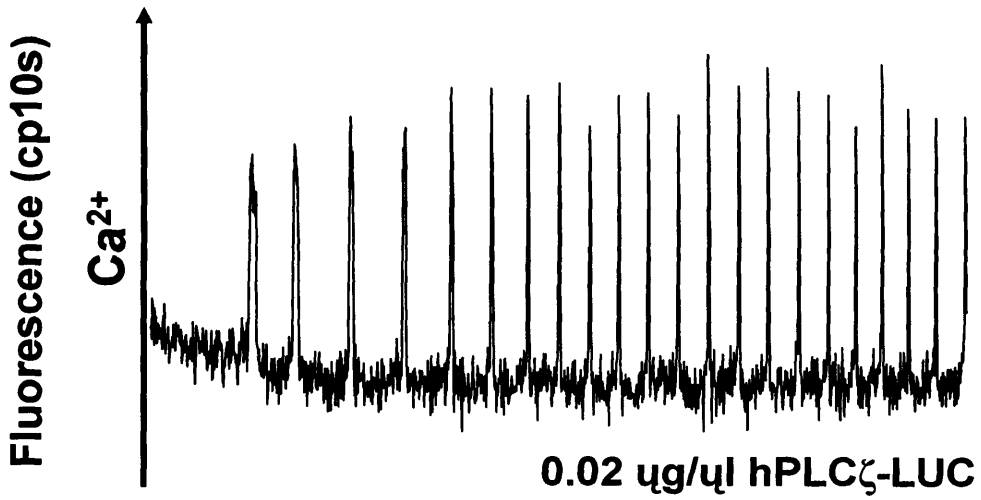

Fig. 7.8 Ca^{2+} oscillations measured in a single egg over a 4 hour period. The frequency of Ca^{2+} oscillations was 6.5 spikes/hour and expression was below detection level (n=13)

Table 7.3 hPLCζ-LUC, sPLCζ-LUC and chimeras

Construct and concentration injected	Ca^{2+} Oscillation frequency (spikes/hour)	Protein level expressed (pg/egg)	Luminescence expression (cps/egg)
Human PLCζ (0.5 µg/µl)	20	1.08	60.5 (n=11)
Monkey PLCζ (1 µg/µl)	1^{st} = 9 2^{nd} = 17	0.15	8 (n=27)
Monkey PLCζ human XY (2 µg/µl)	28	1.4	67 (n=11)
Human PLCζ monkey XY (2.93 µg/µl)	1^{st} = 5 2^{nd} = 20	0.7	27 (n=10)

Table 7.3 Table showing the concentrations of each construct that was injected into mouse eggs. The details of each construct can be found in the accompanying text. The frequency of Ca^{2+} oscillations, level of protein expression and luciferase-luminescence expression are all detailed. The luminescence expression is the average cps/egg obtained by luminescence imaging on the Photek system.

7.3 Discussion

In order to assess the relevance of EF hand and C2 domains in the production of Ca^{2+} oscillations by PLCζ a series of truncated constructs were prepared. The cRNA corresponding to each domain-deletion construct was microinjected into mouse eggs. Although deletion constructs PLCζΔEF1, ζΔC2 and ζD210R showed high expression levels they all failed to produce Ca^{2+} oscillations (Fig. 7.3). The WT mPLCζ, which triggered a series of Ca^{2+} oscillations, was expressed at levels much lower than that of the PLCζ domain-deletion constructs, indicating that the absence of oscillations is due to the absence of the domain and not low expression.

Injection of WT PLCζ-LUC cRNA produced Ca^{2+} oscillations and was expressed at a level determined to be around 190 fg/egg. Assuming a linear increase in PLCζ-LUC protein expression during the 4 hours of recording, it can be estimated that the amount of PLCζ-LUC required to initiate Ca^{2+} oscillations is around 50 fg. This value is comparable to previous estimations that 20-50 fg of PLCζ is required to initiate Ca^{2+} oscillations in eggs (Saunders et al., 2002). It is also similar to the estimate that 10-40 fg of venus tagged GFP-PLCζ is required to initiate a Ca^{2+} release (Yoda et al., 2004). This data, therefore, suggests that PLCζ-LUC has a similar ability to generate Ca^{2+} oscillations via the $InsP_3$ pathway like other N-terminally tagged PLCζ fusion proteins.

The X and Y domains of mPLCζ contain the same active residues 178His (Histidine), 210Asp (Aspartate) and 223His (Histidine) that have

been shown to be involved in catalysis (Ellis et al., 1993; Ellis et al., 1998). These residues are conserved across all PLC families (Katan, 1998). Aspartate at residue 210 in PLCζ was mutated to an arginine residue and this construct, PLCζ D210R has previously been injected into mouse eggs at high (2 μg/μl) concentrations and failed to produce Ca^{2+} oscillations (Saunders et al., 2002). However, protein expression was not confirmed. The construct used in this chapter also failed to induce Ca^{2+} oscillations. It was tagged with luciferase and expression was confirmed when a high (3 μg/μl) concentration was injected. These results suggest that 210Asp is essential for PLCζ enzyme activity.

Microinjection of recombinant PLCδ1 has been shown to produce Ca^{2+} oscillations in mouse eggs at high concentrations (Kouchi et al., 2004). However, injection of cRNA of PLCδ1 was reported not to produce Ca^{2+} oscillations in mouse eggs (Saunders et al., 2002), but protein expression was not confirmed. In this chapter, injection of cRNA PLCδ1 produced low frequency Ca^{2+} oscillations and expression was verified by luciferase luminescence. The amount of protein expressed for PLCδ1 was more than 18 times greater than that of PLCζ suggesting that PLCδ1 is unable to mimic the action of fertilisation even at high concentrations.

Like PLCδ1, microinjection of recombinant PLCγ1 has been reported to produce Ca^{2+} oscillations in mouse eggs (Mehlmann et al., 2001). However, the amount of PLCγ1 protein required to induce oscillations was more than 500 times greater than the PLC activity that is contained a single sperm (Mehlmann et al., 2001). In this chapter, PLCγ1 failed to produce any oscillations even at high protein concentrations. It is

possible that previous observations using recombinant PLCγ1 were contaminated with $InsP_3$ which resulted in Ca^{2+} oscillations. This is a possible explanation since $InsP_3$ alone has been shown to induce Ca^{2+} oscillations (Jones and Nixon, 2000). Such contamination would not occur with cRNA preparations and this could explain the difference in observations. However, in the previous study (Mehlmann et al., 2001), 3 times more protein was expressed in eggs than described in this chapter suggesting that extremely high concentrations of PLCγ1 can induce oscillations.

The PH domain of PLCδ1 is primarily concerned with targeting the enzyme to PIP_2 in the PM (Dowler et al., 2000; Lemmon et al., 1995; Varnai and Balla, 1998). Microinjection and expression of cRNA, corresponding to PLCδ1ΔPH was incapable of generating Ca^{2+} oscillations, even though PLCδ1ΔPH shares a considerable predicted domain homology with PLCζ. Since PLCδ1-LUC requires the PH domain to induce any oscillations in Ca^{2+} it seems that PLCζ is producing $InsP_3$ from a different pool of PIP_2 stores. When PLCζ-δ1PH-LUC was injected, this construct produced a similar frequency of Ca^{2+} oscillations to mPLCζ and showed similar expression levels. This result should be further explored as it does not explain why PLCζ is void of a PH domain, or, explain how PLCζ is targeted to PIP_2 stores to induce oscillations.

Microinjection of untagged hPLCζ into mouse eggs has previously been shown to be more potent than both mPLCζ and sPLCζ (Cox et al., 2002). Using luciferase tagged constructs this chapter has confirmed that hPLCζ is more potent than the mouse. It has also been established that

sPLCζ is also more potent than mPLCζ. Both hPLCζ and sPLCζ can induce oscillations at extremely low expression levels. The minimal detectable expression level on the Photek imaging system used throughout this thesis is around 1cps per egg, which would correlate to a protein level of 10 fg. Therefore, when hPLCζ expression was undetectable (Fig. 7.8) the protein expression was less than 10 fg.

sPLCζ produced two bursts of oscillations which was not recorded when hPLCζ was injected. This was explored further by using XY linker chimeras. The XY linker of PLCζ is the most positively charged region of the protein (Nomikos et al., 2007). The XY linker of hPLCζ is shorter than that of sPLCζ which makes it more positively charged (Cox et al., 2002). The bursts of oscillations were abolished when the XY linker from sPLCζ was replaced with the XY linker from hPLCζ. This could suggest that the XY linker of the monkey is involved with the 2nd series of oscillations. This proposal is further supported by the addition of the sXY linker into hPLCζ. hPLCζ-sXY-LUC produced a series of 3 bursts of Ca^{2+} oscillations with the 3rd burst of oscillations inducing sustained high levels of Ca^{2+}. However, the role of the XY linker is just speculation since the data presented in this chapter is not clear enough to draw any main conclusions from. The data is further complicated by the high frequency Ca^{2+} oscillations that are induced with these constructs. Chapter 5 demonstrated that high Ca^{2+} correlates with low ATP levels. If the ATP is low in eggs injected with PLCζ chimeras then this would suggest low protein expression when the eggs may in fact just be entering cell death.

This chapter has demonstrated the need for both EF1 and C2 domains for PLCζ activity. The requirement of PLCζ for the catalytic 210Asp site on the X domain has also been confirmed. It has also been shown that PLCδ1 is unable to induce oscillations at a similar frequency to PLCζ; while PLCγ1 is unable to induce any Ca^{2+} oscillations. The difference in activity of both sPLCζ and hPLCζ have, in part, been demonstrated and this work has provided a starting point for future investigations with these constructs.

Chapter 8
Main Discussion

8.1 Firefly luciferase luminescence to measure ATP

The work presented in this thesis has demonstrated the usefulness and limitations of using firefly luciferase to measure ATP levels in living cells during physiological and non-physiological stimuli. The luciferase luminescence signal is stable for several hours following stability of the signal. Originally, the initial 'run in' phase was interpreted as protein breakdown due to a rapid decline in flash kinetics (DeLuca and McElroy, 1984). It is for this reason that firefly luciferase was originally and extensively used in assays as a reporter gene (de Wet et al., 1987; Hooper et al., 1990; Pazzagli et al., 1992). In chapter 7, firefly luciferase was used in this manner and proved to be an effective and reliable measure of protein expression.

After the initial 'run in' phase that occurs due to the initial luciferin gradient across the PM, the luminescence signal stabilises within 1 hour (Dumollard et al., 2004; Gandelman et al., 1994). Firefly luciferase has been used as an indicator of ATP levels over the course of several minutes to one hour, in cardiomyocytes and hepatocytes respectively (Bowers et al., 1992; Bowers et al., 1993; Koop and Cobbold, 1993). Throughout chapters 3 – 6 in this thesis, it has been demonstrated that firefly luciferase can be used to measure ATP over several hours.

8.2 ATP levels during fertilisation

The egg to embryo transition that is activated by fertilisation requires many processes to be stimulated that require ATP. Processes that would require ATP include; translation of maternal RNAs, protein degradation,

ionic homeostasis and phosphorylation (Dumollard et al., 2007a). Therefore, it was hypothesised sometime ago that fertilisation induces an overwhelming increase in ATP demand which must be accompanied by the stimulation of energy production. ATP levels in ascidian eggs have not been measured directly, but an increase in mitochondrial O_2 consumption and mitochondrial NADH concentrations indicates that metabolic activity increases at fertilisation in ascidians (Dumollard et al., 2003). Mitochondrial activity has also been shown to oscillate during fertilisation in mouse eggs by measuring NADH and flavoprotein autofluorescence (Dumollard et al., 2004). A slight increase in ATP, measured using firefly luciferase, in mouse eggs at fertilisation has been shown in a minority of eggs (Dumollard et al., 2004). This inconclusive result has been confirmed by data in the thesis which has been published as the first article to measure Ca^{2+} and ATP simultaneously in any cell type (Campbell and Swann, 2006).

The increase in ATP, and the change in luminescence recorded during fertilisation, is very similar to that reported during Ca^{2+} increases in subdomains of living pancreatic β-cells (Kennedy et al., 1999). An increase in ATP during a Ca^{2+} increase has also been reported in HeLa and primary skeletal myotubes (Jouaville et al., 1999). However, the increase in ATP was dependent upon the oxidative substrates that were available to the cells. A transient decrease in ATP was recorded when the cells were supplied with glucose, as opposed to pyruvate and lactate (Jouaville et al., 1999). The use of metabolic substrates shall be discussed in section 8.7. Other somatic cells (muscle fibres) also show a

decrease in ATP during a Ca^{2+} transient (Allen et al., 2002; Jouaville et al., 1999). Moreover, measurements of total ATP levels in sea urchin and fish eggs suggest a substantial decrease in ATP during egg activation (Epel, 1969; Wendling et al., 2004).

A two-phase increase in ATP levels was recorded during fertilisation that was estimated to correspond to a change in ATP levels from 1.88 mM to 3.02 mM. Interestingly, we recorded both increases in ATP levels in the mitochondria and the cytosol. A recent study (Bell et al., 2006) also looked at the changes in cytosolic and mitochondrial ATP levels using luciferase probes in rat myocytes. During stimulation, these cells showed higher changes in the mitochondria than the cytosol (Bell et al., 2006). This suggests that other cell types have an energy demand in the cytosol that is rapidly matched by the mitochondria that responds to increased demand resulting in ATP being rapidly consumed in the cytosol. However, in eggs, it seems that developing embryos prefer to have more ATP than required since cytosolic and mitochondrial ATP levels show a net increase.

8.3 The Second rise in ATP at fertilisation

The second change in ATP levels recorded during fertilisation is an interesting but as yet, unexplainable event that was recorded during fertilisation. It is difficult to investigate the second change in ATP since eggs do not fertilise normally in the presence of cell cycle inhibitors that may not be specific (Chapter 6 discussion). However, the fact that the second change was inhibited with the cell cycle inhibitors MG132 and

nocodazole suggests that it is somehow linked with cell cycle progression. MPF and MAP kinase levels change once an egg becomes fertilised. In mouse eggs, kinase assays performed at specific time points post fertilisation (Moos et al., 1995) demonstrated that MFP levels decline rapidly within the first hour after fertilisation while MAP kinase levels do not show a substantial decline until 7 hours post fertilisation. In fertilising mouse eggs it has been shown, using cyclin B-GFP fusion proteins, that there is an immediate increase in cyclin B destruction that occurs with the first Ca^{2+} spike that continues until meiosis is complete (Marangos and Carroll, 2004; Nixon et al., 2002). This temporal correlation suggests that a change in MPF rather than MAP kinase levels could be responsible for the second change in ATP levels. Additionally, many mitochondrial proteins are activated by Ca^{2+}, such as the F_1F_0 ATPase (Horbinski and Chu, 2005), but it is difficult to predict what is causing the extra production in ATP levels.

A change in cell cycle progression would also involve ER re-organisation which could induce the secondary rise in ATP levels. It has been shown in HEK-293 cells that the movement of mitochondria and the ER are closely linked (Brough et al., 2005). Their study demonstrated similar kinetics profiles of movement for the mitochondria and ER suggesting a common mechanism of regulation. The ER and mitochondria appear to move towards each other to facilitate efficient transfer of Ca^{2+} from the ER to the mitochondria and back. Additionally, it was also shown that sustained high Ca^{2+} levels prevent this movement (Brough et al., 2005). This could explain why Ca^{2+} oscillates in an egg,

since such movement described above is prevented by extended periods of high Ca^{2+}. The shuttling of Ca^{2+} back and forth from the ER to the mitochondria has also been demonstrated in HeLa cells (Ishii et al., 2006). One possibility is that the mitochondria and ER could be moving closer together at the second change in ATP seen during fertilisation. Such movement would allow a greater co-ordination of Ca^{2+} transport between these two organelles and increase the ATP production.

It has been shown in mouse eggs that the ER reorganises during the first few hours of fertilisation (FitzHarris et al., 2003). This event is cell cycle dependent, since it requires a decrease in cyclin B levels. Before fertilisation the ER are present in clusters of around 1-2 μm in diameter. These clusters begin to disperse around the same time of 2nd PB emission from the zygote (FitzHarris et al., 2003). These ER clusters also disappear in Xenopus and nemertean eggs during fertilisation (FitzHarris et al., 2003; Stricker et al., 1998; Terasaki et al., 2001). The re-organisation of the ER could begin around the time of the 2nd change in ATP. Fitzharris et al (2003) looked at the ER organisation after fertilisation and then 3 hours later, but it is possible this process could begin around 1 hour and requires additional ATP levels. To investigate this in detail a probe to measure mitochondrial Ca^{2+} would be needed. As shown in Chapter 6, current recordings of mitochondrial Ca^{2+} during fertilisation are insufficient to draw any conclusions from.

One study has shown a direct link between Ca^{2+} oscillation frequency and metabolic NAD(P)H oscillatory activity in hepatocytes activated using vasopressin (Hajnoczky et al., 1995). Increased Ca^{2+}

frequency increased the oscillatory NAD(P)H activity and indeed, very high Ca^{2+} oscillations caused the NAD(P)H response to run together superimposing on each rather than the individual spike responses seen at low frequencies. This is similar to the responses recorded throughout this thesis, since a single Ca^{2+} spike produces an individual response in ATP, but Ca^{2+} oscillations produce an accumulative response. This again suggests Ca^{2+} oscillations in the mitochondria may get an extra boost after 1 hour, producing the secondary increase. Currently, attempts to measure a change in NADH or flavoprotein autofluorescence during fertilisation have not demonstrated a second change (Dumollard et al., 2004), this could be due to a poor autofluorescence signal. Or, it could be that autofluorescence doesn't have a secondary increase and that Ca^{2+} is inducing the rise in ATP levels.

8.4 Ca^{2+} release and ATP response

At fertilisation, a Ca^{2+} increase in the egg is the universal trigger for the activation of embryo development. Ca^{2+} oscillations stimulate many energy consuming processes which results in an increase in production of ATP (as demonstrated in Chapters 3 – 6). It would be useful to compare the ATP response with the size of the first and subsequent Ca^{2+} transients. Throughout this thesis, the changes in intracellular Ca^{2+} were shown in arbitrary units of relative fluorescence changes however, the mean amplitude of the first and subsequent Ca^{2+} transients are shown in table 8.1. The Ca^{2+} signal was estimated using the equation; Ca^{2+} = KD (F-Fmin)/ (Fmax-F). The values for the KD (170 nM) and Fmin/Fmax ratio

(14) of OGBD were obtained from molecular probes (www. probes.invitrogen.com). A resting Ca^{2+} level in the egg was assumed to be 100 nM (Thomas et al., 2000) and the resting ATP levels were taken to be 1.88 mM as calculated from the calibration in Chapter 3. Table 8.1 shows that the amplitude of the Ca^{2+} rise does not significantly differ between sperm, ionomycin and thapsigargin despite the latter two agents producing an initial decline in ATP levels before a subsequent increase. Since similar changes in ATP during fertilisation are not recorded when various Ca^{2+} stimuli are used it seems that $InsP_3$ independent Ca^{2+} increases could cause the activation of ATP requiring processes in the cytosol (e.g. ion pumps and proteins). Such activation produces an initial decrease or, delayed increase in ATP levels until the Ca^{2+} activates mitochondrial oxidative phosphorylation (Bell et al., 2006). This mechanism has been demonstrated in rat myocytes when increased workload was induced using isoprotenol. The mitochondrial ATP and cytosolic ATP levels decreased before increasing (Bell et al., 2006) which correlates with the data presented in Chapter 4.

When a physiological Ca^{2+} response was produced via carbachol, despite similar Ca^{2+} amplitude of the 1st transient, a delayed ATP increase was recorded. Caged $InsP_3$ has been shown to mimic the pattern of Ca^{2+} oscillations induced by sperm (Jones and Nixon, 2000) and therefore, would be expected to mimic the ATP response seen at fertilisation. However, uncaging $InsP_3$ produced a delayed ATP increase and at high frequencies induced a decrease in ATP. The amplitude of the first and subsequent transients obtained during uncaging of $InsP_3$ were

significantly lower to that of sperm induced oscillations, indicating that the sperm is delivering a specific IICR that produces a high ATP response not recorded with other $InsP_3$ releasing agents. In addition, when the sperm factor PLCζ was used to initiate oscillations, the ATP response was significantly lower compared to fertilisation despite similar Ca^{2+} release. This result further demonstrates that the exact response elicited by the sperm is difficult to reproduce. It could be that the PLCζ expression levels are not high enough at the 1st Ca^{2+} transient that results in the ATP response being lower. This problem may be overcome by injecting recombinant PLCζ protein as opposed to PLCζ cRNA.

The pattern of Ca^{2+} release seems to be essential to induce the correct ATP response. Table 8.1 shows that the amplitude of Ca^{2+} oscillations was significantly lower in aged eggs, when compared to fresh eggs. It is not clear why older eggs have a smaller Ca^{2+} increase. It has been reported that aging eggs have a decreased Ca^{2+} response (Jones and Whittingham, 1996) when exposed to $InsP_3$. It has also been suggested that the Ca^{2+} signal in aged eggs can trigger apoptosis as opposed to development (Gordo et al., 2002). Despite the two-phase ATP increase occurring in aged eggs, the overall ATP increase was significantly lower when compared to control IVF (Table 8.1) and this could partly be due to insufficient Ca^{2+} signalling in the egg.

Table 8.1 Changes in Ca2+ concentrations during physiological and non-physiological stimuli

Stimuli	Amplitude of 1st Ca^{2+} transient (nM) ± s.e.m	Amplitude of subsequent Ca^{2+} transients (nM) ± s.e.m	Initial change in ATP levels (mM)
Control IVF (n=34)	820 ± 12	800 ±9.3	+0.62
IVF (no 2nd change) (n=4)	600 ± 8.3*	800 ± 4.4	+0.17
PLCζ (n=12)	800 ± 9.1	750 ± 2.2	0
Ionomycin (n=16)	896 ± 5.6	N/A	-0.38
Thapsigargin (n=16)	750 ± 2.3	N/A	-0.38
Carbachol (n=9)	800 ± 4.6	500 ± 18**	0
Old eggs (n=4)	700 ± 1.2*	600 ± 12**	+0.5
Uncage (10 mins) (n=6)	675 ±0.78*	600 ± 6**	0
Uncage (5 mins) (n=10)	700 ± 0.55*	600 ± 10**	0
Uncage (2.5 mins) (n=8)	550 ± 0.21*	400 ± 15**	-0.68

Table 8.1 A resting Ca^{2+} level of 100 nM was assumed and the amplitude of the first and subsequent Ca^{2+} transients was calculated. The initial change in ATP was stated assuming, from the calibration in Chapter 3 that resting ATP was 1.88 mM. Only sperm produced an immediate increase in ATP levels. Carbachol, PLCζ and uncaging every 10 and 5 minutes showed no immediate increase in ATP whilst ionomycin, thapsigargin and uncaging every 2.5 minutes produced an initial decline in ATP. (*$P<0.005$ when compared to the 1st Ca^{2+} transient during control IVF and **$P<0.005$ when compared to subsequent oscillations during control IVF).

8.5 ATP and aged eggs

As mentioned above, a similar pattern of ATP changes were recorded during fertilisation in aged eggs, but the overall increase in ATP levels was significantly lower. The first change in ATP was comparable to control conditions but the second change was significantly lower (see Chapter 3). As mentioned in the previous section (section 8.3) MPF levels are maintained at high levels until fertilisation (Brunet and Maro, 2005; Marangos and Carroll, 2004; Moos et al., 1995; Verlhac et al., 1994). In the mouse it has been shown that MII eggs from aged mice (48-52 weeks old) are unable to maintain high MPF levels in culture. MPF begins to decrease within the first 3 hours of culture whereas, MII eggs removed from young mice (4-6 weeks old) do not show a substantial decline in MFP until 9 hours in culture (Tatone et al., 2006). This would suggest that *in vitro* aged eggs would also have decreased MFP levels which could explain why these eggs failed to show the change in ATP during fertilisation like that of fresh eggs. If MPF is already low, fertilisation would not initiate a rapid decrease in MPF and hence be unable to induce such a marked 2nd change in ATP.

Mitochondrial membrane potential associated with oocyte age could also explain why ATP in aged eggs is not as high as fresh eggs Oocytes from mice with advanced maternal age (AMA, >30 weeks) are more sensitive to mitochondrial damage via photosensitive treatment than oocytes taken from pubertal mice (4-6 weeks) (Thouas et al., 2005). Additionally, the membrane potential, and ATP content of aging eggs is

lower than that of younger eggs (Thouas et al., 2005). Lower membrane potential in aging eggs has also been demonstrated in human eggs (Wilding et al., 2003). Aging associated decreases in mitochondrial membrane potential could affect that ability of the mitochondria to induce a large second change. This would also suggest that the second change and overall ATP increase is an important event for the developing embryo since it has been shown aging oocytes have a lower developmental capacity (Thouas et al., 2005; Wilding et al., 2003).

Aged related deficiencies in mitochondria have also been show in somatic cells (Genova et al., 2004). Such cells show an increase in the generation of reactive oxygen species (ROS) due to the inefficient decomposition of oxygen (Genova et al., 2004). Additionally, aging oocytes have a decreased capacity to accumulate and sequester Ca^{2+} which results in high cytoplasmic Ca^{2+} levels and increased risk of Ca^{2+} overload in the mitochondria (Nicholls, 2002). Such problems with aged mitochondria could contribute to the explanation as to why patient with advanced maternal age (AMA) have lower success with IVF and ICSI (Janny and Menezo, 1996; Sandalinas et al., 2001; Shahine and Cedars, 2006).

8.6 Why does ATP levels matter?

The exact function of the rise in ATP during fertilisation in mouse eggs is unknown. A cellular transducer that can directly respond to a physiological increase in ATP is the closure of the K_{ATP} channels (Campbell et al., 2003), but there is no evidence that this channel exists

in eggs. ATP levels also control the activity of mammalian Target of Rapamycin (mTOR), which has Km for ATP of around 1mM (Dennis et al., 2001). Since ATP levels are crucial parameters of cells homeostasis one possibility is that, the ATP increase is a reflection of the egg having a bias towards making more ATP than required as a fail safe. A recent study (Izyumov et al., 2004) demonstrated that a 3-fold reduction in ATP levels in HeLa cells initiated cell suicide even though the decreased ATP levels were still above the Km for the majority of ATP-dependent enzymes; including those enzymes required for apoptosis. Adenosine 5'-monophosphate-activated protein kinase (AMP kinase) are activated when ATP levels drop (Kahn et al., 2005) and could become activated in eggs during transient decreases in ATP levels. Izyumov et al (2004) also demonstrated that recoveries in ATP were insufficient to save the cells (Izyumov et al., 2004). This suggests that the ATP response recorded in eggs is particularly high to overcompensate since a suicide signal could be triggered when the ATP levels drop. Additionally, Izyumov et al (2004) showed that increasing temperature results in a decrease in ATP levels and induces apoptosis even when the temperature is returned to normal. This has also been seen in eggs (unpublished observations Campbell and Swann). Since the activation of an egg is the start of a developing embryo that could eventually become a newborn, it seems the cell would prefer to die than continue developing in an abnormal manner.

Mammalian eggs contain ~100,000 mitochondria which appear to be a critical factor in egg and embryo quality (Ankel-Simons and Cummins, 1996; Duchen, 2004; Van Blerkom, 2004). In mouse, human

and pigs eggs the presence of poorly polarized, displaced or damaged, mitochondria is associated with poor embryo development and apoptosis (Van Blerkom et al., 1995). As suggested above, if the egg was to fall behind in ATP generation this could lead to a decrease in ATP levels that may be detrimental to embryo development. Like the study detailed above (Izyumov et al., 2004), it has been shown that transient exposure of mouse oocytes to mitochondrial uncouplers leads to a transient decrease in ATP levels (Van Blerkom et al., 1995). Such exposed oocytes can go on to mature, fertilise and develop, but the developmental rate is much reduced compared to control embryos (Van Blerkom et al., 1995).

Poor embryo morphology and failure to develop *in vitro* has been shown to correlate with cellular abnormalities (Sathananthan et al., 1990; Van Blerkom, 1989), and chromosome abnormalities (Angell et al., 1988; Angell et al., 1991; Munne et al., 1993). However, it is difficult to explain development failure when the embryo appears normal. The increase in ATP we describe may be an important indicator of the quality of the egg. One particular study established the relationship between ATP content and the clinical outcome in human eggs (Van Blerkom et al., 1995). This study evaluated the ATP content of eggs that were not implanted from a cohort of patients and related these results to the clinical outcome of the eggs that were implanted. It was proposed that eggs with low ATP content would fail to achieve a clinical pregnancy despite the ability of those eggs to develop to normal looking 4-8 cell embryos. The eggs with high ATP levels had higher implantation success but did not develop

faster or show better morphology compared to those eggs with low ATP. This suggests that simply assessing the rate of development and morphology may not be a reliable method for selecting the "best" embryo for transfer into a patient.

Other studies have also shown that the ATP content of eggs or embryos is correlated with the success rates in embryo development in mice and humans (Ginsberg and Hillman, 1973; Quinn and Wales, 1973; Van Blerkom et al., 1995). Collectively, the work in this thesis and previous publications suggest that ATP levels are critical for embryo development and that the ATP content of an embryo during pre-implantation could directly influence or, determine the clinical outcome.

Reports in cow eggs show that eggs with a higher ATP content are the eggs most likely to have normal morphology and the best fertilisation potential (Kolle et al., 2004; Stojkovic et al., 2001). This report, unlike work described above in human eggs (Van Blerkom et al., 1995), showed a direct correlation between morphology and quality with developmental outcome. They also noted a correlation between ATP content and total cell number in blastocytsts. It seems that mitochondrial distribution and re-organisation during maturation plays an important role in cow eggs. Successful re-organisation during maturation resulted in high ATP and good quality embryos, whilst failure of mitochondrial re-organisation resulted in poor ATP levels and poor development. Such re-organisation could also determine the ATP content in mouse and human eggs.

It should be noted that other studies have not found a strong correlation between resting ATP levels and the developmental capacity of

eggs of different types (Brevini et al., 2005; Combelles and Albertini, 2003). In pig eggs it was suggested that no correlation exists between high ATP levels and developmental capacity (Brevini et al., 2005). Instead, in the pig egg, it seems that the most important factor that effects development are the changes in mitochondrial distribution during maturation, like that described above in the cow (Stojkovic et al., 2001). In the pig, it was shown that successful relocation of the mitochondria from the periphery of the egg to the inner region of the cell correlated with good development (Brevini et al., 2005).

One study investigated the effect of repeated ovarian stimulation on the ATP content and developmental capacity of mouse eggs (Combelles and Albertini, 2003). This study showed that ATP decreased with repeated ovarian stimulation, but decreased ATP levels did not effect development. However, it is important to note that this particular study did not report oocyte morphology or, quality (Combelles and Albertini, 2003). It is possible that mitochondrial ATP generation maybe faulty despite normal resting levels. For example, it has been shown that primary fibroblasts containing specific mitochondrial point mutations do not demonstrate a change in mitochondrial function (from control cells) until they undergo stressful conditions (James et al., 1996).

8.7 Metabolism during fertilisation

A relative increase in ATP has also been reported after receptor stimulation of Ca^{2+} release in HeLa cells (Jouaville et al., 1999). The ATP increase in HeLa cells is seen when cells are metabolising pyruvate via

oxidative phosphorylation, but when cells are only supplied with glucose, and hence relied upon glycolytic metabolism, the Ca^{2+} release leads to a decrease in ATP (Jouaville et al., 1999). This suggests that cells that primarily use oxidative phosphorylation for ATP production can respond to Ca^{2+} increases by showing a marked increase in ATP. This mechanism could also exist in eggs during fertilisation since it has been proposed that mitochondrial activity oscillates at fertilisation (Dumollard et al., 2003; Dumollard et al., 2004).

In oviductal fluid and culture media there are 4 main substrates present that are pyruvate (<0.5 mM), lactate (10-25 mM), glucose (0.5-5 mM) and glutamine (1 mM) (Summers and Biggers, 2003). Pyruvate is long known to be the only metabolic substrate required for egg activation in the mouse as glycolysis makes a minor contribution during the first stages of embryonic development (Barbehenn et al., 1974; Dumollard et al., 2006; Dumollard et al., 2007b). Despite this, glucose is required in the fertilised mouse egg to support development to the blastocyst stage (Brown and Whittingham, 1991). In one study (Brown and Whittingham, 1991) mouse embryos could reach the morula stage with only lactate and pyruvate, but arrested before blastocyst unless glucose was present at fertilisation, highlighting the requirement of fertilising eggs for glucose.

To investigate the role of mitochondrial ATP production during fertilisation, cinnamate was used (Chapter 6). Cinnamate was used throughout Chapter 5 since it is known to be a specific inhibitor of pyruvate uptake into the mitochondria. Its action is specific since it does not affect pyruvate uptake into the cell via the H^+ monocarboxylate

cotransporter proteins (MCT1 and MCT3 in mouse embryos) (Dumollard et al., 2007b; Jansen et al., 2006). Additionally, cinnamate does not affect pyruvate metabolism such as pyruvate dehydrogenase or, carboxylase (Williams et al., 1996). Cinnamate has been effectively used on striatal neurons (Williams et al., 1996), the protozoon parasite African trypanosomes (Barnard et al., 1993) and more recently mouse eggs (Dumollard et al., 2007b). The mitochondrial Ca^{2+} uptake inhibitor ruthenium red is unspecific (unpublished observations and (Dumollard et al., 2007a) and mitochondrial poisons such as FCCP, oligomycin and cyanide induce an instant change in cell homeostasis that results in cell death. Therefore, blocking pyruvate uptake into the mitochondria using cinnamate was used as a more subtle attempt to alter mitochondrial activity.

The work in Chapter 5 confirms that mitochondrial metabolism of pyruvate is essential for maintaining cytosolic ATP levels in the unfertilised egg as well as for the up-regulation of energy production at fertilisation. Indeed, inhibiting the mitochondrial import of pyruvate using cinnamate caused ATP levels in the cytosol to decrease in the unfertilised egg. Cinnamate also abolished the up-regulation of ATP production by sperm-triggered Ca^{2+} oscillations. However, cytosolic ATP levels could still be maintained (albeit to a lower level) after inhibition of mitochondrial pyruvate import in the unfertilised oocyte. Furthermore, in the presence of cinnamate, cytosolic ATP levels seemed to be transiently maintained during Ca^{2+} oscillations before disruption of Ca^{2+} homeostasis and

complete ATP depletion. These results suggest that other metabolic substrates might fuel the mitochondrial Kreb's cycle.

To investigate the contribution of other substrates at fertilisation, eggs were fertilised that had been pre incubated in substrate free media for 2 hours to starve the eggs from energy producing substrates. As demonstrated in Chapter 5, the activation of energy deprived eggs showed high frequency Ca^{2+} oscillations that occurred with low ATP levels. These observations are the first direct evidence of an increase in ATP demand at fertilisation, which substantiates the hypothesis that activation of development is accompanied by activation of energy demand and matching energy production. Addition of pyruvate to starved eggs undergoing Ca^{2+} oscillations could restore both ATP levels and low frequency Ca^{2+} oscillations provided that pyruvate import into the mitochondria was not inhibited. Figure 8.1 shows exogenously added pyruvate feeding the TCA cycle and driving oxidative phosphorylation. This shows that the sole mitochondrial metabolism of pyruvate is able to supply all the required energy production.

In contrast, glucose could not restore ATP levels, or, Ca^{2+} oscillations even though in these starved eggs, glycolysis should be more active than in eggs cultured in control medium since ATP and citrate levels would be decreased in a starved egg (Barbehenn et al., 1974). This observation indicates that, even though glucose transport might be stimulated after fertilisation in the cow and the mouse egg (Comizzoli et al., 2003; Urner and Sakkas, 2005); glucose metabolism is poorly active in the mouse zygote. However, it has been shown, in the mouse, that

glucose is required at fertilisation to feed the pentose phosphate pathway (PPP). The PPP converts glucose-6-phosphate to ribose-5-phosphate which results in the production of 2NADPH. NADPH is required by the thiol tripeptide glutathione (GSH) reductase/peroxidise system to protect against excessive reactive oxygen species (ROS). Oxidative stress by ROS results in an imbalance of redox potential towards an oxidised state (Balaban et al., 2005). Such oxidative stress has been shown to be associated with impaired development and fragmentation of embryos (Johnson and Nasr-Esfahani, 1994; Yang and Park, 2003). It can also induce apoptosis (Liu and Keefe, 2000; Liu et al., 2000).

Additionally, the presence of glucose seems to be required for the future fate of that embryo. Exposure, rather than utilisation of glucose is required for the expression of the glucose transporter protein (GLUT1 and GLUT3 in mouse pre-implantation embryos) (Pantaleon et al., 2001) which is essential for blastocyst formation (Pantaleon et al., 2001). Also, the presence of glucose has been shown to be required for the expression of MCT1 which is essential for pyruvate uptake into the embryo (Jansen et al., 2006). Therefore, the need for glucose during fertilisation should not be underestimated.

Both lactate and glutamine can fuel mitochondrial ATP production since lactate is oxidised to pyruvate in the eggs cytosol by lactate dehydrogenase (Wales and Whittingham, 1973) and glutamine is oxidised to α-ketoglutarate (Dumollard et al., 2007b; Lane and Gardner, 2005). Lactate was unable to restore ATP levels or Ca^{2+} oscillations in starved eggs undergoing Ca^{2+} oscillations. The lack of effect of lactate on

mitochondrial ATP production was surprising as lactate is by far the most abundant metabolic substrate in oviductal fluid and in embryo culture media. Lactate-derived pyruvate appears to be diverted from mitochondrial oxidation while exogenous pyruvate is rapidly oxidised by mitochondria. It also seems that glutamine cannot feed the TCA quickly or, efficiently enough to recover an energy substrate deprived egg. Figure 8.1 shows how both exogenous glutamine and glucose could feed into the TCA.

The inability for exogenous lactate to fuel mitochondrial production is rather intriguing even though it is consistent with the facts that lactate cannot support development from fertilisation (Lane et al., 2006). A recent study by Lane and Gardner (2006) suggested lactate cannot fuel mitochondrial ATP production due to poor transfer of cytosolic NADH (generated during oxidation of lactate to pyruvate, (Stryer, 1971)) into the mitochondria. This was reported since restoration of NADH shuttling between cytosol and mitochondria allowed lactate to support development from fertilisation (Lane et al., 2006).

However, lactate-driven NADH production also produces pyruvate that should be oxidised in the mitochondria. By imaging the mitochondrial redox state in mouse eggs it was shown pyruvate derived from lactate cannot reduce the mitochondrial redox state as opposed to exogenous pyruvate (Dumollard et al., 2007b). Since in chapter 5 it was shown that lactate-derived pyruvate does not supply mitochondrial ATP production even in the absence of exogenous pyruvate it strongly suggest that two intracellular pools of pyruvate exist. It seems that one pool of pyruvate

(derived from lactate) is diverted from mitochondrial oxidation (Fig. 8.1). Such compartmentation of pyruvate has been observed in astrocysts (Zwingmann et al., 2001) and cortical neurons (Cruz et al., 2001) where glycolytic pyruvate is preferentially oxidised by mitochondria while exogenous pyruvate is channelled towards reduction into lactate. Alanine has been shown to be produced in cow embryos (Cetica et al., 2003; Gopichandran and Leese, 2003) and alanine aminotransferase, which converts pyruvate to alanine, is present in cow (Cetica et al., 2003; Gopichandran and Leese, 2003), human (Yazigi et al., 1993) and mouse (Dumollard et al., 2007b) eggs. This leads to the hypothesis that lactate-derived pyruvate is metabolised to alanine in the cytosol of mouse zygotes (Dumollard et al., 2007b), a possibility that should be investigated in the future. It is also possible that glucose could also undergo metabolic channelling and this is another route for future investigations.

Fig. 8. 1 Pathways taken by exogenously added metabolic substrates

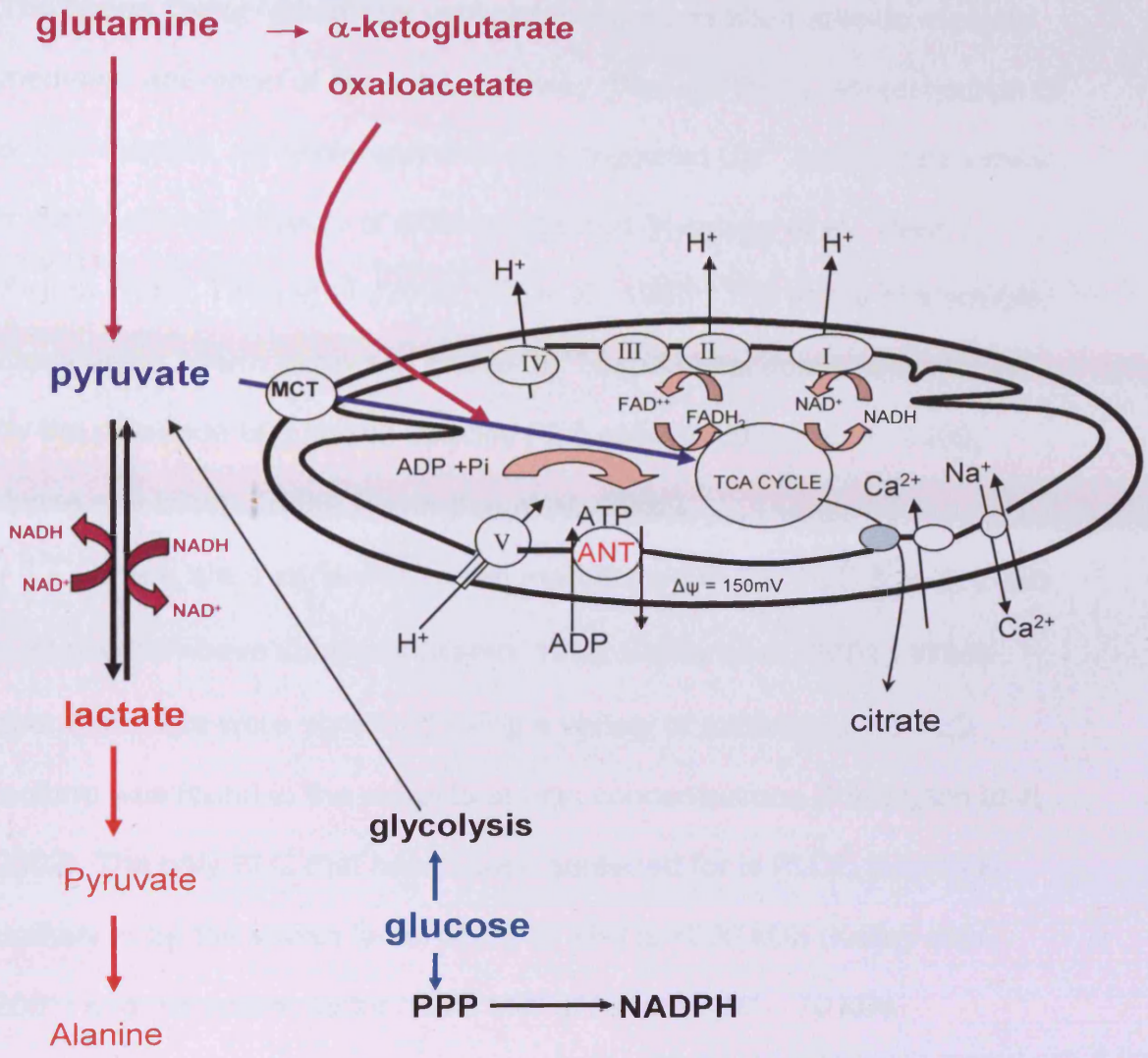

Fig. 8.1 Schematic diagram showing possible pathways taken by exogenously added pyruvate, lactate, glucose and glutamine. See text for details.

8.8 PLCζ

The sperm factor hypothesis was proposed as an alternative to receptor mediated activation of the $InsP_3$ pathway (Swann, 1990). Microinjection of sperm extracts, or whole sperm in eggs triggered Ca^{2+} oscillations similar to fertilisation in a range of different species (Kyozuka et al., 1998; Swann, 1990; Tang et al., 2000; Wu et al., 1997). The ability of a soluble, mammalian sperm extract to cause Ca^{2+} oscillations could be explained by the presence of a sperm-specific PLC activity (Jones et al., 1998; Jones and Nixon, 2000; Parrington et al., 2002).

There are a variety of known mammalian PLCs: PLC δ, γ, β, ε and η all of which have subtypes (Katan, 1998; Kelley et al., 2001). When sperm extracts were screened using a variety of antibodies, no PLC isoform was found in the extracts at high concentrations (Parrington et al., 2002). The only PLC that hasn't been screened for is PLCε, but this is unlikely to be the sperm factor since its MW is >200 kDa (Kelley et al., 2001) and the sperm factor has a MW of between 30 – 70 kDa (Parrington et al., 2002; Wu et al., 1998). PLCγ has been shown to be present in both mammalian eggs and sperm (Dupont et al., 1996). Despite the fact that PLCγ can induce Ca^{2+} oscillations at high concentrations (more than 500 times greater than the PLC activity in a single sperm) (Mehlmann et al., 2001) it is unlikely to be the sperm factor since it was demonstrated in Chapter 7 that it is unable to induce oscillations in mouse eggs, even at high expression.

PLCδ1 has previously been reported to induce oscillations in mouse eggs at high concentrations (Kouchi et al., 2004). The MW of the

sperm factor alone would suggest that a PLCδ is likely to be the cause. However, PLCδs are not present in active sperm extracts (Parrington et al., 2002). PLCδ4 is present in whole sperm, however, the mouse knockout of PLCδ4 failed to inhibit the production of Ca^{2+} oscillations. during fertilisation or, ICSI (Fukami et al., 2001). Additionally, PLCδ1 is unlikely to be the sperm factor since protein levels of PLCδ1 higher than the PLC activity in a single sperm, are required to induce Ca^{2+} oscillations The oscillations produced could be the result of protein over expression in mouse eggs. This result is in overall agreement with the observations of another recent study, in which recombinant PLCδ1 triggered Ca^{2+} oscillations when microinjected at a concentration 20-fold higher than recombinant PLCζ (Kouchi et al., 2004). Even when the PH domain from PLCδ1 was deleted to make it structurally similar to PLCζ it failed to trigger Ca^{2+} changes when microinjected into mouse eggs.

Microinjection of cRNA encoding the mouse (Saunders et al., 2002), human, and simian PLCζ (Cox et al., 2002) into mouse eggs, triggered Ca^{2+} oscillations similar to those observed at fertilisation. Furthermore, Ca^{2+} oscillations were abolished when PLCζ was immunodepleted from native sperm extracts (Saunders et al., 2002). The presence of PLCζ has been also been demonstrated in boar and hamster sperm (Saunders et al., 2002). Microinjecting recombinant PLCζ that was synthesised using a baculovirus expression system was able triggered Ca^{2+} oscillations in mouse eggs (Kouchi et al., 2004). An important feature of PLCζ is that it is able to produce Ca^{2+} oscillations in eggs at very low concentrations (e.g. 10 fg/egg), (Fujimoto et al., 2004; Kouchi et

al., 2004; Saunders et al., 2002). In contrast, other studies have shown that PLC isoforms of PLCβ, γ or δ are either ineffective, or much less effective than PLCζ at causing Ca^{2+} release, when microinjected into eggs at low concentrations (Kouchi et al., 2004; Runft et al., 2002). PLCζ could exist as the sperm factor across mammals and non-mammalian species since it was recently defined in the domestic chicken *(gallus gallus)*. The chicken PLCζ is 639a.a long and like its mammalian forms lacks a PH domain. Injection of chicken PLCζ cRNA was able to induce Ca^{2+} oscillations in mouse eggs at similar potency levels to that of hPLCζ (Coward et al., 2005). From this result, it could be predicted that PLCζ is also the sperm factor in frog and fish since sperm extracts from the fish (Coward et al., 2003) and frog (Dong et al., 2000) can induce oscillations in mouse eggs.

Sperm extract from ascidians, injected into ascidian oocytes can induce Ca^{2+} spikes and activation (Kyozuka et al., 1998), while in the sea urchin there is currently no evidence to suggest a sperm factor exists. It seems that PLCγ present in the egg cytoplasm, plays a role in sea urchin activation (Carroll et al., 1999; Giusti et al., 2003). A role for egg derived PLCγ at fertilisation has also been suggested to exist in ascidians (Runft and Jaffe, 2000). It seems the newt (*cynops pyrrhogaster*) may also have a different mechanism for activation. A 45 kDa protein that is homologous to xenopus citrate synthase, and not a PLC, has been reported to activate newt eggs (Harada et al., 2007). This is an interesting report that ties in with other studies that suggest mitochondria play a crucial role during fertilisation, since citrate synthase is the first committed step in the TCA

cycle. Therefore, it is likely that mitochondria play an essential role in all species during fertilisation, independent of the precise activation procedure, be it a PLC or, an enzyme. However, the newt egg undergoes a single Ca^{2+} transient at fertilisation which can be mimicked by other Ca^{2+} stimuli; therefore, it is difficult to interpret if citrate synthase is a real factor at fertilisation. Recently a 32 kDa protein named, postacrosomal sheath WW domain-binding protein (PAWP), was reported to activate mammalian eggs when the recombinant form of PAWP was injected (Wu et al., 2007). However, the ability of the protein to induce Ca^{2+} oscillations like that of sperm was not investigated making this data inconclusive.

As mentioned previously, it is very difficult to mimic the exact pattern of Ca^{2+} oscillations induced by sperm. Oscillations in $InsP_3$ levels have been shown to underlie Ca^{2+} oscillations in kidney cells (Hirose et al., 1999) and such a mechanism could also exist in eggs during fertilisation. This could indicate regenerative $InsP_3$ production during fertilisation which would explain why hydrolysable $InsP_3$ cannot sustain Ca^{2+} oscillations in hamster eggs (Galione et al., 1994). The mechanism of action of PLCζ is still unclear. However, the results in this thesis have helped to understand which domains are required for successful PLCζ action. The data presented in Chapter 7 shows that PLCζ was unable to stimulate a Ca^{2+} release in eggs when it lacked one of its EF hand domains. This result is consistent with previous observations that a short form of PLCζ lacking the first 110 amino acids at the N-terminus is unable to induce oscillations (Kouchi et al., 2004).

PLCζ accumulates in the PN which is thought to explain why Ca^{2+} oscillations stop at PN formation (Kuroda et al., 2006). The aspartate residue at 210 is an important residue on the catalytic X domain of PLCζ. When this residue is mutated PLCζ is unable to produce oscillations (Chapter 7; (Kuroda et al., 2006; Saunders et al., 2002). When this residue at position 210 is mutated, nuclear localisation still occurs but at significantly slower rate suggesting that the catalytic domain may have some function in nuclear localisation (Kuroda et al., 2006). PN formation is an important step in embryo development since a positive correlation has been found between rate of PN formation and pregnancy rates (Nagy et al., 1994). Human eggs were fertilised via ICSI and studied for morphological nuclear changes and it was determined that eggs forming PN within 8 hours post ICSI, were more likely to result in a successful pregnancy (Nagy et al., 1994).

The requirement of the C2 domain in PLCζ to induce Ca^{2+} oscillations is consistent with other reports (Kuroda et al., 2006). The C2 domain has been well characterised as a membrane associating and intermolecular binding domain in a wide range of proteins (Frazier et al., 2002; Gerber et al., 2001; Medkova and Cho, 1999). The C2 domain could play an important role in targeting PLCζ to the correct sub-cellular source of $PtdInsP_2$ in the eggs. It is possible that association of PLCζ with the PM may be mediated by the interaction of the C2 domain with another membrane-targeting protein, as has been previously demonstrated for the C2 domain of $PLA_2\alpha$ and its associations with vimentin (Nakatani et al., 2000). Vimentin is an intermediate filament component that acts as a

perinuclear adapter for $PLA_2\alpha$ through its associations with the C2 domain of $PLA_2\alpha$ in a Ca^{2+}-sensitive manner (Nakatani et al., 2000).

When PLCζ (0.02 μg/μl) is prepared with the PH domain from PLCδ, a similar pattern of Ca^{2+} oscillations are produced when compared to WT PLCζ. The only difference was the amplitude of the first Ca^{2+} spike (Table 8.2). This could suggest that zeta is in fact producing $InsP_3$ via the PM but it is being targeting there by a PH independent mechanism. The XY linker region of PLCζ contains a cluster of basic residues. This positively charged cluster within the XY linker has been suggested to anchor PLCζ to the PM to hydrolyse PIP_2 (Nomikos et al., 2007). This PM targeting role of positively charged regions has previously been reported in GTPases that also have clusters of basic residues that appear to target them to the PM (McLaughlin, 2006). In addition, this positively charged region in the XY linker of PLCζ has also been shown to enhance local concentrations of PIP_2 adjacent to the catalytic domain (Nomikos et al., 2007).

Table 8.2 Changes in Ca2+ concentrations following injections of either PLCζ or, PLCδ

PLC construct	Amplitude of initial Ca^{2+} transient (nM) ± s.e.m	Amplitude of subsequent Ca^{2+} transients (nM) ± s.e.m
PLCζ (n=23)	800 ± 9.1	750 ± 2.2
PLCδ1 (n=24)	750 ± 2.3	750 ± 3.7
PLCζ-δPH (n=22)	600 ± 5.3*	800 ± 7.1

Table 8.2 Assuming resting Ca^{2+} of 100 nM the relative amplitude of the Ca^{2+} transients were calculated. *significantly different when compared to PLCζ (*P<0.005)

A comparison between mouse, human and monkey PLCζ was investigated previously (Cox et al., 2002). Cox et al (2002) reported that monkey and human shared 90% sequence similarity, but only a 70% similarity was shared between these two species against the mouse. Of the 3 constructs, human PLCζ is the shortest (608 aa) when compared to the mouse (647 aa) and the monkey (641 aa). Human PLCζ has a shorter XY linker region that results in it having less basic residues meaning it has a higher positive charge. This reason was proposed to explain why human PLCζ was more potent than the mouse and monkey (Cox et al., 2002). However, in contrast, the results in this thesis suggest that both human and monkey are more potent than the mouse. This result makes the more positive charge on human PLCζ more complicated and undefined. Since human and monkey appear to be equally as potent it seems XY linker chimeras between human and mouse PLCζ must be explored. The XY linker is the sequence that links together the two domains forming the β/α catalytic barrel. The role of the XY linker is still unclear since it is the only sequence in the protein structure of PLCδ1 that has not been resolved by X-ray crystallography (Saunders et al., 2002).

Independent of the mammalian species, PLCζ appears to be a crucial factor in fertilisation. It has been shown that 90% of failed human ICSI cases were successfully activated by exposure to a calcium ionophore (Tesarik and Sousa, 1995). Low concentrations of PLCζ fail to activate eggs which could explain why 40% of ICSI treatments that fail are due to incomplete egg activation (Rawe et al., 2000). In contrast, high PLCζ concentrations result in cell arrest (Cox et al., 2002) which could

explain why human embryos with normal morphology and development suddenly arrest. Combined, more investigations into both egg metabolism and PLCζ activity has the potential to pioneer a new approach to assisted reproductive medicine.

References

Aitken, R. J. (1989). The role of free oxygen radicals and sperm function. *Int J Androl* **12**, 95-7.
al-Anzi, B. and Chandler, D. E. (1998). A sperm chemoattractant is released from Xenopus egg jelly during spawning. *Dev Biol* **198**, 366-75.
Albertini, D. F., Sanfins, A. and Combelles, C. M. (2003). Origins and manifestations of oocyte maturation competencies. *Reprod Biomed Online* **6**, 410-5.
Albrieux, M., Lee, H. C. and Villaz, M. (1998). Calcium signaling by cyclic ADP-ribose, NAADP, and inositol trisphosphate are involved in distinct functions in ascidian oocytes. *J Biol Chem* **273**, 14566-74.
Allbritton, N. L., Meyer, T. and Stryer, L. (1992). Range of messenger action of calcium ion and inositol 1,4,5-trisphosphate. *Science* **258**, 1812-5.
Allen, D. G., Lannergren, J. and Westerblad, H. (2002). Intracellular ATP measured with luciferin/luciferase in isolated single mouse skeletal muscle fibres. *Pflugers Arch* **443**, 836-42.
Allue, I., Gandelman, O., Dementieva, E., Ugarova, N. and Cobbold, P. (1996). Evidence for rapid consumption of millimolar concentrations of cytoplasmic ATP during rigor-contracture of metabolically compromised single cardiomyocytes. *Biochem J* **319 (Pt 2)**, 463-9.
Angell, R. R., Hillier, S. G., West, J. D., Glasier, A. F., Rodger, M. W. and Baird, D. T. (1988). Chromosome anomalies in early human embryos. *J Reprod Fertil Suppl* **36**, 73-81.
Angell, R. R., Ledger, W., Yong, E. L., Harkness, L. and Baird, D. T. (1991). Cytogenetic analysis of unfertilized human oocytes. *Hum Reprod* **6**, 568-73.
Ankel-Simons, F. and Cummins, J. M. (1996). Misconceptions about mitochondria and mammalian fertilization: implications for theories on human evolution. *Proc Natl Acad Sci U S A* **93**, 13859-63.
Aoki, F., Worrad, D. M. and Schultz, R. M. (1997). Regulation of transcriptional activity during the first and second cell cycles in the preimplantation mouse embryo. *Dev Biol* **181**, 296-307.
Arnold, S. and Kadenbach, B. (1997). Cell respiration is controlled by ATP, an allosteric inhibitor of cytochrome-c oxidase. *Eur J Biochem* **249**, 350-4.
Austin, C.R and Shorts, RV (1982) Reproduction in mammals:1 Germ cells and fertilization second edition, *Cambridge University Press*
Bahat, A., Tur-Kaspa, I., Gakamsky, A., Giojalas, L. C., Breitbart, H. and Eisenbach, M. (2003). Thermotaxis of mammalian sperm cells: a potential navigation mechanism in the female genital tract. *Nat Med* **9**, 149-50.
Bak, J., Billington, R. A., Timar, G., Dutton, A. C. and Genazzani, A. A. (2001). NAADP receptors are present and functional in the heart. *Curr Biol* **11**, 987-90.
Balaban, R. S., Nemoto, S. and Finkel, T. (2005). Mitochondria, oxidants, and aging. *Cell* **120**, 483-95.
Barbehenn, E. K., Wales, R. G. and Lowry, O. H. (1974). The explanation for the blockade of glycolysis in early mouse embryos. *Proc Natl Acad Sci U S A* **71**, 1056-60.

Barnard, J. P., Reynafarje, B. and Pedersen, P. L. (1993). Glucose catabolism in African trypanosomes. Evidence that the terminal step is catalyzed by a pyruvate transporter capable of facilitating uptake of toxic analogs. *J Biol Chem* **268**, 3654-61.

Bell, C. J., Bright, N. A., Rutter, G. A. and Griffiths, E. J. (2006). ATP regulation in adult rat cardiomyocytes: time-resolved decoding of rapid mitochondrial calcium spiking imaged with targeted photoproteins. *J Biol Chem* **281**, 28058-67.

Bennett, D. L., Cheek, T. R., Berridge, M. J., De Smedt, H., Parys, J. B., Missiaen, L. and Bootman, M. D. (1996). Expression and function of ryanodine receptors in nonexcitable cells. *J Biol Chem* **271**, 6356-62.

Berridge, M. J., Lipp, P. and Bootman, M. D. (2000). The versatility and universality of calcium signalling. *Nat Rev Mol Cell Biol* **1**, 11-21.

Beutner, G., Sharma, V. K., Giovannucci, D. R., Yule, D. I. and Sheu, S. S. (2001). Identification of a ryanodine receptor in rat heart mitochondria. *J Biol Chem* **276**, 21482-8.

Biggers, J. D., McGinnis, L. K. and Raffin, M. (2000). Amino acids and preimplantation development of the mouse in protein-free potassium simplex optimized medium. *Biol Reprod* **63**, 281-93.

Biggers, J. D., Whittingham, D. G. and Donahue, R. P. (1967). The pattern of energy metabolism in the mouse oocyte and zygote. *Proc Natl Acad Sci U S A* **58**, 560-7.

Bleil, J. D. and Wassarman, P. M. (1983). Sperm-egg interactions in the mouse: sequence of events and induction of the acrosome reaction by a zona pellucida glycoprotein. *Dev Biol* **95**, 317-24.

Bootman, M. D., Collins, T. J., Peppiatt, C. M., Prothero, L. S., MacKenzie, L., De Smet, P., Travers, M., Tovey, S. C., Seo, J. T., Berridge, M. J. et al. (2001). Calcium signalling--an overview. *Semin Cell Dev Biol* **12**, 3-10.

Bootman, M. D. and Lipp, P. (1999). Ringing changes to the 'bell-shaped curve'. *Curr Biol* **9**, R876-8.

Bootman, M. D., Thomas, D., Tovey, S. C., Berridge, M. J. and Lipp, P. (2000). Nuclear calcium signalling. *Cell Mol Life Sci* **57**, 371-8.

Bos-Mikich, A., Swann, K. and Whittingham, D. G. (1995). Calcium oscillations and protein synthesis inhibition synergistically activate mouse oocytes. *Mol Reprod Dev* **41**, 84-90.

Bouniol, C., Nguyen, E. and Debey, P. (1995). Endogenous transcription occurs at the 1-cell stage in the mouse embryo. *Exp Cell Res* **218**, 57-62.

Bowers, K. C., Allshire, A. P. and Cobbold, P. H. (1992). Bioluminescent measurement in single cardiomyocytes of sudden cytosolic ATP depletion coincident with rigor. *J Mol Cell Cardiol* **24**, 213-8.

Bowers, K. C., Allshire, A. P. and Cobbold, P. H. (1993). Continuous measurements of cytoplasmic ATP in single cardiomyocytes during simulation of the "oxygen paradox". *Cardiovasc Res* **27**, 1836-9.

Bradley, M. P., Geelan, A., Leitch, V. and Goldberg, E. (1996). Cloning, sequencing, and characterization of LDH-C4 from a fox testis cDNA library. *Mol Reprod Dev* **44**, 452-9.

Brand, M. D. (1985). The stoichiometry of the exchange catalysed by the mitochondrial calcium/sodium antiporter. *Biochem J* **229**, 161-6.

Breitbart, H. (2002). Role and regulation of intracellular calcium in acrosomal exocytosis. *J Reprod Immunol* **53**, 151-9.

Breitbart, H., Rubinstein, S. and Nass-Arden, L. (1985). The role of calcium and Ca2+-ATPase in maintaining motility in ram spermatozoa. *J Biol Chem* **260**, 11548-53.
Brevini, T. A., Vassena, R., Francisci, C. and Gandolfi, F. (2005). Role of adenosine triphosphate, active mitochondria, and microtubules in the acquisition of developmental competence of parthenogenetically activated pig oocytes. *Biol Reprod* **72**, 1218-23.
Brind, S., Swann, K. and Carroll, J. (2000). Inositol 1,4,5-trisphosphate receptors are downregulated in mouse oocytes in response to sperm or adenophostin A but not to increases in intracellular Ca(2+) or egg activation. *Dev Biol* **223**, 251-65.
Brough, D., Schell, M. J. and Irvine, R. F. (2005). Agonist-induced regulation of mitochondrial and endoplasmic reticulum motility. *Biochem J* **392**, 291-7.
Brown, J. J. and Whittingham, D. G. (1991). The roles of pyruvate, lactate and glucose during preimplantation development of embryos from F1 hybrid mice in vitro. *Development* **112**, 99-105.
Brown, J. J. and Whittingham, D. G. (1992). The dynamic provision of different energy substrates improves development of one-cell random-bred mouse embryos in vitro. *J Reprod Fertil* **95**, 503-11.
Brunet, S. and Maro, B. (2005). Cytoskeleton and cell cycle control during meiotic maturation of the mouse oocyte: integrating time and space. *Reproduction* **130**, 801-11.
Bunch, D. O., Welch, J. E., Magyar, P. L., Eddy, E. M. and O'Brien, D. A. (1998). Glyceraldehyde 3-phosphate dehydrogenase-S protein distribution during mouse spermatogenesis. *Biol Reprod* **58**, 834-41.
Calarco, P. G. (1995). Polarization of mitochondria in the unfertilized mouse oocyte. *Dev Genet* **16**, 36-43.
Campbell, A. K. (1988) Chemiluminescence Principles and Applications in Biology and Medicine, *Ellis Horwood Ltd.*
Campbell, J. D., Sansom, M. S. and Ashcroft, F. M. (2003). Potassium channel regulation. *EMBO Rep* **4**, 1038-42.
Campbell, K. and Swann, K. (2006). Ca2+ oscillations stimulate an ATP increase during fertilization of mouse eggs. *Dev Biol* **298**, 225-33.
Carroll, D. J., Albay, D. T., Terasaki, M., Jaffe, L. A. and Foltz, K. R. (1999). Identification of PLCgamma-dependent and -independent events during fertilization of sea urchin eggs. *Dev Biol* **206**, 232-47.
Carroll, J. (2001). The initiation and regulation of Ca2+ signalling at fertilization in mammals. *Semin Cell Dev Biol* **12**, 37-43.
Cetica, P., Pintos, L., Dalvit, G. and Beconi, M. (2003). Involvement of enzymes of amino acid metabolism and tricarboxylic acid cycle in bovine oocyte maturation in vitro. *Reproduction* **126**, 753-63.
Chatot, C. L., Ziomek, C. A., Bavister, B. D., Lewis, J. L. and Torres, I. (1989). An improved culture medium supports development of random-bred 1-cell mouse embryos in vitro. *J Reprod Fertil* **86**, 679-88.
Chen, C. and Regehr, W. G. (1999). Contributions of residual calcium to fast synaptic transmission. *J Neurosci* **19**, 6257-66.
Cheng, J., Yusufi, A. N., Thompson, M. A., Chini, E. N. and Grande, J. P. (2001). Nicotinic acid adenine dinucleotide phosphate: a new Ca2+ releasing agent in kidney. *J Am Soc Nephrol* **12**, 54-60.

Chini, E. N., Beers, K. W. and Dousa, T. P. (1995). Nicotinate adenine dinucleotide phosphate (NAADP) triggers a specific calcium release system in sea urchin eggs. *J Biol Chem* **270**, 3216-23.
Ciapa, B. and Whitaker, M. (1986). Two phases of inositol polyphosphate and diacylglycerol production at fertilisation. *FEBS Lett* **195**, 347-51.
Colledge, W. H., Carlton, M. B., Udy, G. B. and Evans, M. J. (1994). Disruption of c-mos causes parthenogenetic development of unfertilized mouse eggs. *Nature* **370**, 65-8.
Colonna, R. and Mangia, F. (1983). Mechanisms of amino acid uptake in cumulus-enclosed mouse oocytes. *Biol Reprod* **28**, 797-803.
Colton, S. A., Humpherson, P. G., Leese, H. J. and Downs, S. M. (2003). Physiological changes in oocyte-cumulus cell complexes from diabetic mice that potentially influence meiotic regulation. *Biol Reprod* **69**, 761-70.
Combelles, C. M. and Albertini, D. F. (2003). Assessment of oocyte quality following repeated gonadotropin stimulation in the mouse. *Biol Reprod* **68**, 812-21.
Comizzoli, P., Urner, F., Sakkas, D. and Renard, J. P. (2003). Up-regulation of glucose metabolism during male pronucleus formation determines the early onset of the s phase in bovine zygotes. *Biol Reprod* **68**, 1934-40.
Conaghan, J., Handyside, A. H., Winston, R. M. and Leese, H. J. (1993). Effects of pyruvate and glucose on the development of human preimplantation embryos in vitro. *J Reprod Fertil* **99**, 87-95.
Conti, M., Andersen, C. B., Richard, F., Mehats, C., Chun, S. Y., Horner, K., Jin, C. and Tsafriri, A. (2002). Role of cyclic nucleotide signaling in oocyte maturation. *Mol Cell Endocrinol* **187**, 153-9.
Cooper, J. A. (1987). Effects of cytochalasin and phalloidin on actin. *J Cell Biol* **105**, 1473-8.
Coursol, S., Pierre, J. N., Vidal, J. and Grisvard, J. (2002). Cloning and characterization of a phospholipase C from the C(4) plant Digitaria sanguinalis. *J Exp Bot* **53**, 1521-4.
Coward, K., Campos-Mendoza, A., Larman, M., Hibbitt, O., McAndrew, B., Bromage, N. and Parrington, J. (2003). Teleost fish spermatozoa contain a cytosolic protein factor that induces calcium release in sea urchin egg homogenates and triggers calcium oscillations when injected into mouse oocytes. *Biochem Biophys Res Commun* **305**, 299-304.
Coward, K., Ponting, C. P., Chang, H. Y., Hibbitt, O., Savolainen, P., Jones, K. T. and Parrington, J. (2005). Phospholipase Czeta, the trigger of egg activation in mammals, is present in a non-mammalian species. *Reproduction* **130**, 157-63.
Cox, L. J., Larman, M. G., Saunders, C. M., Hashimoto, K., Swann, K. and Lai, F. A. (2002). Sperm phospholipase Czeta from humans and cynomolgus monkeys triggers Ca2+ oscillations, activation and development of mouse oocytes. *Reproduction* **124**, 611-23.
Crossley, I., Swann, K., Chambers, E. and Whitaker, M. (1988). Activation of sea urchin eggs by inositol phosphates is independent of external calcium. *Biochem J* **252**, 257-62.
Cruz, F., Villalba, M., Garcia-Espinosa, M. A., Ballesteros, P., Bogonez, E., Satrustegui, J. and Cerdan, S. (2001). Intracellular compartmentation of pyruvate in primary cultures of cortical neurons as detected by (13)C NMR spectroscopy with multiple (13)C labels. *J Neurosci Res* **66**, 771-81.

Csordas, G., Thomas, A. P. and Hajnoczky, G. (1999). Quasi-synaptic calcium signal transmission between endoplasmic reticulum and mitochondria. *Embo J* **18**, 96-108.
Cullen, P. J. (1998). Bridging the GAP in inositol 1,3,4,5-tetrakisphosphate signalling. *Biochim Biophys Acta* **1436**, 35-47.
Cummins, J. M. (2004). The role of mitochondria in the establishment of oocyte functional competence. *Eur J Obstet Gynecol Reprod Biol* **115 Suppl 1**, S23-9.
Cuthbertson, K. S. and Cobbold, P. H. (1985). Phorbol ester and sperm activate mouse oocytes by inducing sustained oscillations in cell Ca2+. *Nature* **316**, 541-2.
Cuthbertson, K. S., Whittingham, D. G. and Cobbold, P. H. (1981). Free Ca2+ increases in exponential phases during mouse oocyte activation. *Nature* **294**, 754-7.
Dale, B., DeFelice, L. J. and Ehrenstein, G. (1985). Injection of a soluble sperm fraction into sea-urchin eggs triggers the cortical reaction. *Experientia* **41**, 1068-70.
de Wet, J. R., Wood, K. V., DeLuca, M., Helinski, D. R. and Subramani, S. (1987). Firefly luciferase gene: structure and expression in mammalian cells. *Mol Cell Biol* 7, 725-37.
Dekel, N. (1988). Regulation of oocyte maturation. The role of cAMP. *Ann N Y Acad Sci* **541**, 211-6.
DeLuca, M. and McElroy, W. D. (1984). Two kinetically distinguishable ATP sites in firefly luciferase. *Biochem Biophys Res Commun* **123**, 764-70.
Denburg, J. L. and McElroy, W. D. (1970). Anion inhibition of firefly luciferase. *Arch Biochem Biophys* **141**, 668-75.
Deng, M. Q. and Shen, S. S. (2000). A specific inhibitor of p34(cdc2)/cyclin B suppresses fertilization-induced calcium oscillations in mouse eggs. *Biol Reprod* **62**, 873-8.
Dennis, P. B., Jaeschke, A., Saitoh, M., Fowler, B., Kozma, S. C. and Thomas, G. (2001). Mammalian TOR: a homeostatic ATP sensor. *Science* **294**, 1102-5.
Digonnet, C., Aldon, D., Leduc, N., Dumas, C. and Rougier, M. (1997). First evidence of a calcium transient in flowering plants at fertilization. *Development* **124**, 2867-74.
Donahue, R. P. (1968). Maturation of the mouse oocyte in vitro. I. Sequence and timing of nuclear progression. *J Exp Zool* **169**, 237-49.
Donahue, R. P. and Stern, S. (1968). Follicular cell support of oocyte maturation: production of pyruvate in vitro. *J Reprod Fertil* **17**, 395-8.
Dong, J. B., Tang, T. S. and Sun, F. Z. (2000). Xenopus and chicken sperm contain a cytosolic soluble protein factor which can trigger calcium oscillations in mouse eggs. *Biochem Biophys Res Commun* **268**, 947-51.
Doree, M. and Hunt, T. (2002). From Cdc2 to Cdk1: when did the cell cycle kinase join its cyclin partner? *J Cell Sci* **115**, 2461-4.
Dowler, S., Montalvo, L., Cantrell, D., Morrice, N. and Alessi, D. R. (2000). Phosphoinositide 3-kinase-dependent phosphorylation of the dual adaptor for phosphotyrosine and 3-phosphoinositides by the Src family of tyrosine kinase. *Biochem J* **349**, 605-10.
Downs, S. M. (1995). The influence of glucose, cumulus cells, and metabolic coupling on ATP levels and meiotic control in the isolated mouse oocyte. *Dev Biol* **167**, 502-12.

Downs, S. M. (1998). Precursors of the purine backbone augment the inhibitory action of hypoxanthine and dibutyryl cAMP on mouse oocyte maturation. *J Exp Zool* **282**, 376-84.
Duchen, M. R. (2000). Mitochondria and calcium: from cell signalling to cell death. *J Physiol* **529 Pt 1**, 57-68.
Duchen, M. R. (2004). Mitochondria in health and disease: perspectives on a new mitochondrial biology. *Mol Aspects Med* **25**, 365-451.
Ducibella, T., Huneau, D., Angelichio, E., Xu, Z., Schultz, R. M., Kopf, G. S., Fissore, R., Madoux, S. and Ozil, J. P. (2002). Egg-to-embryo transition is driven by differential responses to Ca(2+) oscillation number. *Dev Biol* **250**, 280-91.
Duckworth, B. C., Weaver, J. S. and Ruderman, J. V. (2002). G2 arrest in Xenopus oocytes depends on phosphorylation of cdc25 by protein kinase A. *Proc Natl Acad Sci U S A* **99**, 16794-9.
Dumollard, R., Duchen, M. and Carroll, J. (2007a). The role of mitochondrial function in the oocyte and embryo. *Curr Top Dev Biol* **77**, 21-49.
Dumollard, R., Duchen, M. and Sardet, C. (2006). Calcium signals and mitochondria at fertilisation. *Semin Cell Dev Biol* **17**, 314-23.
Dumollard, R., Hammar, K., Porterfield, M., Smith, P. J., Cibert, C., Rouviere, C. and Sardet, C. (2003). Mitochondrial respiration and Ca2+ waves are linked during fertilization and meiosis completion. *Development* **130**, 683-92.
Dumollard, R., Marangos, P., Fitzharris, G., Swann, K., Duchen, M. and Carroll, J. (2004). Sperm-triggered [Ca2+] oscillations and Ca2+ homeostasis in the mouse egg have an absolute requirement for mitochondrial ATP production. *Development* **131**, 3057-67.
Dumollard, R., Ward, Z., Carroll, J. and Duchen, M. R. (2007b). Regulation of redox metabolism in the mouse oocyte and embryo. *Development* **134**, 455-65.
Dupont, G., McGuinness, O. M., Johnson, M. H., Berridge, M. J. and Borgese, F. (1996). Phospholipase C in mouse oocytes: characterization of beta and gamma isoforms and their possible involvement in sperm-induced Ca2+ spiking. *Biochem J* **316 (Pt 2)**, 583-91.
Dym, M. (1994). Spermatogonial stem cells of the testis. *Proc Natl Acad Sci U S A* **91**, 11287-9.
Eckberg, W. R. and Miller, A. L. (1995). Propagated and nonpropagated calcium transients during egg activation in the annelid, Chaetopterus. *Dev Biol* **172**, 654-64.
Eisen, A. and Reynolds, G. T. (1985). Source and sinks for the calcium released during fertilization of single sea urchin eggs. *J Cell Biol* **100**, 1522-7.
Eisenbach, M. and Giojalas, L. C. (2006). Sperm guidance in mammals - an unpaved road to the egg. *Nat Rev Mol Cell Biol* 7, 276-85.
Ellis, M. V., Carne, A. and Katan, M. (1993). Structural requirements of phosphatidylinositol-specific phospholipase C delta 1 for enzyme activity. *Eur J Biochem* **213**, 339-47.
Ellis, M. V., James, S. R., Perisic, O., Downes, C. P., Williams, R. L. and Katan, M. (1998). Catalytic domain of phosphoinositide-specific phospholipase C (PLC). Mutational analysis of residues within the active site and hydrophobic ridge of plcdelta1. *J Biol Chem* **273**, 11650-9.
Epel, D. (1969). Does ADP regulate respiration following fertilization of sea urchin eggs? *Exp Cell Res* **58**, 312-8.

Eppig, J. J., Ward-Bailey, P. F. and Coleman, D. L. (1985). Hypoxanthine and adenosine in murine ovarian follicular fluid: concentrations and activity in maintaining oocyte meiotic arrest. *Biol Reprod* **33**, 1041-9.
Ernster, L. and Schatz, G. (1981). Mitochondria: a historical review. *J Cell Biol* **91**, 227s-255s.
Fabro, G., Rovasio, R. A., Civalero, S., Frenkel, A., Caplan, S. R., Eisenbach, M. and Giojalas, L. C. (2002). Chemotaxis of capacitated rabbit spermatozoa to follicular fluid revealed by a novel directionality-based assay. *Biol Reprod* **67**, 1565-71.
FitzHarris, G., Marangos, P. and Carroll, J. (2003). Cell cycle-dependent regulation of structure of endoplasmic reticulum and inositol 1,4,5-trisphosphate-induced Ca2+ release in mouse oocytes and embryos. *Mol Biol Cell* **14**, 288-301.
Florman, H. M. and Wassarman, P. M. (1985). O-linked oligosaccharides of mouse egg ZP3 account for its sperm receptor activity. *Cell* **41**, 313-24.
Follmann, K., Arnold, S., Ferguson-Miller, S. and Kadenbach, B. (1998). Cytochrome c oxidase from eucaryotes but not from procaryotes is allosterically inhibited by ATP. *Biochem Mol Biol Int* **45**, 1047-55.
Foltz, K. R. and Shilling, F. M. (1993). Receptor-mediated signal transduction and egg activation. *Zygote* **1**, 276-9.
Franzini-Armstrong, C. and Protasi, F. (1997). Ryanodine receptors of striated muscles: a complex channel capable of multiple interactions. *Physiol Rev* **77**, 699-729.
Fraser, L. R. and Quinn, P. J. (1981). A glycolytic product is obligatory for initiation of the sperm acrosome reaction and whiplash motility required for fertilization in the mouse. *J Reprod Fertil* **61**, 25-35.
Frazier, A. A., Wisner, M. A., Malmberg, N. J., Victor, K. G., Fanucci, G. E., Nalefski, E. A., Falke, J. J. and Cafiso, D. S. (2002). Membrane orientation and position of the C2 domain from cPLA2 by site-directed spin labeling. *Biochemistry* **41**, 6282-92.
Freudzon, L., Norris, R. P., Hand, A. R., Tanaka, S., Saeki, Y., Jones, T. L., Rasenick, M. M., Berlot, C. H., Mehlmann, L. M. and Jaffe, L. A. (2005). Regulation of meiotic prophase arrest in mouse oocytes by GPR3, a constitutive activator of the Gs G protein. *J Cell Biol* **171**, 255-65.
Fujimoto, S., Yoshida, N., Fukui, T., Amanai, M., Isobe, T., Itagaki, C., Izumi, T. and Perry, A. C. (2004). Mammalian phospholipase Czeta induces oocyte activation from the sperm perinuclear matrix. *Dev Biol* **274**, 370-83.
Fukami, K., Nakao, K., Inoue, T., Kataoka, Y., Kurokawa, M., Fissore, R. A., Nakamura, K., Katsuki, M., Mikoshiba, K., Yoshida, N. et al. (2001). Requirement of phospholipase Cdelta4 for the zona pellucida-induced acrosome reaction. *Science* **292**, 920-3.
Galione, A., McDougall, A., Busa, W. B., Willmott, N., Gillot, I. and Whitaker, M. (1993). Redundant mechanisms of calcium-induced calcium release underlying calcium waves during fertilization of sea urchin eggs. *Science* **261**, 348-52.
Galione, A., Swann, K., Georgiou, P. and Whitaker, M. (1994). Regenerative and non-regenerative calcium transients in hamster eggs triggered by inositol 1,4,5-trisphosphate. *J Physiol* **480 (Pt 3)**, 465-74.
Gandelman, O., Allue, I., Bowers, K. and Cobbold, P. (1994). Cytoplasmic factors that affect the intensity and stability of bioluminescence from firefly luciferase in living mammalian cells. *J Biolumin Chemilumin* **9**, 363-71.

Gardner, D. K. and Leese, H. J. (1986). Non-invasive measurement of nutrient uptake by single cultured pre-implantation mouse embryos. *Hum Reprod* **1**, 25-7.
Gardner, D. K. and Leese, H. J. (1988). The role of glucose and pyruvate transport in regulating nutrient utilization by preimplantation mouse embryos. *Development* **104**, 423-9.
Genazzani, A. A. and Galione, A. (1997). A Ca2+ release mechanism gated by the novel pyridine nucleotide, NAADP. *Trends Pharmacol Sci* **18**, 108-10.
Genova, M. L., Pich, M. M., Bernacchia, A., Bianchi, C., Biondi, A., Bovina, C., Falasca, A. I., Formiggini, G., Castelli, G. P. and Lenaz, G. (2004). The mitochondrial production of reactive oxygen species in relation to aging and pathology. *Ann N Y Acad Sci* **1011**, 86-100.
Gerber, S. H., Garcia, J., Rizo, J. and Sudhof, T. C. (2001). An unusual C(2)-domain in the active-zone protein piccolo: implications for Ca(2+) regulation of neurotransmitter release. *Embo J* **20**, 1605-19.
Gerhart, J., Wu, M. and Kirschner, M. (1984). Cell cycle dynamics of an M-phase-specific cytoplasmic factor in Xenopus laevis oocytes and eggs. *J Cell Biol* **98**, 1247-55.
Ginsberg, L. and Hillman, N. (1973). ATP metabolism in cleavage-staged mouse embryos. *J Embryol Exp Morphol* **30**, 267-82.
Giojalas, L. C. and Rovasio, R. A. (1998). Mouse spermatozoa modify their motility parameters and chemotactic response to factors from the oocyte microenvironment. *Int J Androl* **21**, 201-6.
Giusti, A. F., O'Neill, F. J., Yamasu, K., Foltz, K. R. and Jaffe, L. A. (2003). Function of a sea urchin egg Src family kinase in initiating Ca2+ release at fertilization. *Dev Biol* **256**, 367-78.
Gopichandran, N. and Leese, H. J. (2003). Metabolic characterization of the bovine blastocyst, inner cell mass, trophectoderm and blastocoel fluid. *Reproduction* **126**, 299-308.
Gordo, A. C., Rodrigues, P., Kurokawa, M., Jellerette, T., Exley, G. E., Warner, C. and Fissore, R. (2002). Intracellular calcium oscillations signal apoptosis rather than activation in in vitro aged mouse eggs. *Biol Reprod* **66**, 1828-37.
Grudzinskas, J. G. and Yovich. J. L. (1995) Gametes: The oocyte, ***Cambridge University Press***
Gunter, T. E., Buntinas, L., Sparagna, G., Eliseev, R. and Gunter, K. (2000). Mitochondrial calcium transport: mechanisms and functions. *Cell Calcium* **28**, 285-96.
Haghighat, N. and Van Winkle, L. J. (1990). Developmental change in follicular cell-enhanced amino acid uptake into mouse oocytes that depends on intact gap junctions and transport system Gly. *J Exp Zool* **253**, 71-82.
Hajnoczky, G., Hager, R. and Thomas, A. P. (1999). Mitochondria suppress local feedback activation of inositol 1,4, 5-trisphosphate receptors by Ca2+. *J Biol Chem* **274**, 14157-62.
Hajnoczky, G., Robb-Gaspers, L. D., Seitz, M. B. and Thomas, A. P. (1995). Decoding of cytosolic calcium oscillations in the mitochondria. *Cell* **82**, 415-24.
Hansen, D. V., Tung, J. J. and Jackson, P. K. (2006). CaMKII and polo-like kinase 1 sequentially phosphorylate the cytostatic factor Emi2/XErp1 to trigger its destruction and meiotic exit. *Proc Natl Acad Sci U S A* **103**, 608-13.

Harada, Y., Matsumoto, T., Hirahara, S., Nakashima, A., Ueno, S., Oda, S., Miyazaki, S. and Iwao, Y. (2007). Characterization of a sperm factor for egg activation at fertilization of the newt Cynops pyrrhogaster. *Dev Biol* **306**, 797-808.

Hashimoto, N., Watanabe, N., Furuta, Y., Tamemoto, H., Sagata, N., Yokoyama, M., Okazaki, K., Nagayoshi, M., Takeda, N., Ikawa, Y. et al. (1994). Parthenogenetic activation of oocytes in c-mos-deficient mice. *Nature* **370**, 68-71.

Hirose, K., Kadowaki, S., Tanabe, M., Takeshima, H. and Iino, M. (1999). Spatiotemporal dynamics of inositol 1,4,5-trisphosphate that underlies complex Ca2+ mobilization patterns. *Science* **284**, 1527-30.

Hogan, B., Costantini, F. and Lacy, E. (1986) Manipulating the mouse embryo A laboratory manual, *Cold Spring Harbour Laboratoty*

Holst, P. A. and Phemister, R. D. (1971). The prenatal development of the dog: preimplantation events. *Biol Reprod* **5**, 194-206.

Hooper, C. E., Ansorge, R. E., Browne, H. M. and Tomkins, P. (1990). CCD imaging of luciferase gene expression in single mammalian cells. *J Biolumin Chemilumin* **5**, 123-30.

Hopper, R. K., Carroll, S., Aponte, A. M., Johnson, D. T., French, S., Shen, R. F., Witzmann, F. A., Harris, R. A. and Balaban, R. S. (2006). Mitochondrial matrix phosphoproteome: effect of extra mitochondrial calcium. *Biochemistry* **45**, 2524-36.

Horbinski, C. and Chu, C. T. (2005). Kinase signaling cascades in the mitochondrion: a matter of life or death. *Free Radic Biol Med* **38**, 2-11.

Huo, L. and Scarpulla, R. C. (2001). Mitochondrial DNA instability and peri-implantation lethality associated with targeted disruption of nuclear respiratory factor 1 in mice. *Mol Cell Biol* **21**, 644-54.

Hyslop, L. A., Carroll, M., Nixon, V. L., McDougall, A. and Jones, K. T. (2001). Simultaneous measurement of intracellular nitric oxide and free calcium levels in chordate eggs demonstrates that nitric oxide has no role at fertilization. *Dev Biol* **234**, 216-30.

Igarashi, H., Takahashi, T., Takahashi, E., Tezuka, N., Nakahara, K., Takahashi, K. and Kurachi, H. (2005). Aged mouse oocytes fail to readjust intracellular adenosine triphosphates at fertilization. *Biol Reprod* **72**, 1256-61.

Ishii, K., Hirose, K. and Iino, M. (2006). Ca2+ shuttling between endoplasmic reticulum and mitochondria underlying Ca2+ oscillations. *EMBO Rep* **7**, 390-6.

Izyumov, D. S., Avetisyan, A. V., Pletjushkina, O. Y., Sakharov, D. V., Wirtz, K. W., Chernyak, B. V. and Skulachev, V. P. (2004). "Wages of fear": transient threefold decrease in intracellular ATP level imposes apoptosis. *Biochim Biophys Acta* **1658**, 141-7.

Jaffe, L. A., Giusti, A. F., Carroll, D. J. and Foltz, K. R. (2001). Ca2+ signalling during fertilization of echinoderm eggs. *Semin Cell Dev Biol* **12**, 45-51.

Jaffe, L. F. (1983). Sources of calcium in egg activation: a review and hypothesis. *Dev Biol* **99**, 265-76.

Jaffe, L. F. (1991). The path of calcium in cytosolic calcium oscillations: a unifying hypothesis. *Proc Natl Acad Sci U S A* **88**, 9883-7.

James, A. M., Wei, Y. H., Pang, C. Y. and Murphy, M. P. (1996). Altered mitochondrial function in fibroblasts containing MELAS or MERRF mitochondrial DNA mutations. *Biochem J* **318 (Pt 2)**, 401-7.

Janny, L. and Menezo, Y. J. (1996). Maternal age effect on early human embryonic development and blastocyst formation. *Mol Reprod Dev* **45**, 31-7.
Jansen, R. P. (2000). Origin and persistence of the mitochondrial genome. *Hum Reprod* **15 Suppl 2**, 1-10.
Jansen, S., Esmaeilpour, T., Pantaleon, M. and Kaye, P. L. (2006). Glucose affects monocarboxylate cotransporter (MCT) 1 expression during mouse preimplantation development. *Reproduction* **131**, 469-79.
Jellerette, T., He, C. L., Wu, H., Parys, J. B. and Fissore, R. A. (2000). Down-regulation of the inositol 1,4,5-trisphosphate receptor in mouse eggs following fertilization or parthenogenetic activation. *Dev Biol* **223**, 238-50.
Johnson, M. H. and Nasr-Esfahani, M. H. (1994). Radical solutions and cultural problems: could free oxygen radicals be responsible for the impaired development of preimplantation mammalian embryos in vitro? *Bioessays* **16**, 31-8.
Johnson, M. T., Freeman, E. A., Gardner, D. K. and Hunt, P. A. (2007). Oxidative Metabolism of Pyruvate Is Required for Meiotic Maturation of Murine Oocytes In Vivo. *Biol Reprod.*
Jones, K. T. (2004). Turning it on and off: M-phase promoting factor during meiotic maturation and fertilization. *Mol Hum Reprod* **10**, 1-5.
Jones, K. T., Cruttwell, C., Parrington, J. and Swann, K. (1998a). A mammalian sperm cytosolic phospholipase C activity generates inositol trisphosphate and causes Ca2+ release in sea urchin egg homogenates. *FEBS Lett* **437**, 297-300.
Jones, K. T., Matsuda, M., Parrington, J., Katan, M. and Swann, K. (2000). Different Ca2+-releasing abilities of sperm extracts compared with tissue extracts and phospholipase C isoforms in sea urchin egg homogenate and mouse eggs. *Biochem J* **346 Pt 3**, 743-9.
Jones, K. T. and Nixon, V. L. (2000). Sperm-induced Ca(2+) oscillations in mouse oocytes and eggs can be mimicked by photolysis of caged inositol 1,4,5-trisphosphate: evidence to support a continuous low level production of inositol 1, 4,5-trisphosphate during mammalian fertilization. *Dev Biol* **225**, 1-12.
Jones, K. T., Soeller, C. and Cannell, M. B. (1998b). The passage of Ca2+ and fluorescent markers between the sperm and egg after fusion in the mouse. *Development* **125**, 4627-35.
Jones, K. T. and Whittingham, D. G. (1996). A comparison of sperm- and IP3-induced Ca2+ release in activated and aging mouse oocytes. *Dev Biol* **178**, 229-37.
Jouaville, L. S., Pinton, P., Bastianutto, C., Rutter, G. A. and Rizzuto, R. (1999). Regulation of mitochondrial ATP synthesis by calcium: evidence for a long-term metabolic priming. *Proc Natl Acad Sci U S A* **96**, 13807-12.
Jung, D. W., Baysal, K. and Brierley, G. P. (1995). The sodium-calcium antiport of heart mitochondria is not electroneutral. *J Biol Chem* **270**, 672-8.
Kahn, B. B., Alquier, T., Carling, D. and Hardie, D. G. (2005). AMP-activated protein kinase: ancient energy gauge provides clues to modern understanding of metabolism. *Cell Metab* **1**, 15-25.
Kalinowski, R. R., Berlot, C. H., Jones, T. L., Ross, L. F., Jaffe, L. A. and Mehlmann, L. M. (2004). Maintenance of meiotic prophase arrest in vertebrate oocytes by a Gs protein-mediated pathway. *Dev Biol* **267**, 1-13.

Kaneda, M., Okano, M., Hata, K., Sado, T., Tsujimoto, N., Li, E. and Sasaki, H. (2004). Essential role for de novo DNA methyltransferase Dnmt3a in paternal and maternal imprinting. *Nature* **429**, 900-3.
Katan, M. (1998). Families of phosphoinositide-specific phospholipase C: structure and function. *Biochim Biophys Acta* **1436**, 5-17.
Kelley, G. G., Reks, S. E., Ondrako, J. M. and Smrcka, A. V. (2001). Phospholipase C(epsilon): a novel Ras effector. *Embo J* **20**, 743-54.
Kennedy, H. J., Pouli, A. E., Ainscow, E. K., Jouaville, L. S., Rizzuto, R. and Rutter, G. A. (1999). Glucose generates sub-plasma membrane ATP microdomains in single islet beta-cells. Potential role for strategically located mitochondria. *J Biol Chem* **274**, 13281-91.
Kimura, Y. and Yanagimachi, R. (1995). Intracytoplasmic sperm injection in the mouse. *Biol Reprod* **52**, 709-20.
Kline, D. and Kline, J. T. (1992a). Repetitive calcium transients and the role of calcium in exocytosis and cell cycle activation in the mouse egg. *Dev Biol* **149**, 80-9.
Kline, D. and Kline, J. T. (1992b). Thapsigargin activates a calcium influx pathway in the unfertilized mouse egg and suppresses repetitive calcium transients in the fertilized egg. *J Biol Chem* **267**, 17624-30.
Kline, D. and Zagray, J. A. (1995). Absence of an intracellular pH change following fertilisation of the mouse egg. *Zygote* **3**, 305-11.
Kline, J. T. and Kline, D. (1994). Regulation of intracellular calcium in the mouse egg: evidence for inositol trisphosphate-induced calcium release, but not calcium-induced calcium release. *Biol Reprod* **50**, 193-203.
Kolle, S., Stojkovic, M., Reese, S., Reichenbach, H. D., Wolf, E. and Sinowatz, F. (2004). Effects of growth hormone on the ultrastructure of bovine preimplantation embryos. *Cell Tissue Res* **317**, 101-8.
Kono, T., Obata, Y., Wu, Q., Niwa, K., Ono, Y., Yamamoto, Y., Park, E. S., Seo, J. S. and Ogawa, H. (2004). Birth of parthenogenetic mice that can develop to adulthood. *Nature* **428**, 860-4.
Koop, A. and Cobbold, P. H. (1993). Continuous bioluminescent monitoring of cytoplasmic ATP in single isolated rat hepatocytes during metabolic poisoning. *Biochem J* **295 (Pt 1)**, 165-70.
Kouchi, Z., Fukami, K., Shikano, T., Oda, S., Nakamura, Y., Takenawa, T. and Miyazaki, S. (2004). Recombinant phospholipase Czeta has high Ca2+ sensitivity and induces Ca2+ oscillations in mouse eggs. *J Biol Chem* **279**, 10408-12.
Kubiak, J. Z., Weber, M., de Pennart, H., Winston, N. J. and Maro, B. (1993). The metaphase II arrest in mouse oocytes is controlled through microtubule-dependent destruction of cyclin B in the presence of CSF. *Embo J* **12**, 3773-8.
Kunz, W. S. (1986). Spectral properties of fluorescent flavoproteins of isolated rat liver mitochondria. *FEBS Lett* **195**, 92-6.
Kuo, R. C., Baxter, G. T., Thompson, S. H., Stricker, S. A., Patton, C., Bonaventura, J. and Epel, D. (2000). NO is necessary and sufficient for egg activation at fertilization. *Nature* **406**, 633-6.

Kuroda, K., Ito, M., Shikano, T., Awaji, T., Yoda, A., Takeuchi, H., Kinoshita, K. and Miyazaki, S. (2006). The role of X/Y linker region and N-terminal EF-hand domain in nuclear translocation and Ca2+ oscillation-inducing activities of phospholipase Czeta, a mammalian egg-activating factor. *J Biol Chem* **281**, 27794-805.

Kyozuka, K., Deguchi, R., Mohri, T. and Miyazaki, S. (1998). Injection of sperm extract mimics spatiotemporal dynamics of Ca2+ responses and progression of meiosis at fertilization of ascidian oocytes. *Development* **125**, 4099-105.

Lane, M. and Gardner, D. K. (2005). Mitochondrial malate-aspartate shuttle regulates mouse embryo nutrient consumption. *J Biol Chem* **280**, 18361-7.

Lane, M. E., Brennan, F. S. and Corrigan, O. I. (2006). Influence of post-emulsification drying processes on the microencapsulation of human serum albumin. *Int J Pharm* **307**, 16-22.

Lawrence, Y., Ozil, J. P. and Swann, K. (1998). The effects of a Ca2+ chelator and heavy-metal-ion chelators upon Ca2+ oscillations and activation at fertilization in mouse eggs suggest a role for repetitive Ca2+ increases. *Biochem J* **335 (Pt 2)**, 335-42.

Lawrence, Y., Whitaker, M. and Swann, K. (1997). Sperm-egg fusion is the prelude to the initial Ca2+ increase at fertilization in the mouse. *Development* **124**, 233-41.

Lax, Y., Rubinstein, S. and Breitbart, H. (1994). Epidermal growth factor induces acrosomal exocytosis in bovine sperm. *FEBS Lett* **339**, 234-8.

Lee, H. C., Walseth, T. F., Bratt, G. T., Hayes, R. N. and Clapper, D. L. (1989). Structural determination of a cyclic metabolite of NAD+ with intracellular Ca2+-mobilizing activity. *J Biol Chem* **264**, 1608-15.

Lee, S. B. and Rhee, S. G. (1996). Molecular cloning, splice variants, expression, and purification of phospholipase C-delta 4. *J Biol Chem* **271**, 25-31.

Lee, S. L., Kuo, Y. M., Kao, C. C., Hong, C. Y. and Wei, Y. H. (1992). Purification of a sperm motility stimulator from porcine follicular fluid. *Comp Biochem Physiol B* **101**, 591-4.

Leese, H. J. and Barton, A. M. (1984). Pyruvate and glucose uptake by mouse ova and preimplantation embryos. *J Reprod Fertil* **72**, 9-13.

Leese, H. J. and Barton, A. M. (1985). Production of pyruvate by isolated mouse cumulus cells. *J Exp Zool* **234**, 231-6.

Lemmon, M. A., Ferguson, K. M., O'Brien, R., Sigler, P. B. and Schlessinger, J. (1995). Specific and high-affinity binding of inositol phosphates to an isolated pleckstrin homology domain. *Proc Natl Acad Sci U S A* **92**, 10472-6.

Lindsay, L. L. and Clark, W. H., Jr. (1992). Preloading of micromolar intracellular Ca2+ during capacitation of Sicyonia ingentis sperm, and the role of the pHi decrease during the acrosome reaction. *J Exp Zool* **262**, 219-29.

Lindsay, L. L., Hertzler, P. L. and Clark, W. H., Jr. (1992). Extracellular Mg2+ induces an intracellular Ca2+ wave during oocyte activation in the marine shrimp Sicyonia ingentis. *Dev Biol* **152**, 94-102.

Liu, J. and Maller, J. L. (2005). Calcium elevation at fertilization coordinates phosphorylation of XErp1/Emi2 by Plx1 and CaMK II to release metaphase arrest by cytostatic factor. *Curr Biol* **15**, 1458-68.

Liu, L., Hammar, K., Smith, P. J., Inoue, S. and Keefe, D. L. (2001). Mitochondrial modulation of calcium signaling at the initiation of development. *Cell Calcium* **30**, 423-33.
Liu, L. and Keefe, D. L. (2000). Cytoplasm mediates both development and oxidation-induced apoptotic cell death in mouse zygotes. *Biol Reprod* **62**, 1828-34.
Liu, L., Trimarchi, J. R. and Keefe, D. L. (2000). Involvement of mitochondria in oxidative stress-induced cell death in mouse zygotes. *Biol Reprod* **62**, 1745-53.
Madgwick, S., Hansen, D. V., Levasseur, M., Jackson, P. K. and Jones, K. T. (2006). Mouse Emi2 is required to enter meiosis II by reestablishing cyclin B1 during interkinesis. *J Cell Biol* **174**, 791-801.
Manfredi, G., Yang, L., Gajewski, C. D. and Mattiazzi, M. (2002). Measurements of ATP in mammalian cells. *Methods* **26**, 317-26.
Marangos, P. and Carroll, J. (2004). Fertilization and InsP3-induced Ca2+ release stimulate a persistent increase in the rate of degradation of cyclin B1 specifically in mature mouse oocytes. *Dev Biol* **272**, 26-38.
Marangos, P., FitzHarris, G. and Carroll, J. (2003). Ca2+ oscillations at fertilization in mammals are regulated by the formation of pronuclei. *Development* **130**, 1461-72.
Masui, Y. (1991). Roles of protein synthesis in the control of chromosome behavior during egg maturation and activation. *Bull Assoc Anat (Nancy)* **75**, 81-3.
Masui, Y. (2000). The elusive cytostatic factor in the animal egg. *Nat Rev Mol Cell Biol* **1**, 228-32.
Masui, Y. and Markert, C. L. (1971). Cytoplasmic control of nuclear behavior during meiotic maturation of frog oocytes. *J Exp Zool* **177**, 129-45.
Matson, S. and Ducibella, T. (2007). The MEK inhibitor, U0126, alters fertilization-induced [Ca(2+)](i) oscillation parameters and secretion: Differential effects associated with in vivo and in vitro meiotic maturation. *Dev Biol* **306**, 538-48.
McAvey, B. A., Wortzman, G. B., Williams, C. J. and Evans, J. P. (2002). Involvement of calcium signaling and the actin cytoskeleton in the membrane block to polyspermy in mouse eggs. *Biol Reprod* **67**, 1342-52.
McCulloh, D. H. and Chambers, E. L. (1992). Fusion of membranes during fertilization. Increases of the sea urchin egg's membrane capacitance and membrane conductance at the site of contact with the sperm. *J Gen Physiol* **99**, 137-75.
McDougall, A. and Levasseur, M. (1998). Sperm-triggered calcium oscillations during meiosis in ascidian oocytes first pause, restart, then stop: correlations with cell cycle kinase activity. *Development* **125**, 4451-9.
McGrath, J. and Solter, D. (1984). Completion of mouse embryogenesis requires both the maternal and paternal genomes. *Cell* **37**, 179-83.
McLaughlin, S. (2006). Cell biology. Tools to tamper with phosphoinositides. *Science* **314**, 1402-3.
McLay, D. W. and Clarke, H. J. (2003). Remodelling the paternal chromatin at fertilization in mammals. *Reproduction* **125**, 625-33.
Medkova, M. and Cho, W. (1999). Interplay of C1 and C2 domains of protein kinase C-alpha in its membrane binding and activation. *J Biol Chem* **274**, 19852-61.

Mehlmann, L. M., Carpenter, G., Rhee, S. G. and Jaffe, L. A. (1998). SH2 domain-mediated activation of phospholipase Cgamma is not required to initiate Ca2+ release at fertilization of mouse eggs. *Dev Biol* **203**, 221-32.
Mehlmann, L. M., Chattopadhyay, A., Carpenter, G. and Jaffe, L. A. (2001). Evidence that phospholipase C from the sperm is not responsible for initiating Ca(2+) release at fertilization in mouse eggs. *Dev Biol* **236**, 492-501.
Mehlmann, L. M., Jones, T. L. and Jaffe, L. A. (2002). Meiotic arrest in the mouse follicle maintained by a Gs protein in the oocyte. *Science* **297**, 1343-5.
Meng, X., Lindahl, M., Hyvonen, M. E., Parvinen, M., de Rooij, D. G., Hess, M. W., Raatikainen-Ahokas, A., Sainio, K., Rauvala, H., Lakso, M. et al. (2000). Regulation of cell fate decision of undifferentiated spermatogonia by GDNF. *Science* **287**, 1489-93.
Mitchell, P. (1961). Coupling of phosphorylation to electron and hydrogen transfer by a chemi-osmotic type of mechanism. *Nature* **191**, 144-8.
Miyazaki, S. and Igusa, Y. (1981). Fertilization potential in golden hamster eggs consists of recurring hyperpolarizations. *Nature* **290**, 702-4.
Miyazaki, S., Hashimoto, N., Yoshimoto, Y., Kishimoto, T., Igusa, Y. and Hiramoto, Y. (1986). Temporal and spatial dynamics of the periodic increase in intracellular free calcium at fertilization of golden hamster eggs. *Dev Biol* **118**, 259-67.
Miyazaki, S. and Ito, M. (2006). Calcium signals for egg activation in mammals. *J Pharmacol Sci* **100**, 545-52.
Miyazaki, S., Shirakawa, H., Nakada, K. and Honda, Y. (1993). Essential role of the inositol 1,4,5-trisphosphate receptor/Ca2+ release channel in Ca2+ waves and Ca2+ oscillations at fertilization of mammalian eggs. *Dev Biol* **158**, 62-78.
Miyazaki, S., Yuzaki, M., Nakada, K., Shirakawa, H., Nakanishi, S., Nakade, S. and Mikoshiba, K. (1992). Block of Ca2+ wave and Ca2+ oscillation by antibody to the inositol 1,4,5-trisphosphate receptor in fertilized hamster eggs. *Science* **257**, 251-5.
Moller, C. C. and Wassarman, P. M. (1989). Characterization of a proteinase that cleaves zona pellucida glycoprotein ZP2 following activation of mouse eggs. *Dev Biol* **132**, 103-12.
Monk, M. and McLaren, A. (1981). X-chromosome activity in foetal germ cells of the mouse. *J Embryol Exp Morphol* **63**, 75-84.
Monroy, A. (1965). An analysis of the process of activation of protein synthesis upon fertilization. *Arch Biol (Liege)* **76**, 511-22.
Montero, M., Alonso, M. T., Carnicero, E., Cuchillo-Ibanez, I., Albillos, A., Garcia, A. G., Garcia-Sancho, J. and Alvarez, J. (2000). Chromaffin-cell stimulation triggers fast millimolar mitochondrial Ca2+ transients that modulate secretion. *Nat Cell Biol* **2**, 57-61.
Montero, M., Lobaton, C. D., Moreno, A. and Alvarez, J. (2002). A novel regulatory mechanism of the mitochondrial Ca2+ uniporter revealed by the p38 mitogen-activated protein kinase inhibitor SB202190. *Faseb J* **16**, 1955-7.
Moos, J., Visconti, P. E., Moore, G. D., Schultz, R. M. and Kopf, G. S. (1995). Potential role of mitogen-activated protein kinase in pronuclear envelope assembly and disassembly following fertilization of mouse eggs. *Biol Reprod* **53**, 692-9.

Mori, C., Nakamura, N., Welch, J. E., Gotoh, H., Goulding, E. H., Fujioka, M. and Eddy, E. M. (1998). Mouse spermatogenic cell-specific type 1 hexokinase (mHk1-s) transcripts are expressed by alternative splicing from the mHk1 gene and the HK1-S protein is localized mainly in the sperm tail. *Mol Reprod Dev* **49**, 374-85.

Moses, R. M. and Kline, D. (1995). Release of mouse eggs from metaphase arrest by protein synthesis inhibition in the absence of a calcium signal or microtubule assembly. *Mol Reprod Dev* **41**, 264-73.

Motta, P. M., Nottola, S. A., Makabe, S. and Heyn, R. (2000). Mitochondrial morphology in human fetal and adult female germ cells. *Hum Reprod* **15 Suppl 2**, 129-47.

Munne, S., Lee, A., Rosenwaks, Z., Grifo, J. and Cohen, J. (1993). Diagnosis of major chromosome aneuploidies in human preimplantation embryos. *Hum Reprod* **8**, 2185-91.

Murray, A. W., Solomon, M. J. and Kirschner, M. W. (1989). The role of cyclin synthesis and degradation in the control of maturation promoting factor activity. *Nature* **339**, 280-6.

Nagai, T., Sawano, A., Park, E. S. and Miyawaki, A. (2001). Circularly permuted green fluorescent proteins engineered to sense Ca2+. *Proc Natl Acad Sci U S A* **98**, 3197-202.

Nagy, Z. P., Liu, J., Joris, H., Devroey, P. and Van Steirteghem, A. (1994). Time-course of oocyte activation, pronucleus formation and cleavage in human oocytes fertilized by intracytoplasmic sperm injection. *Hum Reprod* **9**, 1743-8.

Nakatani, Y., Tanioka, T., Sunaga, S., Murakami, M. and Kudo, I. (2000). Identification of a cellular protein that functionally interacts with the C2 domain of cytosolic phospholipase A(2)alpha. *J Biol Chem* **275**, 1161-8.

Narisawa, S., Hecht, N. B., Goldberg, E., Boatright, K. M., Reed, J. C. and Millan, J. L. (2002). Testis-specific cytochrome c-null mice produce functional sperm but undergo early testicular atrophy. *Mol Cell Biol* **22**, 5554-62.

Navazio, L., Bewell, M. A., Siddiqua, A., Dickinson, G. D., Galione, A. and Sanders, D. (2000). Calcium release from the endoplasmic reticulum of higher plants elicited by the NADP metabolite nicotinic acid adenine dinucleotide phosphate. *Proc Natl Acad Sci U S A* **97**, 8693-8.

Nicholls, D. G. (2002). Mitochondrial function and dysfunction in the cell: its relevance to aging and aging-related disease. *Int J Biochem Cell Biol* **34**, 1372-81.

Nishi, Y., Takeshita, T., Sato, K. and Araki, T. (2003). Change of the mitochondrial distribution in mouse ooplasm during in vitro maturation. *J Nippon Med Sch* **70**, 408-15.

Nixon, V. L., Levasseur, M., McDougall, A. and Jones, K. T. (2002). Ca(2+) oscillations promote APC/C-dependent cyclin B1 degradation during metaphase arrest and completion of meiosis in fertilizing mouse eggs. *Curr Biol* **12**, 746-50.

Nomikos, M., Mulgrew-Nesbitt, A., Pallavi, P., Mihalyne, G., Zaitseva, I., Swann, K., Lai, F. A., Murray, D. and McLaughlin, S. (2007). Binding of Phosphoinositide-specific Phospholipase C-{zeta} (PLC-{zeta}) to Phospholipid Membranes: POTENTIAL ROLE OF AN UNSTRUCTURED CLUSTER OF BASIC RESIDUES. *J Biol Chem* **282**, 16644-53.

Nuccitelli, R. (1991). How do sperm activate eggs? *Curr Top Dev Biol* **25**, 1-16.

Nurse, P. (1990). Universal control mechanism regulating onset of M-phase. *Nature* **344**, 503-8.

Ohsumi, K., Koyanagi, A., Yamamoto, T. M., Gotoh, T. and Kishimoto, T. (2004). Emi1-mediated M-phase arrest in Xenopus eggs is distinct from cytostatic factor arrest. *Proc Natl Acad Sci U S A* **101**, 12531-6.
Oliveira, R. G., Tomasi, L., Rovasio, R. A. and Giojalas, L. C. (1999). Increased velocity and induction of chemotactic response in mouse spermatozoa by follicular and oviductal fluids. *J Reprod Fertil* **115**, 23-7.
Ozil, J. P., Markoulaki, S., Toth, S., Matson, S., Banrezes, B., Knott, J. G., Schultz, R. M., Huneau, D. and Ducibella, T. (2005). Egg activation events are regulated by the duration of a sustained [Ca2+]cyt signal in the mouse. *Dev Biol* **282**, 39-54.
Pantaleon, M., Ryan, J. P., Gil, M. and Kaye, P. L. (2001). An unusual subcellular localization of GLUT1 and link with metabolism in oocytes and preimplantation mouse embryos. *Biol Reprod* **64**, 1247-54.
Parrington, J., Jones, M. L., Tunwell, R., Devader, C., Katan, M. and Swann, K. (2002). Phospholipase C isoforms in mammalian spermatozoa: potential components of the sperm factor that causes Ca2+ release in eggs. *Reproduction* **123**, 31-9.
Parrington, J., Swann, K., Shevchenko, V. I., Sesay, A. K. and Lai, F. A. (1996). Calcium oscillations in mammalian eggs triggered by a soluble sperm protein. *Nature* **379**, 364-8.
Pazzagli, M., Devine, J. H., Peterson, D. O. and Baldwin, T. O. (1992). Use of bacterial and firefly luciferases as reporter genes in DEAE-dextran-mediated transfection of mammalian cells. *Anal Biochem* **204**, 315-23.
Peters, J. M. (2006). The anaphase promoting complex/cyclosome: a machine designed to destroy. *Nat Rev Mol Cell Biol* **7**, 644-56.
Phillips, K. P. and Baltz, J. M. (1996). Intracellular pH change does not accompany egg activation in the mouse. *Mol Reprod Dev* **45**, 52-60.
Piko, L. and Chase, D. G. (1973). Role of the mitochondrial genome during early development in mice. Effects of ethidium bromide and chloramphenicol. *J Cell Biol* **58**, 357-78.
Poulton, J. and Marchington, D. R. (2002). Segregation of mitochondrial DNA (mtDNA) in human oocytes and in animal models of mtDNA disease: clinical implications. *Reproduction* **123**, 751-5.
Presicce, G. A. and Yang, X. (1994). Parthenogenetic development of bovine oocytes matured in vitro for 24 hr and activated by ethanol and cycloheximide. *Mol Reprod Dev* **38**, 380-5.
Quinn, P. and Wales, R. G. (1973). The effect of culture in vitro on the levels of adenosine triphosphate in preimplantation mouse embryos. *J Reprod Fertil* **32**, 231-41.
Ralt, D., Manor, M., Cohen-Dayag, A., Tur-Kaspa, I., Ben-Shlomo, I., Makler, A., Yuli, I., Dor, J., Blumberg, S., Mashiach, S. et al. (1994). Chemotaxis and chemokinesis of human spermatozoa to follicular factors. *Biol Reprod* **50**, 774-85.
Rauh, N. R., Schmidt, A., Bormann, J., Nigg, E. A. and Mayer, T. U. (2005). Calcium triggers exit from meiosis II by targeting the APC/C inhibitor XErp1 for degradation. *Nature* **437**, 1048-52.
Rawe, V. Y., Olmedo, S. B., Nodar, F. N., Doncel, G. D., Acosta, A. A. and Vitullo, A. D. (2000). Cytoskeletal organization defects and abortive activation in human oocytes after IVF and ICSI failure. *Mol Hum Reprod* **6**, 510-6.

Raz, T., Ben-Yosef, D. and Shalgi, R. (1998). Segregation of the pathways leading to cortical reaction and cell cycle activation in the rat egg. *Biol Reprod* **58**, 94-102.
Regehr, W. G. and Atluri, P. P. (1995). Calcium transients in cerebellar granule cell presynaptic terminals. *Biophys J* **68**, 2156-70.
Regehr, W. G. and Tank, D. W. (1991). Selective fura-2 loading of presynaptic terminals and nerve cell processes by local perfusion in mammalian brain slice. *J Neurosci Methods* **37**, 111-9.
Reijo, R., Lee, T. Y., Salo, P., Alagappan, R., Brown, L. G., Rosenberg, M., Rozen, S., Jaffe, T., Straus, D., Hovatta, O. et al. (1995). Diverse spermatogenic defects in humans caused by Y chromosome deletions encompassing a novel RNA-binding protein gene. *Nat Genet* **10**, 383-93.
Reimann, J. D., Freed, E., Hsu, J. Y., Kramer, E. R., Peters, J. M. and Jackson, P. K. (2001a). Emi1 is a mitotic regulator that interacts with Cdc20 and inhibits the anaphase promoting complex. *Cell* **105**, 645-55.
Reimann, J. D., Gardner, B. E., Margottin-Goguet, F. and Jackson, P. K. (2001b). Emi1 regulates the anaphase-promoting complex by a different mechanism than Mad2 proteins. *Genes Dev* **15**, 3278-85.
Rizzuto, R., Bernardi, P. and Pozzan, T. (2000). Mitochondria as all-round players of the calcium game. *J Physiol* **529 Pt 1**, 37-47.
Rizzuto, R., Simpson, A. W., Brini, M. and Pozzan, T. (1992). Rapid changes of mitochondrial Ca2+ revealed by specifically targeted recombinant aequorin. *Nature* **358**, 325-7.
Roegiers, F., Djediat, C., Dumollard, R., Rouviere, C. and Sardet, C. (1999). Phases of cytoplasmic and cortical reorganizations of the ascidian zygote between fertilization and first division. *Development* **126**, 3101-17.
Ruestow, E. G. (1983). Images and ideas: Leeuwenhoek's perception of the spermatozoa. *J Hist Biol* **16**, 185-224.
Runft, L. L. and Jaffe, L. A. (2000). Sperm extract injection into ascidian eggs signals Ca(2+) release by the same pathway as fertilization. *Development* **127**, 3227-36.
Runft, L. L., Jaffe, L. A. and Mehlmann, L. M. (2002). Egg activation at fertilization: where it all begins. *Dev Biol* **245**, 237-54.
Sagata, N. (1997). What does Mos do in oocytes and somatic cells? *Bioessays* **19**, 13-21.
Sakkas, D., Urner, F., Menezo, Y. and Leppens, G. (1993). Effects of glucose and fructose on fertilization, cleavage, and viability of mouse embryos in vitro. *Biol Reprod* **49**, 1288-92.
Sandalinas, M., Sadowy, S., Alikani, M., Calderon, G., Cohen, J. and Munne, S. (2001). Developmental ability of chromosomally abnormal human embryos to develop to the blastocyst stage. *Hum Reprod* **16**, 1954-8.
Santella, L., Kyozuka, K., Hoving, S., Munchbach, M., Quadroni, M., Dainese, P., Zamparelli, C., James, P. and Carafoli, E. (2000). Breakdown of cytoskeletal proteins during meiosis of starfish oocytes and proteolysis induced by calpain. *Exp Cell Res* **259**, 117-26.
Sathananthan, H., Bongso, A., Ng, S. C., Ho, J., Mok, H. and Ratnam, S. (1990). Ultrastructure of preimplantation human embryos co-cultured with human ampullary cells. *Hum Reprod* **5**, 309-18.

Saunders, C. M., Larman, M. G., Parrington, J., Cox, L. J., Royse, J., Blayney, L. M., Swann, K. and Lai, F. A. (2002). PLC zeta: a sperm-specific trigger of Ca(2+) oscillations in eggs and embryo development. *Development* **129**, 3533-44.

Schini, S. A. and Bavister, B. D. (1988). Two-cell block to development of cultured hamster embryos is caused by phosphate and glucose. *Biol Reprod* **39**, 1183-92.

Schmidt, A., Duncan, P. I., Rauh, N. R., Sauer, G., Fry, A. M., Nigg, E. A. and Mayer, T. U. (2005). Xenopus polo-like kinase Plx1 regulates XErp1, a novel inhibitor of APC/C activity. *Genes Dev* **19**, 502-13.

Schmidt, T., Patton, C. and Epel, D. (1982). Is there a role for the Ca2+ influx during fertilization of the sea urchin egg? *Dev Biol* **90**, 284-90.

Schneider, D. A. and Gourse, R. L. (2004). Relationship between growth rate and ATP concentration in Escherichia coli: a bioassay for available cellular ATP. *J Biol Chem* **279**, 8262-8.

Schomer, B. and Epel, D. (1998). Redox changes during fertilization and maturation of marine invertebrate eggs. *Dev Biol* **203**, 1-11.

Schultz, R. M. and Kopf, G. S. (1995). Molecular basis of mammalian egg activation. *Curr Top Dev Biol* **30**, 21-62.

Schultz, R. M., Montgomery, R. R. and Belanoff, J. R. (1983a). Regulation of mouse oocyte meiotic maturation: implication of a decrease in oocyte cAMP and protein dephosphorylation in commitment to resume meiosis. *Dev Biol* **97**, 264-73.

Schultz, R. M., Montgomery, R. R., Ward-Bailey, P. F. and Eppig, J. J. (1983b). Regulation of oocyte maturation in the mouse: possible roles of intercellular communication, cAMP, and testosterone. *Dev Biol* **95**, 294-304.

Schwartz, M. and Vissing, J. (2002). Paternal inheritance of mitochondrial DNA. *N Engl J Med* **347**, 576-80.

Seliger, H. H. and Mc, E. W. (1960). Spectral emission and quantum yield of firefly bioluminescence. *Arch Biochem Biophys* **88**, 136-41.

Sette, C., Bevilacqua, A., Bianchini, A., Mangia, F., Geremia, R. and Rossi, P. (1997). Parthenogenetic activation of mouse eggs by microinjection of a truncated c-kit tyrosine kinase present in spermatozoa. *Development* **124**, 2267-74.

Shah, J. V. and Cleveland, D. W. (2000). Waiting for anaphase: Mad2 and the spindle assembly checkpoint. *Cell* **103**, 997-1000.

Shahine, L. K. and Cedars, M. I. (2006). Preimplantation genetic diagnosis does not increase pregnancy rates in patients at risk for aneuploidy. *Fertil Steril* **85**, 51-6.

Shepard, T. H., Muffley, L. A. and Smith, L. T. (2000). Mitochondrial ultrastructure in embryos after implantation. *Hum Reprod* **15 Suppl 2**, 218-28.

Shoji, S., Yoshida, N., Amanai, M., Ohgishi, M., Fukui, T., Fujimoto, S., Nakano, Y., Kajikawa, E. and Perry, A. C. (2006). Mammalian Emi2 mediates cytostatic arrest and transduces the signal for meiotic exit via Cdc20. *Embo J* **25**, 834-45.

Smith, L. D. and Ecker, R. E. (1971). The interaction of steroids with Rana pipiens Oocytes in the induction of maturation. *Dev Biol* **25**, 232-47.

Soukhomlinova, M. Y., Fais, D., Kireev, II, Gianguzza, F., Morici, G., Giudice, G. and Poliakov, V. Y. (2001). Division and motility of mitochondria in sea urchin embryogenesis. *J Submicrosc Cytol Pathol* **33**, 433-42.

Speksnijder, J. E., Corson, D. W., Sardet, C. and Jaffe, L. F. (1989). Free calcium pulses following fertilization in the ascidian egg. *Dev Biol* **135**, 182-90.
Spungin, B., Margalit, I. and Breitbart, H. (1995). A 70 kDa protein is transferred from the outer acrosomal to the plasma membrane during capacitation. *FEBS Lett* **357**, 98-102.
Steinhardt, R. A., Epel, D., Carroll, E. J., Jr. and Yanagimachi, R. (1974). Is calcium ionophore a universal activator for unfertilised eggs? *Nature* **252**, 41-3.
Stephano, J. L. and Gould, M. C. (1997). The intracellular calcium increase at fertilization in Urechis caupo oocytes: activation without waves. *Dev Biol* **191**, 53-68.
Stock, D., Leslie, A. G. and Walker, J. E. (1999). Molecular architecture of the rotary motor in ATP synthase. *Science* **286**, 1700-5.
Stojkovic, M., Machado, S. A., Stojkovic, P., Zakhartchenko, V., Hutzler, P., Goncalves, P. B. and Wolf, E. (2001). Mitochondrial distribution and adenosine triphosphate content of bovine oocytes before and after in vitro maturation: correlation with morphological criteria and developmental capacity after in vitro fertilization and culture. *Biol Reprod* **64**, 904-9.
Stricker, S. A. (1996). Repetitive calcium waves induced by fertilization in the nemertean worm Cerebratulus lacteus. *Dev Biol* **176**, 243-63.
Stricker, S. A. (1999). Comparative biology of calcium signaling during fertilization and egg activation in animals. *Dev Biol* **211**, 157-76.
Stricker, S. A., Silva, R. and Smythe, T. (1998). Calcium and endoplasmic reticulum dynamics during oocyte maturation and fertilization in the marine worm Cerebratulus lacteus. *Dev Biol* **203**, 305-22.
Stricker, S. A., Swann, K., Jones, K. T. and Fissore, R. A. (2000). Injections of porcine sperm extracts trigger fertilization-like calcium oscillations in oocytes of a marine worm. *Exp Cell Res* **257**, 341-7.
Sugiura, K., Pendola, F. L. and Eppig, J. J. (2005). Oocyte control of metabolic cooperativity between oocytes and companion granulosa cells: energy metabolism. *Dev Biol* **279**, 20-30.
Summers, M. C. and Biggers, J. D. (2003). Chemically defined media and the culture of mammalian preimplantation embryos: historical perspective and current issues. *Hum Reprod Update* **9**, 557-82.
Surani, M. A., Barton, S. C. and Norris, M. L. (1984). Development of reconstituted mouse eggs suggests imprinting of the genome during gametogenesis. *Nature* **308**, 548-50.
Sutovsky, P., Moreno, R. D., Ramalho-Santos, J., Dominko, T., Simerly, C. and Schatten, G. (2000). Ubiquitinated sperm mitochondria, selective proteolysis, and the regulation of mitochondrial inheritance in mammalian embryos. *Biol Reprod* **63**, 582-90.
Swann, K. (1990). A cytosolic sperm factor stimulates repetitive calcium increases and mimics fertilization in hamster eggs. *Development* **110**, 1295-302.
Swann, K., Larman, M. G., Saunders, C. M. and Lai, F. A. (2004). The cytosolic sperm factor that triggers Ca2+ oscillations and egg activation in mammals is a novel phospholipase C: PLCzeta. *Reproduction* **127**, 431-9.
Swann, K. and Ozil, J. P. (1994). Dynamics of the calcium signal that triggers mammalian egg activation. *Int Rev Cytol* **152**, 183-222.
Takahashi, T., Takahashi, E., Igarashi, H., Tezuka, N. and Kurachi, H. (2003). Impact of oxidative stress in aged mouse oocytes on calcium oscillations at fertilization. *Mol Reprod Dev* **66**, 143-52.

Takahashi, Y. and First, N. L. (1992). In vitro development of bovine one-cell embryos: Influence of glucose, lactate, pyruvate, amino acids and vitamins. *Theriogenology* **37**, 963-78.
Tang, T. S., Dong, J. B., Huang, X. Y. and Sun, F. Z. (2000). Ca(2+) oscillations induced by a cytosolic sperm protein factor are mediated by a maternal machinery that functions only once in mammalian eggs. *Development* **127**, 1141-50.
Tatone, C., Carbone, M. C., Gallo, R., Delle Monache, S., Di Cola, M., Alesse, E. and Amicarelli, F. (2006). Age-associated changes in mouse oocytes during postovulatory in vitro culture: possible role for meiotic kinases and survival factor BCL2. *Biol Reprod* **74**, 395-402.
Terasaki, M., Runft, L. L. and Hand, A. R. (2001). Changes in organization of the endoplasmic reticulum during Xenopus oocyte maturation and activation. *Mol Biol Cell* **12**, 1103-16.
Territo, P. R., Mootha, V. K., French, S. A. and Balaban, R. S. (2000). Ca(2+) activation of heart mitochondrial oxidative phosphorylation: role of the F(0)/F(1)-ATPase. *Am J Physiol Cell Physiol* **278**, C423-35.
Tesarik, J. and Sousa, M. (1995). Key elements of a highly efficient intracytoplasmic sperm injection technique: Ca2+ fluxes and oocyte cytoplasmic dislocation. *Fertil Steril* **64**, 770-6.
Thomas, D., Tovey, S. C., Collins, T. J., Bootman, M. D., Berridge, M. J. and Lipp, P. (2000). A comparison of fluorescent Ca2+ indicator properties and their use in measuring elementary and global Ca2+ signals. *Cell Calcium* **28**, 213-23.
Thouas, G. A., Trounson, A. O. and Jones, G. M. (2005). Effect of female age on mouse oocyte developmental competence following mitochondrial injury. *Biol Reprod* **73**, 366-73.
Travis, A. J., Foster, J. A., Rosenbaum, N. A., Visconti, P. E., Gerton, G. L., Kopf, G. S. and Moss, S. B. (1998). Targeting of a germ cell-specific type 1 hexokinase lacking a porin-binding domain to the mitochondria as well as to the head and fibrous sheath of murine spermatozoa. *Mol Biol Cell* **9**, 263-76.
Trimarchi, J. R., Liu, L., Porterfield, D. M., Smith, P. J. and Keefe, D. L. (2000). Oxidative phosphorylation-dependent and -independent oxygen consumption by individual preimplantation mouse embryos. *Biol Reprod* **62**, 1866-74.
Tung, J. J., Hansen, D. V., Ban, K. H., Loktev, A. V., Summers, M. K., Adler, J. R., 3rd and Jackson, P. K. (2005). A role for the anaphase-promoting complex inhibitor Emi2/XErp1, a homolog of early mitotic inhibitor 1, in cytostatic factor arrest of Xenopus eggs. *Proc Natl Acad Sci U S A* **102**, 4318-23.
Tunquist, B. J. and Maller, J. L. (2003). Under arrest: cytostatic factor (CSF)-mediated metaphase arrest in vertebrate eggs. *Genes Dev* **17**, 683-710.
Turner, R. M. (2006). Moving to the beat: a review of mammalian sperm motility regulation. *Reprod Fertil Dev* **18**, 25-38.
Ugarova, N. N., Filippova, N. and Berezin, I. V. (1981). [Inhibition of luciferase from fireflies Luciola mingrelica by inorganic salts]. *Biokhimiia* **46**, 851-8.
Urner, F. and Sakkas, D. (2005). Involvement of the pentose phosphate pathway and redox regulation in fertilization in the mouse. *Mol Reprod Dev* **70**, 494-503.

Van Blerkom, J. (1989). The origin and detection of chromosomal abnormalities in meiotically mature human oocytes obtained from stimulated follicles and after failed fertilization in vitro. *Prog Clin Biol Res* **296**, 299-310.
Van Blerkom, J. (2004). Mitochondria in human oogenesis and preimplantation embryogenesis: engines of metabolism, ionic regulation and developmental competence. *Reproduction* **128**, 269-80.
Van Blerkom, J., Davis, P. W. and Lee, J. (1995). ATP content of human oocytes and developmental potential and outcome after in-vitro fertilization and embryo transfer. *Hum Reprod* **10**, 415-24.
Varnai, P. and Balla, T. (1998). Visualization of phosphoinositides that bind pleckstrin homology domains: calcium- and agonist-induced dynamic changes and relationship to myo-[3H]inositol-labeled phosphoinositide pools. *J Cell Biol* **143**, 501-10.
Verlhac, M. H., Kubiak, J. Z., Clarke, H. J. and Maro, B. (1994). Microtubule and chromatin behavior follow MAP kinase activity but not MPF activity during meiosis in mouse oocytes. *Development* **120**, 1017-25.
Visconti, P. E. and Kopf, G. S. (1998). Regulation of protein phosphorylation during sperm capacitation. *Biol Reprod* **59**, 1-6.
Visconti, P. E., Moore, G. D., Bailey, J. L., Leclerc, P., Connors, S. A., Pan, D., Olds-Clarke, P. and Kopf, G. S. (1995). Capacitation of mouse spermatozoa. II. Protein tyrosine phosphorylation and capacitation are regulated by a cAMP-dependent pathway. *Development* **121**, 1139-50.
Vivarelli, E., Conti, M., De Felici, M. and Siracusa, G. (1983). Meiotic resumption and intracellular cAMP levels in mouse oocytes treated with compounds which act on cAMP metabolism. *Cell Differ* **12**, 271-6.
Wales, R. G. and Whittingham. (1973). The metabolism of specifically labelled lactate and pyruvate by two-cell mouse embryos. *J Reprod Fertil* **33**, 207-22.
Wang, T., Dowal, L., El-Maghrabi, M. R., Rebecchi, M. and Scarlata, S. (2000). The pleckstrin homology domain of phospholipase C-beta(2) links the binding of gbetagamma to activation of the catalytic core. *J Biol Chem* **275**, 7466-9.
Wang, T., Pentyala, S., Rebecchi, M. J. and Scarlata, S. (1999). Differential association of the pleckstrin homology domains of phospholipases C-beta 1, C-beta 2, and C-delta 1 with lipid bilayers and the beta gamma subunits of heterotrimeric G proteins. *Biochemistry* **38**, 1517-24.
Wassarman, P. M. (1988). Zona pellucida glycoproteins. *Annu Rev Biochem* **57**, 415-42.
Wassarman, P. M. (1991). Construction of the zona pellucida during production of fertilizable mouse eggs. *Bull Assoc Anat (Nancy)* **75**, 115-7.
Wassarman, P. M., Josefowicz, W. J. and Letourneau, G. E. (1976). Meiotic maturation of mouse oocytes in vitro: inhibition of maturation at specific stages of nuclear progression. *J Cell Sci* **22**, 531-45.
Wassarman, P. M., Jovine, L., Qi, H., Williams, Z., Darie, C. and Litscher, E. S. (2005). Recent aspects of mammalian fertilization research. *Mol Cell Endocrinol* **234**, 95-103.
Wassarman, P. M. and Mortillo, S. (1991). Structure of the mouse egg extracellular coat, the zona pellucida. *Int Rev Cytol* **130**, 85-110.

Wendling, N. C., Bencic, D. C., Nagler, J. J., Cloud, J. G. and Ingermann, R. L. (2004). Adenosine triphosphate levels in steelhead (Oncorhynchus mykiss) eggs: an examination of turnover, localization and role. *Comp Biochem Physiol A Mol Integr Physiol* **137**, 739-48.
Westhoff, D. and Kamp, G. (1997). Glyceraldehyde 3-phosphate dehydrogenase is bound to the fibrous sheath of mammalian spermatozoa. *J Cell Sci* **110 (Pt 15)**, 1821-9.
Whitaker, M. (2006). Calcium at fertilization and in early development. *Physiol Rev* **86**, 25-88.
Wilding, M., De Placido, G., De Matteo, L., Marino, M., Alviggi, C. and Dale, B. (2003). Chaotic mosaicism in human preimplantation embryos is correlated with a low mitochondrial membrane potential. *Fertil Steril* **79**, 340-6.
Williams, C. J., Mehlmann, L. M., Jaffe, L. A., Kopf, G. S. and Schultz, R. M. (1998). Evidence that Gq family G proteins do not function in mouse egg activation at fertilization. *Dev Biol* **198**, 116-27.
Williams, R. J., Maus, M., Stella, N., Glowinski, J. and Premont, J. (1996). Reduced glucose metabolism enhances the glutamate-evoked release of arachidonic acid from striatal neurons. *Neuroscience* **74**, 461-8.
Wilson, T. and Hastings, J. W. (1998). Bioluminescence. *Annu Rev Cell Dev Biol* **14**, 197-230.
Wolosker, H., Kline, D., Bian, Y., Blackshaw, S., Cameron, A. M., Fralich, T. J., Schnaar, R. L. and Snyder, S. H. (1998). Molecularly cloned mammalian glucosamine-6-phosphate deaminase localizes to transporting epithelium and lacks oscillin activity. *Faseb J* **12**, 91-9.
Wouters-Tyrou, D., Martinage, A., Chevaillier, P. and Sautiere, P. (1998). Nuclear basic proteins in spermiogenesis. *Biochimie* **80**, 117-28.
Wu, A. T., Sutovsky, P., Manandhar, G., Xu, W., Katayama, M., Day, B. N., Park, K. W., Yi, Y. J., Xi, Y. W., Prather, R. S. et al. (2007). PAWP, a sperm-specific WW domain-binding protein, promotes meiotic resumption and pronuclear development during fertilization. *J Biol Chem* **282**, 12164-75.
Wu, H., He, C. L. and Fissore, R. A. (1997). Injection of a porcine sperm factor triggers calcium oscillations in mouse oocytes and bovine eggs. *Mol Reprod Dev* **46**, 176-89.
Wu, H., He, C. L., Jehn, B., Black, S. J. and Fissore, R. A. (1998). Partial characterization of the calcium-releasing activity of porcine sperm cytosolic extracts. *Dev Biol* **203**, 369-81.
Yamamoto, T., Takeuchi, H., Kanematsu, T., Allen, V., Yagisawa, H., Kikkawa, U., Watanabe, Y., Nakasima, A., Katan, M. and Hirata, M. (1999). Involvement of EF hand motifs in the Ca(2+)-dependent binding of the pleckstrin homology domain to phosphoinositides. *Eur J Biochem* **265**, 481-90.
Yang, J. H. and Park, J. W. (2003). Oxalomalate, a competitive inhibitor of NADP+-dependent isocitrate dehydrogenase, enhances lipid peroxidation-mediated oxidative damage in U937 cells. *Arch Biochem Biophys* **416**, 31-7.
Yazigi, R. A., Chi, M. M., Mastrogiannis, D. S., Strickler, R. C., Yang, V. C. and Lowry, O. H. (1993). Enzyme activities and maturation in unstimulated and exogenous gonadotropin-stimulated human oocytes. *Am J Physiol* **264**, C951-5.
Yoda, A., Oda, S., Shikano, T., Kouchi, Z., Awaji, T., Shirakawa, H., Kinoshita, K. and Miyazaki, S. (2004). Ca2+ oscillation-inducing phospholipase C zeta expressed in mouse eggs is accumulated to the pronucleus during egg activation. *Dev Biol* **268**, 245-57.

The relationship between calcium and metabolism in mouse eggs at fertilisation

Karen Campbell

Department of Obstetrics and Gynaecology

Cardiff University

A thesis submitted for the degree of Doctor of Philosophy

July 2007

APPENDIX 1:
Specimen Layout for Thesis Summary and Declaration/Statements page to be included in a Thesis

DECLARATION

This work has not previously been accepted in substance for any degree and is not concurrently submitted in candidature for any degree.

Signed ..... (candidate) Date 10/07/07

STATEMENT 1

This thesis is being submitted in partial fulfillment of the requirements for the degree of PhD (~~insert MCh, MD, MPhil,~~ PhD etc, as appropriate)

Signed ..... (candidate) Date 10/07/07

STATEMENT 2

This thesis is the result of my own independent work/investigation, except where otherwise stated.
Other sources are acknowledged by explicit references.

Signed ..... (candidate) Date 10/07/07

STATEMENT 3

I hereby give consent for my thesis, if accepted, to be available for photocopying and for inter-library loan, and for the title and summary to be made available to outside organisations.

Signed ..... (candidate) Date 10/07/07

STATEMENT 4 - BAR ON ACCESS APPROVED

I hereby give consent for my thesis, if accepted, to be available for photocopying and for inter-library loans **after expiry of a bar on access** approved by the Graduate Development Committee.

Signed ..... (candidate) Date .....

Acknowledgements

Firstly I would like to thank Karl for being my PhD supervisor and providing invaluable support and guidance throughout the past 3 years. Also, I would like to thank Remi for his advice and encouragement during the past year.

I also have to thank Sharon, Katherine, Sally, Katie, Lorraine, Jo and Dr Yu for their support in and out of the lab. All your friendships have helped make my PhD an enjoyable experience.

Thanks to my mum and dad who have always believed in me. Your encouragement and love have always been my inspiration! Thanks to my sister for making the last few months even more exciting by announcing that my first little niece/nephew is on the way! Last but not least, I would like to thank Ryan, whose love, friendship and encouragement has been invaluable to me; you're the best!